

# UNCLASSIFIED

|   |
|---|
|   |
|   |
|   |
|   |
| AD NUMBER   |
| AD405766  |
| NEW LIMITATION CHANGE   |
| TO<br>Approved for public release, distribution unlimited   |
| FROM<br>Distribution authorized to U.S. Gov't. agencies and their contractors; Administrative/Operational Use; MAR 1963. Other requests shall be referred to Aeronautical Systems Division, Attn: Directorate of Aeromechanics, Wright-Patterson AFB, OH 45433. |
| AUTHORITY   |
| AFFDL ltr, 25 Apr 1972  |

THIS PAGE IS UNCLASSIFIED

**UNCLASSIFIED**

**405 766**

**DOCUMENTATION CENTER**

**FOR**

**C AND TECHNICAL INFORMATION**

**STATION, ALEXANDRIA, VIRGINIA**



**UNCLASSIFIED**

NOTICE: When government or other drawings, specifications or other data are used for any purpose other than in connection with a definitely related government procurement operation, the U. S. Government thereby incurs no responsibility, nor any obligation whatsoever; and the fact that the Government may have formulated, furnished, or in any way supplied the said drawings, specifications, or other data is not to be regarded by implication or otherwise as in any manner licensing the holder or any other person or corporation, or conveying any rights or permission to manufacture, use or sell any patented invention that may in any way be related thereto.

ASD-TDR-62-527

Part I

WJ

# ATMOSPHERIC CONTROL SYSTEMS FOR SPACE VEHICLES

TECHNICAL DOCUMENTARY REPORT NO. ASD-TDR-62-527, Part I

14 March 1963

Directorate of Aeromechanics  
Aeronautical Systems Division  
Air Force Systems Command  
Wright-Patterson Air Force Base, Ohio

Project No. 6146, Task No. 614609

(Prepared under Contract No. AF 33(616)-8323  
by AirResearch Manufacturing Company, Los Angeles  
California; J. Rousseau, author)

405 766

NO OTS

DDC  
MAY 1 1963  
FISIA D



**Best  
Available  
Copy**

## NOTICES

When Government drawings, specifications, or other data are used for any purpose other than in connection with a definitely related Government procurement operation, the United States Government thereby incurs no responsibility nor any obligation whatsoever; and the fact that the Government may have formulated, furnished, or in any way supplied the said drawings, specifications, or other data, is not to be regarded by implication or otherwise as in any manner licensing the holder or any other person or corporation, or conveying any rights or permission to manufacture, use, or sell any patented invention that may in any way be related thereto.

**ASTIA release to OTS not authorized.**

Qualified requesters may obtain copies of this report from the Armed Services Technical Information Agency, (ASTIA), Arlington Hall Station, Arlington 12, Virginia.

Copies of this report should not be returned to the Aeronautical Systems Division unless return is required by security considerations, contractual obligations, or notice on a specific document.

**D**

FOREWORD

This report was prepared by the AIResearch Manufacturing Company at Los Angeles, a division of The Garrett Corporation, under subcontract to the Space and Information Systems Division of North American Aviation, Inc. It is one of a series summarizing the work performed on Phase II of a study covering various aspects of the thermal and atmospheric control of space vehicles. Other reports of the series, including analytical and experimental studies, are listed below.

Thermal and Atmospheric Control  
Study Program Published Reports

|                  |  |                     |
|------------------|--|---------------------|
| 1 ASD TR 61-164  | Environmental Control Systems Selection for Unmanned Space Vehicles                            | -Part I<br>-Part II |
| 2 ASD TR 61-240  | Environmental Control System Selection for Manned Space Vehicles                               | -Part I<br>-Part II |
| 3 ASD TR 61-161  | Space Vehicle Environmental Control Requirements Based on Equipment and Physiological Criteria | -Part I<br>-Part II |
| 4 ASD TR 61-119  | Radiation Heat Transfer Analysis for Space Vehicles  | -Part I<br>-Part II |
| 5 ASD TR 61-30   | Space Radiator Analysis and Design   | -Part I<br>-Part II |
| 6 ASD TR 61-176  | Integration and Optimization of Space Vehicle Environmental Control Systems                    | -Part I<br>-Part II |
| 7 ASD TDR 62-493 | Temperature Control Systems for Space Vehicles   | -Part I             |
| 8 ASD TR 61-162  | Analytical Methods for Space Vehicle Atmospheric Control Processes                             | -Part I<br>-Part II |
| 9 ASD TDR 62-527 | Atmospheric Control Systems for Space Vehicles   | -Part I             |

ASD-TDR-62-527

FOREWORD (Contd)

Test Reports

| <u>ASD No.</u> | <u>Title</u>   | <u>Contractor's No.</u> |
|----------------|--|-------------------------|
| TDR 62-543     | Space Vehicle Transient Thermal Test                                 | SID 62-394              |
| TDR 62-567     | Performance of Extended Surface Space Model                          | SID 62-433              |
| TDR 62-583     | Potassium Superoxide Canister Evaluation for Manned Space Vehicles   | NA 62-283               |
| TDR 62-560     | Low Temperature Carbon Dioxide Adsorption and Adsorbent Regeneration | SS-715-R                |
| TDR 62-581     | Hydrogenation of Carbon Dioxide                                      | SS-712-R                |
| In preparation | Subcritical Pressure Cryogenic Storage Vessel Test                   | In preparation          |

Computer Program Reports

| <u>ASD No.</u> | <u>Title</u>   | <u>Contractor's No.</u> |
|----------------|--|-------------------------|
| TN 61-83       | Program for Determining the Thermal Environment and Temperature History of Orbiting Space Vehicles | SID 62-313              |
| TN 61-129      | Program for Determining Total Emissivity and Absorptivity  | SID 61-446              |
| TN 61-101      | General Computer Program for the Determination of Radiant Interchange Configuration Factors        | SID 62-393              |
| TDR 62-98      | Cryogenic Storage Vessel Design Computer Program   | SS-642-R                |
| TDR 62-599     | Gas to Liquid Heat Exchanger Design Computer Program (Plate Fin V)                                 | SS-707-R                |

## FOREWORD

This report was prepared by the AResearch Manufacturing Company at Los Angeles, a division of The Garrett Corporation, under subcontract to the Space and Information Systems Division of North American Aviation, Inc. It is one of a series summarizing the work performed on Phase II of a study covering various aspects of the thermal and atmospheric control of space vehicles. Other reports of the series, including analytical and experimental studies, are listed below.

Thermal and Atmospheric ControlStudy Program Published Reports

|                  |  |                     |
|------------------|--|---------------------|
| 1 ASD TR 61-164  | Environmental Control Systems<br>Selection for Unmanned Space<br>Vehicles                            | -Part I<br>-Part II |
| 2 ASD TR 61-240  | Environmental Control System<br>Selection for Manned Space<br>Vehicles                               | -Part I<br>-Part II |
| 3 ASD TR 61-161  | Space Vehicle Environmental Control<br>Requirements Based on Equipment and<br>Physiological Criteria | -Part I<br>-Part II |
| 4 ASD TR 61-119  | Radiation Heat Transfer Analysis<br>for Space Vehicles   | -Part I<br>-Part II |
| 5 ASD TR 61-30   | Space Radiator Analysis and Design   | -Part I<br>-Part II |
| 6 ASD TR 61-176  | Integration and Optimi-<br>zation of Space Vehicle Environmental<br>Control Systems                  | -Part I<br>-Part II |
| 7 ASD TDR 62-493 | Temperature Control Systems for<br>Space Vehicles  | -Part I             |
| 8 ASD TR 61-162  | Analytical Methods for Space Vehicle<br>Atmospheric Control Processes                                | -Part I<br>-Part II |
| 9 ASD TDR 62-527 | Atmospheric Control Systems for<br>Space Vehicles  | -Part I             |

ASD-TDR-62-527

FOREWORD (Contd)

The study program is sponsored by the Flight Accessories Laboratory of the Aeronautical Systems Division of the USAF. It is under the direction of A. L. Ingelfinger and A. Gross of the Environmental Control Section. ASD Monitor of this report is W. Fox. R. E. Sexton of the Space and Information Systems Division of North American Aviation, Inc., is the program project manager. At AiResearch, C. S. Coe is the principal investigator.

This report was prepared by J. Rousseau of AiResearch; other personnel who assisted in the preparation are W. L. Burriss, C. S. Coe, and L. E. Hummel. Acknowledgement is given to F. H. Green who prepared the sections on system requirements, system parameters, and leakage detection and repairs. The Contractor's Report Number is SS-716-R.

**ABSTRACT**

Studies are presented of subsystems performing one single atmosphere control function and of complete atmospheric control systems. The subsystems considered are the following: gas supply, humidity control, carbon dioxide management, trace contaminant removal, and oxygen recovery from carbon dioxide. Parametric data are presented whereby the subsystems and systems are characterized in terms of vehicle and mission parameters; interfaces between the atmospheric control system and other vehicle systems also are taken into account.

Comparison of the subsystems considered are performed on an equivalent weight basis where the equivalent weight includes hardware weight as well as penalties for material balance, power consumption, and heat rejection load. Areas of utilization of the various subsystems are defined in terms of mission duration, crew complement, and cabin atmosphere parameters.

**This report has been reviewed and is approved.**

  
WILLIAM C. SAVAGE  
Chief, Environmental Branch  
Flight Accessories Laboratory

# CONTENTS

| <u>Section</u> |  | <u>Page</u> |
|----------------|--|-------------|
| <b>I</b>       | <b>INTRODUCTION</b>                            | <b>1</b>    |
|                | Thermal and Atmospheric Control Study Program  | 1           |
|                | Purpose and Scope of Report                    | 2           |
| <b>II</b>      | <b>NOMENCLATURE</b>                            | <b>3</b>    |
| <b>III</b>     | <b>GENERAL APPROACH TO SYSTEM DESIGN</b>       | <b>5</b>    |
|                | System Requirements                            | 5           |
|                | System Parameters                              | 12          |
|                | Weight   | 12          |
|                | Power Requirements                             | 12          |
|                | Volume   | 13          |
|                | Reliability                                    | 14          |
|                | Development Status                             | 14          |
|                | Interfaces with Other Systems                  | 14          |
|                | System Evaluation Criteria                     | 15          |
|                | Subsystem Considerations                       | 17          |
|                | Physiological Performance Charts               | 19          |
|                | Subsystem Comparison                           | 22          |
| <b>IV</b>      | <b>BREATHING AND PRESSURIZING GAS SUPPLIES</b> | <b>23</b>   |
|                | Introduction and Summary                       | 23          |
|                | High-Pressure Gas Storage                      | 23          |
|                | General  | 23          |
|                | Storage Vessel Weight and Volume               | 24          |
|                | Supercritical Storage of Cryogenic Fluids      | 27          |
|                | General  | 27          |
|                | Methods of Thermal Pressurization              | 29          |
|                | Storage Vessel Weight and Volume               | 30          |



## CONTENTS (Contd)

| <u>Section</u> |  | <u>Page</u> |
|----------------|--|-------------|
| <b>IV</b>      | <b>Subcritical Storage of Cryogenic Fluids</b>                   | <b>35</b>   |
| <b>(Contd)</b> | <b>Methods of Pressurization</b>                                 | <b>35</b>   |
|                | <b>Storage Vessel Weight</b>                                     | <b>35</b>   |
|                | <b>Chemical Generation of Atmospheric Gases</b>                  | <b>36</b>   |
|                | <b>General</b>   | <b>36</b>   |
|                | <b>Oxygen Generation by Decomposition of Lithium Perchlorate</b> | <b>39</b>   |
|                | <b>Oxygen Generation by Decomposition of Hydrogen Peroxide</b>   | <b>41</b>   |
|                | <b>Oxygen Generation by Electrolysis of Water</b>                | <b>43</b>   |
|                | <b>Nitrogen Generation by Decomposition of Lithium Azide</b>     | <b>46</b>   |
|                | <b>Comparison of Gas Supply Subsystems</b>                       | <b>46</b>   |
|                | <b>Component Integration</b>                                     | <b>46</b>   |
|                | <b>Subsystem Comparison</b>                                      | <b>50</b>   |
|                | <b>Conclusions and Design Data</b>                               | <b>54</b>   |
|                | <b>Conclusions</b>   | <b>54</b>   |
|                | <b>Parametric Data</b>   | <b>55</b>   |
| <b>V</b>       | <b>HUMIDITY CONTROL SUBSYSTEMS</b>                               | <b>65</b>   |
|                | <b>General Considerations</b>                                    | <b>65</b>   |
|                | <b>Summary</b>   | <b>65</b>   |
|                | <b>Moisture Removal by Chemical Absorption</b>                   | <b>65</b>   |
|                | <b>Moisture Removal by Adsorption</b>                            | <b>66</b>   |
|                | <b>General</b>   | <b>66</b>   |
|                | <b>Non-regenerable Silica Gel Subsystem</b>                      | <b>68</b>   |
|                | <b>Regenerable Silica Gel Subsystem</b>                          | <b>68</b>   |

## CONTENTS (Contd)

| <u>Section</u> |  | <u>Page</u> |
|----------------|--|-------------|
| <b>V</b>       | <b>Moisture Removal by Cooler-Condenser</b>                  | <b>76</b>   |
| <b>(Contd)</b> |  |             |
|                | General  | 76          |
|                | Cooler-Condenser Performance                                 | 78          |
|                | Liquid Water Separator                                       | 84          |
|                | Subsystem Integration  | 88          |
|                | Subsystem Comparison   | 90          |
|                | Equivalent Weight  | 90          |
|                | Reliability  | 91          |
|                | Process Air Outlet Temperature                               | 91          |
|                | Integration Potential  | 91          |
| <b>VI</b>      | <b>CARBON DIOXIDE MANAGEMENT SUBSYSTEMS</b>                  | <b>93</b>   |
|                | Introduction   | 93          |
|                | Summary and Conclusions                                      | 93          |
|                | Carbon Dioxide Removal by Lithium Hydroxide Absorption       | 94          |
|                | General  | 94          |
|                | Subsystem Characteristics                                    | 98          |
|                | Conclusions  | 114         |
|                | Carbon Dioxide Removal by Alkali Metal Superoxide Absorption | 114         |
|                | General  | 114         |
|                | Subsystem Characteristics                                    | 115         |
|                | Conclusions  | 122         |
|                | Carbon Dioxide Removal by Molecular Sieve                    | 125         |
|                | General  | 125         |
|                | Subsystem Characteristics                                    | 132         |
|                | Conclusions  | 154         |

## CONTENTS (Contd)

| <u>Section</u>              |   | <u>Page</u> |
|-----------------------------|---|-------------|
| <b>VI</b><br><b>(Contd)</b> | <b>Carbon Dioxide Removal By Freeze-out Process</b>                                 | <b>156</b>  |
|                             | General   | 156         |
|                             | Simple Carbon Dioxide Freeze-out Subsystem Characteristics                          | 164         |
|                             | Discussions of Other Freeze-out Subsystems  | 174         |
|                             | Conclusions   | 177         |
|                             | <b>Carbon Dioxide Removal by Electrodialysis Process</b>                            | <b>183</b>  |
|                             | General   | 183         |
|                             | Performance Characteristics   | 185         |
|                             | Conclusions   | 188         |
| <b>VII</b>                  | <b>RECOVERY OF OXYGEN FROM CARBON DIOXIDE BY HYDROGENATION TO WATER AND METHANE</b> | <b>189</b>  |
|                             | General   | 189         |
|                             | System Description  | 191         |
|                             | Subsystem Characteristics   | 194         |
|                             | Conclusions   | 198         |
| <b>VIII</b>                 | <b>TRACE CONTAMINANT MANAGEMENT</b>   | <b>201</b>  |
|                             | General   | 201         |
|                             | System Description  | 204         |
|                             | System Analysis   | 204         |
| <b>IX</b>                   | <b>LEAKAGE DETECTION AND REPAIR</b>   | <b>211</b>  |
| <b>X</b>                    | <b>ATMOSPHERIC CONTROL SYSTEMS</b>  | <b>213</b>  |
|                             | General   | 213         |
|                             | Gas Supply Subsystem  | 214         |
|                             | Cabin Leakage Detection   | 214         |
|                             | Humidity Control Subsystem  | 214         |

## CONTENTS (Contd)

| <u>Section</u>   | <u>Page</u> |
|--|-------------|
| <b>X</b>   |             |
| <b>(Contd)</b>   |             |
| Trace Contaminant Removal Subsystem  | 214         |
| Redundancy for Safety and Reliability                                      | 215         |
| Lithium Hydroxide Atmospheric Control System                               | 216         |
| General  | 216         |
| System Description   | 216         |
| System Characteristics   | 216         |
| Freeze-out Atmospheric Control System                                      | 220         |
| General  | 220         |
| System Description   | 220         |
| System Characteristics   | 222         |
| Molecular Sieve Atmospheric Control System                                 | 229         |
| General  | 229         |
| System Description   | 229         |
| System Characteristics   | 229         |
| Electrodialysis Cell Atmospheric Control System                            | 232         |
| System Description   | 232         |
| System Characteristics   | 236         |
| Atmospheric Control by Molecular Sieve with Carbon Dioxide Methanation     | 236         |
| System Description   | 236         |
| System Characteristics   | 239         |
| Atmospheric Control System by Electrodialysis Process with Oxygen Recovery | 241         |
| System Description   | 241         |
| System Characteristics   | 241         |

ASD-TDR-62-527

CONTENTS (Contd)

| <u>Section</u> | <u>Page</u> |
|----------------|-------------|
| XI CONCLUSIONS | 245         |
| REFERENCES     | 247         |

## LIST OF FIGURES

| <u>Figure No.</u> |  | <u>Page</u> |
|-------------------|--|-------------|
| 1                 | Typical Flight Plans - Lunar Vehicle   | 6           |
| 2                 | Psychrometric Chart - 7.5 psia, 50 Per Cent Oxygen, 50 Per Cent Nitrogen                           | 9           |
| 3                 | Psychrometric Chart - 3.5 psia, 100 Per Cent Oxygen  | 11          |
| 4a                | Physiological Performance Chart - Oxygen-Pressure Effects  | 20          |
| 4b                | Physiological Performance Chart - Temperature-Humidity Effects                                     | 21          |
| 5                 | Oxygen High-Pressure Gas Storage Vessel Characteristics  | 25          |
| 6                 | Nitrogen High-Pressure Gas Storage Vessel Characteristics  | 26          |
| 7                 | Cryogenic Storage With Positive Expulsion  | 28          |
| 8                 | Thermally Pressurized Supercritical Storage - Fluid Recirculation by Means of a Fan                | 28          |
| 9                 | Thermally Pressurized Supercritical Storage - Fluid Circulation Through an Internal Heat Exchanger | 28          |
| 10                | Supercritical Oxygen Storage Vessel Weight Penalty   | 31          |
| 11                | Supercritical Oxygen Storage Vessel Volume Penalty   | 32          |
| 12                | Supercritical Nitrogen Storage Vessel Weight Penalty   | 33          |
| 13                | Supercritical Nitrogen Storage Vessel Volume Penalty   | 34          |
| 14                | Subcritical Oxygen Storage Vessel Weight Penalty   | 37          |
| 15                | Subcritical Nitrogen Storage Vessel Weight Penalty   | 38          |

## LIST OF FIGURES (Contd)

| <u>Figure No.</u> |  | <u>Page</u> |
|-------------------|--|-------------|
| 16                | Oxygen Generation by Lithium Perchlorate - System Weight                                   | 40          |
| 17                | Chemical Oxygen Supply Using Hydrogen Peroxide   | 42          |
| 18                | Hydrogen Peroxide Storage Weight Penalty   | 44          |
| 19                | Electrolytic Cell Subsystem Weight Penalty   | 45          |
| 20                | High-Pressure Gas Storage - Gas Supply Subsystem Diagram                                   | 47          |
| 21                | Supercritical Cryogenic Fluid Storage - Gas Supply Subsystem Diagram                       | 48          |
| 22                | Subcritical Cryogenic Fluid Storage With Positive Expulsion - Gas Supply Subsystem Diagram | 49          |
| 23                | Gas Supply Subsystems Weight Comparison (Oxygen)   | 52          |
| 24                | Oxygen Supply Subsystem Weight (N=1)   | 56          |
| 25                | Oxygen Supply Subsystem Weight (N=2)   | 57          |
| 26                | Oxygen Supply Subsystem Weight (N=3)   | 58          |
| 27                | Oxygen Supply Subsystem Weight (N=4)   | 59          |
| 28                | Oxygen Supply Subsystem (N=5)  | 60          |
| 29                | Oxygen Supply Subsystem Weight (N=6)   | 61          |
| 30                | Nitrogen Supply Subsystem Weight   | 62          |
| 31                | Nitrogen and Oxygen Penalty for 2 Bottles Sharing Load                                     | 63          |
| 32                | Supercritical Vessel No-Loss Hold Duration   | 64          |
| 33                | Water Adsorption Isotherms at 77°F   | 67          |
| 34                | Non-Regenerable Silica Gel Humidity Control Subsystem Weight                               | 69          |

## LIST OF FIGURES (Contd)

| <u>Figure No.</u> |  | <u>Page</u> |
|-------------------|--|-------------|
| 35                | Regenerable Silica Gel Humidity Control Subsystem  | 70          |
| 36                | Silica Gel Bed Characteristic Weight<br>(One Canister)   | 72          |
| 37                | Cooler-Condenser Humidity Control Subsystem  | 77          |
| 38                | Flow Requirement and Heat Load for Humidity<br>Control - Condenser Temperature, 35°F             | 79          |
| 39                | Flow Requirement and Heat Load for Humidity<br>Control - Condenser Temperature, 40°F             | 80          |
| 40                | Flow Requirement and Heat Load for Humidity<br>Control - Condenser Temperature, 45°F             | 81          |
| 41                | Flow Requirement Variation With Outlet<br>Temperature  | 82          |
| 42                | Heat Load Variation With Temperature   | 83          |
| 43                | Cooler-Condenser Characteristic Weight (RH=60%)  | 85          |
| 44                | Cooler-Condenser Characteristic Weight (RH=70%)  | 86          |
| 45                | Cooler-Condenser Optimization  | 87          |
| 46                | Humidity Control Subsystems Comparison   | 92          |
| 47                | Temperature and Carbon Dioxide Concentration<br>Profiles in a Typical Lithium Hydroxide Canister | 95          |
| 48                | Typical Closed-Circuit Lithium Hydroxide<br>Performance  | 96          |
| 49                | Lithium Hydroxide Absorption Capacity for<br>Carbon Dioxide                                      | 97          |
| 50                | Lithium Hydroxide Subsystem Flow Requirement   | 99          |
| 51                | Lithium Hydroxide Subsystem Process Air<br>Temperature Rise                                      | 100         |



## LIST OF FIGURES (Contd)

| <u>Figure No.</u> |  | <u>Page</u> |
|-------------------|--|-------------|
| 52                | Lithium Hydroxide Subsystem Schematic Diagram  | 102         |
| 53                | Lithium Hydroxide Canister Weight  | 105         |
| 54                | Lithium Hydroxide Bed Pressure Drop  | 106         |
| 55                | Lithium Hydroxide Bed Power Loss   | 107         |
| 56                | Single Canister Weight   | 108         |
| 57                | Lithium Hydroxide Subsystem Equivalent Weight<br>(No Credit for Water Production)            | 112         |
| 58                | Lithium Hydroxide Subsystem Equivalent Weight<br>(Credit for Water Production)               | 113         |
| 59                | Process Air Temperature Rise Through Sodium<br>Superoxide and Potassium Superoxide Canisters | 117         |
| 60                | Alkali Metal Superoxide Subsystem Schematic<br>Diagram                                       | 118         |
| 61                | Alkali Metal Superoxide Canister Weight  | 120         |
| 62                | Sodium Superoxide Subsystem Equivalent Weight<br>(No Credit for Oxygen Production)           | 123         |
| 63                | Sodium Superoxide Subsystem Equivalent Weight<br>(Credit for Oxygen Production)              | 124         |
| 64                | Carbon Dioxide Absorption Subsystem Comparison   | 126         |
| 65                | Comparison of Adsorption Capacity of<br>Three Types of Molecular Sieves at 77°F              | 128         |
| 66                | Adsorption Isotherms for Type 5A Molecular Sieve   | 129         |
| 67                | Typical Regenerable Adsorbent Carbon Dioxide<br>Removal Subsystem (No Waste Heat Recovery)   | 130         |
| 68                | Typical Regenerable Adsorbent Carbon Dioxide<br>Removal Subsystem (With Waste Heat Recovery) | 131         |

## LIST OF FIGURES (Contd)

| <u>Figure No.</u> |   | <u>Page</u> |
|-------------------|---|-------------|
| 69                | Flow Requirement Through the Molecular Sieve Subsystem            | 133         |
| 70                | Water Vapor Flow to the Carbon Dioxide Management Subsystem       | 134         |
| 71                | Heat Rejection Load from Water Adsorption                         | 134         |
| 72                | Process Air Temperature Rise Across Desiccant Bed                 | 135         |
| 73                | Silica Gel Charge Weight for Process Air Drying                   | 137         |
| 74                | Desiccant Bed Canister Weight                                     | 138         |
| 75                | Power Loss Through Silica Gel Canister                            | 140         |
| 76                | Effect of Recuperator on Subsystem                                | 142         |
| 77                | Process Air Temperature Rise Across the Molecular Sieve Bed       | 143         |
| 78                | Molecular Sieve Weight for Carbon Dioxide Removal                 | 145         |
| 79                | Molecular Sieve Bed Canister Weight                               | 146         |
| 80                | Molecular Sieve Bed Pumping Power Losses                          | 147         |
| 81                | Molecular Sieve System Power Requirement                          | 148         |
| 82                | Molecular Sieve System Heat Rejection Loads                       | 150         |
| 83                | Molecular Sieve Subsystem Hardware Weight                         | 151         |
| 84                | Molecular Sieve Subsystem Equivalent Weight                       | 152         |
| 85                | Lithium Hydroxide and Molecular Sieve Break-even Mission Duration | 155         |
| 86                | Simple Carbon Dioxide Freeze-out Subsystem Diagram                | 157         |

## LIST OF FIGURES (Contd)

| <u>Figures No.</u> |  | <u>Page</u> |
|--------------------|--|-------------|
| 87                 | Fluid Temperature for Constant Pressure Delivery - Supercritical Oxygen Storage                    | 158         |
| 88                 | Thermodynamic Properties of Oxygen   | 159         |
| 89                 | Carbon Dioxide Freeze-out With Water Recovery  | 161         |
| 90                 | Carbon Dioxide Freeze-out Subsystem Flow Requirement   | 162         |
| 91                 | Water Vapor Flow To The Carbon Dioxide Freeze-out System   | 163         |
| 92                 | Heat Load for Water Freezing   | 163         |
| 93                 | Simple Freeze-out Subsystem Metabolic and Cabin Leakage Flow Requirement ( $p_{CO_2} = 3.8$ mm Hg) | 165         |
| 94                 | Simple Freeze-out Subsystem Metabolic and Cabin Leakage Flow Requirement ( $p_{CO_2} = 5.7$ mm Hg) | 166         |
| 95                 | Simple Freeze-out Subsystem Metabolic and Cabin Leakage Flow Requirement ( $p_{CO_2} = 7.6$ mm Hg) | 167         |
| 96                 | Simple Freeze-out Heat Exchanger Weight ( $p_{CO_2} = 3.8$ mm Hg)                                  | 170         |
| 97                 | Simple Freeze-out Heat Exchanger Weight ( $p_{CO_2} = 5.7$ mm Hg)                                  | 171         |
| 98                 | Simple Freeze-out Heat Exchanger Weight ( $p_{CO_2} = 7.6$ mm Hg)                                  | 172         |
| 99                 | Simple Carbon Dioxide Freeze-out Subsystem Equivalent Weight                                       | 175         |

## LIST OF FIGURES (Contd)

| <u>Figures No.</u> |  | <u>Page</u> |
|--------------------|--|-------------|
| 100                | Freeze-out Heat Exchanger Weight -<br>Subsystem with External Heat Sink                                  | 176         |
| 101                | Carbon Dioxide Removal Subsystem Comparison  | 178         |
| 102                | Freeze-out Subsystem Break-even Weight -<br>Water Balance not Considered                                 | 180         |
| 103                | Freeze-out Subsystem Weight and Utilization<br>Field ( $P = 7.0$ psia, $P_{CO_2} = 7.6$ mm Hg)           | 181         |
| 104                | Freeze-out Subsystem Equivalent Weight and<br>Utilization Field ( $P = 10$ psia, $P_{CO_2} = 7.6$ mm Hg) | 182         |
| 105                | Ion Exchange Electrodialysis Unit for<br>Continuous Carbon Dioxide Removal                               | 184         |
| 106                | Carbon Dioxide Removal by Electrodialysis<br>Process - Subsystem Schematic Diagram                       | 186         |
| 107                | Catalyst Bed Design for Carbon Dioxide<br>Methanation  | 190         |
| 108                | Carbon Dioxide Reduction Subsystem Schematic<br>Diagram  | 192         |
| 109                | Carbon Dioxide Reduction Subsystem Material<br>and Heat Balance  | 195         |
| 110                | Mission Duration for Utilization of Carbon<br>Dioxide Reduction Subsystem                                | 199         |
| 111                | Trace Contaminant Removal Subsystem  | 205         |
| 112                | Activated Charcoal Canister  | 206         |
| 113                | Heater Power Requirement   | 208         |
| 114                | Cabin Atmospheric Gas Weight   | 208         |
| 115                | Trace Contaminant Subsystem Equivalent Weight  | 210         |

## LIST OF FIGURES (Contd)

| <u>Figures No.</u> |  | <u>Page</u> |
|--------------------|--|-------------|
| 116                | Lithium Hydroxide Atmospheric Control System   | 217         |
| 117                | Lithium Hydroxide Atmospheric Control System Weight  | 218         |
| 118                | Lithium Hydroxide Atmospheric Control System Power Requirement                                     | 219         |
| 119                | Lithium Hydroxide Atmospheric Control System Heat Rejection  | 219         |
| 120                | Freeze-out Atmospheric Control System  | 221         |
| 121                | Freeze-out Atmospheric Control System Weight (Cabin Pressure: 7 psia)                              | 223         |
| 122                | Freeze-out Atmospheric Control System Weight (Cabin Pressure: 10 psia)                             | 224         |
| 123                | Freeze-out Atmospheric Control System Power Requirement  | 225         |
| 124                | Freeze-out Atmospheric Control System Heat Load  | 225         |
| 125                | Rate of Water Evacuated Overboard in a Simple Freeze-out Atmospheric Control System                | 226         |
| 126                | Water Entrained to the Carbon Dioxide Removal Subsystem in a Freeze-out Atmospheric Control System | 227         |
| 127                | Water Recovered in Simple Freeze-out Atmospheric Control System                                    | 228         |
| 128                | Molecular Sieve Atmospheric Control System   | 230         |
| 129                | Molecular Sieve System Weight  | 231         |
| 130                | Molecular Sieve System Power Requirement   | 233         |
| 131                | Heat Rejected to Vehicle Cooling System - Molecular Sieve Atmospheric Control System               | 234         |

## LIST OF FIGURES (Contd)

| <u>Figures No.</u> |   | <u>Page</u> |
|--------------------|---|-------------|
| 132                | Heat Carried by the Process Air - Molecular Sieve Atmospheric Control System  | 234         |
| 133                | Atmospheric Control System with Electrodialysis Cell                          | 235         |
| 134                | Atmospheric Control System by Molecular Sieve with Carbon Dioxide Methanation | 238         |
| 135                | Molecular Sieve System with Methanation - Power Requirements                  | 240         |
| 136                | Atmospheric Control System by Electrodialysis with Carbon Dioxide Reduction   | 243         |

## LIST OF TABLES

|   | <u>Page</u> |
|---|-------------|
| TABLE 1    System and Subsystem Design Parameters and Data Assumptions                            | 18          |
| TABLE 2    High-Pressure Gas Storage Optimum Design   | 24          |
| TABLE 3    Supercritical Vessel Design Data   | 30          |
| TABLE 4    Subcritical Vessel Design Data   | 36          |
| TABLE 5    Typical Gas Supply Subsystems Accessory Weights  | 51          |
| TABLE 6    Oxygen Gas Supply Subsystem Characteristics  | 53          |
| TABLE 7    Regenerable Silica Gel Subsystem Accessory Weight (3-Man System)                       | 73          |
| TABLE 8    Heat Required for Desorption at 150°F and Heat Rejected During Adsorption (Btu/Man-Hr) | 75          |
| TABLE 9    Typical Silica Gel Subsystem Pumping Losses (Watts)                                    | 75          |
| TABLE 10   Cooler-Condenser Subsystem Accessory Weight (3-Man System)                             | 89          |
| TABLE 11   Pumping Power Loss in the Separator and Piping of a Cooler-Condenser System (Watts)    | 89          |
| TABLE 12   Comparison of Subsystem Characteristics  | 90          |
| TABLE 13   Lithium Hydroxide Subsystem Accessory Weight   | 110         |
| TABLE 14   Sodium Superoxide Subsystem Accessory Weight (3-Man System)                            | 121         |
| TABLE 15   Molecular Sieve Subsystem Accessory Weight (3-Man System)                              | 153         |
| TABLE 16   Simple Freeze-Out System Optimum Heat Exchanger Characteristics                        | 169         |
| TABLE 17   Simple Carbon Dioxide Freeze-Out Subsystem Accessory Weight (3-Man System)             | 173         |

## LIST OF TABLES

|  | <u>Page</u> |
|--|-------------|
| TABLE 18 Electrodialysis Subsystem Accessory Weight<br>(3-Man Subsystem)                                     | 187         |
| TABLE 19 Electrodialysis Subsystem Characteristics<br>(10 psia Subsystem)                                    | 188         |
| TABLE 20 Carbon Dioxide Reduction Subsystem Characteristics  | 196         |
| TABLE 21 Carbon Dioxide Reduction Subsystem Weight Breakdown   | 197         |
| TABLE 22 Possible Contaminants of Space Cabin Atmosphere   | 202         |
| TABLE 23 Electrodialysis Cell Atmospheric Control System<br>Characteristics (10 psia System)                 | 237         |
| TABLE 24 Atmospheric Control by Molecular Sieve with Carbon<br>Dioxide Methanation - System Material Balance | 242         |
| TABLE 25 Atmospheric Control System by Electrodialysis with<br>Oxygen Recovery - System Characteristics      | 244         |



## SECTION I

### INTRODUCTION\*

#### THERMAL AND ATMOSPHERIC CONTROL STUDY PROGRAM

This report is one of a series summarizing the results of a study entitled "Space Vehicle Thermal and Atmospheric Control" being performed for the Aeronautical Systems Division of the United States Air Force. This study comprises a broad program concerned with analytical and experimental investigation of the problems in providing suitable thermal and atmospheric control for men and equipment in future military space vehicles.

The Space Vehicle Thermal and Atmospheric Control Study has three general objectives:

1. Development of improved analytical methods for predicting the requirements for, and performance of, space vehicle thermal and atmospheric control systems.
2. Development of improved methods, techniques, systems, and equipment for thermal and atmospheric control.
3. Development of criteria and techniques for the optimization of thermal and atmospheric control systems and integration of these systems with other systems of a space vehicle.

To attain these objectives requires that program studies employing a wide range of technical disciplines be conducted on several levels. Thus, on the one hand, the basic characteristics of processes and equipment components required for thermal and atmospheric control are being analyzed and organized to permit rational synthesis and optimization of thermal and atmospheric control systems. On the other hand, to guide study endeavors along lines which would find immediate and practical application, the thermal and atmospheric requirements associated with a series of hypothetical manned and unmanned space vehicles are being investigated. These vehicles, representative of a number of earth orbiting and cislunar missions, are being carried through the preliminary design stage and used as thermal and atmospheric control models for system optimization and integration studies.

\*Manuscript released July 1962 by the author for publication as an ASD Technical Documentary Report

## PURPOSE AND SCOPE OF REPORT

The principal purpose of this report is to analyze and compare competing systems and subsystems for space vehicle atmospheric control. An atmospheric control system includes those components which supply required oxygen, which maintain humidity and contaminant concentrations at optimum levels, and which, for missions of extended duration, recover oxygen from contaminants. Systems are compared on the basis of weight as a function of crew complement and mission duration where the equivalent weight of power penalties, associated with requirements for heating, cooling, fluid circulation, and control, are included. Other system characteristics, such as safety, reliability considerations, and convenience, also are emphasized.

Initial comparisons will be made on the basis of subsystems, the subsystem being an arrangement of components serving a single function such as carbon dioxide management. Final comparison will be made on complete systems which perform the entire atmospheric control function.

Space vehicle atmospheric requirements are reviewed briefly, for both manned and unmanned space vehicles, as a basis for the subsequent system and subsystem design and analysis. These designs also are based on the process and component analytical methods developed in the ASD Technical Report entitled "Analytical Methods for Space Vehicle Atmospheric Control Processes, Part I and Part II." These reports, concerned with the analysis of components and processes, logically preceded the completion of the present study.

In some cases, information pertinent to certain atmospheric control processes is incomplete or preliminary. In this case estimates were made on the basis of theoretical considerations or simplified assumptions.

SECTION II

NOMENCLATURE

|           |   |
|-----------|---|
| $A_F$     | Face area, $\text{ft}^2$  |
| $D_p$     | Particle equivalent diameter, ft  |
| $f$       | Friction factor, dimensionless  |
| $G$       | Mass velocity, $\text{lb}/\text{ft}^2\text{-sec}$   |
| $K$       | Constant  |
| $L$       | Length, ft  |
| $M$       | Molecular weight, $\text{lb}/\text{mole}$   |
| $N$       | Number of crew members  |
| $NTU$     | Number of heat transfer units, dimensionless  |
| $p$       | Partial pressure, mm Hg   |
| $P$       | Pressure, psia or $\text{lb}/\text{ft}^2$   |
| (PL)      | Power loss, watts   |
| (PP)      | Vehicle power penalty, $\text{lb}/\text{watt}$  |
| (PS)      | Power saving, watts   |
| $Q$       | Heat load, $\text{Btu}/\text{hr}$   |
| $Re$      | Reynolds number, dimensionless  |
| (RP)      | Vehicle heat rejection penalty, $\text{lb}/\text{watt}$ or $\text{lb}/(\text{Btu}/\text{hr})$ |
| $T$       | Temperature, $^{\circ}\text{F}$ ( $^{\circ}\text{K}$ )  |
| $V$       | Volume, $\text{ft}^3$   |
| $W$       | Weight flow, $\text{lb}/\text{sec}$ or $\text{lb}/\text{day}$                                 |
| $\bar{W}$ | Unit weight flow, $\text{lb}/\text{man-day}$  |
| $W$       | Weight, lb  |
| $y$       | Mole fraction, dimensionless  |

## NOMENCLATURE (continued)

### Greek Letters

|        |                               |
|--------|-------------------------------|
| $\eta$ | Efficiency                    |
| $\mu$  | Absolute viscosity, lb/ft-sec |
| $\rho$ | Density, lb/ft <sup>3</sup>   |
| $\tau$ | Time, days                    |

### Subscripts

|     |                |
|-----|----------------|
| A   | Accessory      |
| B   | Bed            |
| c   | Carbon dioxide |
| C   | Canister       |
| D   | Desorption     |
| E   | Equivalent     |
| g   | Gas            |
| H   | Hardware       |
| MAT | Material       |
| P   | Power          |
| Q   | Heat           |
| R   | Rejection      |
| sep | Separator      |
| T   | Total          |
| u   | Useful         |

### SECTION III

#### GENERAL APPROACH TO SYSTEM DESIGN

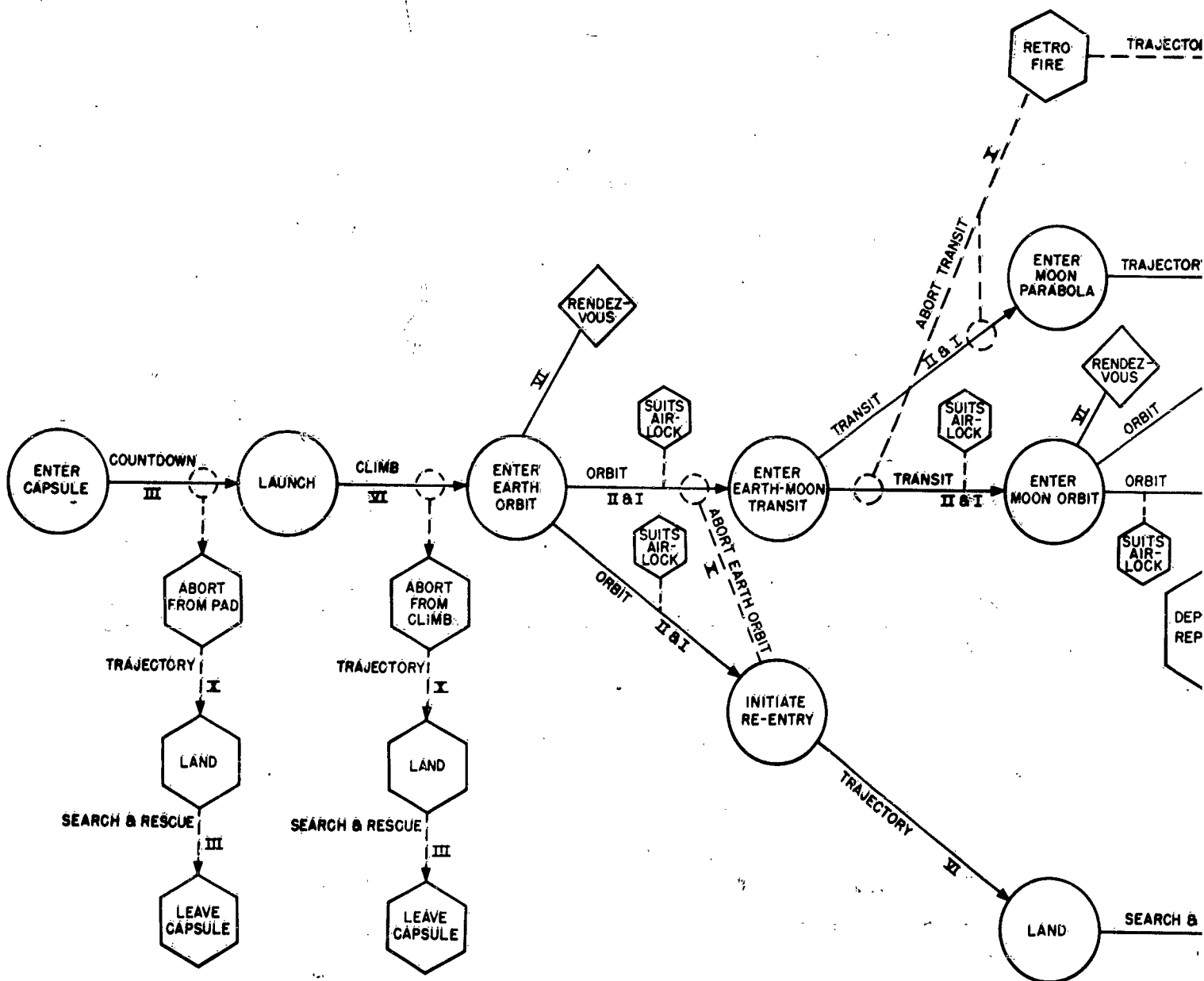
#### SYSTEM REQUIREMENTS

In determining the requirements for an atmospheric control system for a space vehicle, it is important to learn the relations between these requirements and the particular events included in the anticipated mission of the space vehicle. A method of presenting this is shown in Figure 1. On this chart, reading from the left, are listed all expected events and their probable sequence. Events occurring as part of a normal flight plan are shown in circles. Those events which must be allowed for but which are considered emergency conditions are shown in hexagons. Any rendezvous between one vehicle and another is represented by a diamond.

By setting up this chart and later filling in the periods of time involved for each event, and the resulting requirements, a full picture is presented of the relation between the space vehicle mission and the requirements for the atmospheric control system. In expressing the requirements, it is important to consider both the rate of use of the particular requirement and its total use over the entire mission.

The following considerations are apropos of such a chart as Figure 1:

1. It will be necessary to plan for the possibilities of a flight abort from almost any condition, and the succeeding events must be anticipated to result in safe recovery of the astronauts.
2. It will be necessary to allow for the possibility of depressurizing and repressurizing the capsule at least once due to leakage, fire or contamination, with this event likely to occur anywhere within the flight plan.
3. If the crew are to get into their suits rapidly, as in a depressurization operation, then excess oxygen will be needed to scavenge the suit system. If the men must leave the vehicle in pressure suits, then this must be shown on the chart; in computing the requirements for the use of pressure suits, the air used in the airlock must be included.
4. After takeoff, a typical flight, such as shown in Figure 1, would probably first go into earth orbit, then, with further acceleration, start a transit to the moon; on approaching the moon, it would go into a lunar orbit, and, from this orbit, after proper observation, would initiate the moon-landing.



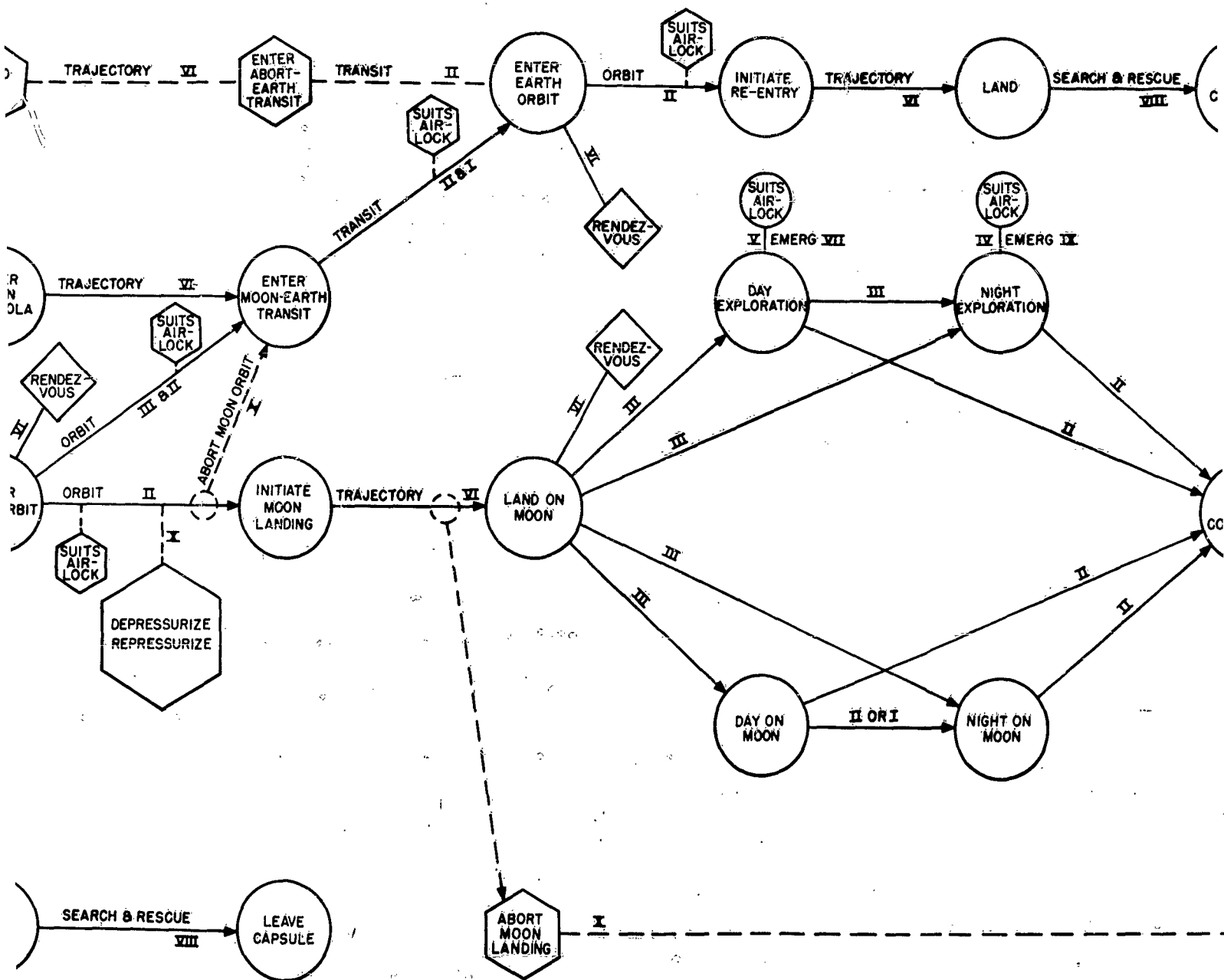
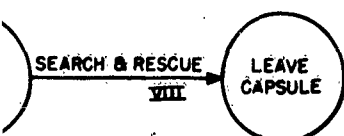
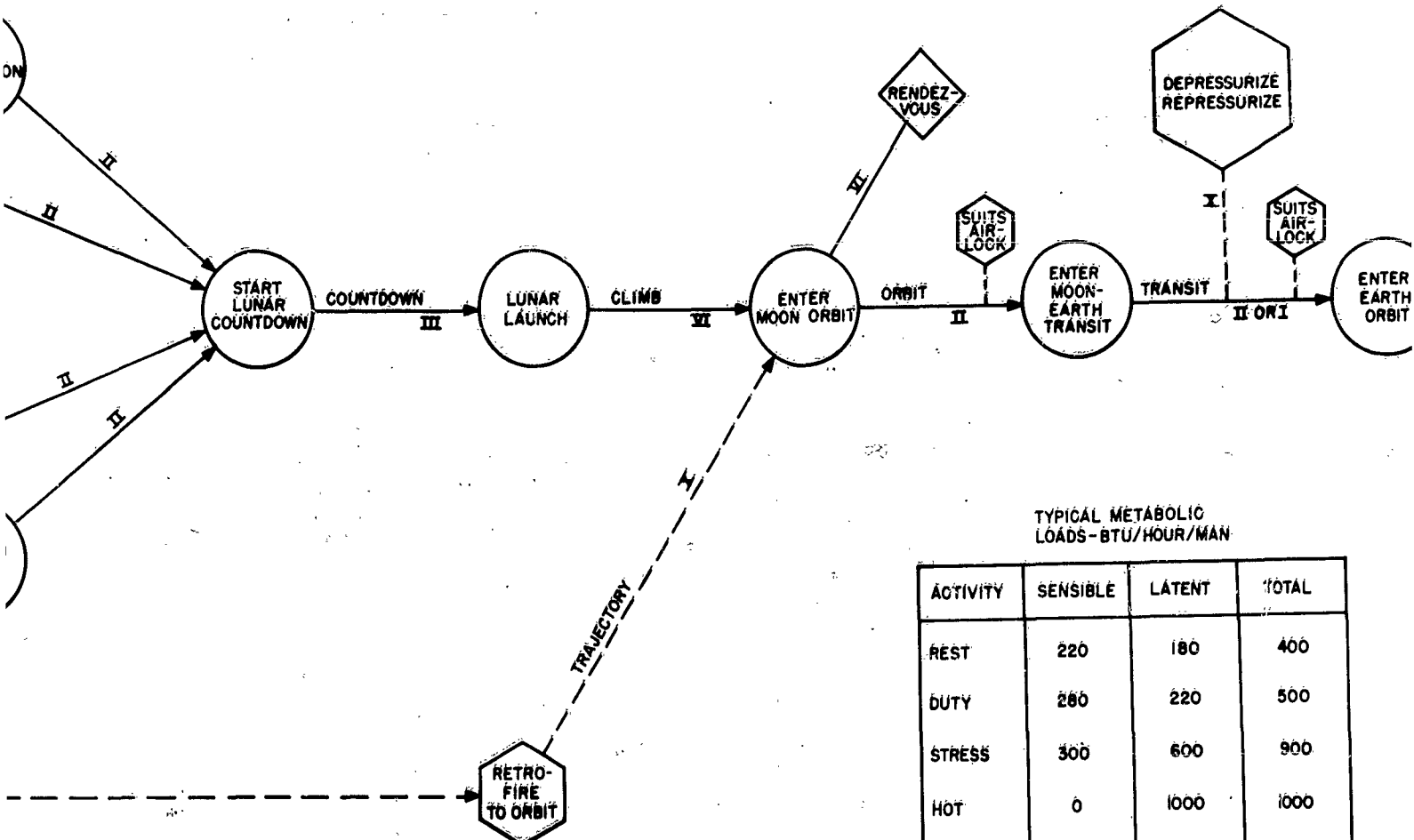


Figure 1. Typical Flight Plans - Lunar Vehicle



ERG IX

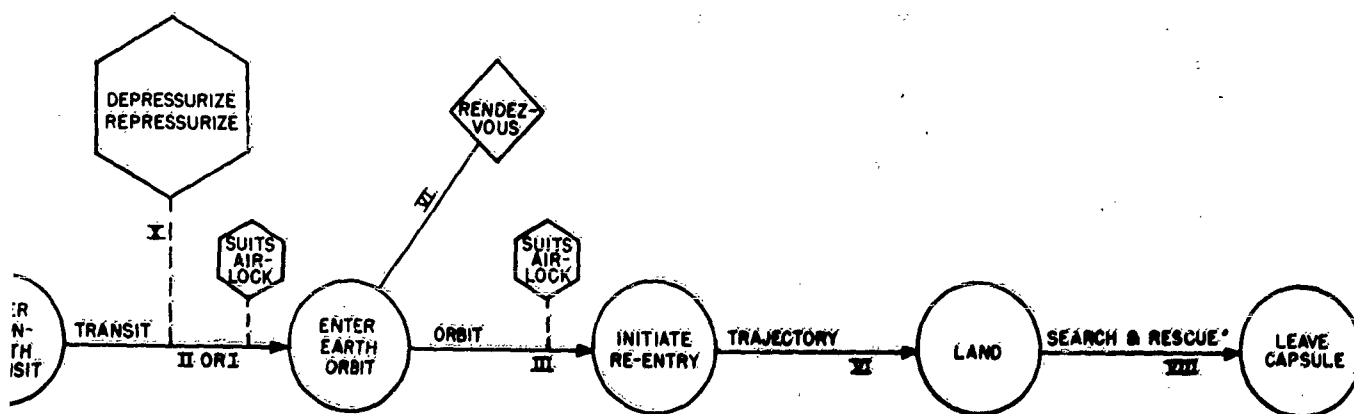


- Lunar Vehicle

TYPICAL METABOLIC LOADS-BTU/HOUR/MAN

| ACTIVITY  | SENSIBLE | LATENT | TOTAL |
|-----------|----------|--------|-------|
| REST      | 220      | 180    | 400   |
| DUTY      | 280      | 220    | 500   |
| STRESS    | 300      | 600    | 900   |
| HOT       | 0        | 1000   | 1000  |
| EMERGENCY | 250      | 1250   | 1500  |

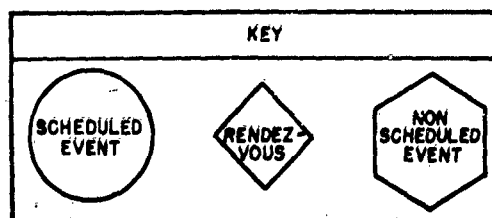




AL METABOLIC  
-BTU/HOUR/MAN

| BLE | LATENT | TOTAL |
|-----|--------|-------|
| 0   | 180    | 400   |
| 0   | 220    | 500   |
| 0   | 600    | 900   |
|     | 1000   | 1000  |
| 0   | 1250   | 1500  |

| LOAD TYPE | NUMBER OF MEN AT: |      |        |     |           |
|-----------|-------------------|------|--------|-----|-----------|
|           | REST              | DUTY | STRESS | HOT | EMERGENCY |
| I         | 2                 | 1    |        |     |           |
| II        | 1                 | 2    |        |     |           |
| III       |                   | 3    |        |     |           |
| IV        |                   | 2    | 1      |     |           |
| V         |                   | 2    |        | 1   |           |
| VI        |                   |      | 3      |     |           |
| VII       |                   |      | 1      | 2   |           |
| VIII      |                   |      |        | 3   |           |
| IX        |                   |      | 1      |     | 2         |
| X         |                   |      |        |     | 3         |



sequence. After landing, probably, one or more of the crew would leave the vehicle for exploration. Subsequently, take-off must be made from the moon to a lunar orbit, a transit made to an orbit above the earth, and then the final re-entry, landing, and recovery operations accomplished.

5. At almost any orbit or stationary location, as on the moon, rendezvous with other vehicles, manned or unmanned, may well form part of the flight program. If such a rendezvous is made, there will probably be an exchange of supplies, equipment, energy, or other items which can be allowed for on the chart.

Although this chart resembles the PERT chart used for program evaluation, it is not necessary to make as much detailed use of the chart as is done in that program. Rather, the chart is presented to form the basis of a clear definition of the entire problem, so that no likely event will be overlooked in studying the requirements for the atmospheric control system.

In determining the detailed atmospheric requirements for specific pieces of equipment in the vehicle, especially an unmanned vehicle, the most important considerations usually are the presence of an atmosphere and the handling of the load of the equipment. It should be remembered that any energy going into a piece of equipment used on a space vehicle will eventually appear in the form of heat; that is, any electrical equipment drawing a current will have a heat output exactly equal to that of the electric current operating the equipment. In case the equipment is hydraulic or pneumatic, then a similar situation applies. In the case of heat loads, the temperature level, the type of coolant, the coolant flow rate, and the coolant pumping method all are likely to influence the actual requirements. In some cases, of course, the coolant may be a liquid. When the coolant is a gas, then it is probable that its control system will be similar to that of the atmospheric control system for the men.

In studying the loads, it is considered easier to assume that the loads introduced by the environmental control systems themselves are part of the systems and affect system operation directly, rather than considering them as external loads on the systems. By this is meant that, if the atmospheric temperature rises in passing through a compressor, it should be represented by showing a temperature change in the circuit itself, rather than reducing it to a certain number of Btu's of load.

The type of equipment will have a large effect on the type of atmospheric control necessary. Photographic equipment, for example, has temperature and humidity requirements similar to those of a man. Electronic equipment generally is relatively sensitive to temperature, particularly affecting high reliability and long life of the equipment. In some cases, a difference of a few degrees in temperature may mean a change of 50 per cent in the reliability of the equipment. In this connection also, it may be desirable to arrange the system so that the air passes

successively over higher temperature limit equipment and makes the most efficient use of the available cooling.

In a manned space vehicle, it is necessary to determine the relative metabolic loads on the atmospheric control system at each of the various levels of activity which will result from each of the events contained in the flight plan. A chart on Figure 1 indicates typical metabolic loads in Btu per hr per man. It has seemed desirable to divide the crew's work into five different levels of activity: rest, duty, stress, "heat," and emergency. For the rest activity, the total load is low, representing a basal metabolic rate of slightly less than 1. For normal duty, the load is higher but by no means stressful. Under some conditions, it will be necessary to go to a stress load nearly twice as high as the duty load. All of these loads show a variation in sensible and latent heat.

When a man is in a pressure suit and working in the sunlight, during and immediately following re-entry, and possibly at other times, the load can best be expressed as "hot," a condition in which the inlet air through the suit is at a temperature high enough that transfer of heat from the body must take place as latent heat, and none of it can take place as sensible heat. In other words, in such a condition, the air does not change dry bulb temperature, but cools entirely by picking up a large amount of moisture. This effect is, of course, much more prominent at the low pressures which will probably be used in any pressurized suit.

The highest loads, or the emergency conditions, will occur when some unplanned event takes place; in this case, the latent load goes very high, leading to a total perhaps three times as high as that of normal duty. It should be noted that tolerability to the three highest load levels is limited, both at a specific time and also limited in their total extent within a particular mission. Although the probability of these intervals' becoming extended does not seem high, the capability of handling them for reasonable periods of time must be part of the atmospheric control system.

Figure 1 also contains a chart showing the probable load types identified by Roman numerals, ranging from I to X. The lightest load likely to occur for a three-man vehicle would be Type I: two men at rest and one man on duty. The highest load would be Type X: three men under emergency conditions. The probable normal operating load during orbits and transits would be Type II: one man at rest and two men on duty. The other types represent various estimates of the loads involved in landings, takeoffs, rendezvous, and various operations outside the vehicle or on the moon. Each type is indicated by a Roman numeral at the appropriate location on the main chart of Figure 1.

In actually planning the operation of the atmospheric control system, the psychrometric chart is a very useful tool. It is necessary, of course, to have a chart made for the particular conditions which will exist within the vehicle. Such a chart is shown in Figure 2, which has been drawn for a total pressure of 7.5 psia with 50-volume per cent oxygen and

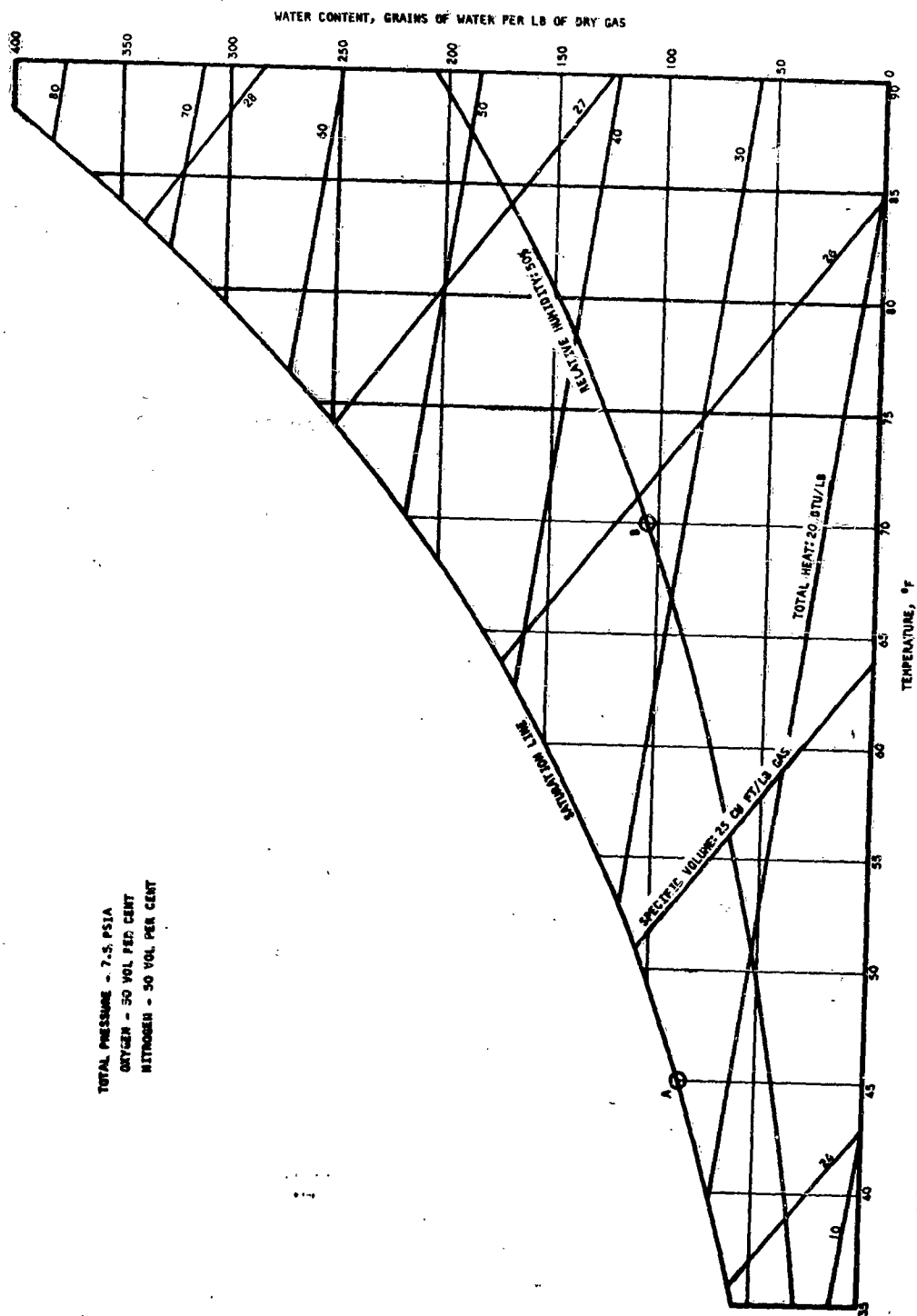
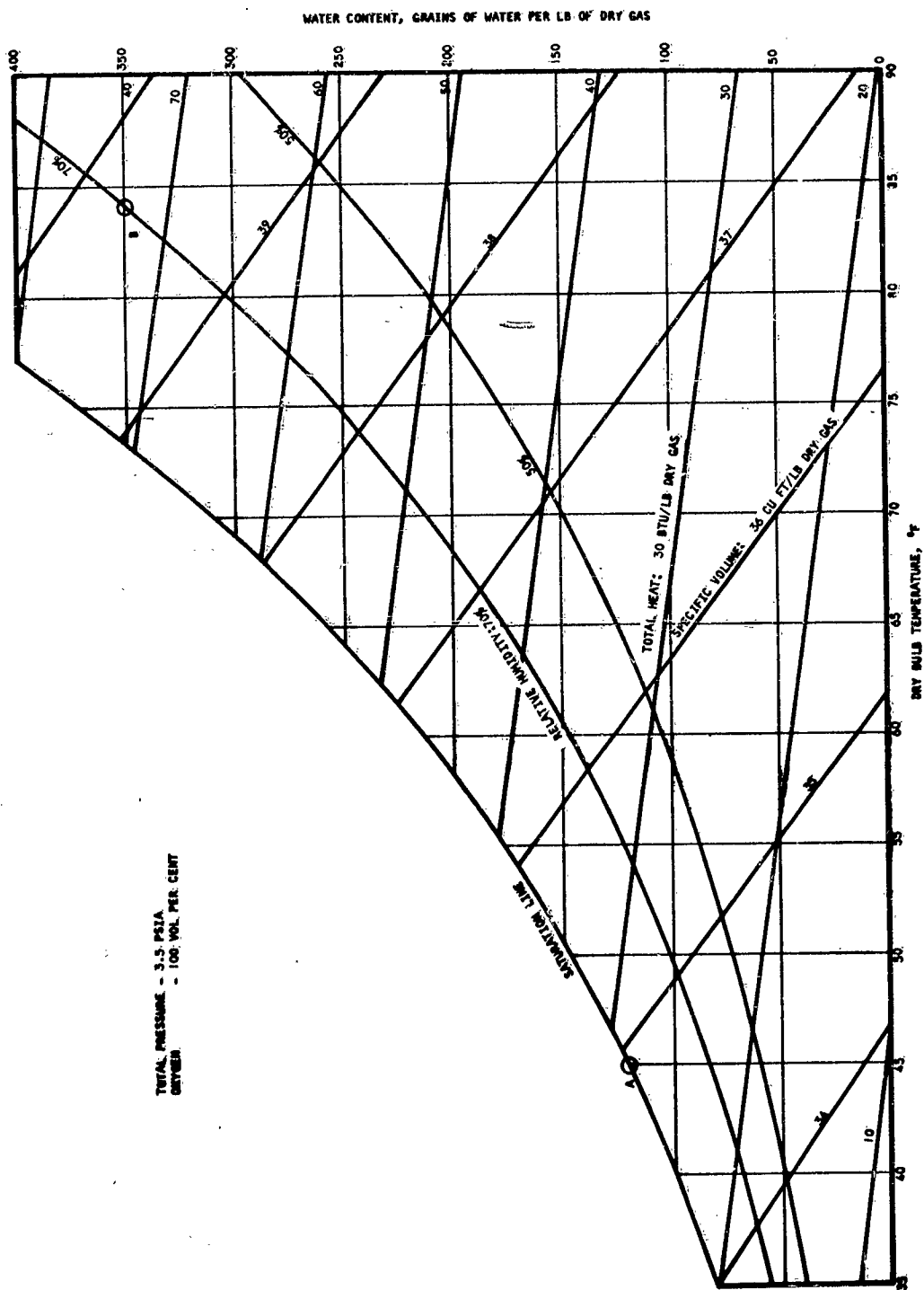


Figure 2. Psychrometric Chart - 7.5 psia, 50 Per Cent Oxygen, 50 Per Cent Nitrogen

50-volume per cent nitrogen. Other reports show it desirable to maintain temperature close to 70°F and relative humidity at about 50 per cent. Experience shows it is better to compute the results relative to the latent heat load and then determine their applicability to the sensible heat load. In Condition II of Figure 1, the normal orbit or transit condition, the total heat loads will be a sensible heat load of 780 Btu per hr and a latent heat load of 620 Btu per hr, or 10.3 Btu per min. This is equivalent to 69 gr of water per min. At the inlet to the equipment, the limitation is the dew point temperature which can be readily obtained, as in an evaporating water-to-air heat exchanger. This may be conservatively estimated as 45°F, since the evaporating temperature is controlled to 35°F to prevent freezing. A dew point of 45°F (Point A on Figure 2) corresponds to 84 grains of water per lb of dry air. The water content at the operating point (Point B of Figure 2) is 105 grains per lb. Thus, there is a possible pickup, in passing through the capsule, of 21 grains per lb of dry air. This would give a dry air flow requirement of 69 divided by 21, or 3.29 lb of airflow per min.

Regarding the sensible heat load, if the air enters at 45°F and the sensible load is 780 Btu per hr, or 13 Btu per min, the dry bulb temperature of the air will rise some 17°F. If the air enters at 45°F dry bulb, the crew would raise the temperature, due to sensible heat, only to 62°F, rather than the 70°F originally estimated. However, other heat sources likely would contribute further to the increase in dry bulb temperature of the capsule air. If not, it becomes a question of studying the air conditioning system to determine whether there is some other, more satisfactory arrangement of flow and dew point or to incorporate within the air conditioning system a dry reheating cycle which would increase the dry bulb temperature of the air but not increase the humidity, before the air is returned to the capsule for use.

The psychrometric chart in Figure 3, drawn for a pure oxygen atmosphere at 5 psia, relates to men in the suits at lower pressure. Experiments with pressure suits tend to indicate that for moderate work loads the air coming from the man's suit will be on the order of 85°F, regardless of the exact inlet temperature. In other words, the human metabolism changes somewhat to allow for various amounts of pickup. Also, in actual practice, it is found that 10 cfm per suit at the operating pressure is about the maximum which can readily be accommodated. At 5 psi oxygen, this is a flow of about 0.29 lb per min per suit. A latent heat load of 600 Btu per hr, or 10 Btu per min, will require the evaporation of 65 grains of water per min. Since the flow is 0.29 lb per min, it will require 226 grains per lb change in moisture content of the oxygen to provide the necessary evaporation for cooling. Oxygen entering the suit at 45°F saturated (Point A), or 121 grains per lb, would leave the suit at 347 grains per lb, which corresponds to a temperature of about 84°F and 70 per cent relative humidity (Point B). This corresponds to a sensible heat pickup of about 175 Btu per hr. If this is insufficient, the metabolic processes will change slightly to provide a higher latent heat load. There is still considerable leeway for this, since the humidity at 84°F and saturation is 516 grains per lb.



TOTAL PRESSURE - 3.5 PSIA  
 DRYER - 100 VOL PER CENT

Figure 3. Psychrometric Chart - 3.5 psia, 100 Per Cent Oxygen

Although a less comfortable condition, it certainly would be acceptable in an emergency. Once the cycle has been worked out on a psychrometric chart, it may be advisable to check it by hand, since even small changes in total pressure in the circuit itself may make some little difference in the psychrometric conditions for these relatively low total pressures.

#### SYSTEM PARAMETERS

Significant criteria to be considered in evaluation of an atmospheric control system include:

- Weight
- Power requirement
- Volume
- Reliability
- Development status
- Interfaces with other systems

For any given application, it will be necessary to consider all of these criteria, since no single one can be assumed to be controlling in the selection of the optimum system. Also, the criteria are not independent of one another.

##### Weight

Weight includes the weights of fixed equipment, ducts and connecting fixtures, any supplies, such as activated charcoal, necessary to the operation of the system, and related control mechanisms and instrumentation. In addition, the power requirement is often considered in terms of the weight required for the power sources, of whatever kind.

##### Power Requirements

Power requirements include mechanical or pneumatic power for circulation of the atmosphere, heat power for use in the catalytic burner, mechanical or pneumatic power for the water separator, and pneumatic or electrical power for operation of control elements and instrumentation. Mechanical power may come from electric motors, and heat power may come from electric resistance elements; that is, the entire power supply may be electrical. Pneumatic power is customary in capsule pressure controls and pressure relief valves.

The preferred type of power will depend upon the design of the equipment and on the relative availability of the different types. For continuously rotating devices, such as compressors, electrical power may be better than pneumatic, while for periodically actuated devices, such as water separator sponges or control valves, pneumatic power may have distinct advantages.

Both the maximum rate at which power will be used and the average rate must be considered. The penalty imposed by any power source will

be a combination of the influences of the maximum rate and the average rate times the use.

Two philosophies are used in computing power. The first, which is machine-oriented, is to set up the flow circuit and then compute the total gross power required by the components to maintain operation of the circuit. In practice, one assumes a flow rate, composition, density, and temperature. The pressure drops of the individual equipment and ducts are computed and added to give the total pressure drop in the circuit. A compressor capable of providing a pressure rise equal to the computed pressure drop is then chosen. The power required by the compressor driving means (an electric motor) is then said to be the power required to maintain the desired fluid circulation in the circuit.

The second method, which is function-oriented, determines with respect to each equipment and duct section, the power equivalent, at 100 per cent efficiency, of the pressure drop in the device. The resulting total power equivalent is then modified to reflect attainable power conversion efficiencies, and the required total power is found. This function-oriented method has two drawbacks when compared with the machine-oriented method. The resulting calculations are more complex, without being more accurate. Also, unless great care is used, violation of the principles of continuity and conservation of energy may occur, resulting in meaningless values.

#### Volume

The volume of an atmospheric control system is relatively difficult to determine at an early stage of the program. This is due to the fact that a substantial percentage of the total volume is necessarily devoted to ducts and fitting, the actual size of which is very dependent upon the layout or arrangement of components. The total volume includes:

- a. Core volume or volume of heat exchanger element, or volume of reacting substance, such as lithium hydroxide
- b. Volume of the supports for the core
- c. Volume of the pans and manifolds
- d. Volume of associated or integral ducts
- e. Volume of auxiliary items, spare parts, tools, and replacement chemicals such as lithium hydroxide
- f. Volume, space clearance necessary for access to equipment and for repairs, on the ground or in flight

It is essential that a layout, or better a mock-up, be used to arrange circuit components for minimum volume.



## Reliability

Reliability is an important criterion in evaluating atmospheric control systems. Although, in certain cases, there is little information on which to base component failure rates, the use of good engineering judgment will tend to give reasonably valid system reliabilities, especially when these results are to be used primarily in a relative, rather than absolute, comparison.

Reliability studies should be made with full cognizance of the critical nature of specific malfunctions and the results of failures of parts and systems. Advantage should be taken, and reflected in the reliability calculations, of the possibilities of redundancy and of replacement and repair of components when a human operator is present.

## Development Status

The development status of each component and subsystem should be determined to provide an evaluation as to the probability that the total system can be developed within the known limitations of time and budget. For example, the design of some components, such as heat exchangers and ducts, is so well advanced that they may be assumed to perform as required, with little or no development. On the other hand, a regenerative chemical system for space application will require extensive development, together with some risk that it will not be possible to reach the goals at the desired time. A closely related problem is the adaptability of the system to different mission profiles, a requirement which is becoming essential.

## Interfaces with Other Systems

There are numerous interfaces between the atmospheric control system and the other vehicle systems. All of these must be taken into consideration in arriving at conclusions relative to the advantages and disadvantages of competing systems. (Interfaces also may be considered as placing restraints or requirements on the system; however, the emphasis is different.) Typical interfaces include:

- a. Thermal loads to and from other vehicle systems, including vehicle structure
- b. Power requirements, including quality, type, amount, and variation of rate
- c. Supplies of oxygen, nitrogen, and any other gases required. This is especially important when the gases are stored remotely or depend upon another process, such as fuel cells. Each gas should be separately considered. Also, the energy connected with the storage and delivery of the gas must be taken into account.

- d. Metabolic inputs from occupants, carbon dioxide, water vapor, odors and the like
- e. Water from water separator, and water to evaporators in the atmosphere control circuit
- f. Chemical process supplies, such as lithium hydroxide, molecular sieves, activated charcoal, and catalysts
- g. Vibration and shock loads, including those generated within the system and those received from outside
- h. Noise generated by operation of the system
- i. Control linkages for operation of the atmospheric control system itself
- j. Space and relative location requirements within the vehicle. The resolution of this item usually requires the use of mock-ups and trade-off studies with other spacecraft systems.
- k. The ground checkout system
- l. Onboard display instrumentation
- m. Instrumentation providing information to be telemetered
- n. Provision for supplying an atmosphere for use in a backpack to provide atmospheric control for a pressure suit used for extravehicular operation
- o. Provision for use of an airlock to enable occupants in pressure suits to leave and re-enter the space vehicle
- p. Detection of malfunctions within the system and the transmission of the information to the astronauts
- q. Interaction with operator; manual control required; extent and scheduling of operator's time; special skills required, if any
- r. Mechanical support of system components on vehicle load-bearing points

#### SYSTEM EVALUATION CRITERIA

In the preceding discussions, the numerous parameters that must be considered to realistically assess the relative merits of competing systems are reviewed. From these parameters, general evaluation criteria must be derived that will make possible system comparison on an integrated basis, taking into account major system variables as well as the

interfaces between the system under consideration and other vehicle systems.

The most important system parameters for space vehicle installation are the weight, volume, power requirement, heat rejection load, and system material balance. These have all been discussed above. As pointed out, the volume of a system is very difficult to determine in a study of this type; it depends to a great extent on the designer's ingenuity; for this reason, it will be ignored in this study.

In the analyses conducted in this report, competing systems and subsystems are compared on an equivalent weight basis. The equivalent weight is made up of several terms and is defined algebraically by the equation

$$W_E = W_H + W_P + W_Q + W_{MAT} \quad (1)$$

The terms of this equation are in turn defined and discussed below:

- a.  $W_H$  is the system hardware weight comprising heat exchangers, canisters, valves, ducts, etc. This weight is the actual system weight, including all its components and associated hardware such as sensors and system flow controllers.
- b.  $W_P$  is the weight of the vehicle power source chargeable to the system under consideration. It can be expressed as the product of the system power requirement by the vehicle power penalty. The system power requirement includes the power expended to circulate the process air through the circuit, the power necessary for system control, and the power required for heating or any other process used in the system.

The vehicle power penalty depends mainly on the size of the vehicle power installation and on the mission duration. Short mission duration vehicles have relatively high specific weight power sources, on the order of 400 lb per kilowatt of installed power. On the other hand, for long mission durations, the power penalty is lower, in the range of 200 to 300 lb per kilowatt.

- c.  $W_Q$  is the weight of the vehicle cooling system that can be charged to the particular system or subsystem considered.  $W_Q$  is the product of the vehicle cooling system specific weight, in lb per watt, by the system heat rejection load. However, this penalty depends not only on the size of the heat load but also on the temperature level at which the heat load is rejected to the cooling system. This temperature level must be taken into account when determining the term  $W_Q$ .

- d.  $W_{MAT}$  depends on the system material balance. As an example, if a non-regenerable absorbent is used for the removal of carbon dioxide from the cabin atmosphere, the weight of the absorbent must be charged against the system. Also, if water is used in a system, either absorbed or evacuated overboard, then the system, in certain cases, must be charged for this amount of water expended. On the other hand, if a system produces water or oxygen, it can, depending on the application, be credited for the production of these materials.

All the possible interface conditions cannot be examined in a general study of this type; however, subsystem comparisons can be conducted along the lines defined here, which yield realistic results. Vehicle parameters, such as power penalty used in the following analyses, were determined mainly on the basis of mission duration. Where the interface parameters play an important role in the choice of competing systems, data are presented for several values of the penalties involved.

#### SUBSYSTEM CONSIDERATIONS

In Sections IV through IX, space vehicle atmospheric control subsystems are analyzed, compared, and evaluated. A subsystem is defined as an assembly of components performing one single function. From this definition, several subsystems can be recognized as integral parts of a complete atmospheric control system:

- Gas Supply Subsystem
- Humidity Control Subsystem
- Carbon Dioxide Management Subsystem
- Trace Contaminant Removal Subsystem
- Cabin Leakage Detection Subsystem
- Oxygen Recovery Subsystem

All these subsystems incorporate a number of components which, when integrated, can be analyzed as a unit in terms of parameters related to the cabin atmosphere, to the vehicle itself, or to the vehicle mission. These subsystems are not all affected by the same parameters, since their particular function differs greatly. However, most of the systems are affected by design variables, such as mission duration, number of crew members in the vehicle, cabin pressure, etc.

The analyses presented in this report are based on data assumptions relative to the cabin atmospheric composition and the crew metabolic behavior which can be found in the literature. Reference is made here to two reports prepared as part of the Thermal and Atmospheric Control of Space Vehicle Study: ASD TR61-162 and ASD TR61-240 (References 1 and 3), from which design data assumptions were obtained. Table 1 lists the main system and subsystem design variables and the particular values assigned to some of them in this study.

**TABLE 1**  
**SYSTEM AND SUBSYSTEM DESIGN PARAMETERS**  
**AND DATA ASSUMPTIONS**

| Parameter   | Value  |
|---|--|
| Cabin temperature                                     | 70°F   |
| Cabin total pressure                                  | 5 to 14.7 psia                               |
| Leakage rate from the cabin                           | Variable (0 to 20 lb/day)                    |
| Oxygen partial pressure in the cabin                  | (See Figure 4a)                              |
| Carbon dioxide partial pressure in the cabin          | 3.8 to 7.6 mm Hg                             |
| Relative humidity                                     | Within the comfort zone defined by Figure 4b |
| Metabolic oxygen consumption                          | 2.0 lb/man-day                               |
| Carbon dioxide production by respiration              | 2.25 lb/man-day                              |
| Water vapor generated by respiration and perspiration | 2.2 lb/man-day                               |

## PHYSIOLOGICAL PERFORMANCE CHARTS

Figure 4a is a physiological performance chart presenting the physiological effects of the relation between the percentage of oxygen in the atmosphere of an airplane or space vehicle and the total pressure of that atmosphere. It is based on continuous exposure or occupancy for one week or more.

Atmospheric air contains 21 per cent oxygen by volume. At sea level, this leads to a blood saturation of 95 per cent. To maintain the same degree of oxygen in the blood at lower pressures, the percentage of oxygen in the atmosphere must increase as shown by the sea level equivalent curve. The Unimpaired Performance Zone indicates the range of variations that can be tolerated without performance decrement.

The maximum tolerance for long periods has not been investigated extensively but is believed to be about as shown. At points to the left of the Unimpaired Performance Zone, acclimatization is required. Acclimatization is considered to be continuous exposure to conditions of successively lower pressure, with no intermediate return to higher pressure. For example, if a person is to remain for one week at 25,000 ft with 21 per cent oxygen, he will require an acclimatization period of four to six weeks.

The minimum tolerable total pressure is based upon the effective partial pressure of oxygen, disregarding aero-embolism which may occur below 300 mm Hg total pressure in the absence of adequate denitrogenation. The aero-embolism limitation is shown by the interrupted horizontal line.

Figure 4b is a physiological performance chart presenting the physiological effects of the relation between the dry bulb temperature and the humidity of the atmosphere of a space vehicle or airplane. The humidity is expressed in terms of the dew point temperature, or vapor pressure, thus providing a chart which is valid for any of the pressures shown in the oxygen-pressure graph.

For a shirt-sleeve atmosphere, the conditions should be within the Unimpaired Performance Zone. The limits of this zone are (1) a dew point of 35°F, below which excessive drying of the respiratory passages takes place, (2) a relative humidity of about 70 per cent, above which skin and clothes are uncomfortable, (3) a dry bulb temperature of 65°F, below which extra clothing is required, and (4) a dry bulb temperature of 80 to 85°F depending upon dew point.

At points to the right of the Unimpaired Performance Zone, appreciable perspiration will occur as the body seeks to maintain a heat balance. At the normal limit, the perspiration rate will be of the order of one pint per hour; at the extreme limit, to which many individuals are unable to adjust, the perspiration rate will reach one quart per hour.

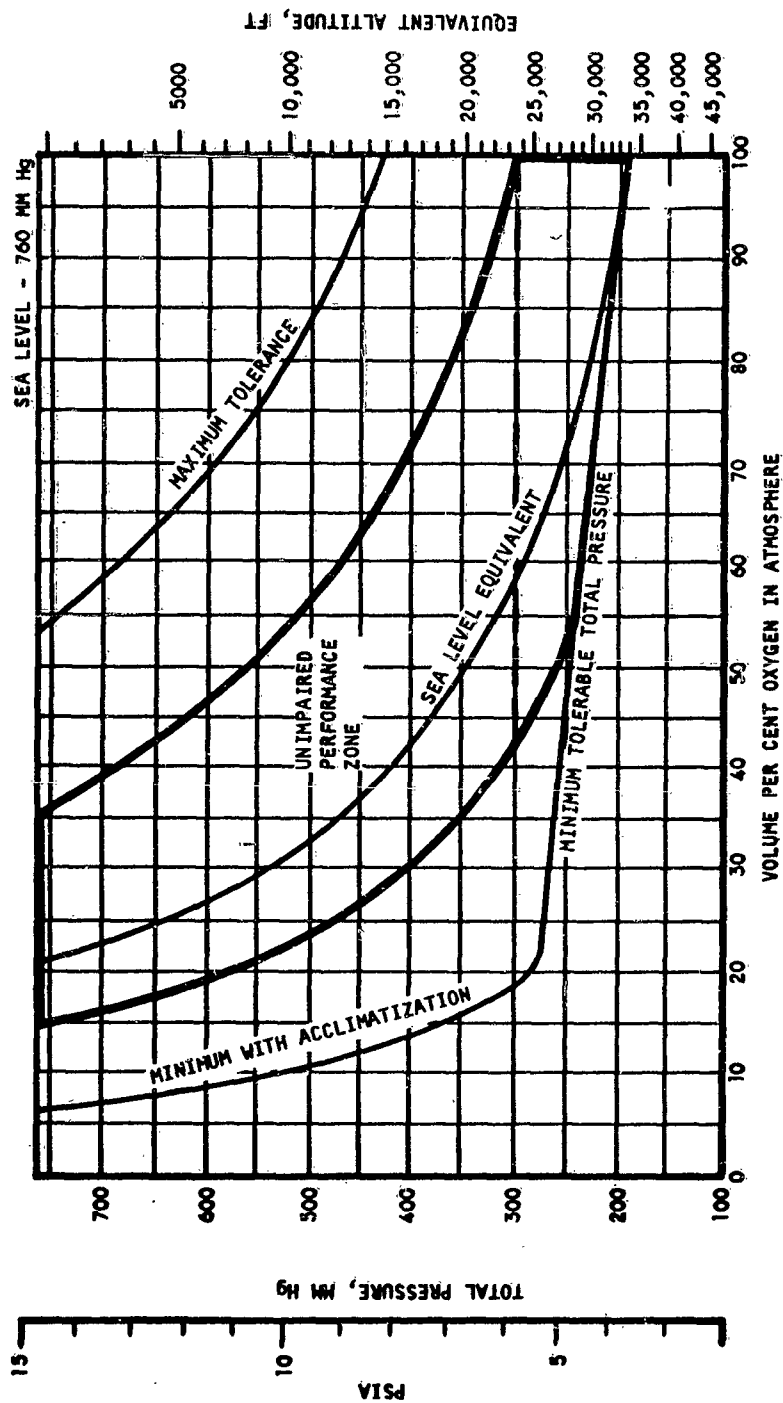


Figure 4a. Physiological Performance Chart - Oxygen-Pressure Effects

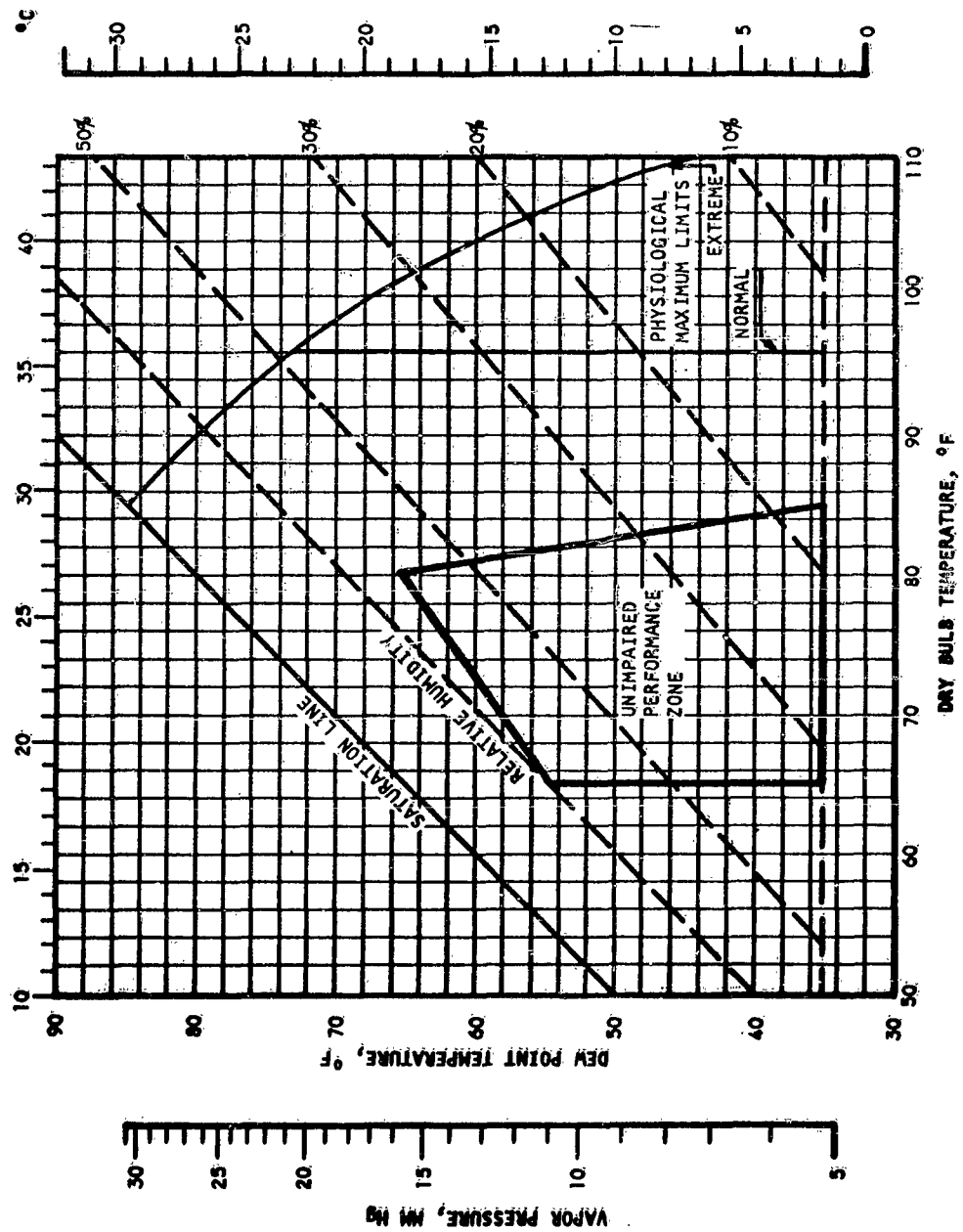


Figure 4b. Physiological Performance Chart - Temperature-Humidity Effects



To use the charts to establish long-term, efficient, shirt-sleeve conditions, an atmosphere is selected whose characteristics lie within the Unimpaired Performance Zones of both charts. The carbon dioxide partial pressure should not exceed 4 mm Hg, the odor should be unobjectionable, and the air movement should be 10 to 50 ft per minute.

The Lovelace Foundation was consulted in the preparation of Figures 4a and 4b.

#### SUBSYSTEM COMPARISON

Subsystem comparison is made on an equivalent weight basis as defined previously. The field of application of each subsystem is defined in terms of mission duration and cabin parameters wherever possible. This simplifies considerably the selection of a particular system for a given application. In the system discussions and comparison, due consideration is given to crew safety and system reliability; although the full influence of these factors on system selection is difficult to assess, they certainly play an important role in system evaluation.

## SECTION IV

### BREATHING AND PRESSURIZING GAS SUPPLIES

#### INTRODUCTION AND SUMMARY

In this section are reviewed various means of supplying the cabin with the oxygen and nitrogen necessary for respiration and cabin pressurization. Storage techniques considered are:

- High-Pressure Gas Storage
- Supercritical Storage of Cryogenic Fluids
- Subcritical Storage of Cryogenic Fluids
- Chemical Generation of Atmospheric gases, including Water Electrolysis

These storage methods are analyzed and compared on a subsystem basis. Subsystem evaluation is performed with the parameters discussed in Section III, e.g., weight and size of the subsystem, reliability, safety, and control problems associated with use in a zero-gravity environment. For mission durations in excess of a few days, supercritical storage of atmospheric constituents appears the most attractive. High-pressure gas storage technique finds its application in emergency systems and in bladder expulsion systems. For extended missions, water electrolysis presently seems the only means of hydrogen production applicable to the reduction of carbon dioxide.

#### HIGH-PRESSURE GAS STORAGE

##### General

Storage of atmospheric constituents as a high-pressure gas offers several important advantages over other storage techniques. First, it is the most reliable storage method available at the present time. The state of the art in the design of high-pressure gas vessels is advanced, and vessels satisfying space vehicle requirements have been thoroughly developed and tested for use on the Mercury capsule. Second, high-pressure gas storage methods offer the advantage of being considerably less sensitive to standby time and to ambient temperature than are cryogenic storage methods. Third, gas mixtures can be stored and delivered from high-pressure bottles at constant composition. Finally, this storage method is insensitive to gravity environment.

Several studies of high-pressure gas vessels have been conducted. The most recent and comprehensive treatment of the subject is given in ASD TR 61-162, Part II, (Reference 1), where due consideration is given to gas compressibility factor. In addition, the effect on the maximum vessel charge of the temperature and pressure tolerances at fill and at the end of vessel operation are considered.

### Storage Vessel Weight and Volume

Following the analytical methods presented in ASD TR 61-162, the weight and volume of spherical oxygen and nitrogen vessels were calculated to determine the optimum storage pressure. Fatigue failure was used as the vessel design criterion, and the working strength of the materials, namely C120-AV for nitrogen storage and SAE 4340 for oxygen, was taken as 60 per cent of the material yield strength. The weight and volume penalties thus calculated are plotted in Figures 5 and 6 as a function of pressure.

Here it is assumed that the vessel volume penalty has the same importance as the weight penalty. Thus, the optimum vessel is selected on a minimum ( $W \cdot V$ ) product, which under these conditions defines the vessel optimization criterion. This parameter is also plotted in Figures 5 and 6. It should be noted that the minimum vessel weight occurs at a much lower pressure than the minimum vessel volume, and consequently than the minimum optimization criterion.

In Table 2 are listed the optimum values of the weight and volume penalties for oxygen and nitrogen vessels. These values correspond to a minimum optimization criterion.

TABLE 2

#### HIGH-PRESSURE GAS STORAGE OPTIMUM DESIGN

| Parameter  | Oxygen | Nitrogen |
|--|--------|----------|
| Optimum pressure, psia                                       | 10,500 | 9,500    |
| Weight penalty, $W$ , lb per lb of useful fluid              | 3.46   | 3.66     |
| Volume penalty, $V$ , ft <sup>3</sup> per lb of useful fluid | 0.0296 | 0.0446   |
| Optimization criterion                                       | 0.1025 | 0.163    |

It should be noted here that the weights plotted in Figures 5 and 6 do not include the weight of the lines, brackets, or valves; an allowance should be made for these accessories. The valve weight depends only on the number of vessels and on the number of valves installed on each vessel for redundancy and for installation requirements. Mounting bracket design depends primarily on the size of the vessel, on the number of vessels, and on the installation. These weights, in general, are small; an allowance should be made, however, on the total vessel weight for accessory weight.

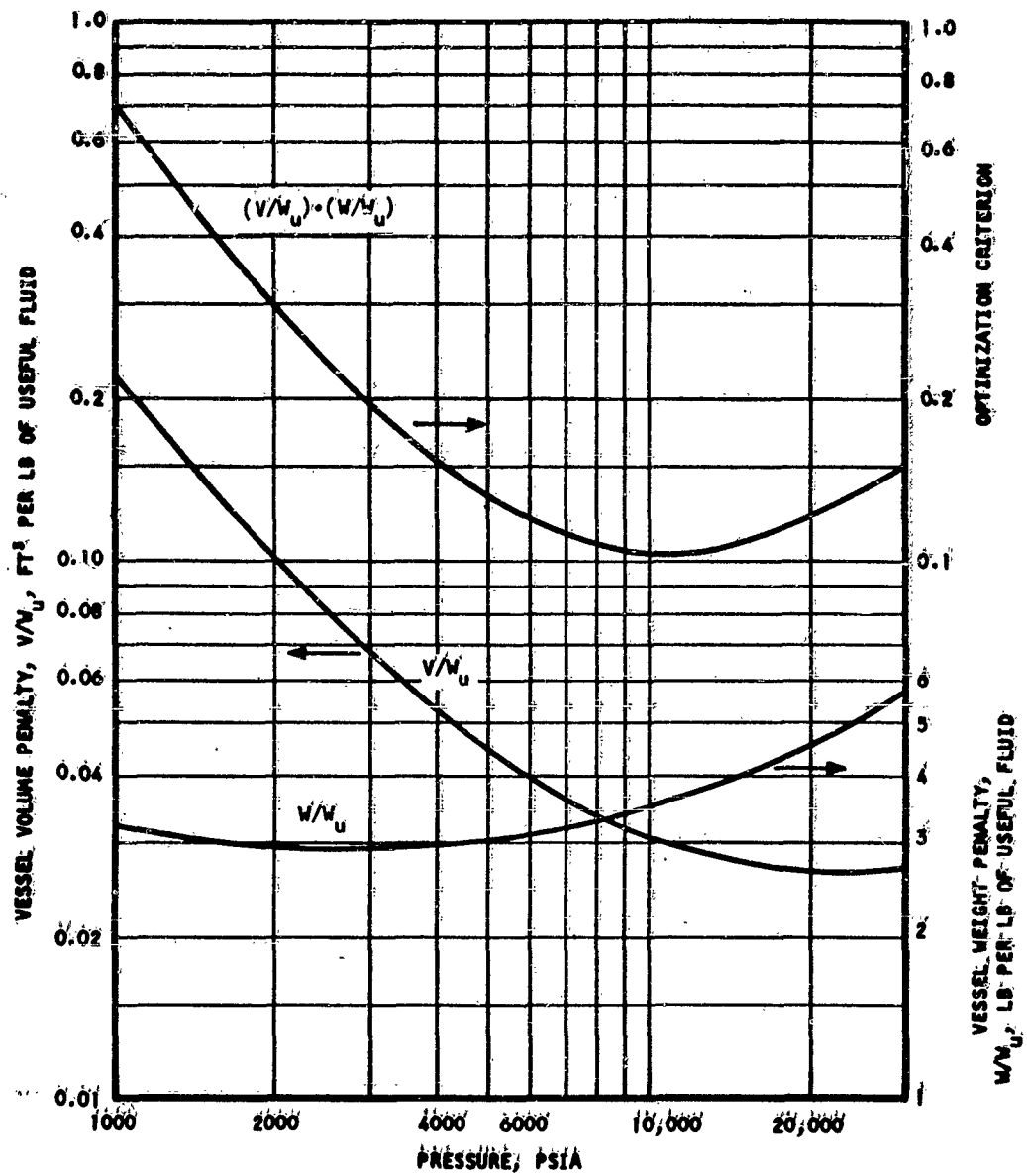


Figure 5. Oxygen High-Pressure Gas Storage Vessel Characteristics

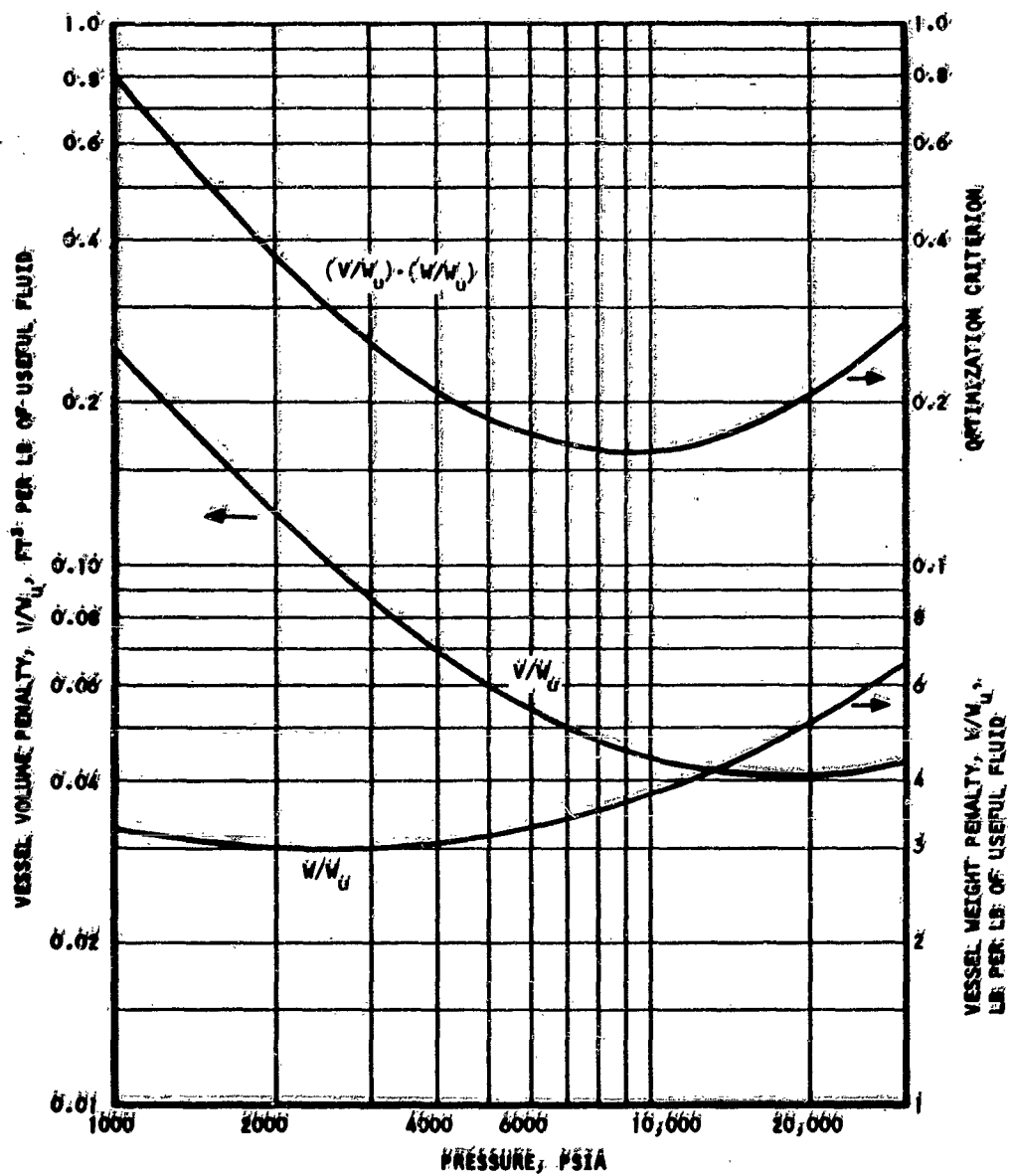


Figure 8. Nitrogen High-Pressure Gas Storage Vessel Characteristics

## SUPERCRITICAL STORAGE OF CRYOGENIC FLUIDS

### General

Storage of cryogenic fluids at supercritical pressures offers the same general advantages as other cryogenic storage techniques, namely, (1) high fluid density at moderate pressure and (2) low-temperature storage which provides a potential heat sink. The first advantage leads to low storage vessel volume and weight. The second one makes this storage method very attractive for space vehicle system integration. In addition, supercritical storage methods do not suffer from the phase separation problems associated with subcritical storage of cryogenic fluids. Since the fluid is stored and delivered as a single phase, it greatly simplifies the metering and quantity measurement of the stored fluid. Other advantages of supercritical storage over its subcritical counterpart are its increased standby potential and its reduced sensitivity to heat leaks because of the higher stored fluid temperature. A thermodynamic treatment of supercritical storage is given in Reference 1.

Supercritical storage methods are divided into two broad types, depending on the vessel pressurization method.

#### 1. Thermally Pressurized Vessels

Pressurization under delivery conditions is achieved by addition of heat to the mass of the stored fluid. The total amount of heat input into the fluid is made up of the parasitic heat leak through the lines, insulation, and pressure shell supports, plus the heat introduced for the purpose of vessel pressurization under delivery conditions. This additional heat input or flow control heat input can be derived from several sources discussed later in this section.

#### 2. Positive Expulsion Vessels

In this case, the fluid is contained in a bladder within the pressure shell. The fluid is pressurized by introducing a high-pressure gas between the shell and bladder. The pressurizing gas, for reasons of weight, safety, and thermodynamic behavior, is usually helium. Such a system is depicted in Figure 7.

Previous studies (Reference 2) have shown that on a weight basis alone, these two types of supercritical storage are competitive, with the thermally pressurized vessel being slightly heavier. However, thermally pressurized storage vessels are simpler in design and operation. The use of a high-pressure gas bottle, with its reduction and safety valves, tends to reduce, somewhat, the reliability of the positive expulsion system. A reliability problem arises from the use of a bladder, and vessel fabrication and insulation space evacuation is further complicated by the presence of the bladder inside the pressure shell. In addition, accurate fluid quantity measurement within the vessel is complicated by the presence of the bladder; an estimate of the fluid

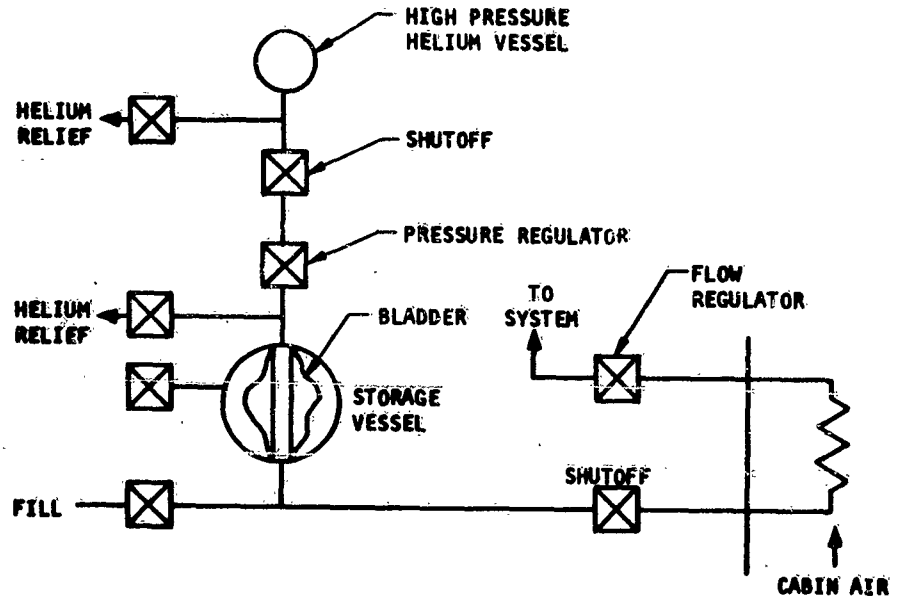


Figure 7. Cryogenic Storage With Positive Expulsion

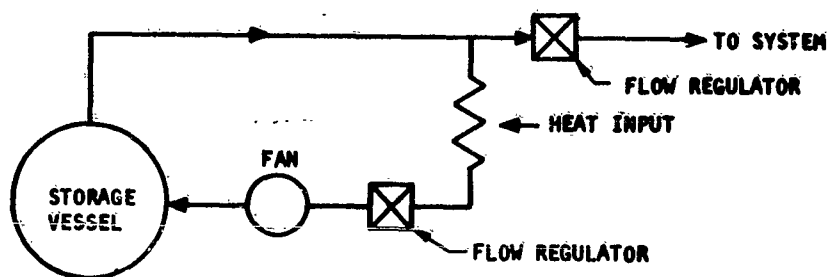


Figure 8. Thermally Pressurized Supercritical Storage - Fluid Recirculation by Means of a Fan

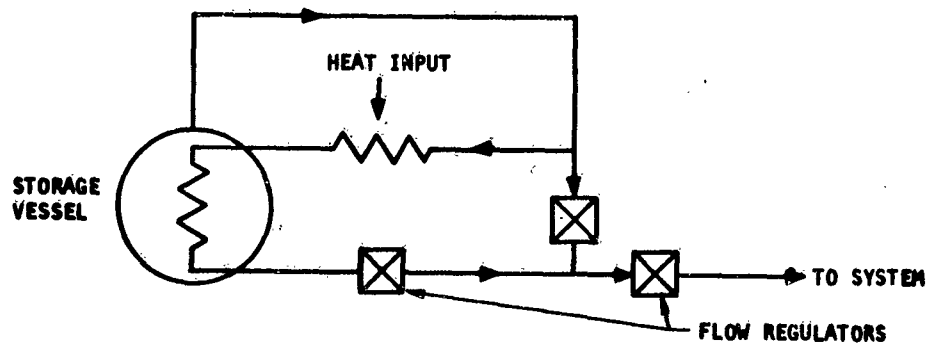


Figure 9. Thermally Pressurized Supercritical Storage - Fluid Circulation Through an Internal Heat Exchanger

left in the bladder can be made from the pressure in the gas bottle; this method, however, does not take venting into account and lacks accuracy.

For these reasons, thermally pressurized vessels are, at present, technologically more advanced and show more promise.

#### Methods of Thermal Pressurization

Several alternate methods of controlling the heat input into a thermally pressurized storage vessel are possible; the more interesting are listed and discussed below.

- a. Electrical power can be supplied to the fluid through heating elements located inside the pressure shell. This method is somewhat wasteful, since electrical power aboard a space vehicle is, in general, at a premium. Also, it does not use advantageously the sizeable heat sink potential of the stored fluid. Other heat sources are usually preferred for normal vessel operation and electrical power heat supply is attractive as an emergency heat source.
- b. A preferred method of vessel thermal pressurization makes use of waste heat from the vehicle atmosphere or from other vehicle systems. In order to simplify the vessel control system, the fluid itself is used to carry the vehicle waste heat into the pressure shell. Two different types of control systems are shown schematically in Figures 8 and 9. In the system depicted in Figure 8, a portion of the delivery flow from the vessel is heated externally with cabin air or other vehicle waste heat and returned to the storage space by means of the fan. The heat is supplied to the stored fluid by mixing of the hot recirculated fluid to the mass of the colder stored fluid. In the system shown in Figure 9, the pressurization heat requirements are satisfied by directing a portion of the delivery flow through two heat exchangers in series: in the first one, waste heat from the vehicle is dumped into the circulated fluid; in the second one, this heat is transferred from the circulated fluid to the stored fluid. In this system, fluid circulation is insured by the pressure differential existing between the vessel and the system.

Pressurization by means of an internal heat exchanger offers several important advantages over fluid recirculation by means of a fan. These advantages are listed below.

- a. Reliability - No fan is necessary to circulate the pressurizing flow through the internal heat exchanger. This leads to a more reliable system.
- b. Power Requirements - No power is required by this system other than that necessary for system valve control.



c. Safety - The system is inherently safer as leakage should present no problem. Unless a canned fan-motor were used in the recirculation system, leakage of gases would occur with its associated hazards.

d. Simplicity - The fan of the recirculation system has to handle a wide range of flow at high pressure; in addition, the temperature of the fluid recirculated will increase considerably during tank operation. Fan reliability, under these operating conditions, is a serious problem. Since the fan-controlled pressurization system has only dubious advantages over the simple internal heat exchanger system, and since the fan itself introduces reliability and safety problems, the simpler heat exchanger pressurization method is preferred for supercritical storage vessel control.

#### Storage Vessel Weight and Volume

The weight and volume penalties of thermally pressurized supercritical vessels were computed for a range of useful fluid loads. The calculations were based on the analytical methods of Reference 1 and the data assumptions tabulated in Table 3.

TABLE 3  
SUPERCritical VESSEL DESIGN DATA

| Parameter                              | Oxygen    | Nitrogen  |
|--|-----------|-----------|
| Design pressure, psia                  | 800       | 725       |
| Maximum pressure, psia                 | 875       | 850       |
| Inner shell material                   | Rene 41   | Rene 41   |
| Minimum insulation thickness, in.      | 0.75      | 0.75      |
| Insulation density, lb/ft <sup>3</sup> | 5.0       | 5.0       |
| Outer shell material                   | Al6061-T6 | Al6061-T6 |
| Liquid fraction at fill                | 0.95      | 0.95      |
| Vessel shape                           | Spherical | Spherical |

The results of these computations are plotted in Figures 10 and 11 for oxygen vessels and in Figures 12 and 13 for nitrogen.

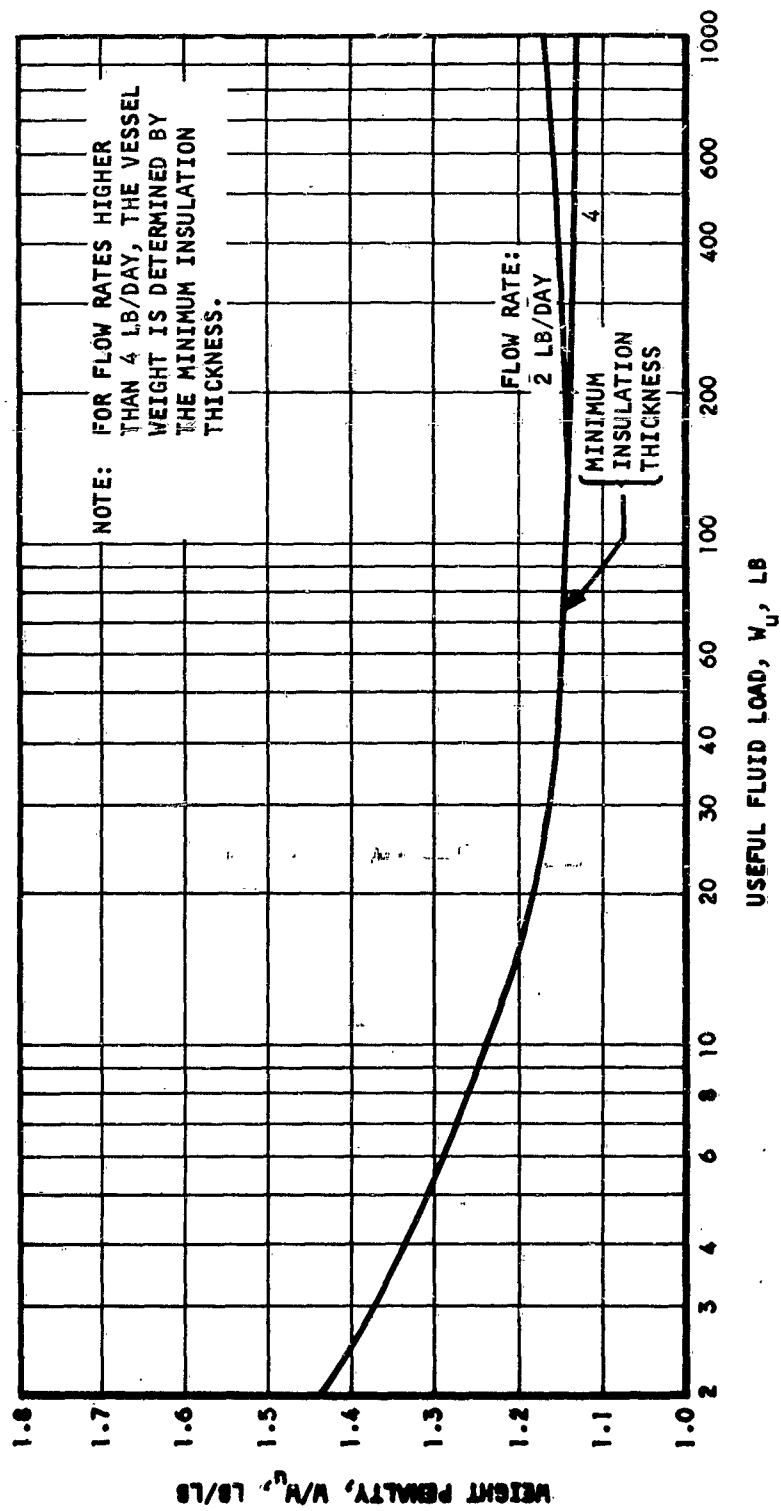


Figure 10. Supercritical Oxygen Storage Vessel Weight Penalty

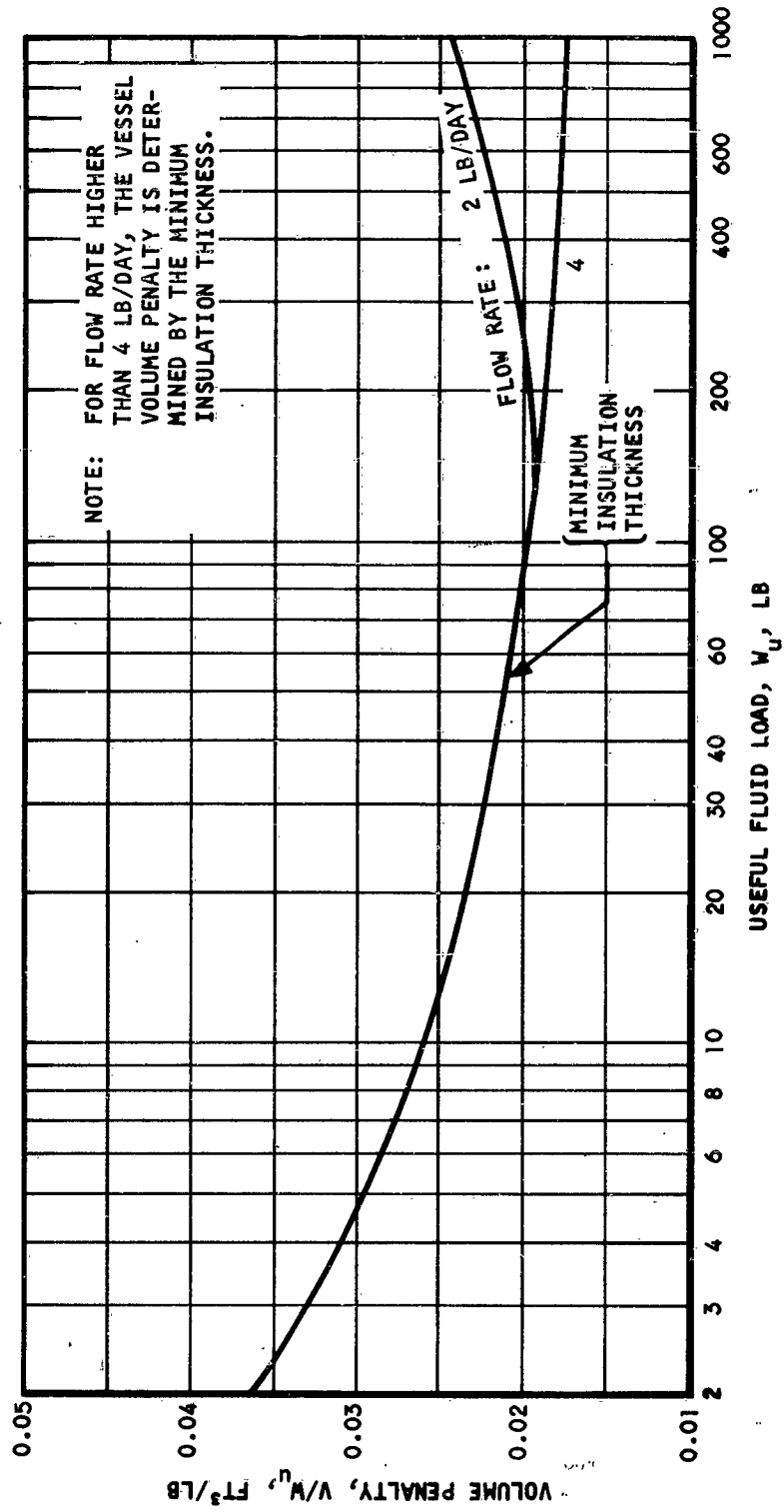


Figure 11. Supercritical Oxygen Storage Vessel Volume Penalty

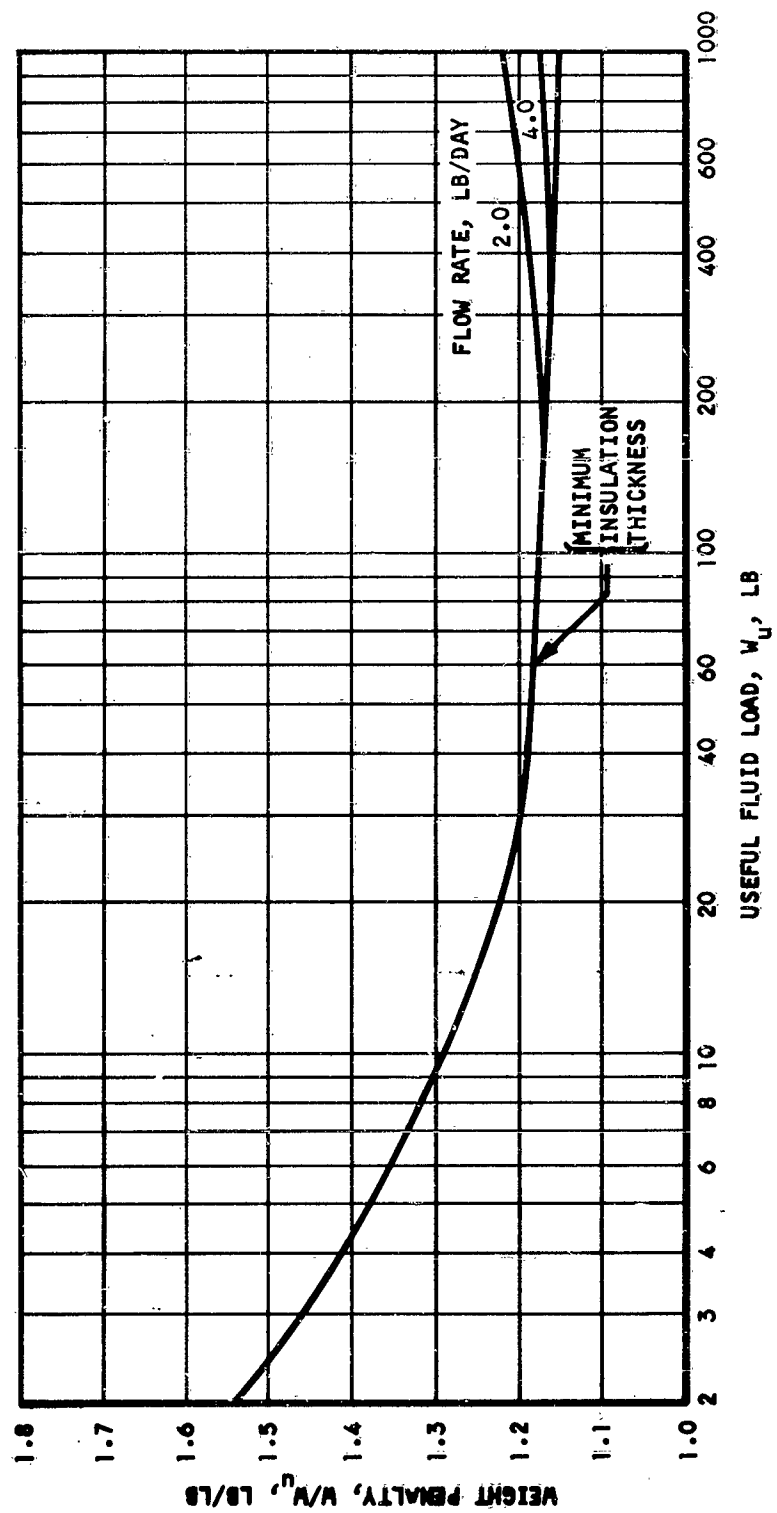


Figure 12. Supercritical Nitrogen Storage Vessel Weight Penalty

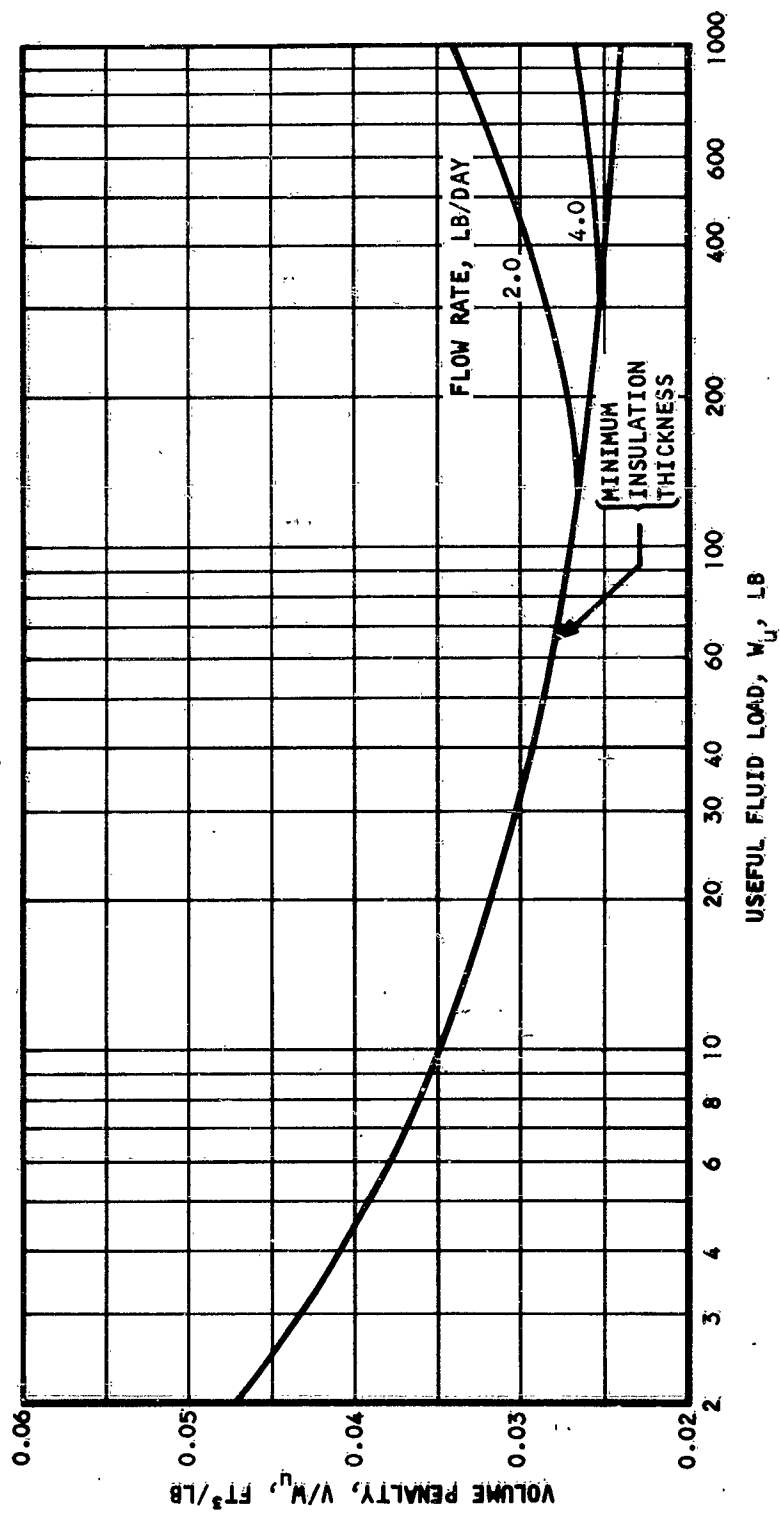


Figure 13. Supercritical Nitrogen Storage Vessel Volume Penalty

## SUBCRITICAL STORAGE OF CRYOGENIC FLUIDS

### Methods of Pressurization

As for the supercritical storage techniques, two types of subcritical storage of cryogenic fluids can be recognized, depending on the method of fluid pressurization.

- a. Positive expulsion vessels, where the fluid is stored in a bladder contained within the vessel inner shell, and fluid delivery is insured by introducing a high-pressure gas in the space between the bladder and the pressure shell. The schematic diagram of this system is shown in Figure 7.
- b. Thermally pressurized vessels, where the pressure is maintained during fluid delivery by means of heat addition to the mass of the stored fluid. The methods of heat addition are the same here as for supercritical storage vessels that have been described previously. Figures 8 and 9 are schematic diagrams showing two types of heat input control loops.

In subcritical thermally pressurized storage vessels, the fluid is stored under two phases. Delivery of a single-phase fluid under zero gravity conditions is possible by means of phase separation devices located within the inner shell. Among these are centrifugal type separators and internal heat exchangers, where the fluid is circulated after throttling and heated up by the mass of the stored fluid, thus insuring vapor delivery. Other suggested methods involve use of capillary forces, and, for oxygen vessels, of the magnetic properties of the fluid. None of these methods of phase separation are developed or have been tested at present. Previous studies (Reference 2) have shown that little weight advantages, if any, are to be expected from thermally pressurized subcritical storage systems, as compared to either the simpler supercritical storage system with thermal pressurization or the subcritical storage system with positive expulsion.

### Storage Vessel Weight

Positive expulsion subcritical storage vessels do not present the same phase separation problem, since the fluid is stored as a subcooled liquid. An analysis, based on the methods developed in Reference 1, has been conducted to determine the weight of this type of vessel. The calculations were based on the data assumptions for oxygen and nitrogen shown in Table 4.

TABLE 4  
SUBCRITICAL VESSEL DESIGN DATA

| Parameter                              | Oxygen     | Nitrogen   |
|--|------------|------------|
| Design pressure, psia                  | 100        | 100        |
| Maximum pressure, psia                 | 120        | 120        |
| Inner shell material                   | Al         | Al         |
| Insulation thickness, in.              | 1.0        | 1.0        |
| Insulation density, lb/ft <sup>3</sup> | 5.0        | 5.0        |
| Outer shell material                   | Al 6061-T6 | Al 6061-T6 |
| Liquid fraction at fill                | 0.95       | 0.95       |
| Accessory weight (gas bottle), lb      | 7.0        | 7.0        |
| Pressurizing gas                       | Helium     | Helium     |
| Liquid residue, %                      | 3          | 3          |
| Vessel shape                           | Spherical  | Spherical  |

Using a factor of 2 on the maximum pressure, calculations show that the inner shell thickness is determined by the minimum gage compatible with present fabrication techniques. Aluminum alloy 6061-T6, because of its low density, is, in this case, the material choice. Pressure shells up to 20 in. in diameter fabricated of 6061-T6 minimum gage material (.020") can withstand the maximum specified pressure of 120 psia.

The weight of oxygen and nitrogen subcritical vessels is shown plotted in Figures 14 and 15 as function of the total vessel loads. These weights include the weight of the pressurizing gas subsystem; the accessory weight used in the calculations includes the valves associated with the pressurizing helium system.

#### CHEMICAL GENERATION OF ATMOSPHERIC GASES

##### General

It is possible to generate atmospheric gases for breathing and leakage make-up from chemical compounds either by reaction or by decomposition. The interest in these methods springs from the fact that these compounds are, in general, stable and storable as liquids or solids at normal pressures and temperatures. In Reference 1, various methods of generating

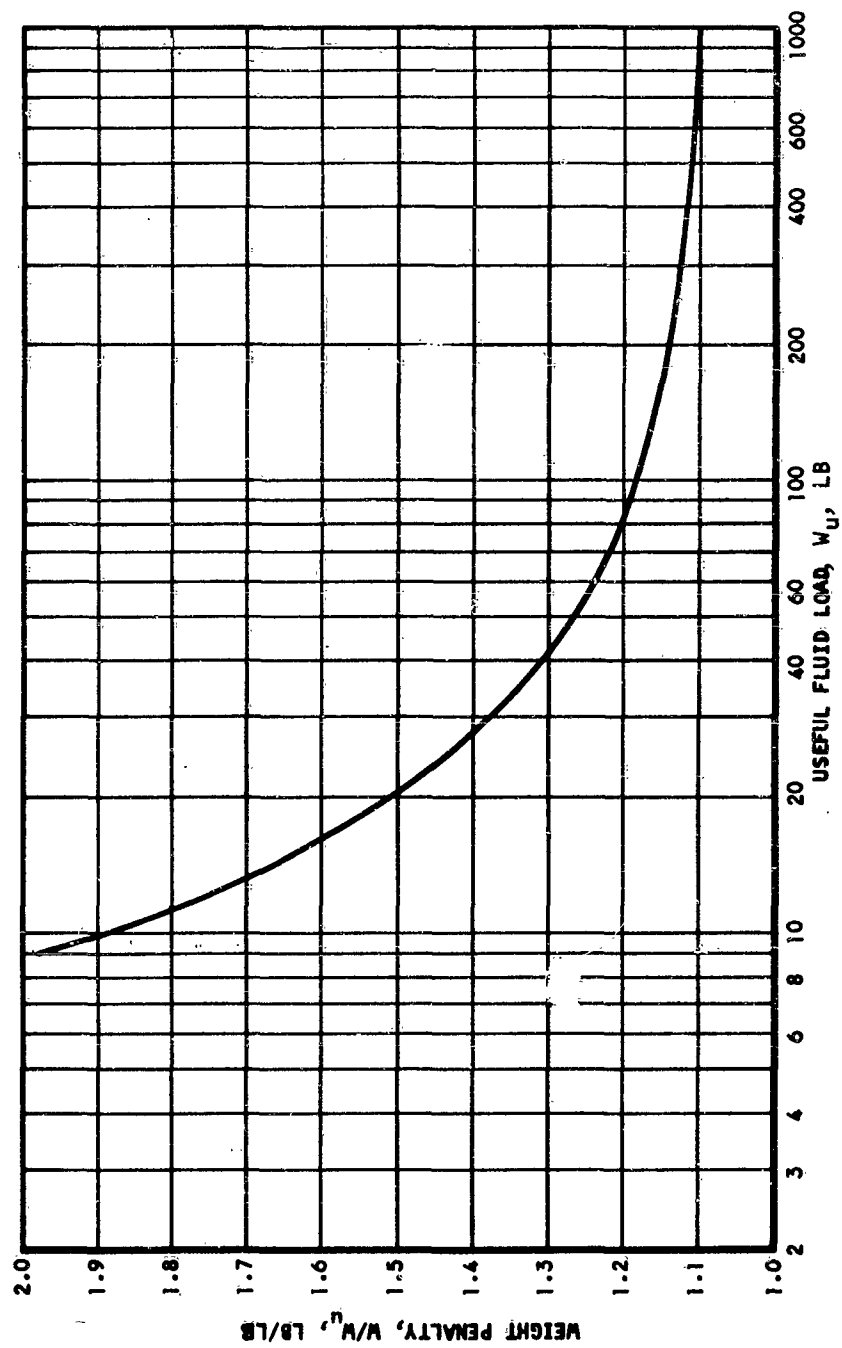


Figure 14. Subcritical Oxygen Storage Vessel Weight Penalty



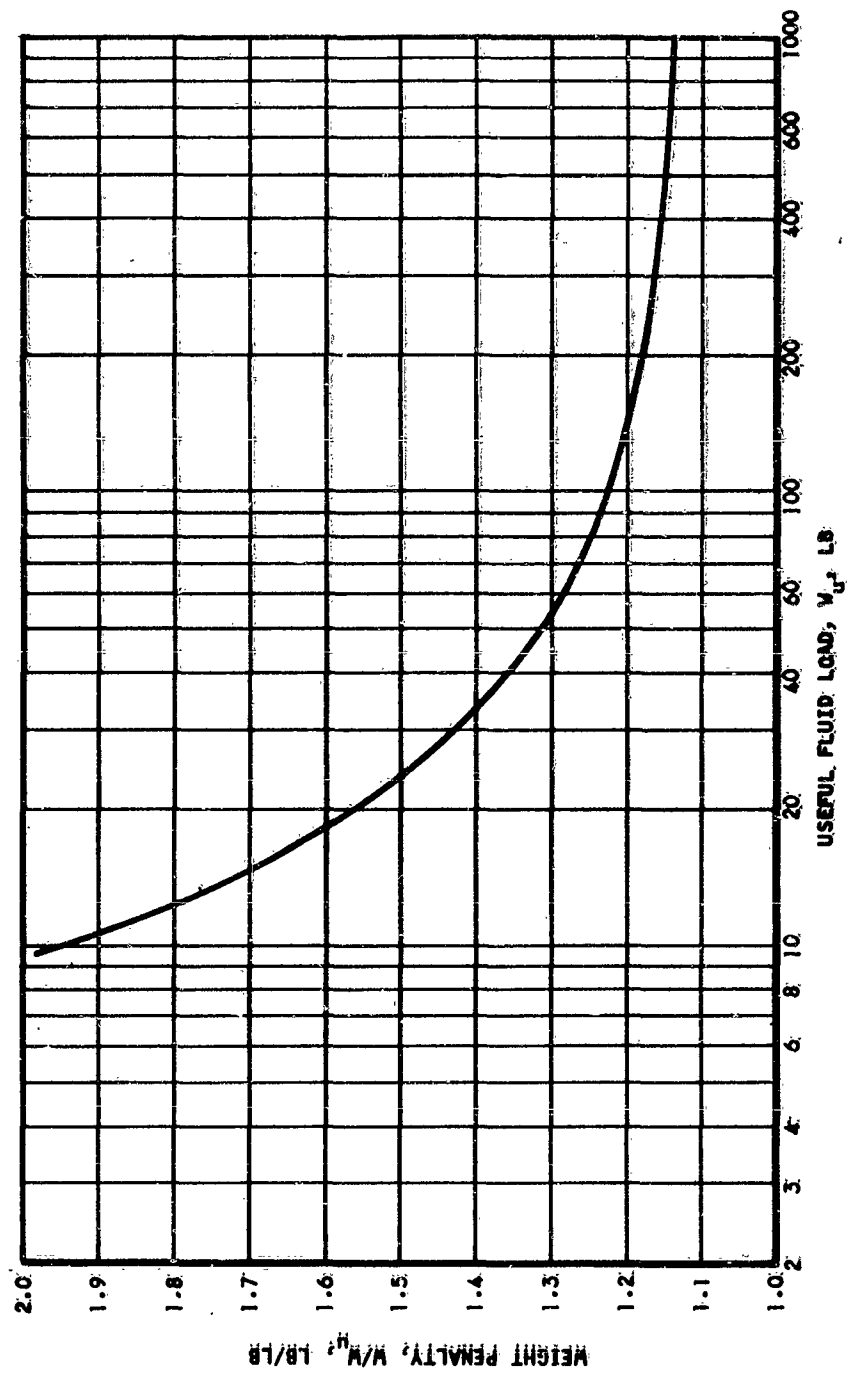


Figure 15. Subcritical Nitrogen Storage Vessel Weight Penalty

oxygen and nitrogen are discussed; here, only a brief review of the most promising chemical processes is given with their pertinent characteristics.

Methods of chemical generation of atmospheric gases considered in this section are listed below.

a. Oxygen Generation

Reaction of carbon dioxide and/or water with sodium or potassium superoxide with generation of oxygen

Lithium perchlorate decomposition

Hydrogen peroxide decomposition

Water electrolysis in ion exchange membrane electrolytic cell

b. Nitrogen generation by alkali metal azides

The use of sodium and potassium superoxide as a source of oxygen is discussed in a subsequent section of this report in conjunction with carbon dioxide management subsystems.

Oxygen Generation by Decomposition of Lithium Perchlorate

Lithium perchlorate decomposes into lithium chloride liberating oxygen (60.1 per cent by weight). The following equation describes the chemical reaction.



The temperature necessary to initiate the reaction is approximately 720°F, which is approximately 280°F higher than the melting point of the perchlorate. A heat input of 991 Btu per lb. of oxygen produced is required to sustain the reaction.

A problem of separating the gaseous oxygen from the liquid compound in the decomposition chamber arises in a zero-gravity environment. Separation can possibly be achieved by use of a porous diaphragm. The rate of oxygen production appears difficult to control, since little is known about the decomposition mechanism. This can probably be achieved, however, by controlling the heat input into the decomposition chamber.

A rough estimate of the weight of a simple lithium perchlorate decomposition system is given in Reference 2 and is shown here as Figure 16. The calculations from which this plot was obtained are based on the following data assumptions:

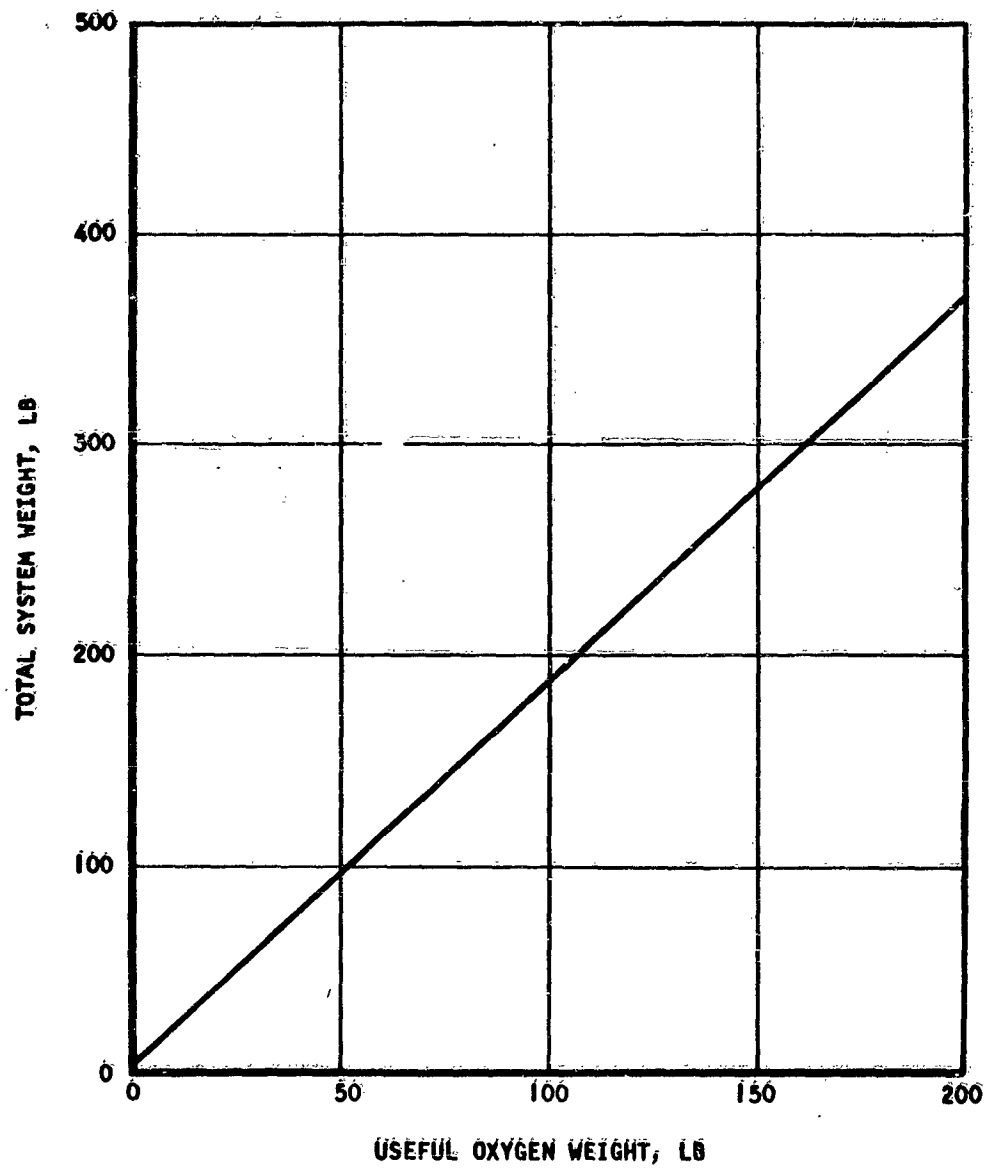


Figure 16: Oxygen Generation by Lithium Perchlorate = System Weight

Ullage: 50 per cent

Decomposition chamber wall: stainless steel, 0.050 in. thick

Decomposition chamber insulation: fiberglass, 1.0 in. thick

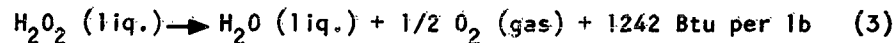
Porous diaphragm for phase separation: ceramic, 0.15 in. thick

Even with this simple system, lithium perchlorate does not appear on a weight basis alone to be competitive with other sources of oxygen for use aboard space vehicles.

#### Oxygen Generation by Decomposition of Hydrogen Peroxide

Hydrogen peroxide,  $H_2O_2$ , is available commercially at a concentration of 90 wt per cent or lower. A concentration of 98 per cent is now available on a semi-commercial basis. Higher concentrations are desirable since they have a higher content of oxygen and greater stability.

To generate oxygen, hydrogen peroxide decomposes according to the equation



The water produced in the reaction may be found useful in the vehicle water management system. Catalysts are required for smooth and rapid decomposition of hydrogen peroxide. These materials have been thoroughly investigated in connection with propellant uses of hydrogen peroxide so that few problems remain. Silver screen packs appear to be the most advanced catalyst at the present time. Zero-gravity conditions increase the complexity of the decomposition and feed system.

Disadvantages of hydrogen peroxide include its high toxicity. Concentrated peroxide blisters the skin on contact. Vapors and aerosols entrained with the oxygen are deleterious to the respiratory system. On contact with most structural materials, the decomposition of peroxide is catalyzed. Storage in pure aluminum appears practical for long durations in vented tanks; however, accidental contamination could be disastrous.

Figure 17 shows an arrangement of a peroxide decomposition system. Hydrogen peroxide is stored in a positive expulsion type tank and expelled through a silver-screen type gas generator. The water vapor and oxygen produced are then circulated through a heat exchanger where the water vapor is condensed and subsequently removed as a liquid.

The temperature of the gas at the outlet of the gas generator depends on the heat leaking from the generator and on the purity of the hydrogen peroxide used. The adiabatic temperature of decomposition of a 90 per cent purity solution is estimated to be  $1364^\circ F$ .

An estimate of the weight of the hydrogen peroxide storage vessel and pressurizing system was made based on the assumptions listed below.

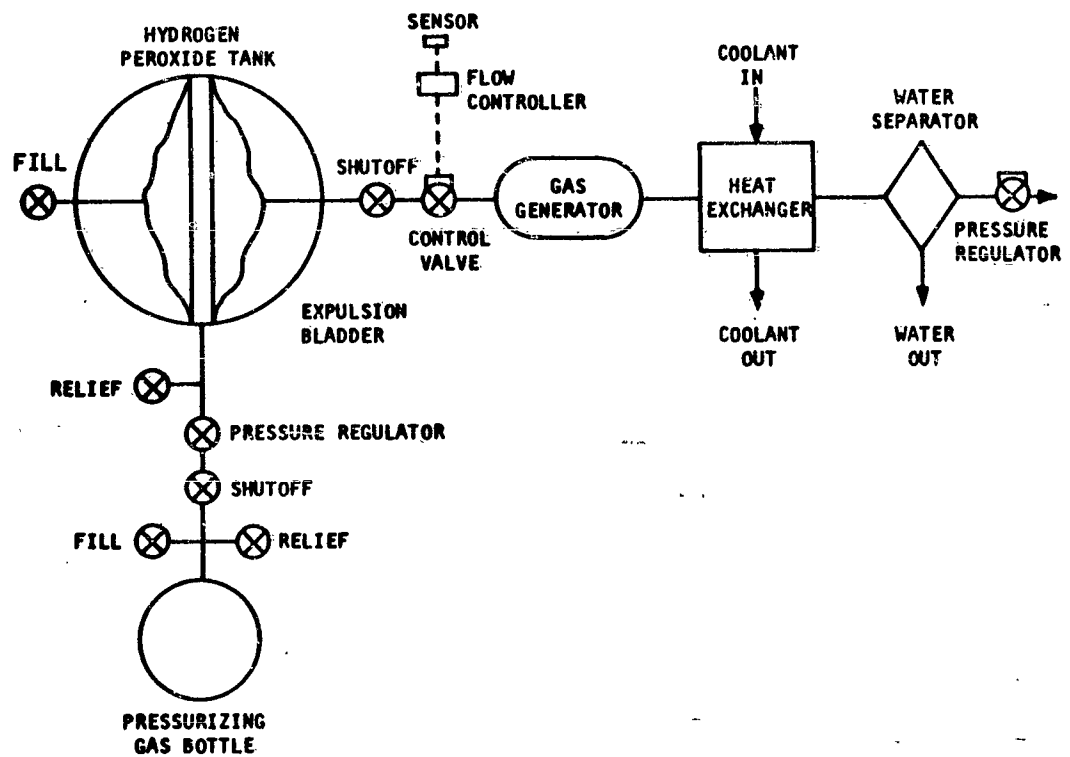


Figure 17. Chemical Oxygen Supply Using Hydrogen Peroxide

Spherical storage vessel  
Hydrogen peroxide purity: 0.90  
Tank material: aluminum  
Utilization efficiency: .98  
Pressurizing gas: helium  
Pressurizing gas subsystem control valves: 7.0 lb  
System is credited for the water evolved in the reaction.

The results of these calculations are given in Figure 18, where the hydrogen peroxide storage vessel weight penalty is plotted vs the useful oxygen load. It should be noted that the weight penalty plotted is lower than the tankage and pressurization subsystem weight by 1.125 lb per lb of oxygen generated due to the credit given to the water of reaction.

#### Oxygen Generation by Electrolysis of Water

Electrolytic processes have been treated in detail in Reference 1. The electrolytic cell considered here is an ion membrane type cell which appears promising for zero-gravity operation.

Reported parameters for a system satisfying the oxygen metabolic requirements of a three-man vehicle are as follows:

Power input: 702 watts  
Weight: 112 lb  
Volume: 1.97 ft<sup>3</sup>

It is believed that the voltage across the cell electrode was on the order of 1.8 volts, and that the gases were delivered at approximately 50 psia. The heat rejected by the three-man cell is estimated to be 447 Btu per hr and the cell operating temperature as 122°F. Water is pumped to the electrode by means of a wick.

The weight of an ion membrane electrolytic cell, including a positive expulsion type water storage subsystem, has been estimated from the data given above and the following assumptions:

Water storage vessel pressurizing gas: helium  
Pressurizing gas subsystem control valves: 7.0 lb  
Hydrogen is discharged overboard, and no credit is given for its production.  
Water storage tank material: aluminum

The results of these computations are plotted in Figure 19.

This oxygen production technique does not appear competitive on a weight basis with the other storage methods discussed previously, especially for short duration missions. In addition, the high power requirements of the electrolytic cell are a serious disadvantage for space vehicle installation.

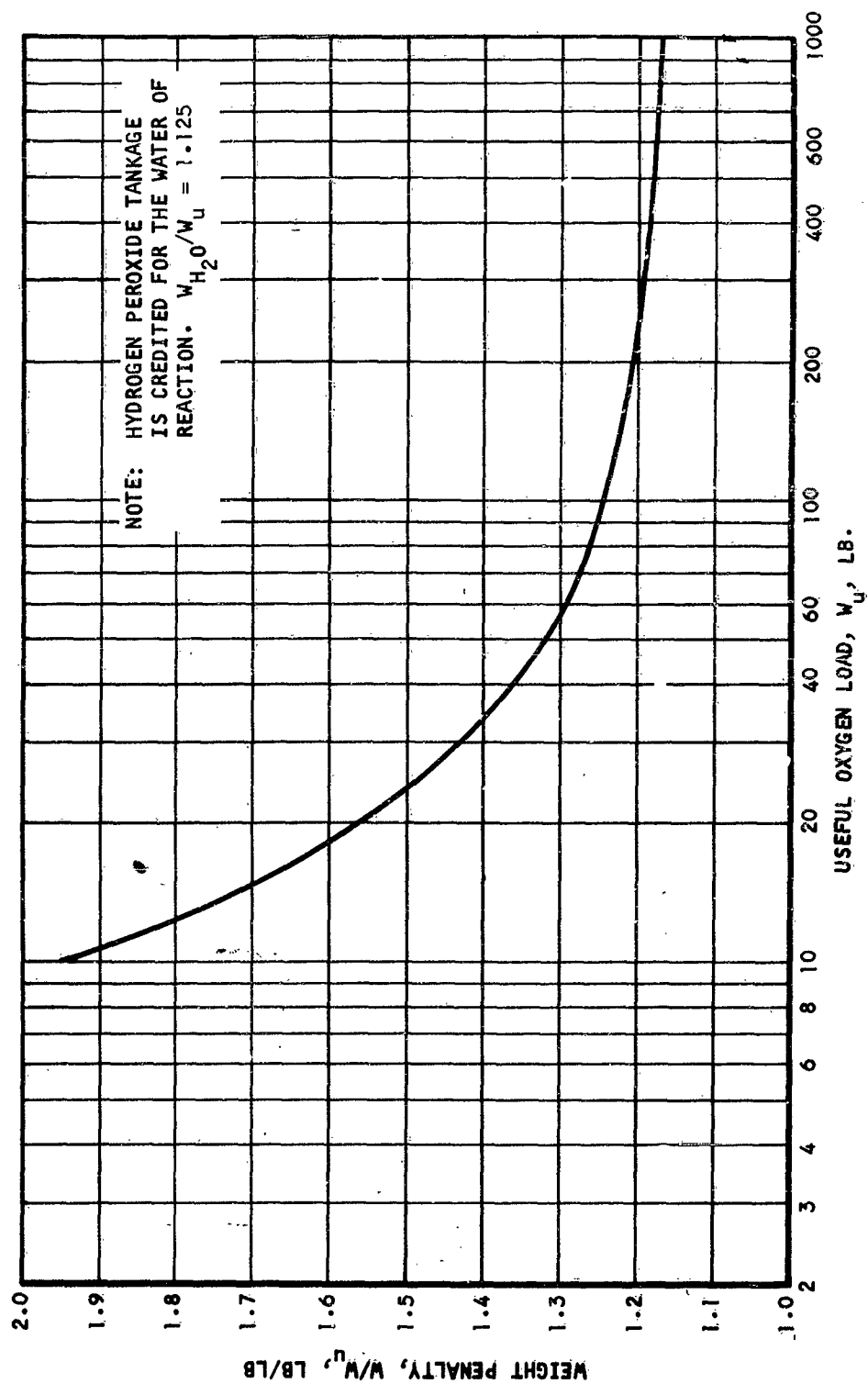


Figure 18. Hydrogen Peroxide Storage Weight Penalty

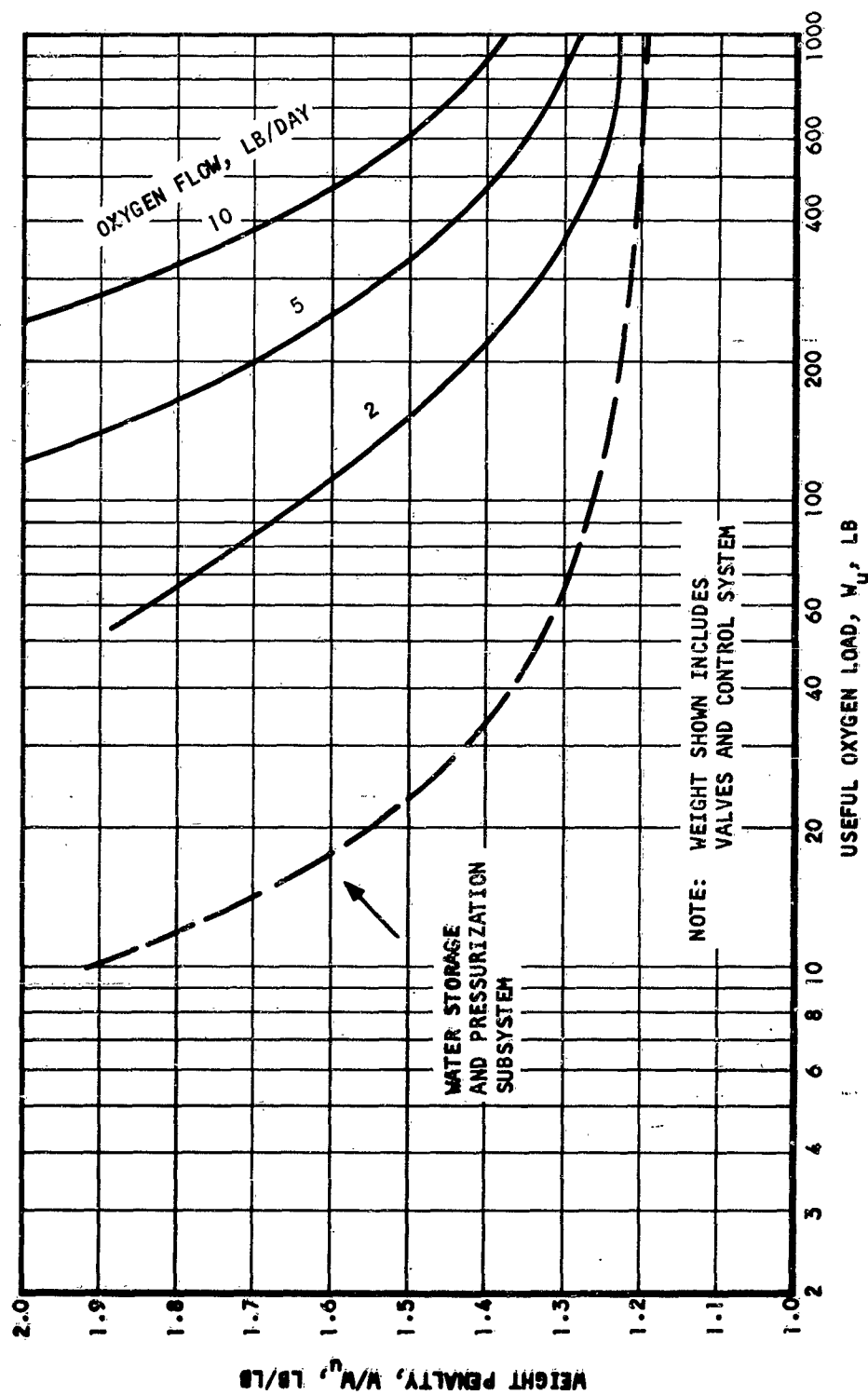
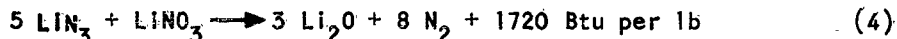


Figure 19. Electrolytic Cell Subsystem Weight Penalty



#### Nitrogen Generation by Decomposition of Lithium Azide

On decomposition at 550°F, lithium azide yields 85.8 per cent nitrogen and 95 Btu per lb. To provide heat for initiation and maintenance of decomposition, a reactant can be provided which produces a more stable lithium compound as reaction product. Oxidants such as lithium nitrate or fluorocarbons have been used to form nitrogen-producing solid propellants. In the case of lithium nitrate, the chemical reaction is given by Equation 4.



This reaction produces 71.5 per cent nitrogen. For practical use, extensive filters must be provided to remove lithium oxide and heat exchangers to cool the product nitrogen. Because the reaction operates more smoothly at elevated pressures, the nitrogen-producing mixture would be used to pressurize a small storage tank, required nitrogen being obtained through a pressure-regulating valve on the tank. The nitrogen-producing azide mixture burns like a solid propellant and is not amenable to simple control.

Material balance alone, without considering any weight penalty for the storage of the azide or the disposal (or storage) of the lithium oxide, shows a weight penalty ( $W/W_{\text{N}_2}$ ) equal to 1.14 and is not competitive

with the cryogenic methods described previously. In addition, the reaction is difficult to control and presents a safety problem which makes the process prohibitive for space vehicle usage.

#### COMPARISON OF GAS SUPPLY SUBSYSTEMS

##### Component Integration

In addition to the storage vessels and their pressurization subsystem, other components such as valves, heat transfer equipment, etc., are integral parts of the complete gas supply subsystems. As these accessories can contribute a large percentage of the total gas supply system weight, comparison of the various storage techniques discussed previously can only be made on an integrated basis.

The weight and size of the accessories is, in general, independent of the size of the storage vessel and, in most cases, of the delivery flow rates. While this is true of valves and sensors, it does not apply to items such as heat exchangers whose weight is a direct function of the flow rates in the system. Schematic diagrams showing the arrangement of the following subsystems are given here:

High-pressure gas storage: Figure 20

Supercritical storage of cryogenic fluid with thermal pressurization: Figure 21.

Subcritical storage of cryogenic fluid with positive expulsion: Figure 22.

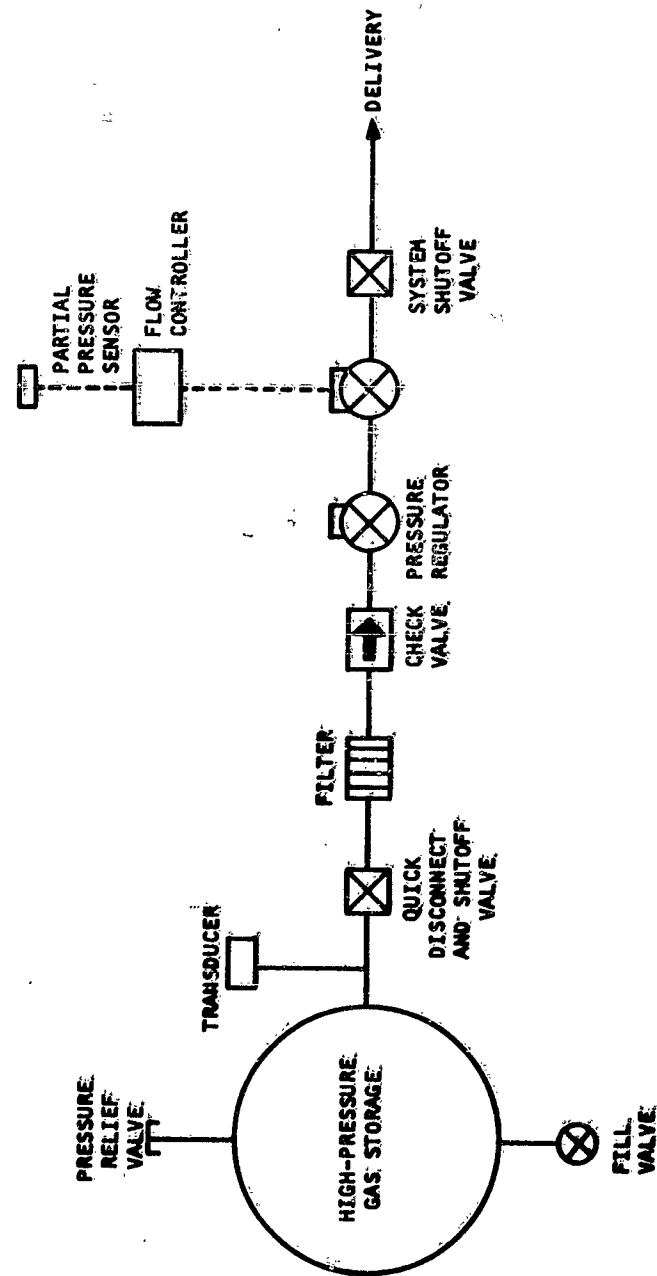


Figure 20: High-Pressure Gas Storage - Gas Supply Subsystem Diagram

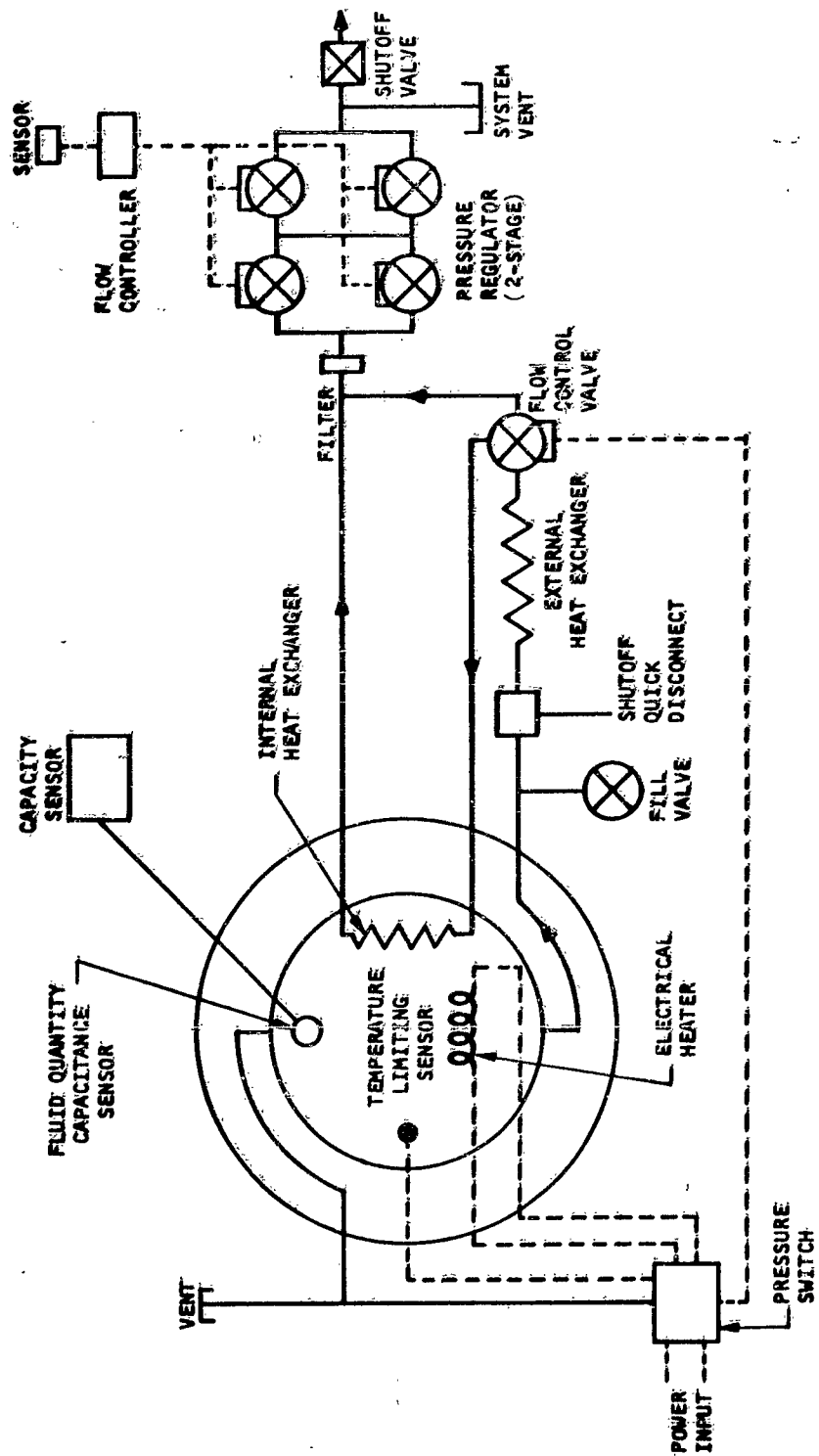


Figure 21. Supercritical Cryogenic Fluid Storage - Gas Supply Subsystem Diagram

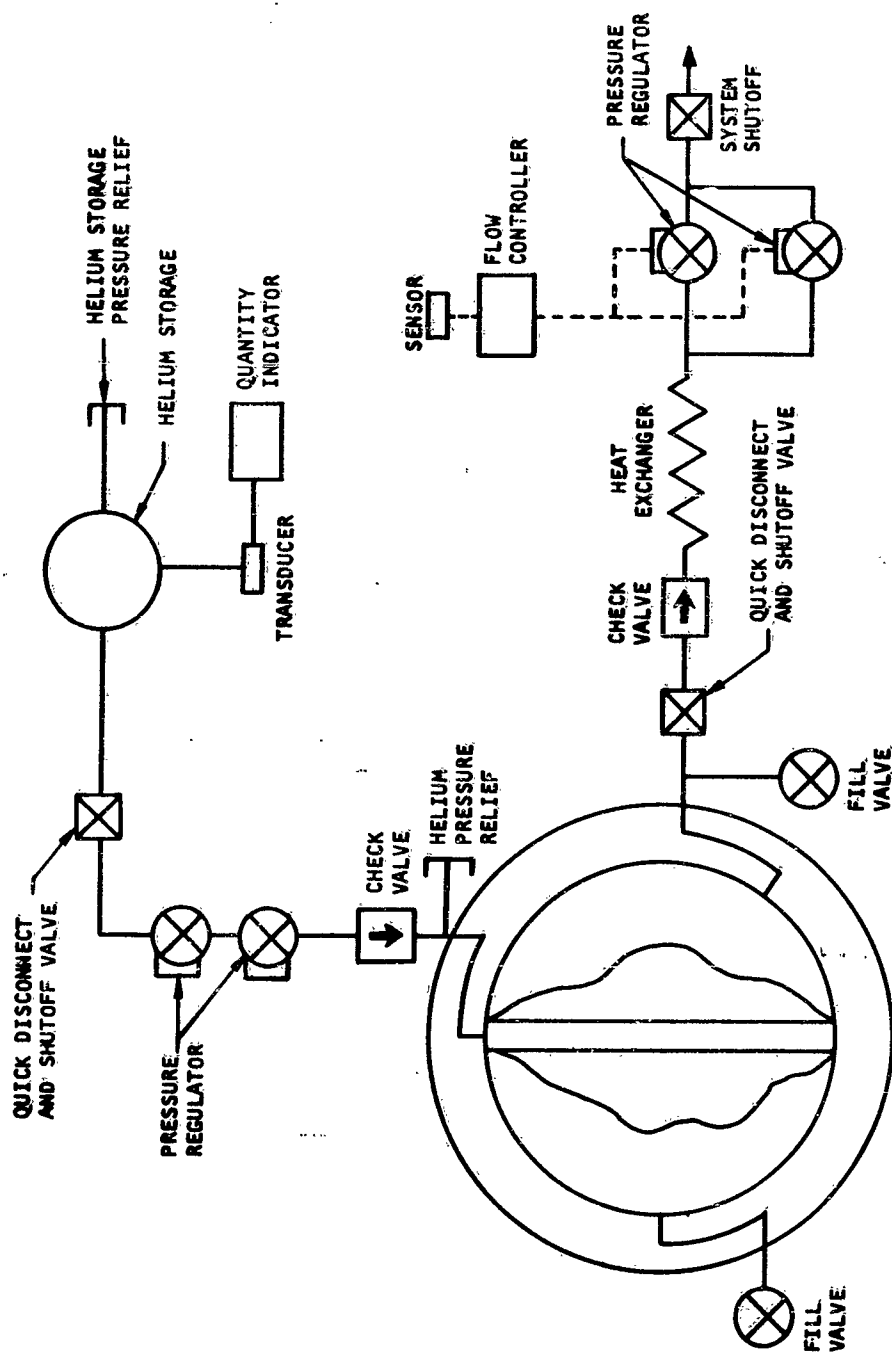


Figure 22. Subcritical Cryogenic Fluid Storage With Positive Expulsion. -  
Gas Supply Subsystem Diagram

These arrangements are typical of space vehicle installation. In some cases, components are duplicated to improve the subsystem reliability by redundancy. The estimated weight of the accessories shown in the schematics is listed in Table 5.

#### Subsystem Comparison

Since weight is usually the determining factor in the selection of a space vehicle system, a plot of the gas supply subsystem weight considered in this report is presented for comparison in Figure 23. This plot has been prepared using the accessory weights tabulated above and the storage vessel weights plots of Figures 5, 10, 14, 18, and 19. The curves are given for oxygen only, since the conclusions drawn from it also apply to nitrogen storage vessels.

Other parameters of importance in system selection are listed in Table 6. These include maximum subsystem pressure (excluding the pressurizing gas components), maximum estimated temperature in the subsystem, power requirements, the heat evolved, and the heat sink potential of the subsystem. Also listed in Table 6 is the water consumed (or produced) by the subsystem. Complete system evaluation cannot be made without taking into account these parameters. Normally, the gas supply subsystem would be penalized (or credited) for each one of the items listed above; the penalties involved are discussed in Section III of this report.

Cryogenic fluid storage subsystems are, on a weight basis, superior to all the other subsystems considered. This weight advantage increases markedly as the capacity of the supply system decreases. At a total fluid load of 100 lb, the weight of the two cryogenic subsystems is about the same. Above 100 lb of fluid storage capacity, the subcritical system is slightly lighter than its supercritical counterpart. Below 100 lb, the weight picture is reversed. The weight difference is so small that system selection must be based on other considerations.

The weight penalty of the high-pressure gas storage subsystem is approximately 3 times as large as that of cryogenic subsystems at large fluid loads. For this reason, high-pressure gas storage vessels are not very attractive for space vehicle applications other than emergency gas supply. In this case, maximum reliability, indefinite stand-by periods, and short-duration usage are the design criteria, and weight is a secondary consideration. At a stored weight lower than approximately 6 to 8 lb, the high-pressure gas subsystem shows a lower weight penalty than all the other subsystems analyzed.

None of the chemical systems are competitive on a weight basis with either of the cryogenic storage techniques. No suitable chemical generation method for nitrogen supply has been found to date.

Oxygen generation from hydrogen peroxide decomposition could find a use on vehicles where the water management subsystem shows a water deficit. This would occur in missions of short duration when water is not recovered

TABLE 5  
TYPICAL GAS SUPPLY SUBSYSTEMS ACCESSORY WEIGHTS

| Accessory   | Weight, lb | Accessory  | Weight, lb |
|---|------------|--|------------|
| <b>1. High-Pressure Gas Storage (Figure 20)</b>       |            | <b>3. Subcritical Cryogenic Storage (Figure 22)</b>                            |            |
| a. Pressure relief valve                              | 0.3        | a. Helium pressurization subsystem<br>(accounted for in storage vessel weight) |            |
| b. Fill valve   | 1.1        | b. Transducer  | 0.4        |
| c. Transducer   | 0.4        | c. Fluid quantity indicator  | 0.4        |
| d. Quick disconnect and shutoff valve                 | 0.2        | d. Vent valve  | 0.2        |
| e. Filter   | 0.1        | e. Fill valve  | 0.3        |
| f. Check valve  | 0.2        | f. Vessel shutoff valve  | 0.2        |
| g. High-pressure regulating valve                     | 0.9        | g. Heat exchanger  | 0.7        |
| h. Demand pressure regulating valve                   | 1.4        | h. Check valve   | 0.2        |
| i. Partial pressure sensor                            | 0.2        | i. Demand pressure regulating valve  | 2 x 1.4    |
| j. Flow controller                                    | 2.5        | j. Partial pressure sensor   | 0.2        |
| k. Shutoff valve                                      | 0.4        | k. Flow controller   | 2.5        |
| Total Weight  | 7.7        | l. System shutoff valve  | 0.4        |
| <b>2. Supercritical Cryogenic Storage (Figure 21)</b> |            | Total Weight   | 6.5        |
| a. Vessel vent and pressure relief valve              | 0.2        | <b>4. Hydrogen Peroxide Storage (Figure 17)</b>                                |            |
| b. Pressure controller                                | 0.4        | a. Helium pressurization subsystem<br>(accounted for in storage vessel weight) |            |
| c. Electrical heater                                  | 0.8        | b. Vent valve  | 0.2        |
| d. Internal heat exchanger                            | 0.9        | c. Fill valve  | 0.3        |
| e. Fluid quantity capacitance sensor                  | 0.5        | d. Vessel shutoff valve  | 0.2        |
| f. Capacity indicator                                 | 0.6        | e. Flow control valve  | 1.5        |
| g. Fill valve   | 0.3        | f. Partial pressure sensor   | 0.2        |
| h. Vessel shutoff valve                               | 0.2        | g. Flow controller   | 2.5        |
| i. External heat exchanger                            | 0.5        | h. Gas generator   | 2.2        |
| j. Flow control valve                                 | 1.2        | i. Heat exchanger  | 2.5        |
| k. Check valve  | 0.1        | j. Water separator   | 1.5        |
| l. Check valve  | 0.2        | k. Pressure regulator  | 1.4        |
| m. High-pressure regulating valve                     | 2 x 0.9    | Total Weight   | 12.1       |
| n. Demand pressure regulating valve                   | 2 x 1.4    |  |            |
| o. Partial pressure sensor                            | 0.2        |  |            |
| p. Flow controller                                    | 2.5        |  |            |
| q. System shutoff valve                               | 0.4        |  |            |
| r. Pipes and fittings                                 | 0.50       |  |            |
| s. Bosses   | 0.30       |  |            |
| Total Weight  | 14.4       |  |            |

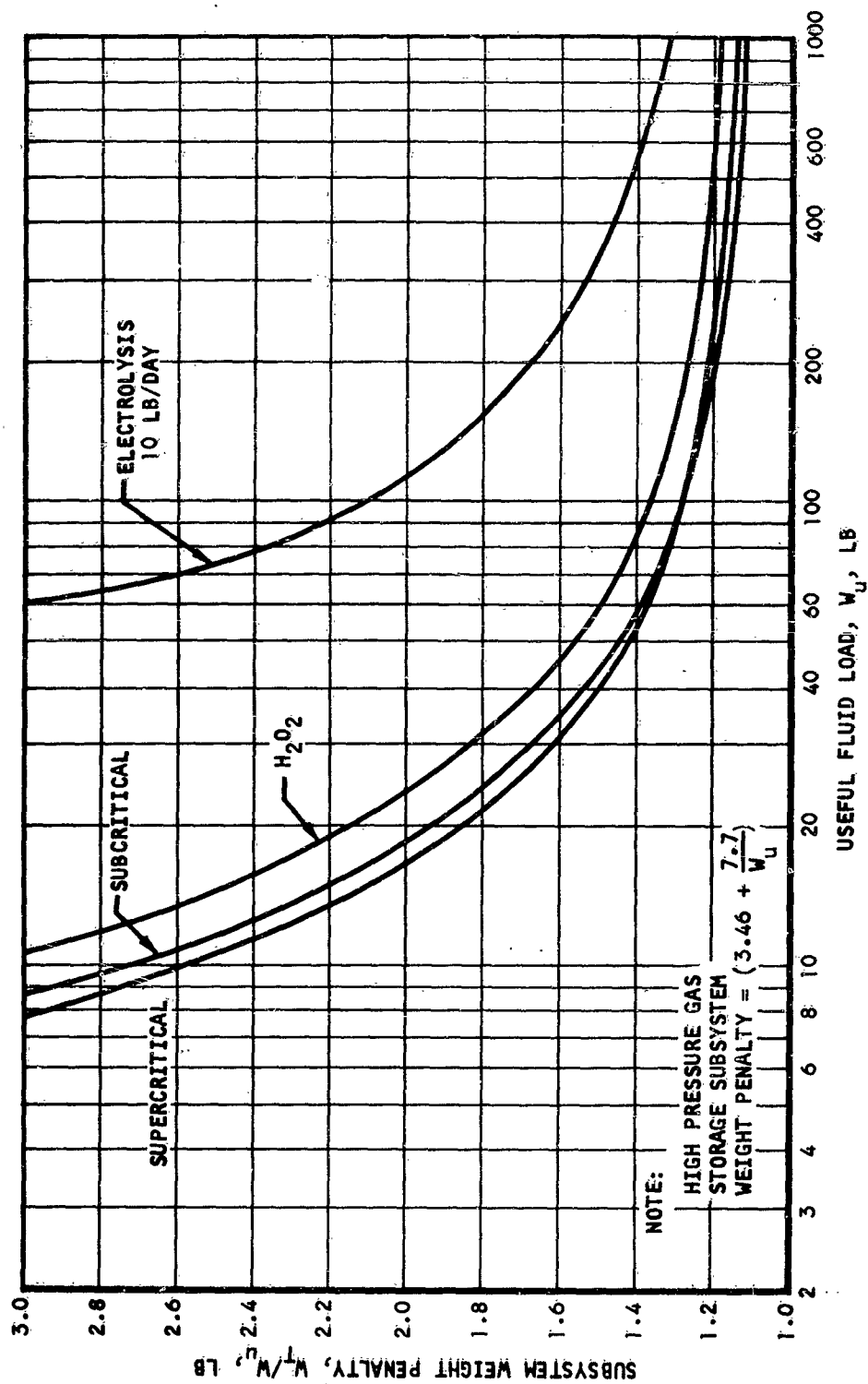


Figure 23. Gas Supply Subsystems Weight Comparison (Oxygen)

TABLE 6  
OXYGEN GAS SUPPLY SUBSYSTEM CHARACTERISTICS

| Subsystem                       | Maximum System Pressure<br>psia | Maximum System Temp.<br>°F | Power Requirement<br>watts per lb O <sub>2</sub> | Heat Evolved<br>Btu per lb O <sub>2</sub> | Heat Sink Potential<br>Btu per lb O <sub>2</sub> |
|---------------------------------|---------------------------------|----------------------------|--|---|--|
| High-pressure gas               | 10,500                          | ambient                    | none   | none                                      | none   |
| Supercritical storage           | 875                             | ambient                    | none   | none                                      | 90* @270°R                                       |
| Subcritical storage             | 100**                           | ambient                    | none   | none                                      | 155 @170°R                                       |
| Hydrogen peroxide decomposition | 50**                            | 1360                       | none   | 2610                                      | none   |
| Water electrolysis              | 50**                            | 122                        | 117  | 75  | none   |

\* Average

\*\* Pressurizing gas stored at 2000 psia



from the waste or wash products. In this case, however, the small gas storage capacity requirement and the high hydrogen peroxide subsystem weight offsets the advantages of water generation as a by-product of oxygen production. In addition, hydrogen peroxide systems for breathing oxygen supply are comparatively underdeveloped, are not easily controlled, and lack safe operational characteristics.

Because of the high electrolytic cell weight, oxygen production from water by electrolysis is attractive only for missions in excess of one year. The weight of this system, as shown, greatly improves if, in the overall vehicle material balance, an excess of water is produced which can be used for the electrolysis process. The weight plotted can, in this case, be reduced by the amount of excess water production. In a mission of this type, it is very likely that vehicle electrical power would be derived from nuclear or solar sources, and that a very low penalty would be paid for supplying power to the electrolytic cell. This type of gas supply system, therefore, offers potentialities for long mission duration, especially if hydrogen is required for carbon dioxide reduction.

As shown in Figure 23, the two cryogenic gas supply subsystems are competitive on a weight basis. However, other advantages of the supercritical system make it the preferred storage system for space vehicle installation. These advantages are briefly discussed below:

- a. The bladder of the subcritical liquid delivery system introduces problems of fabrication and reliability which have already been discussed in conjunction with positive expulsion supercritical storage systems. These problems are particularly difficult in large storage vessels in the range where subcritical vessels with positive expulsion are competitive with supercritical vessels.
- b. The presence of a bladder makes difficult accurate fluid quantity measurements inside the vessel. This also has been pointed out in the discussion of subcritical vessels.
- c. Since heat is leaking from the ambient atmosphere and from the pressurizing gas into the cooler stored fluid, a problem of fluid temperature stratification within the bladder and consequent fluid vaporization on the bladder wall arises. Presence of vapor within the bladder defeats the purpose of the design and could hardly be tolerated.

## CONCLUSIONS AND DESIGN DATA

### Conclusions

From the above discussion, it appears that even for missions of long duration supercritical storage of cryogenic fluids in thermally pressurized vessels is the most attractive method for breathing and pressurizing gas supply. For extended missions, oxygen production by water electrolysis could find its application. High-pressure gas storage appears attractive for emergency system gas supply.

### Parametric Data

Data pertinent to supercritical thermally pressurized gas supply subsystems are given here in graphical form. The plots for spherical vessels are based on the data assumptions listed on Page 30 of this report. In addition, the oxygen and nitrogen weight fraction in the cabin atmosphere is here assumed to be 0.339 and 0.638, respectively.

The following plots are given:

- a. Oxygen supply subsystem weight as a function of the mission duration with the leakage rate as a parameter. This plot is given for a number of crew members from 1 to 6 (Figures 24 through 29).
- b. Same plot for nitrogen (Figure 30).
- c. Oxygen and nitrogen weight penalty for redundancy (Figure 31). Here the added vessel weight incurred when the total gas stored is divided equally between two vessels is plotted as a function of the total gas storage load.
- d. The estimated stand-by period without venting of the supercritical oxygen and nitrogen vessels designed on the data of Page 30 is plotted as a function of the total fluid load in Figure 32.
- e. Heat sink potential (Table 6).

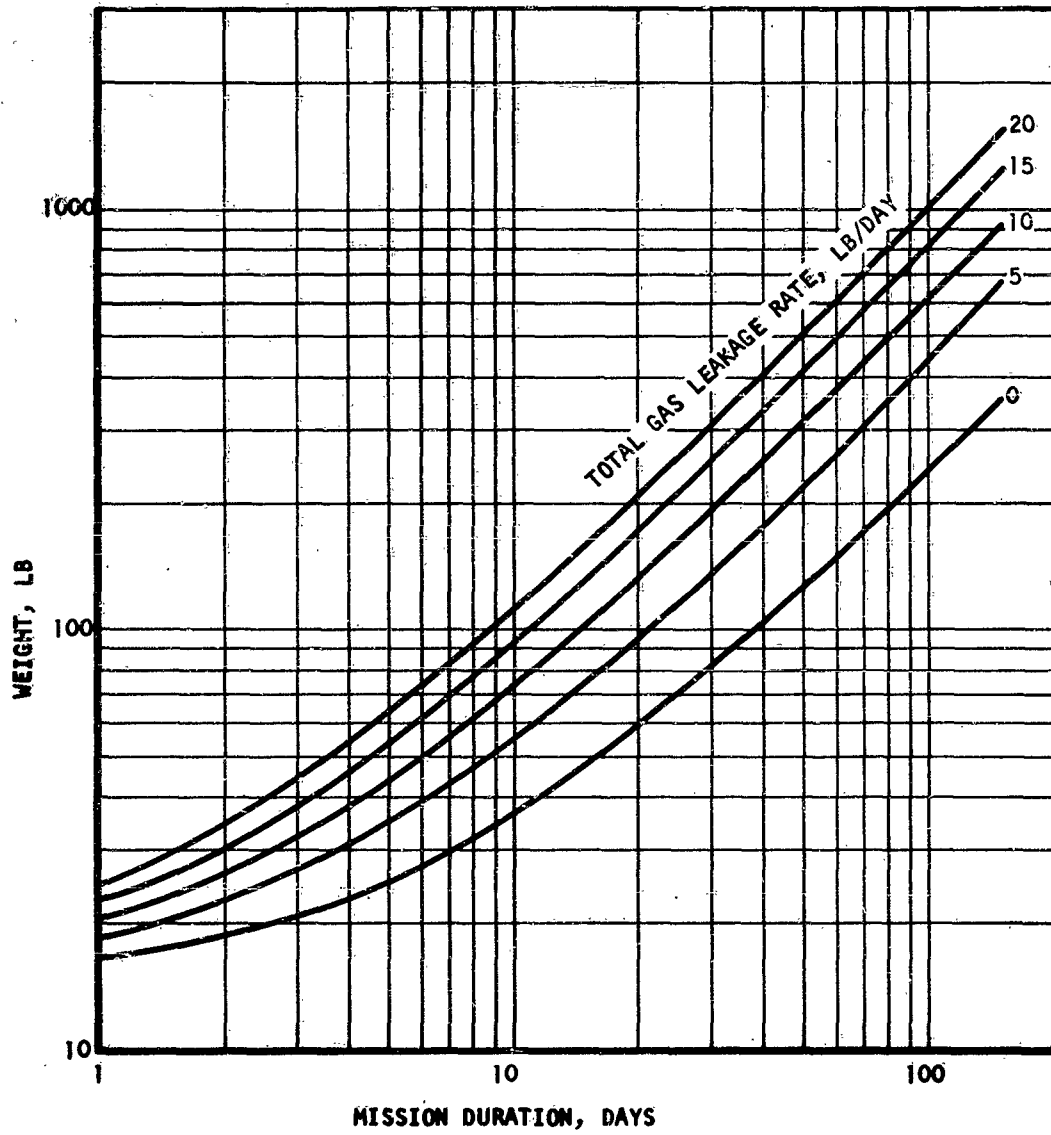


Figure 24. Oxygen Supply Subsystem Weight (N=1)

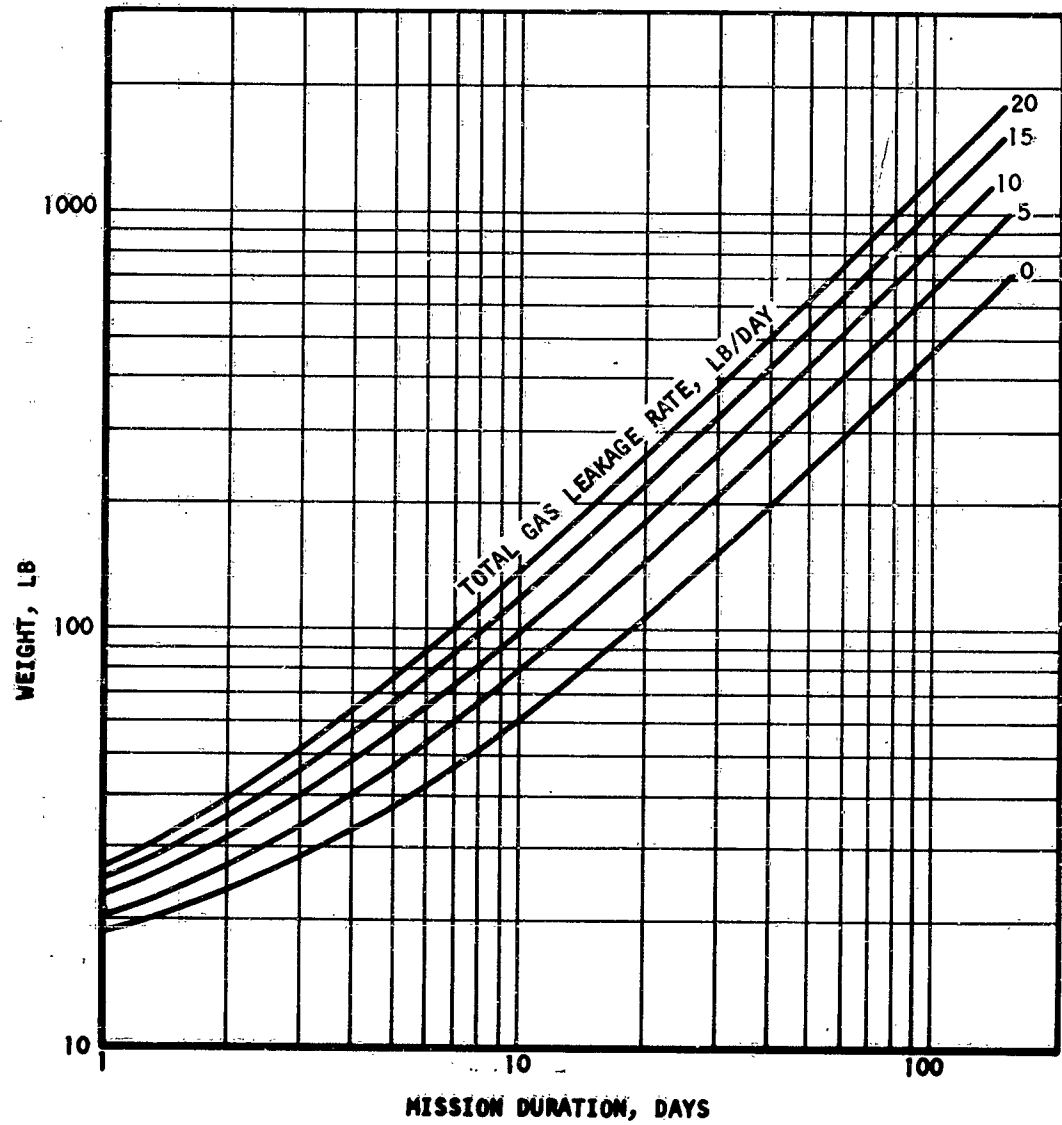


Figure 25. Oxygen Supply Subsystem Weight (N=2)

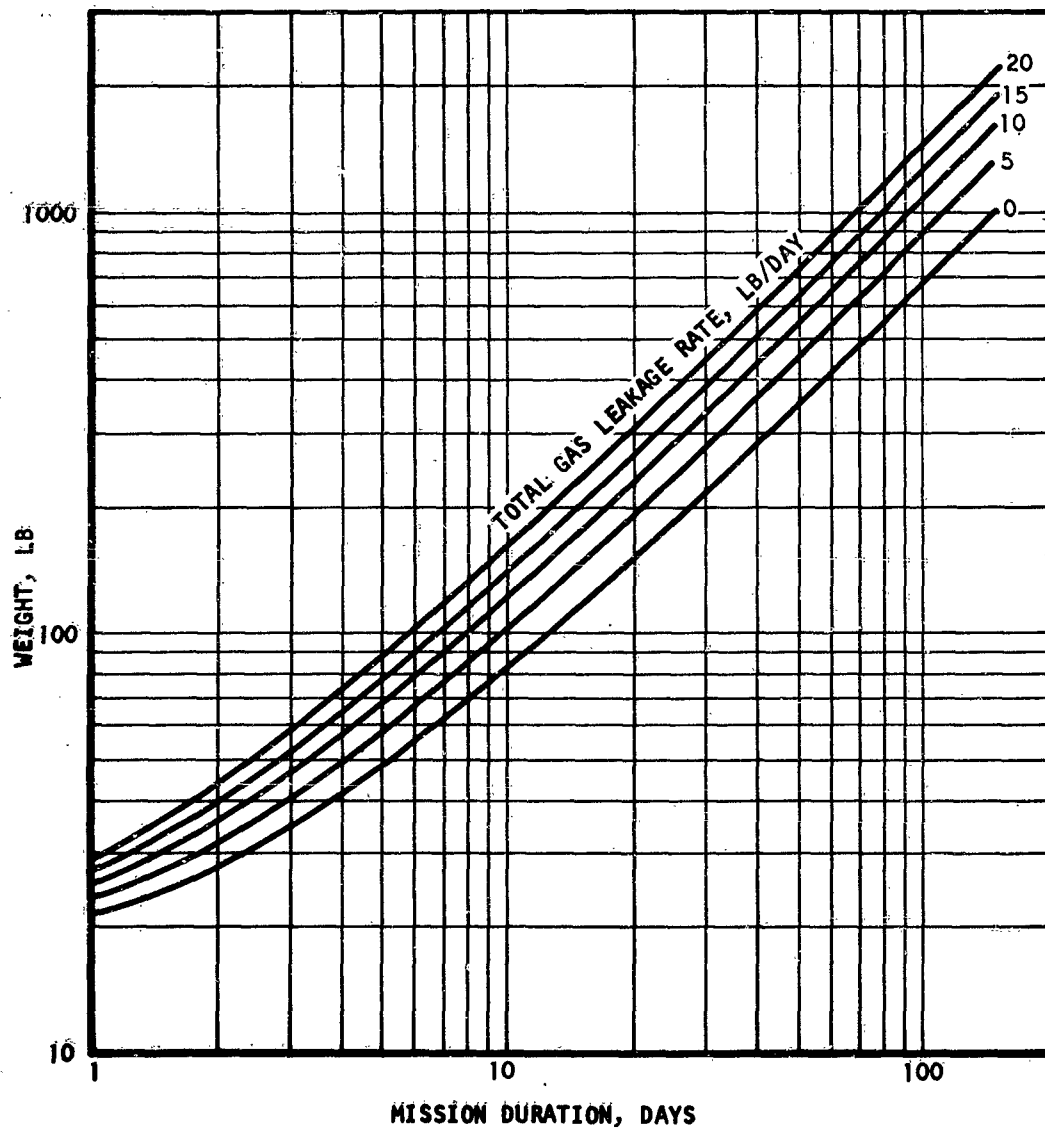


Figure 26. Oxygen Supply Subsystem Weight (N=3)

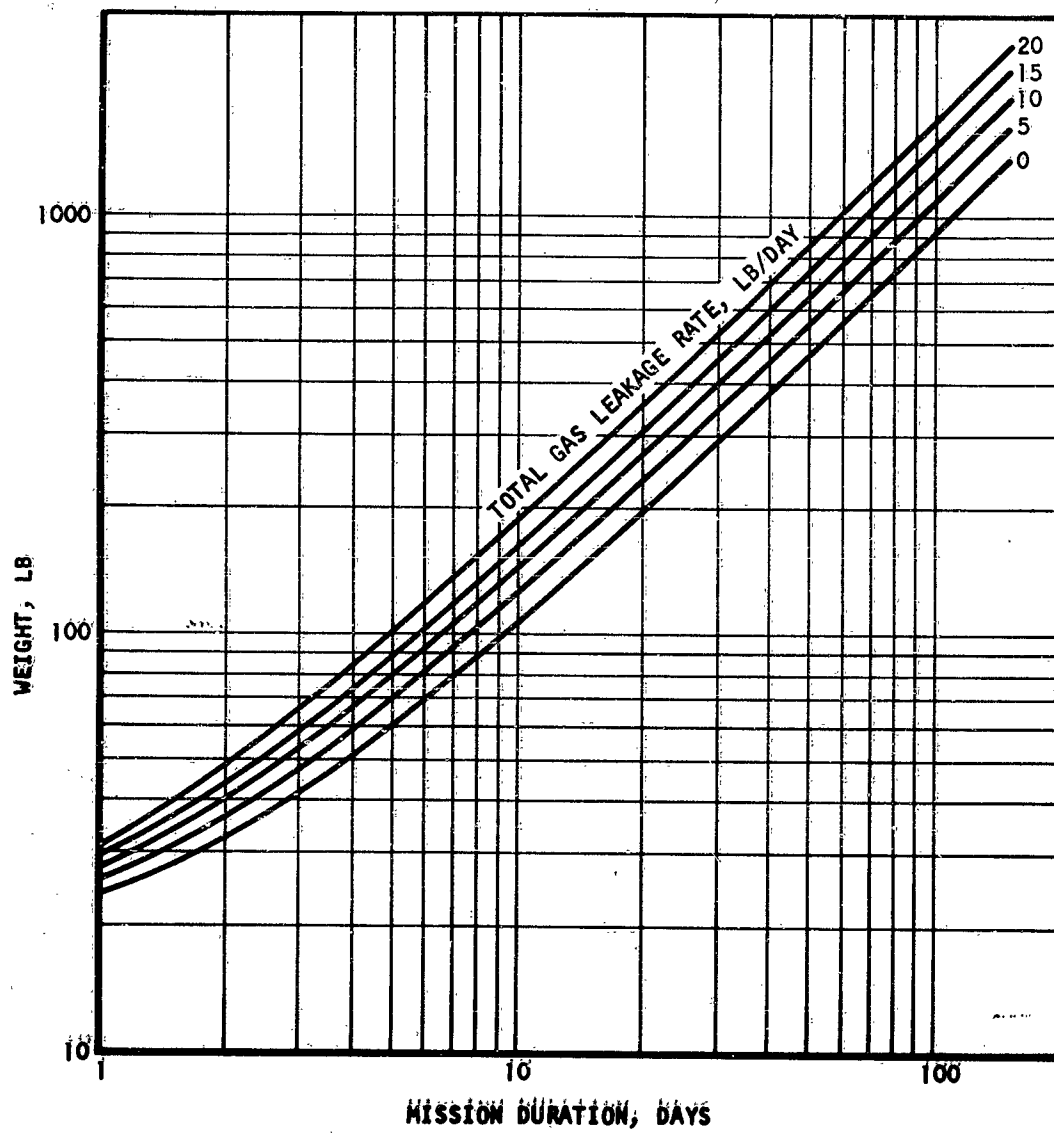


Figure 27. Oxygen Supply Subsystem Weight (N=4)

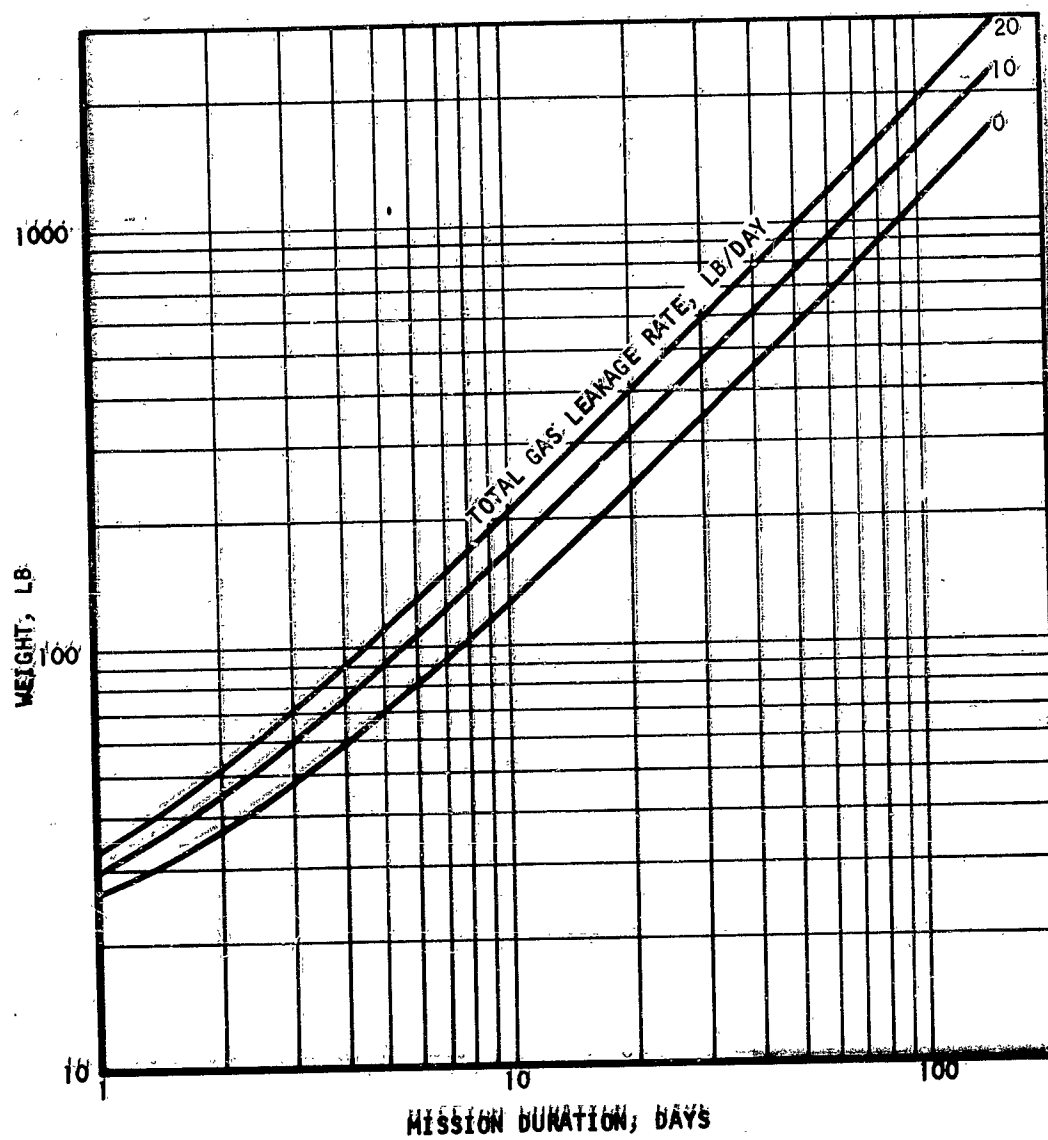


Figure 28: Oxygen supply subsystem (N=5)

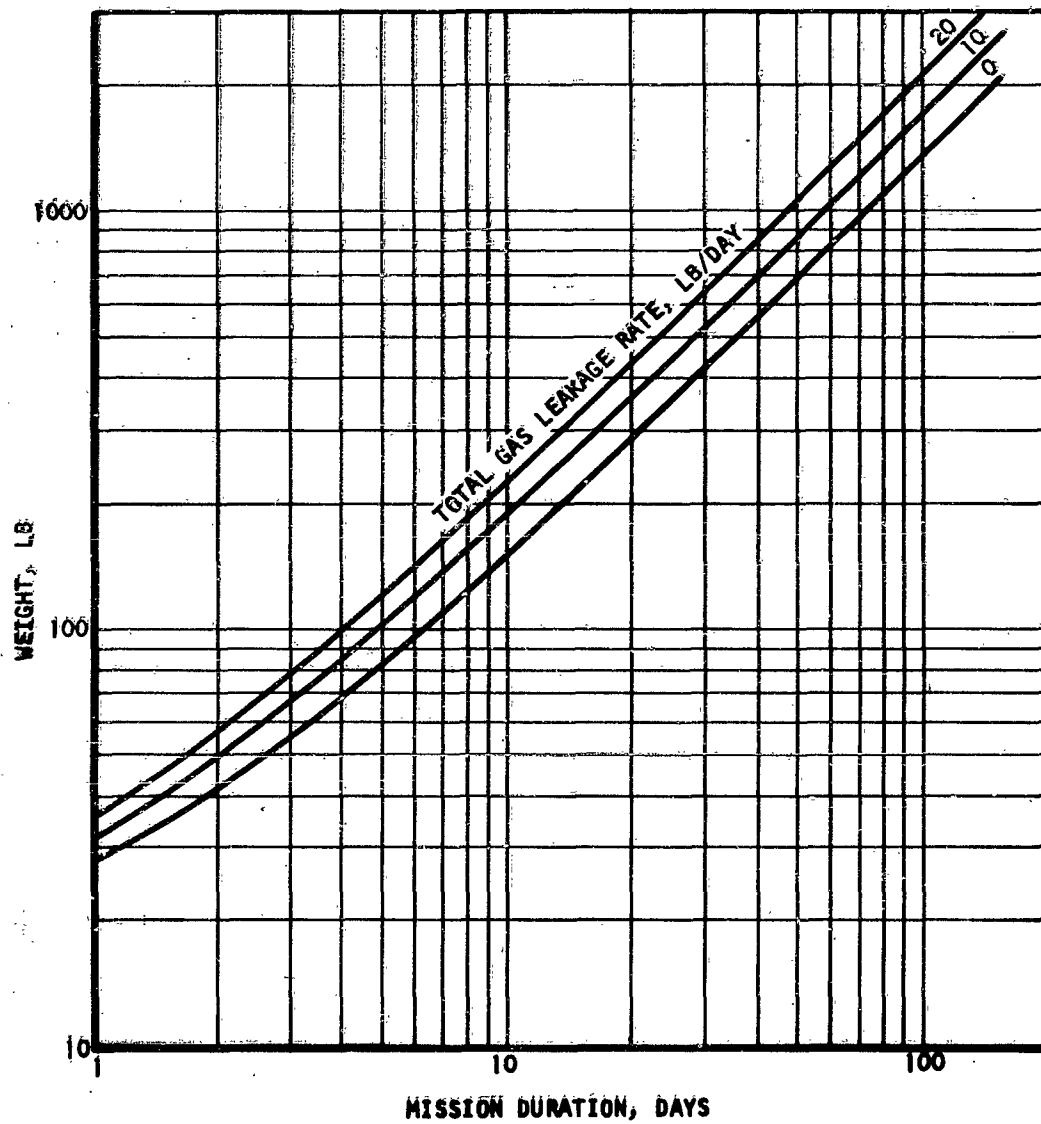


Figure 29: Oxygen Supply Subsystem Weight (N=6)



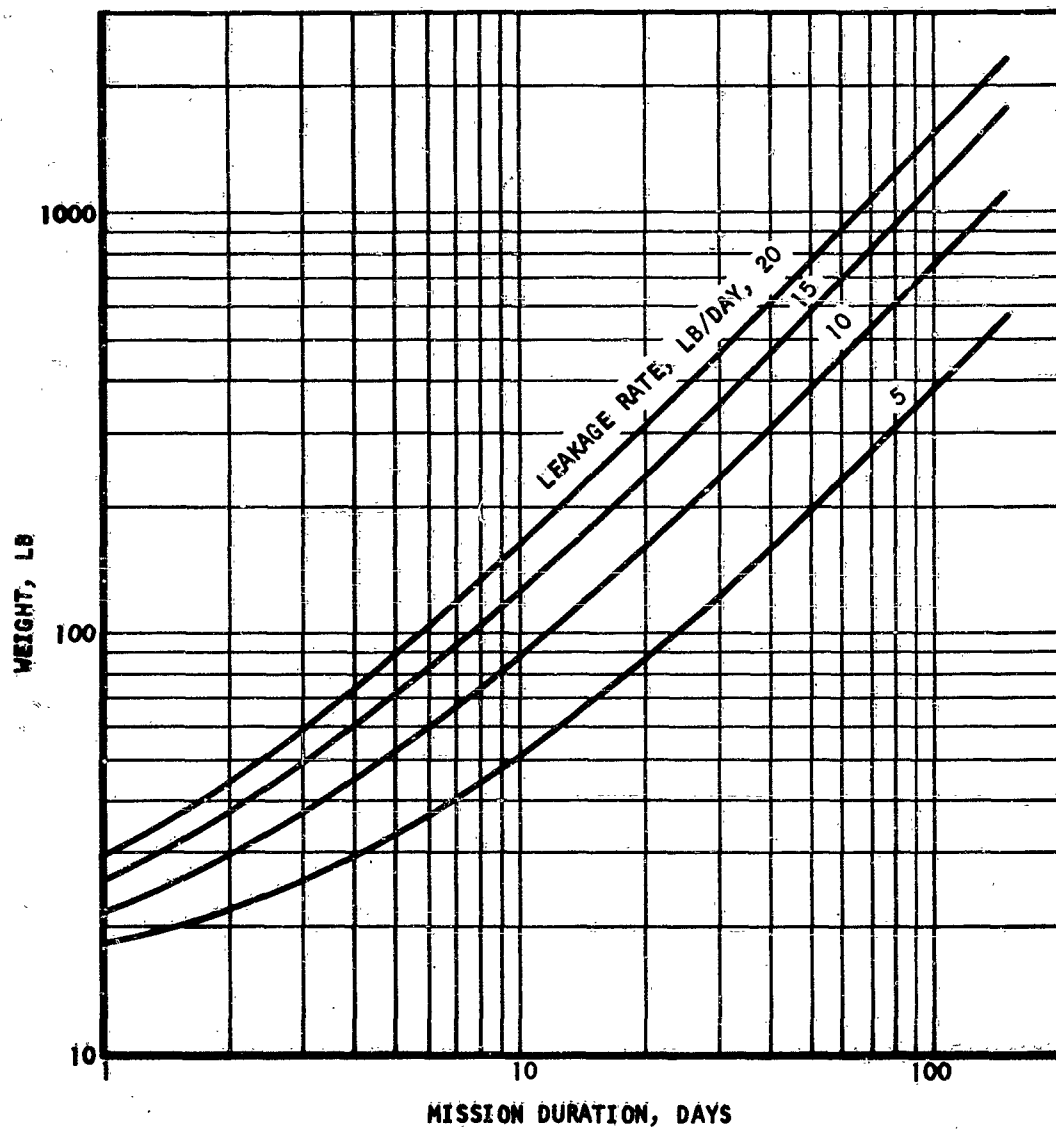


Figure 30. Nitrogen Supply Subsystem Weight

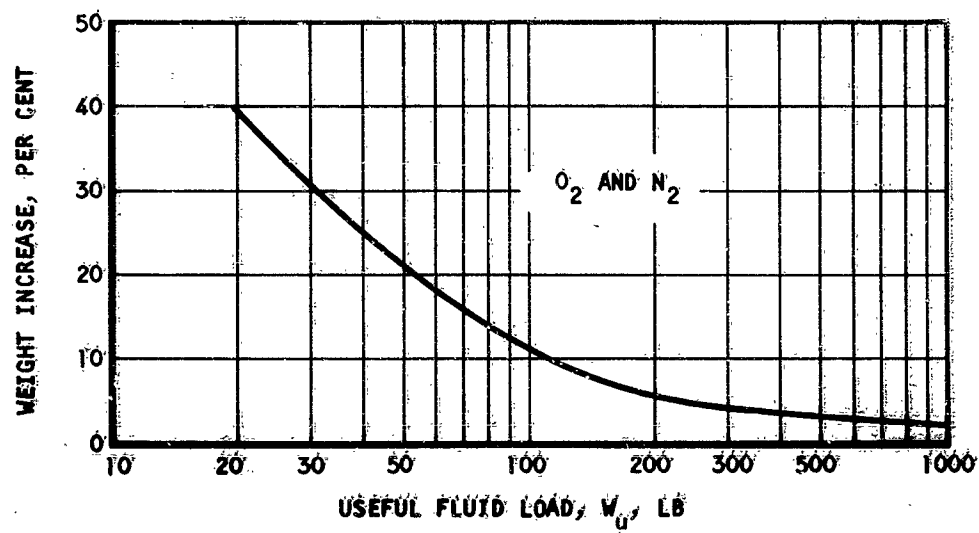


Figure 31. Nitrogen and Oxygen Penalty for 2 Bottles Sharing Load

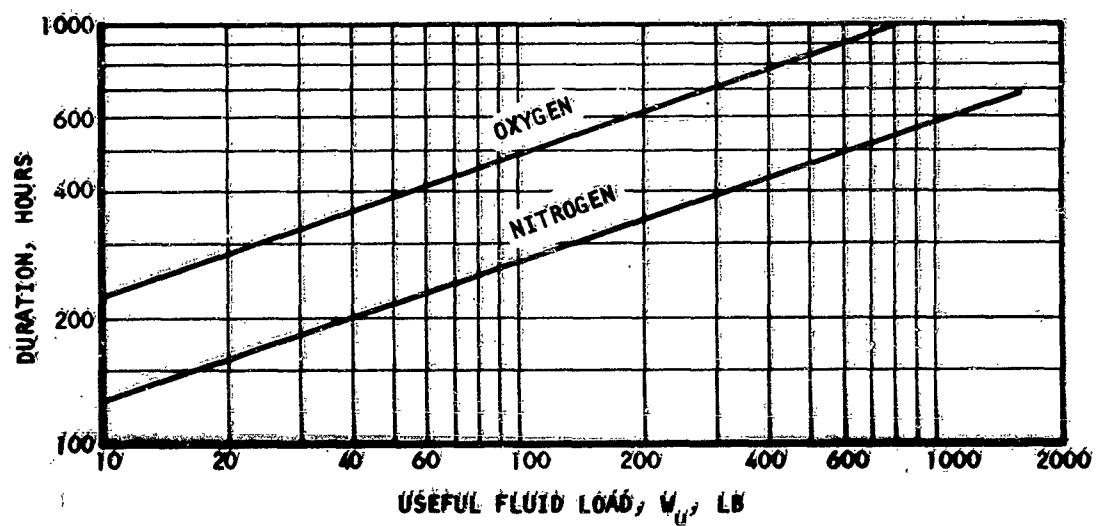


Figure 32. Supercritical Vessel No-Loss Hold Duration

## SECTION V

### HUMIDITY CONTROL SUBSYSTEMS

#### GENERAL CONSIDERATIONS

Humidity control of a space vehicle cabin atmosphere involves the removal of the water vapor produced by the crew members. As discussed in Section I of this report, the rate of production of water vapor by respiration and perspiration varies greatly, depending on the occupants' metabolic rate and also on their activity. In this section, the rate of water vapor emitted is taken as the average value of 2.2 lb per man-day. If water is produced at a rate higher than average, the cabin relative humidity will rise slightly; this does not present any disadvantage, since the requirements for relative humidity are very broad, as seen by the comfort zone definition in Figures 4a and 4b.

The water recovered from the cabin atmosphere is relatively pure and can easily be made potable. The purification process involves simple filtration through activated carbon beds. This fact should be borne in mind when comparing the possible means of moisture removal.

In this section, the various methods of controlling the moisture level in the space vehicle cabin are reviewed and compared on a subsystem basis. A summary of the conclusions drawn from this study follows.

#### SUMMARY

Humidity control by moisture condensation in a cooler-condenser with subsequent liquid water separation is the best process available at this time. Simplicity, low specific weight, relatively low heat rejection loads, and pumping power requirements are the attributes of the cooler-condenser process which make it a preferred method of humidity control of space vehicle cabin atmosphere. In addition, the water recovered is easily processed for drinking.

Cooler-condenser heat exchangers have been developed for some time, and no special problems are anticipated for zero-gravity environment, since the water condensed in the cooler is blown through the exchanger by the process air being cooled. Of the several possible methods of liquid water separation from the process air stream, cyclone type separators appear promising. They have no moving parts, are simple in design and fabrication, and are essentially lightweight. Although cyclone separators have been extensively used in industrial applications, they are still in the development stages for operation under zero-gravity operation.

#### Moisture Removal by Chemical Absorption

Water removal by absorbent materials is not attractive for space vehicle installation because of the several serious disadvantages common to most absorbing materials. These are listed below.

- a. The reactions involving water absorption by a solid liberates an amount of heat equal to the heat of condensation of the water, plus the heat of reaction. The total amount of heat rejected in the process is in general much higher than that involved in a simple condensation process (Reference 1).
- b. For long mission duration, absorbents must be of the regenerable type to minimize weight. Most chemical absorbents need temperatures on the order of 400 to 500°F or above for regeneration. A heat source at these high temperatures is not readily available aboard space vehicles; electrical power would most probably be used for regeneration of the absorption beds and this at a considerable penalty, since the heat of regeneration is the sum of the heat of reaction and the heat of condensation.
- c. The specific weight of the chemical absorbents is, in general, heavier than that of the available adsorbents which have lower heat rejection load and power requirements.
- d. The water removed cannot be recovered as a liquid even in regenerable systems.

In conclusion, it seems that for space vehicle applications, no specific advantage favors the use of absorbing materials in preference to the other methods of moisture removal.

#### MOISTURE REMOVAL BY ADSORPTION

##### General

Humidity control by solid adsorbents, such as silica gel or molecular sieves, is more attractive than water removal by chemical absorbents. No heat of reaction is involved in the process, and the heat of adsorption released is roughly the heat of vaporization of the water. The saturated adsorbents can be regenerated by addition of heat to the bed at a much lower temperature level than required to regenerate the chemical absorbents; 250°F is usually quoted for silica gel. Regeneration also can be achieved partially by evacuating the bed to vacuum; this process, however, is relatively slow, and its dynamic characteristics are not well known at the present time. It appears that heat addition to the saturated bed, coupled with evacuation to vacuum, would be very satisfactory for systems in which water is dumped overboard. A desorption temperature of 150°F is sufficient in this case.

The characteristic adsorption curves for silica gel and three types of molecular sieves are given in Figure 33. Silica gel has a much higher capacity than the molecular sieves at the water vapor pressures encountered in space vehicle humidity control systems; it is the only adsorbent considered for moisture removal.

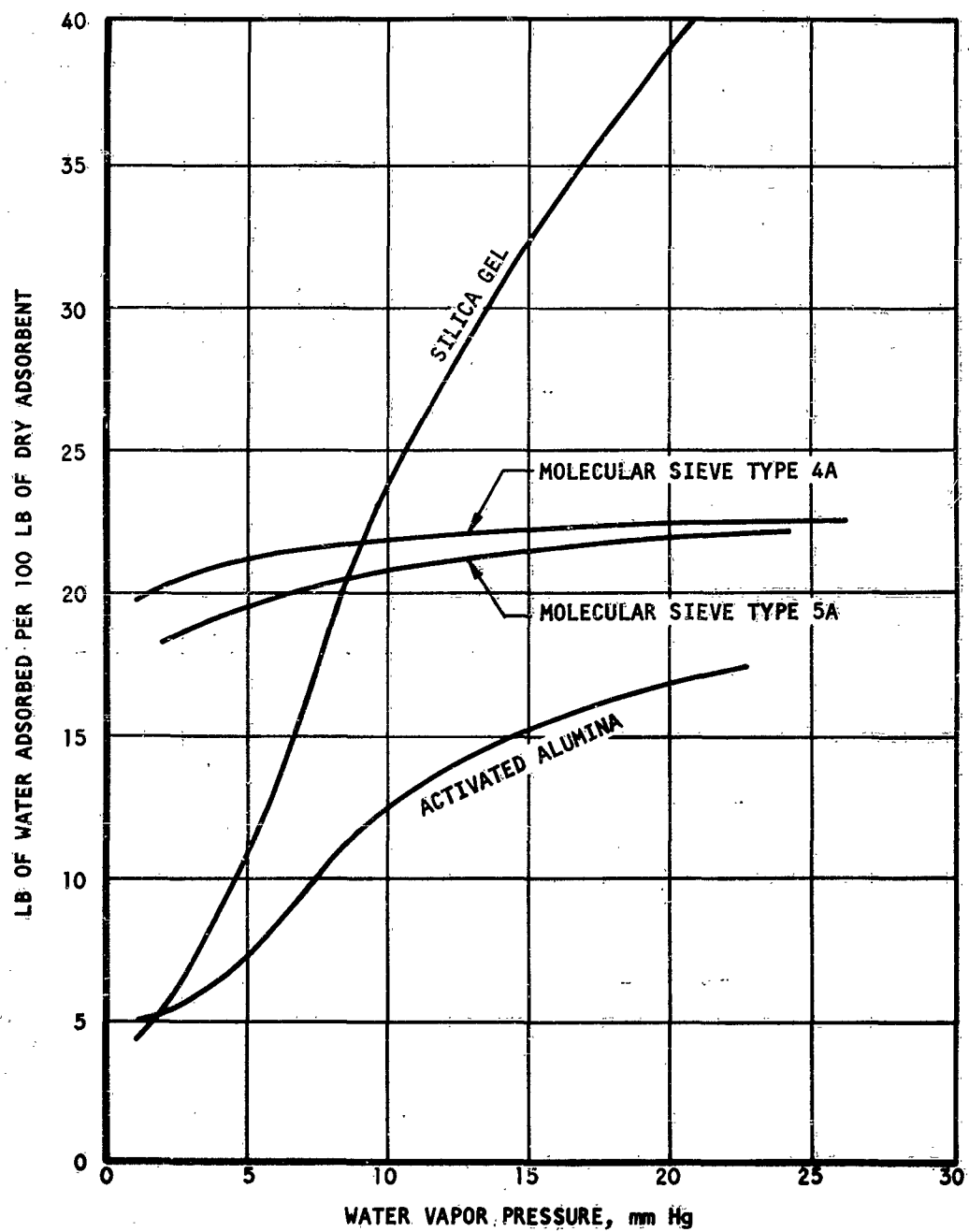


Figure 33. Water Adsorption Isotherms at 77°F

### Non-Regenerable Silica Gel Subsystem

For missions of brief duration, a system in which the humidity is removed from the cabin air by circulating it through a silica gel bed is very attractive because of its simplicity. This system requires no valving, heating loops, nor cooling. The weight of such a system is readily estimated from Figure 33, and is shown plotted in Figure 34 as a function of the mission duration.

Calculations show that the canister weight is only a small portion of the total subsystem weight. It varies between 3 and 5 per cent, depending on the pumping power expended to circulate the process air through the silica gel bed and also on the pressure level of the air in the system. Here, it was assumed that the bed utilization efficiency, based on the isotherm adsorption capacity of the silica gel, was 0.75. The weight of the system, neglecting secondary effects, is proportional to the number of crew members. It should be noted that, for high utilization efficiency, the length of the silica gel bed must be kept above a minimum length which depends on the bed face area and on the process gas superficial velocity.

Since the weight of this non-regenerable silica gel system is proportional to the mission duration, its field of application is severely restricted to short-duration missions.

### Regenerable Silica Gel Subsystem

#### 1. System Description

For mission durations in excess of a few days, regeneration of the silica gel bed is indicated. A water removal system of this type is depicted in Figure 35. Two identical silica gel beds are required, one adsorbing and the other desorbing. Operation is fairly simple: when the process water concentration at bed outlet reaches a certain preset value, all the valves of the system are turned 90° from the position shown, and heat is applied to the saturated bed, which is then evacuated to vacuum. The process air is routed through the other silica gel bed. Water vapor from the saturated bed is dumped overboard. Switching of the valves is usually automatic at fixed time intervals. The valve actuating mechanism can be a cam shaft driven by an electric motor.

The heater provided for bed desorption can serve a dual purpose: it can be used for removing the heat adsorption from the bed during the adsorption period, thus increasing the capacity of the silica gel. However, this adds to system complication and is possible only when the heat of desorption is provided by a hot fluid. Often no suitable fluid loop at the temperature required for desorption (150°F) is available aboard the vehicle, and electrical power must be used.

It is to be noted here that water is not easily recovered from a saturated bed and is evacuated overboard. If the regenerable silica gel system is considered for installation aboard a vehicle where no excess water is produced, then the system must be penalized by the amount of water dumped overboard.

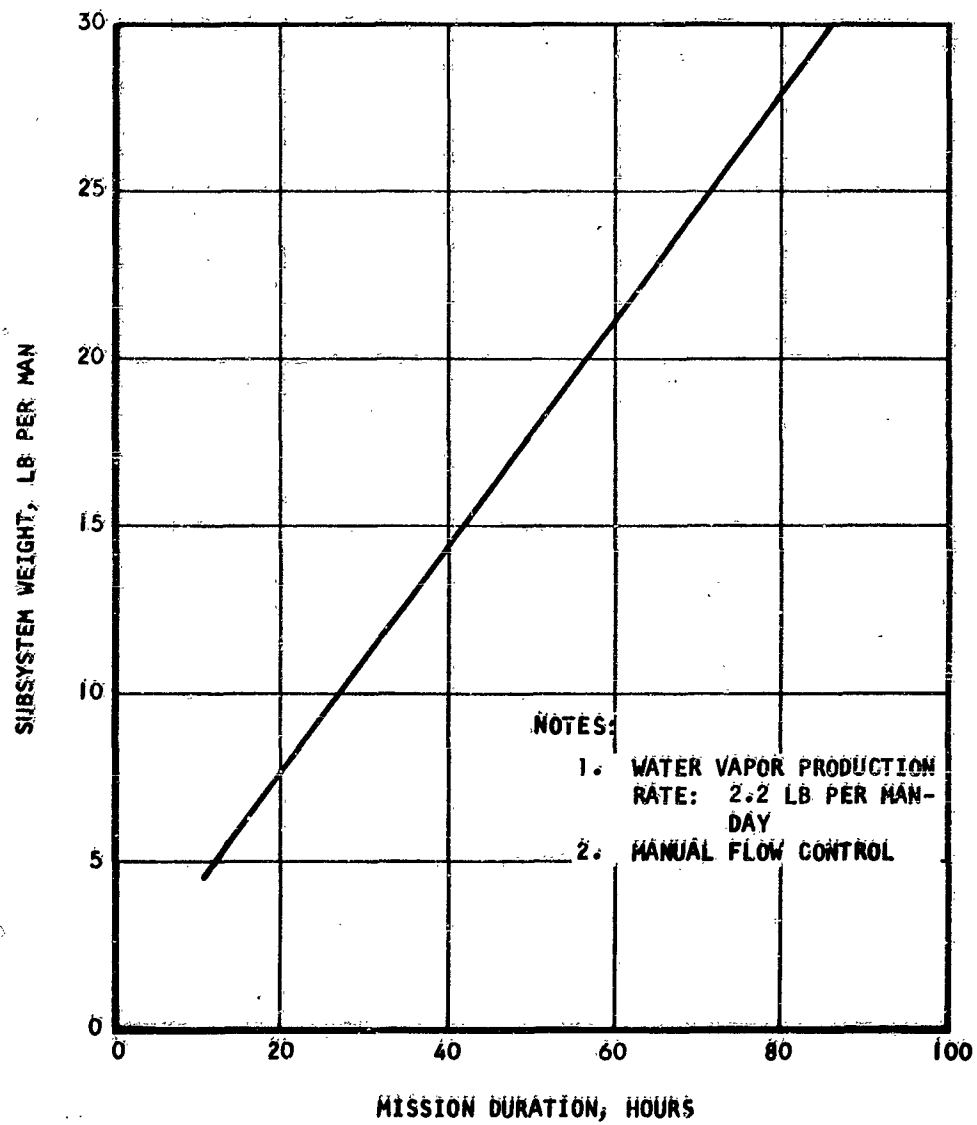


Figure 34. Non-Regenerable Silica Gel Humidity Control Subsystem Weight



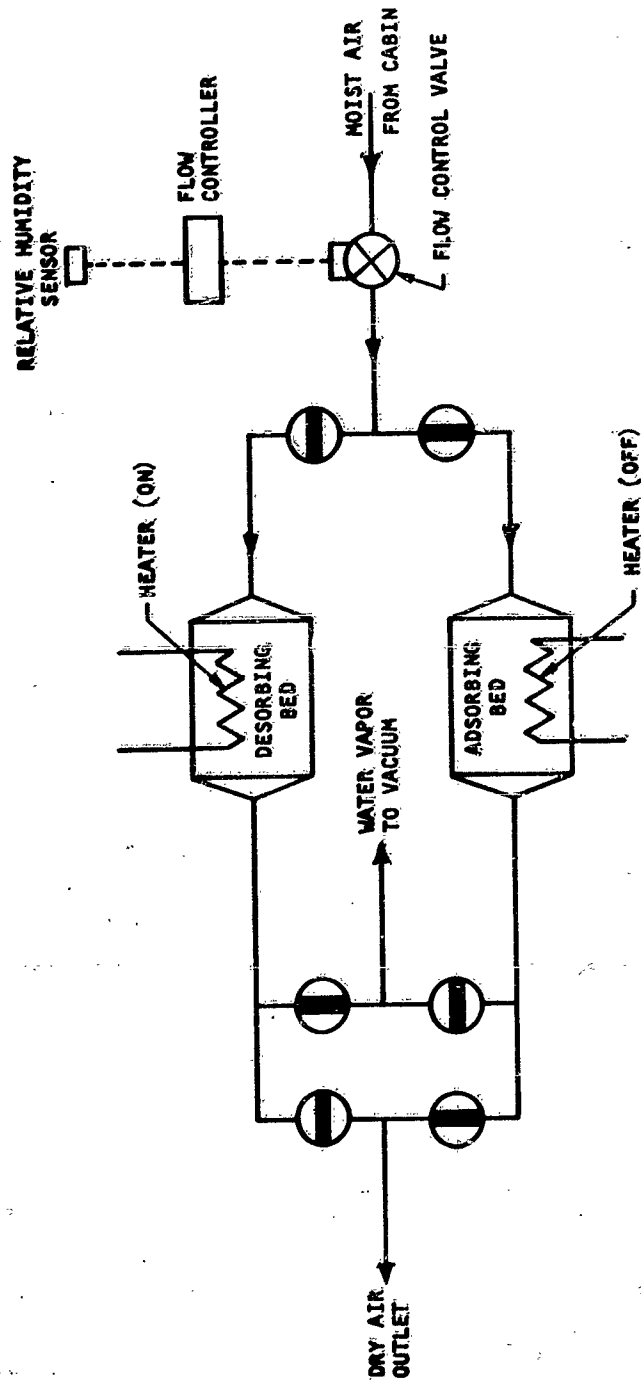


Figure 35. Regenerable Silica Gel Humidity Control Subsystem

## 2. Silica Gel Bed Characteristics

Calculations were performed to determine the weight of a system such as that depicted in Figure 35. The following assumptions were used in the computations:

- a. The silica gel is dry at the beginning of the adsorption cycle.
- b. The water vapor concentration in the air exhausting from the system is negligible.
- c. The rate of water adsorption is taken as 2.2 lb per man-day.
- d. Calculations were performed for isothermal adsorption; an allowance of 20 per cent on the bed length is made to account for non-isothermal operation.
- e. The pressure drop through the silica gel bed is calculated by the method presented in Reference 1.
- f. The pumping power is calculated from the pressure drop assuming a fan motor efficiency of 0.45.
- g. Canister weight is calculated from a model using the following expression:

$$W_c = 3.6 A_F + 2.552 \sqrt{A_F} L, \text{ lb} \quad (5)$$

- h. The system was not penalized for the water dumped overboard.
- i. The weight includes the average water content of two beds over the cycling period. This is about equal to the water content of one bed at the end of its adsorption period.
- j. The silica gel particle size is taken as 6 to 8 mesh.
- k. The cycling time is one hour.

The results of the computations given in Figure 36 show the effect on the silica gel bed weight of the pumping power expended to circulate the air through the bed. The plot is given for three values of the cabin relative humidity, namely, 50, 60, and 70 per cent, and cabin pressures of 5, 7, 10, and 14.7 psia. Low pumping power results from large face areas and short bed lengths for a given adsorption period. Short lengths, in general, lead to low utilization efficiency and correspondingly high weight. On the other hand, high pumping losses occur at the higher superficial air velocities which also produce low bed utilization efficiencies.

## 3. Subsystem Integration

The weights of the components of the regenerable silica gel humidity control subsystem depicted in Figure 35 are listed in Table 7. In addition to the accessory weight, the total subsystem weight includes the weight of the water contained in the bed during operation.

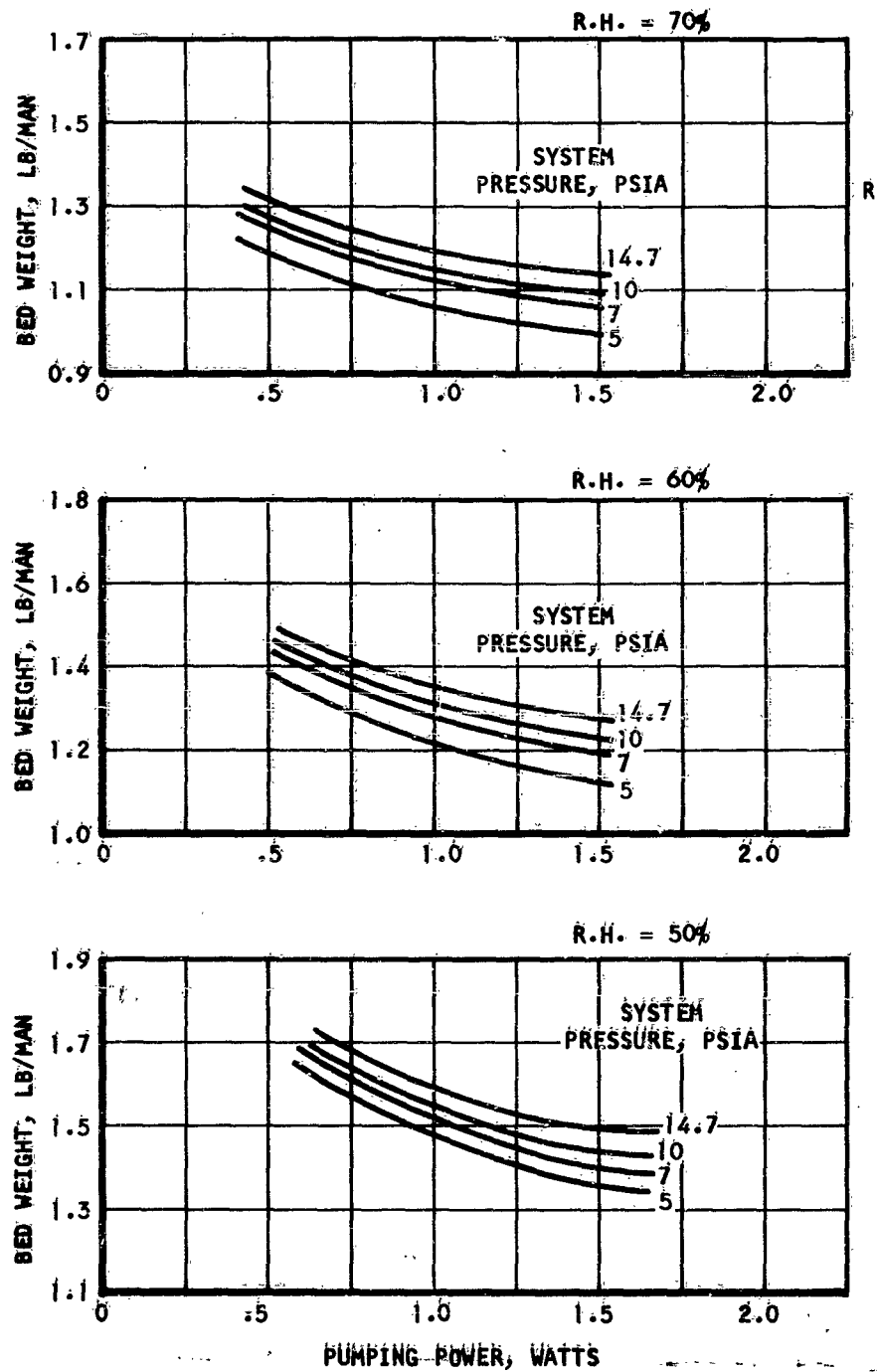


Figure 36. Silica Gel Bed Characteristic Weight  
(One Canister)

TABLE 7  
REGENERABLE SILICA GEL SUBSYSTEM ACCESSORY WEIGHT  
(3-MAN SYSTEM)

| Component                 | Number<br>Required | Total<br>Weight, lb |
|---------------------------|--------------------|---------------------|
| Heater                    | 2                  | 0.6                 |
| Switching valves          | 12**               | 4.2                 |
| Valve actuator and drive* | 1                  | 2.5                 |
| Flow control valve        | 1                  | 0.6                 |
| Flow controller*          | 1                  | 2.5                 |
| Sensor*                   | 1                  | 0.1                 |
| Ducts                     | --                 | 0.5                 |
| Total Weight              |                    | 11.0                |

\* Fixed weight accessory

\*\*Valving is redundant for safety reasons

Since the fixed portion of the accessory weight is a sizeable percentage of the total subsystem weight, the total weight of the system cannot be averaged on a number-of-crew-member basis. Instead, the variable portion of the accessory weight is taken as proportional to the square root of the number of crew members, and the total subsystem weight is expressed by

$$W_T = W_B N + 3.41 \sqrt{N} + 5.1, \text{ lb} \quad (6)$$

where  $N$  is the number of crew members, and  $W_B$  is the weight of the two silica gel canisters.  $W_B$  can be obtained for various cabin atmosphere conditions from the plots of Figure 36.

Another subsystem characteristic of importance for space vehicle installation is the heat required by the system for desorption of the bed. As pointed out previously, the silica gel desorption temperature is approximately 150°F. If electrical power is used as a heat source for bed desorption, the penalty incurred by the subsystem can be expressed by the following equation:

$$W_{PI} = \frac{Q_D N (PP)}{3.413}, \text{ lb} \quad (7)$$

where  $Q_D$  is the heat requirement for desorption as given in Table 8,  $N$  is the number of crew members, and (PP) the vehicle power penalty in lb per watt of power consumed.

After desorption, the bed temperature is 150°F, and the heat stored in the bed is rejected partly to the environment and partly to the process air stream after valve switching. In any case, this amount of heat constitutes a heat load on the vehicle thermal management system. In addition, since no cooling of the bed is provided, the heat released during adsorption is dumped into the process air, thus raising its temperature; part of the heat of adsorption is expended in warming the bed itself. This amount of heat, however, is small compared to the load rejected to the air. The total heat rejection from the silica gel system to the vehicle thermal management system is the same as required for bed desorption, which is given in Table 8. The penalty associated with this heat rejection load is given by the expression

$$W_Q = Q_R N (RP), \text{ lb} \quad (8)$$

where  $Q_R$  is listed in Table 8, and (RP) is the vehicle heat rejection penalty in lb per Btu/hr.

The water removed from the process air is dumped overboard upon desorption of the silica gel bed. In vehicles where no surplus of water exists, this is a serious disadvantage for which the system should be penalized. This penalty is obviously a function of the number of crew members and of the mission duration; it can be expressed by

$$W_{H_2O} = 2.2 N \tau, \text{ lb} \quad (9)$$

**TABLE 8**  
**HEAT REQUIRED FOR DESORPTION AT 150°F**  
**AND**  
**HEAT REJECTED DURING ADSORPTION**  
**(BTU/MAN-HR)**

| System Pressure, psia   |     | 5     | 7     | 10    | 14.7  |
|-------------------------|-----|-------|-------|-------|-------|
| Cabin relative humidity | 50% | 148.0 | 148.5 | 148.7 | 149.1 |
|                         | 60% | 144.5 | 146.2 | 146.4 | 146.6 |
|                         | 70% | 143.7 | 144.2 | 144.3 | 145.0 |

**TABLE 9**  
**TYPICAL SILICA GEL SUBSYSTEM PUMPING LOSSES (WATTS)**

| System Pressure, psia   |     | 5    | 7    | 10   | 14.7 |
|-------------------------|-----|------|------|------|------|
| Cabin relative humidity | 50% | .635 | .657 | .632 | .622 |
|                         | 60% | .484 | .546 | .534 | .519 |
|                         | 70% | .451 | .467 | .451 | .444 |

where  $\tau$  is the mission duration in days.

Another factor, which must be accounted for in the system equivalent weight, is the pumping losses incurred for circulating the process air through the system. The silica gel bed weight was plotted against the system pumping losses which can, in turn, be translated into system weight by the expression

$$W_{p2} = (PL)_T (PP) \quad (10)$$

where  $(PL)_T$  is the system pumping losses in watts, and  $(PP)$  is the vehicle power penalty. Here the subsystem power loss is made up of the bed, valves, and piping losses. Table 9 gives the pumping losses in the system valves and piping for a fan motor efficiency of 0.45.

The subsystem total equivalent weight, taking into account all the penalties associated with its installation aboard a space vehicle, can then be expressed by collecting all the weights defined in the preceding paragraphs; the subsystem is then characterized fully by -

$$W_E = 5.1 + 3.41 \sqrt{N} + W_B N + (PP) \left[ \frac{Q_D N}{3.413} + (PL) \right] + (RP) Q_R N + 2.2 N\tau \quad (11)$$

It should be noted that the vehicle power penalty can be a function of the mission duration (e.g., if the power source is chemically fueled).

#### MOISTURE REMOVAL BY COOLER-CONDENSER

##### General

A relatively simple method of controlling the humidity of the cabin air is to condense the moisture in a heat exchanger and to remove the condensate from the process air stream. Figure 37 is a schematic diagram of such a system. Water from the moist air stream condenses on the surface of the cooler-condenser and is blown downstream by the air flowing through the heat exchanger. Part of the liquid water droplets are separated from the main air stream in a water separator; the air is then returned to the cabin or to another subsystem for further processing. The condensate is channeled to a reservoir (shown here as a bellows), pumped to the water management subsystem, and dumped overboard or returned to the cold side of the cooler-condenser, where it is evaporated at low pressure, to provide part of the heat sink for humidity condensation.

The system diagram illustrates a possible arrangement for the collection and disposal of the water separated, suitable for operation in a zero-gravity environment. The condensate is ducted by means of wicks from the water separator to a bellows-type reservoir. As the water in the reservoir accumulates, an electrical contact activates a solenoid actuator which compresses the bellows and thus pumps the water through a check valve

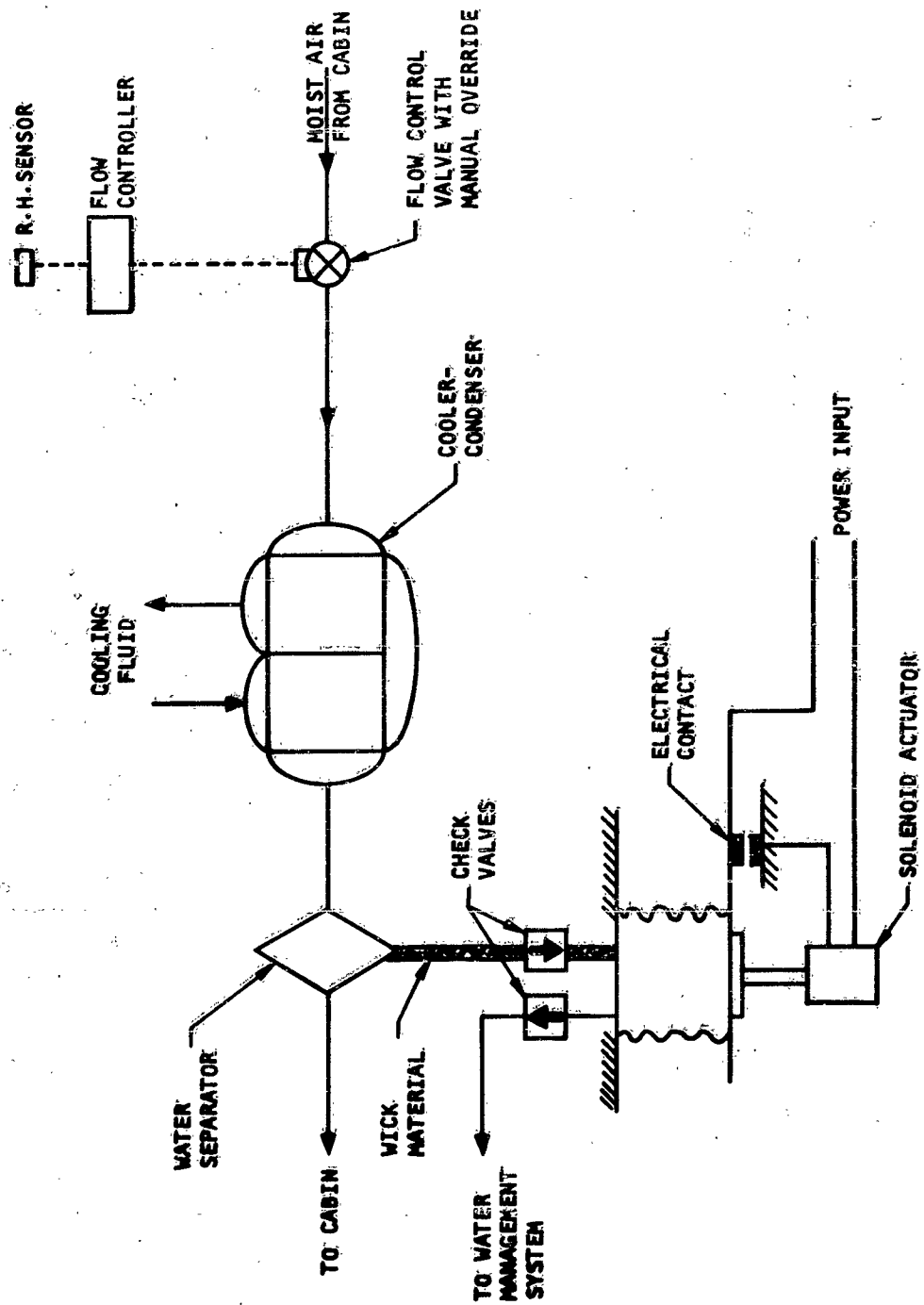


Figure 37. Cooler-Condenser Humidity Control Subsystem



to the water management subsystem. As the bellows is depressed, the contact is broken and the cycle repeated.

In the following discussions, the characteristics of the cooler-condenser are given in terms of system parameters, and the various means of separating the condensate from the process air stream are reviewed and discussed.

#### Cooler-Condenser Performance

The flow required through the system for the removal of 2.2 lb of water per man-day is a function of the inlet and outlet water concentrations in the process air stream, of the cabin pressure, and of the water separator efficiency. The expression for the flow requirement is given by the equation

$$w_g = N_1 M_1 = \frac{\bar{w}_{H_2O} M_1}{18 \eta_{sep}} \frac{(1 - y_2)}{(y_1 - y_2)} \quad (12)$$

Graphic solution of this equation is shown in Figures 38 to 40, where the flow requirement is plotted against the cabin relative humidity for cooler-condenser outlet temperatures of 35, 40, and 45°F and cabin pressures of 5, 7, 10, and 14.7 psia. Also, the flow requirement for water removal is plotted against cooler-condenser outlet temperature in Figure 41. In Figures 38 to 40, the humidity control system cooling requirements are also plotted as a function of the cabin relative humidity and cabin pressure. Figure 42 shows the cooling requirements as a function of condenser outlet temperature.

The sharp rise in flow requirement and cooling load at low cabin relative humidity with a flattening characteristic at about 60 per cent relative humidity points to the desirability of maintaining the cabin humidity as high as possible. The comfort zone inside the cabin extends over a wide range of relative humidities with the maximum values compatible with unimpaired crew performance varying between 60 and 70 per cent (see Figure 4b).

These plots also indicate the savings ensuring from low condenser outlet temperatures. This, however, is more difficult to satisfy than high relative humidity. Heat sink temperatures lower than about 40 to 45°F normally impose very high weight penalties on space vehicle liquid cooling loops. These penalties result from the large radiator areas required to cool the heat transport fluid to the temperature level desired for operation of the humidity control system. Temperatures on the order of 40 to 45°F can, however, be achieved by evaporating water or another fluid at low pressure and dumping the vapor overboard. This process can be advantageously used aboard vehicles where material balance shows a surplus production of water. Where a refrigeration system is installed, it is advantageous to operate the heat exchanger at a temperature as low as possible. It should be noted here that the surface temperature of the cooler-condenser must be kept above the freezing temperature of the water. The operating temperature range of the cooler-condenser surface is, therefore, restricted to 32°F.

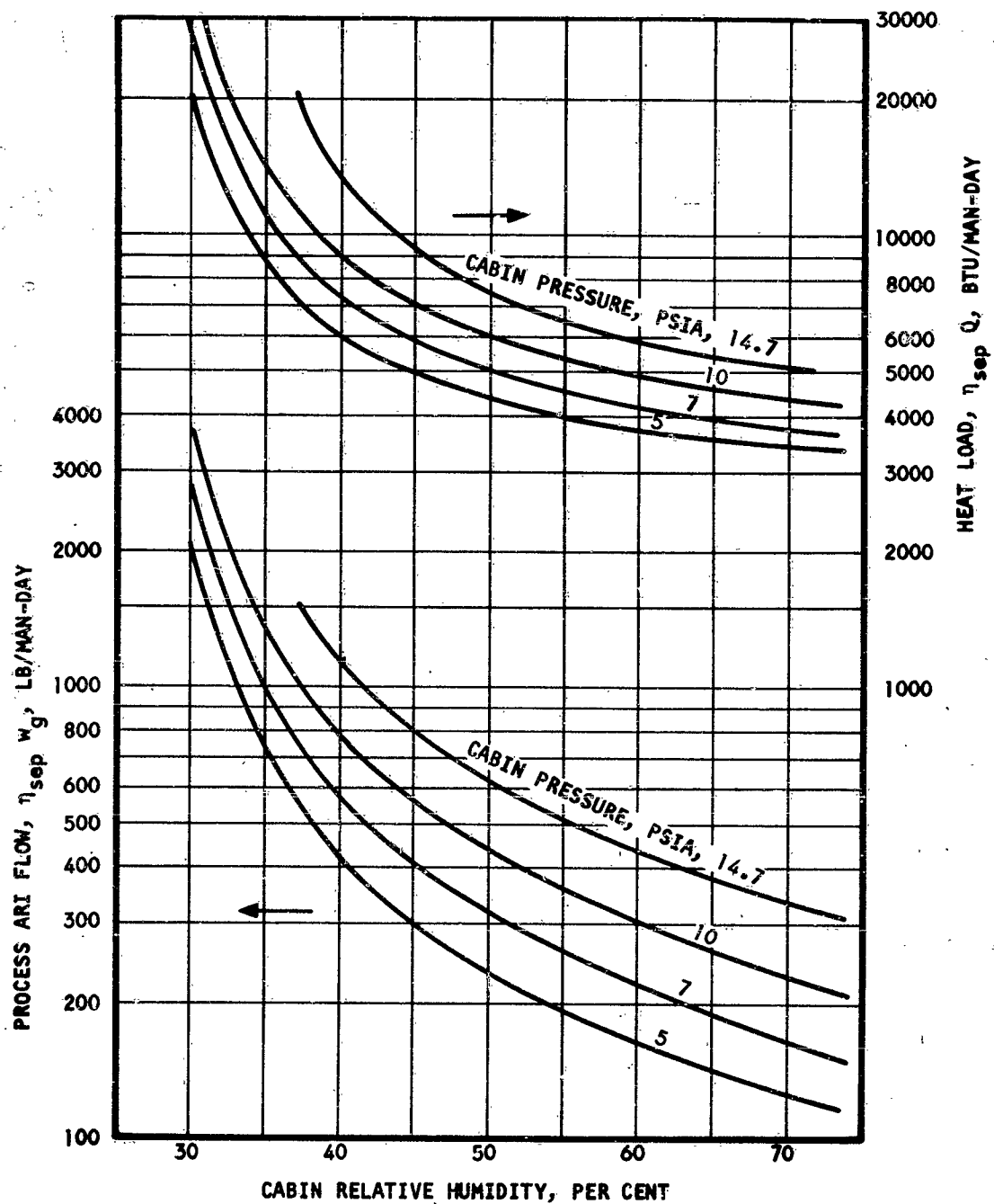


Figure 38. Flow Requirement and Heat Load for Humidity Control-  
Condenser Temperature: 35°F

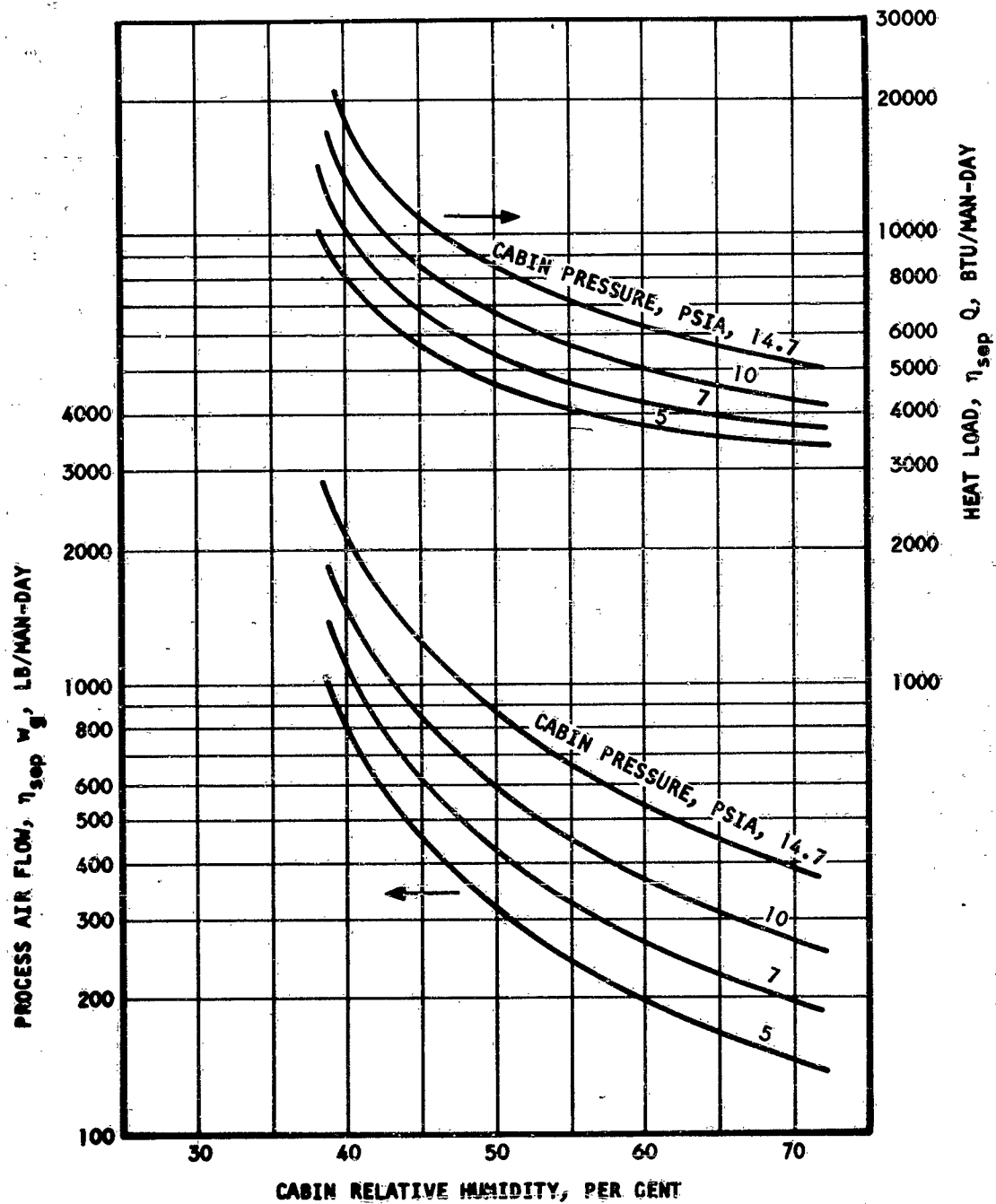


Figure 39. Flow Requirement and Heat Load for Humidity Control-  
Condenser Temperature: 40°F

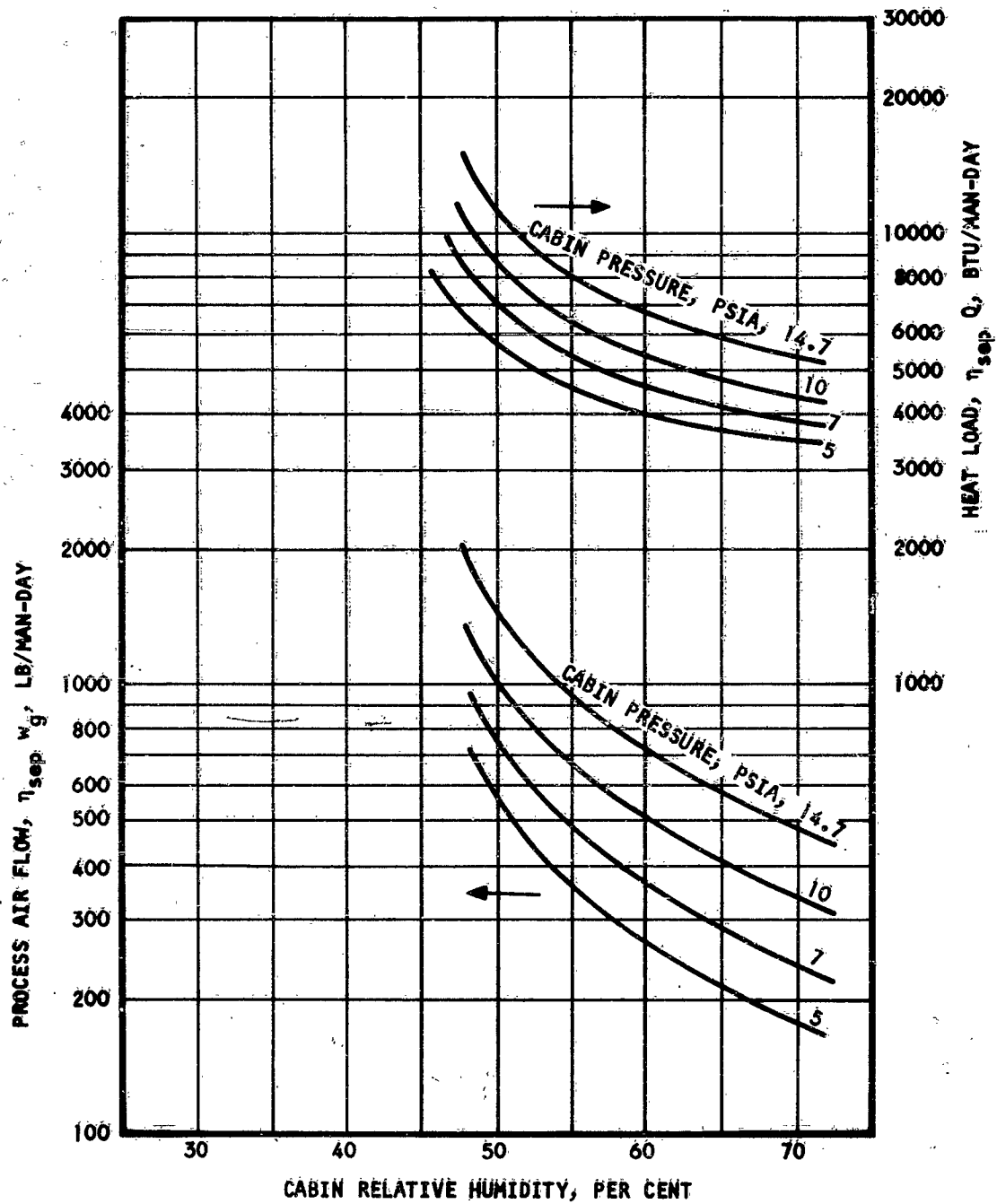
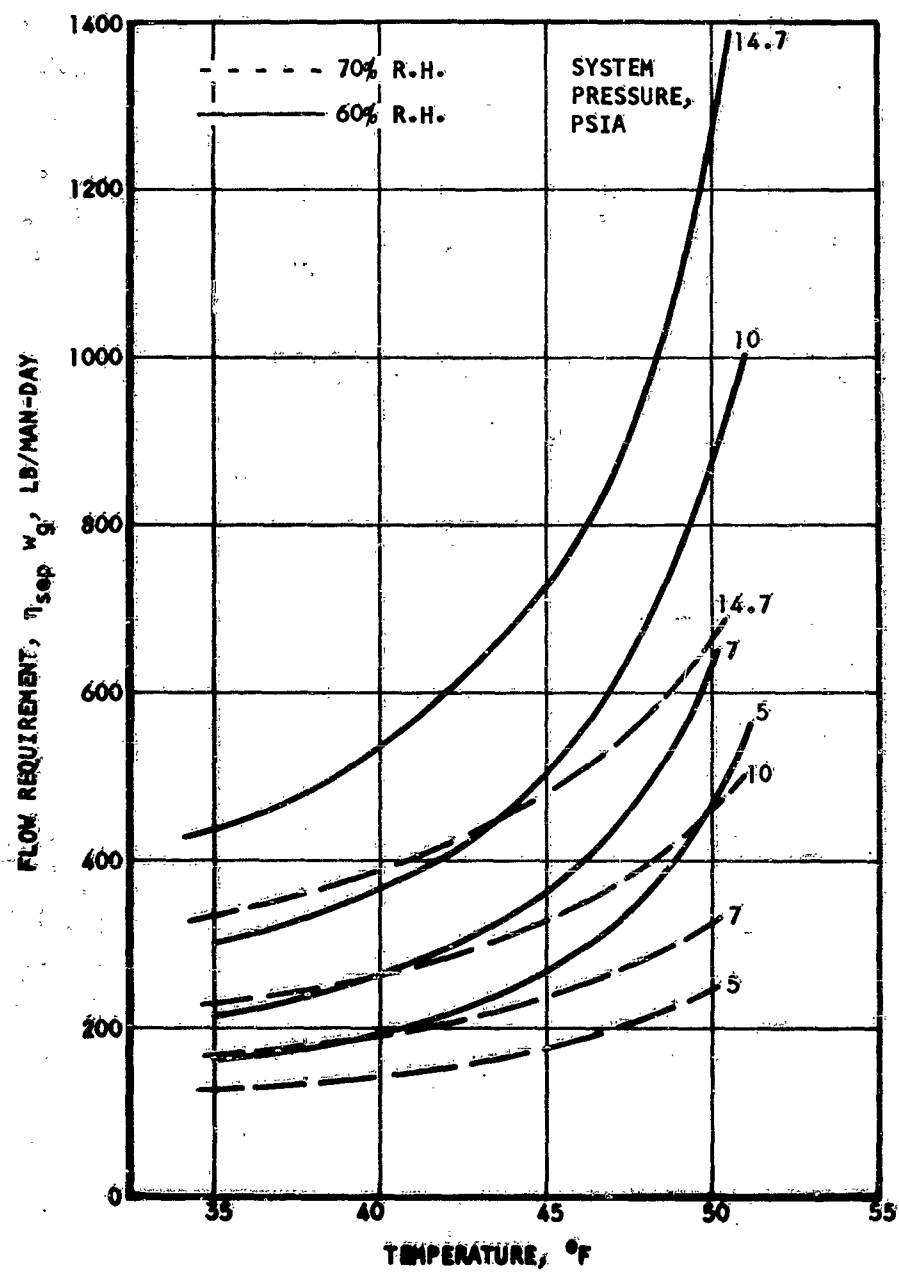


Figure 40. Flow Requirement and Heat Load for Humidity Control-  
Condenser Temperature: 45°F



**Figure 41. Flow Requirement Variation With Outlet Temperature**

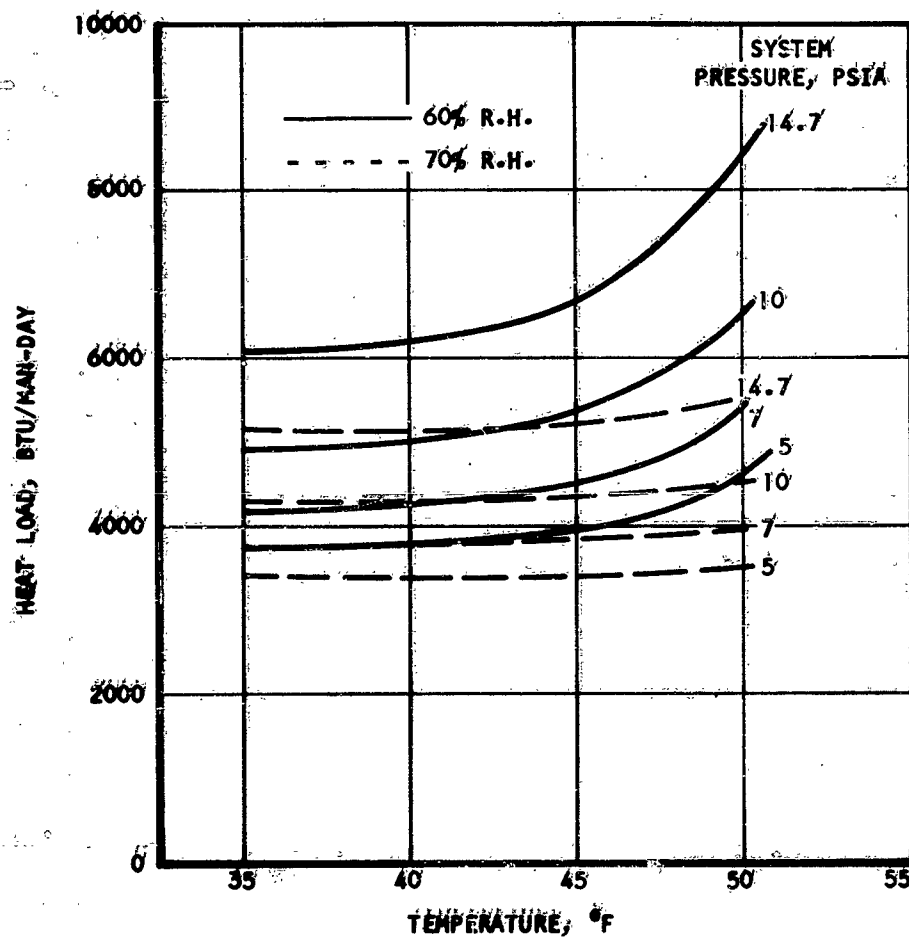


Figure 42. Heat Load Variation With Temperature

The weight of the cooler-condenser was estimated by the methods presented in Reference 1. The calculations were performed assuming a heat exchanger effectiveness of 0.8 for cabin relative humidities of 60 and 70 per cent. The plate fin arrangement used in the design with the air side extended surface defined is given below.

Fin type: rectangular

Offset:  $1/7$  in.

Fin height: 0.153 in.

Fin thickness: 0.020 in.

Number of fins per inch: 16

Plate thickness: 0.020 in.

Material: aluminum

Construction: Double sandwich arrangement

The cold fluid was assumed to be ethylene glycol, and the heat transfer surface on the liquid side was the same as the air side fin, but in a single sandwich arrangement. The results of the calculations are presented in Figures 43 and 44 where the total heat exchanger weight is plotted as a function of the pumping power expended to flow the moist air through the exchanger. The curves are plotted for cabin pressures of 5, 10, and 14.7 psia. Here, the efficiency of the fan and motor drive is taken as 0.45. These plots indicate that not much will be gained by increasing the pumping losses above about 2 or 3 watts.

Selection of the heat exchanger can only be made on the basis of a trade-off study between the pumping losses and the heat exchanger weight. As an example of such a study, heat exchanger weight and pumping power are plotted in Figure 45 against the vehicle power penalty expressed in lb per watt. The trade-off study was conducted for a cooler-condenser outlet temperature of 45°F and cabin relative humidity of 60 per cent.

#### Liquid Water Separator

The condensate blown out of the cooler-condenser by the process air stream is partly entrained in the form of small droplets and partly as drops of liquid water attached to the duct walls. Several means of removing the liquid water from the air stream have been proposed for zero-gravity operation. Among these are the filter separators, such as sponges, and the centrifugal types, such as bend separators, cyclone separators, and rotating separators. All of these types are discussed and analyzed in Reference 1. At present, a certain amount of experience on the sponge separators has been developed from its use in the Mercury capsule. Separators using artificially induced centrifugal fields, on the other hand, are in various stages of development.

Sponge separators are inherently high-energy loss devices; their squeezing mechanism is relatively complex, and their weight is higher than centrifugal-type separators. Of the centrifugal separators, the most attractive for simplicity and reliability is the cyclone separator. It is

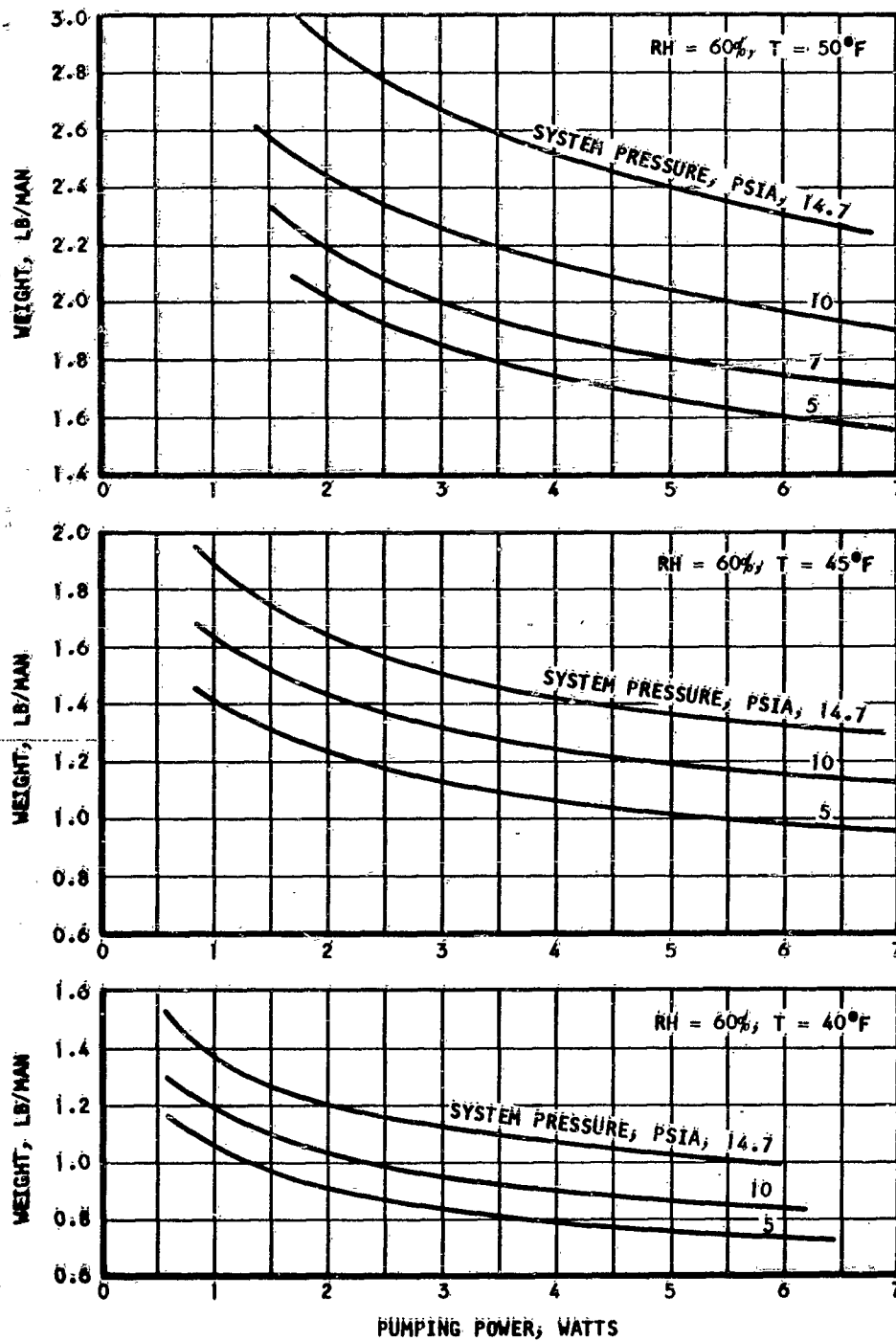


Figure 43. Cooler-Condenser Characteristic Weight (RH=60%)



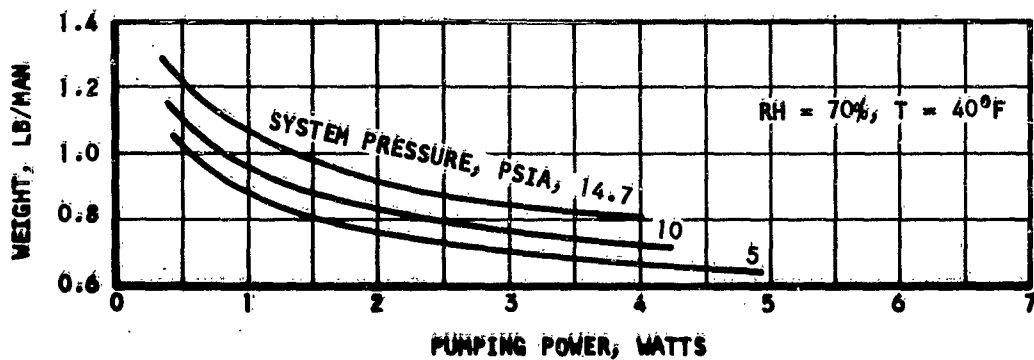
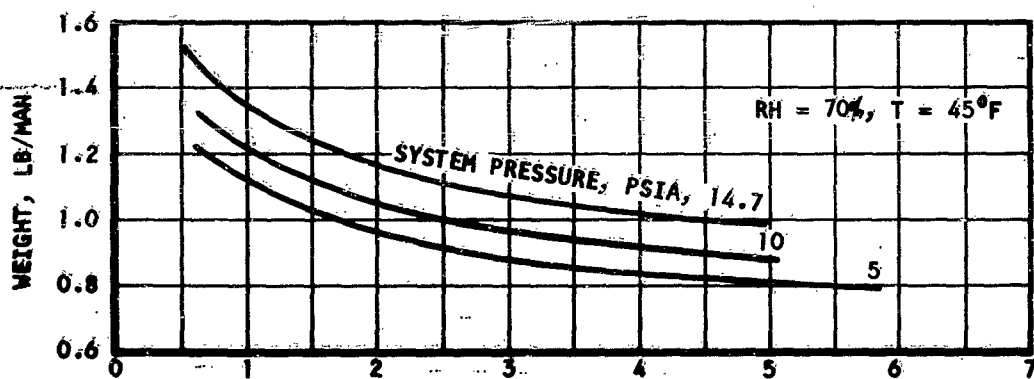
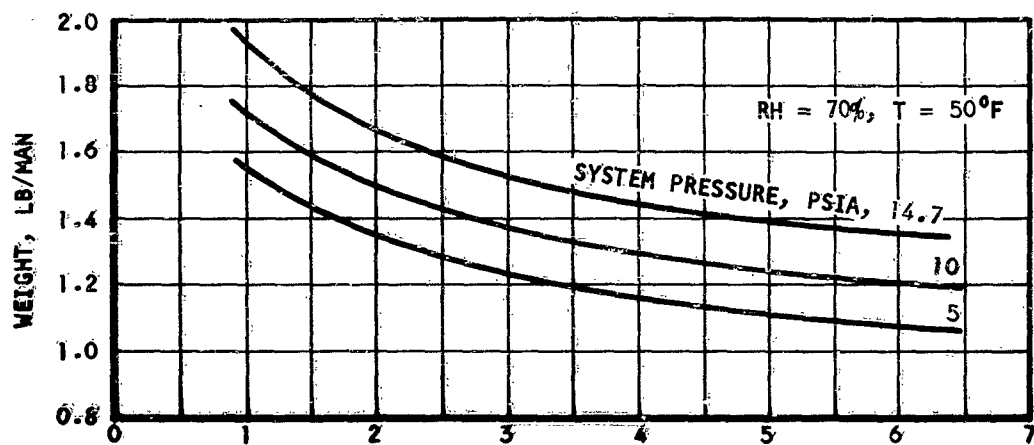


Figure 44. Cooler-Condenser Characteristic Weight ( $RH=70\%$ )

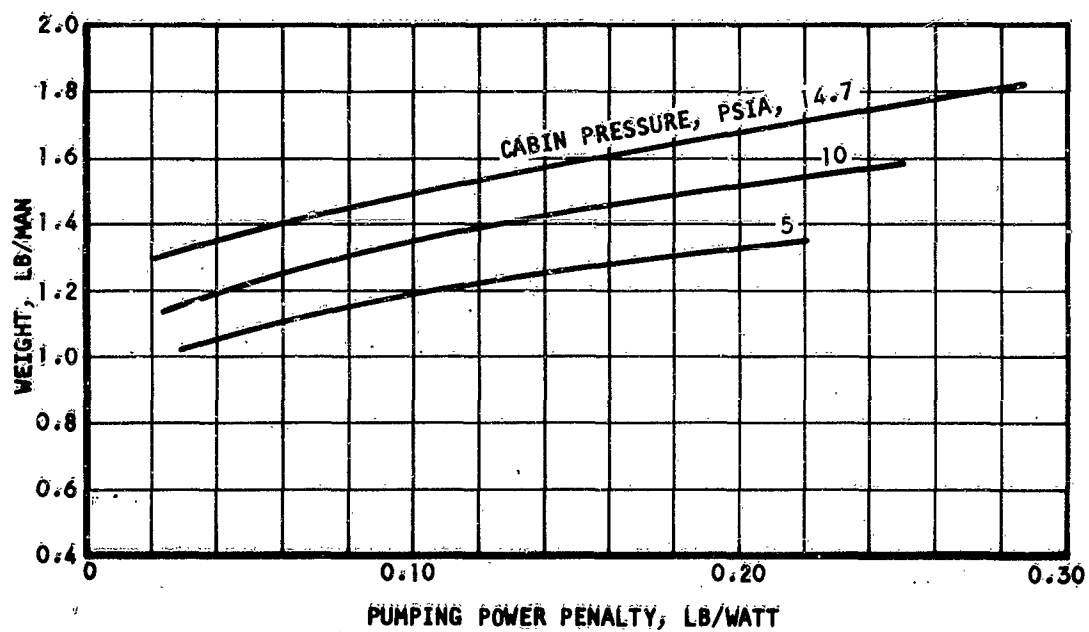
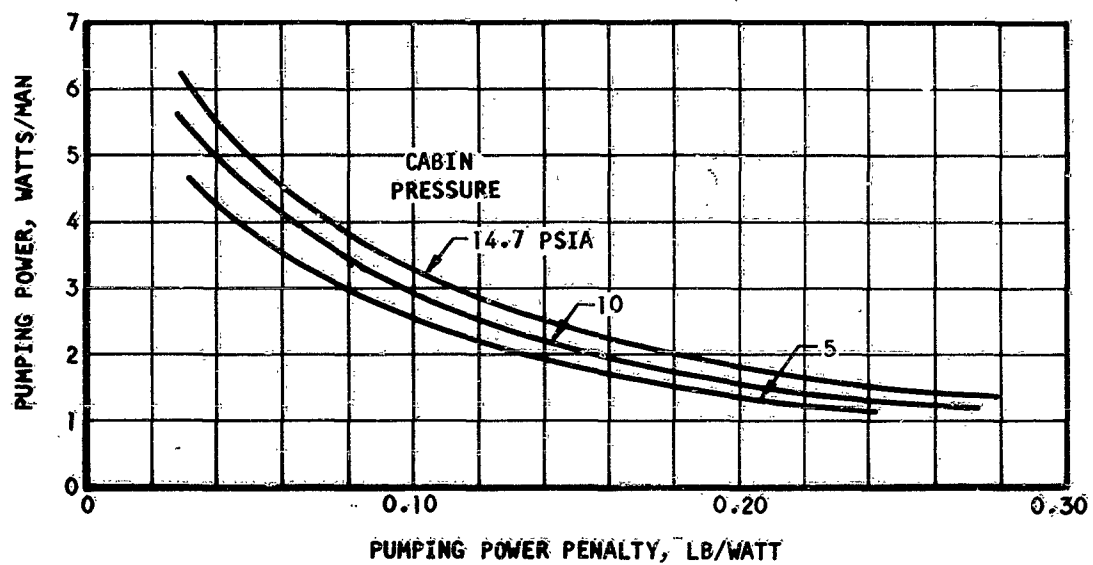


Figure 45. Cooler-Condenser Optimization

felt that with a moderate effort, a low-loss cyclone separator can be developed for zero-gravity operation. The analysis of Reference 1 suggests that pressure drop on the order of 1.5 in. of water is within the expected performance of these separators. However, all of the liquid water entrained by the air stream into the separator is not in small droplet form, as assumed in the analysis, and an experimental program is required to confirm the results of the analysis of Reference 1. Because of all the development work being pursued presently in the area of water separation, it is safe to assume in this report, for the purpose of systems analysis, that a water separator of the centrifugal type can be used in space vehicle humidity control systems. The weight of the separator in the following analyses will be assumed to be 0.5 lb per man, and it will further be assumed that the power losses in the separator are equivalent to a process air pressure drop of 1.5 in. of water.

#### Subsystem Integration

The weight of the accessories of the humidity control subsystem shown diagrammatically in Figure 37 is listed in Table 10. The total weight of the subsystem hardware can be expressed as a function of the number of crew members by

$$W_T = 2.6 + W_{HX} N + 2.19 \sqrt{N}, \text{ lb} \quad (13)$$

The various penalties to be charged against the subsystem and added to its basic weight can be found below.

#### 1. Heat Rejection Penalty

The cooling load requirement of the cooler-condenser,  $Q_R$ , is plotted in Figure 38, 39, and 40, for cabin pressures of 5, 7, 10, and 14.7 psia, and cabin relative humidities of 30 to 70 per cent. The corresponding equivalent subsystem weight is expressed in terms of the vehicle heat rejection penalty, RP (in lb per Btu/hr) as

$$W_Q = Q_R N (RP), \text{ lb} \quad (14)$$

#### 2. Pumping Power Penalty

The weight of the cooler-condenser,  $W_{HX}$ , is plotted in Figures 43 and 44 as a function of the pumping losses through the heat exchanger itself. The total subsystem pumping power is made up of the losses in the cooler-condenser itself, and the losses in the rest of the circuit. These calculations for air temperatures of 40°F and 45°F are listed in Table 11. The subsystem weight equivalent to the pumping losses is, therefore, expressed as

$$W_P = (PL)_T (PP) \quad (15)$$

where  $(PL)_T$  is the total pumping power through the system from Figures 43 or 44 and Table 11.

TABLE 10  
COOLER-CONDENSER SUBSYSTEM ACCESSORY WEIGHT  
(3-MAN SYSTEM)

| Component                 | Weight, lb |
|---------------------------|------------|
| Flow control valve        | 0.6        |
| Flow controller*          | 2.5        |
| Relative humidity sensor* | 0.1        |
| Water separator           | 0.7        |
| Check valves              | 0.6        |
| Pump reservoir            | 1.2        |
| Solenoid actuator         | 0.7        |
| Total Weight: 6.4 lb      |            |

\* Fixed weight accessory

TABLE 11  
PUMPING POWER LOSS IN THE SEPARATOR AND PIPING OF A  
COOLER-CONDENSER SYSTEM (WATTS)

| Pressure, psia    |     | 5    | 7    | 10   | 14.7  |
|-------------------|-----|------|------|------|-------|
| Relative humidity | 60% | 2.69 | 2.81 | 2.74 | 2.68  |
|                   | 70% | 1.76 | 1.85 | 1.80 | 1.765 |

### 3. Electrical Power

The electrical power required to activate the solenoid actuator is negligible.

The total subsystem equivalent weight can finally be written as

$$W_E = 2.6 + W_{HX} N + 2.19 \sqrt{N} + Q_R N \text{ (RP)} \\ + (PS)_T \text{ (PP)} \quad (16)$$

It is interesting to note that the total subsystem equivalent weight is independent of the mission duration as such. Mission duration can, however, indirectly influence the weight if it has an effect on the vehicle power penalty.

#### SUBSYSTEM COMPARISON

The two competing humidity control subsystems considered in this section are compared here on the basis of their equivalent weight and other characteristics pertaining to space vehicle installation.

##### Equivalent Weight

The hardware weight, heat rejection load, heating requirement, power consumption, and water balance for the cooler-condenser and the silica gel subsystem were calculated for the following typical vehicle and mission parameters:

Cabin pressure: 7 psia

Cabin relative humidity: 60%

Number of crew members: 3

Cooler-condenser subsystem air outlet temperature: 45°F

For these conditions, the subsystem parameters are listed in Table 12.

TABLE 12  
COMPARISON OF SUBSYSTEM CHARACTERISTICS

| Parameter                   | Silica-Gel Subsystem | Cooler-Condenser Subsystem |
|-----------------------------|----------------------|----------------------------|
| Hardware weight, lb         | 28.1                 | 10.3                       |
| Pumping losses, watts       | 1.55                 | 4.81                       |
| Heat rejection load, Btu/hr | 439                  | 569                        |
| at a temperature of, °F     | 70                   | 45                         |
| Heating requirement, Btu/hr | 439                  | ---                        |
| at a temperature of, °F     | 150                  | ---                        |
| Water balance, lb/day       | -6.6*                | +6.6**                     |

\* Dumped overboard

\*\* Recovered

The equivalent weight of the subsystem is plotted in Figure 46 for various penalties considered. Here it is assumed that the heat rejection penalty (RP), in lb per watt, is 10 per cent of the power penalty, (PP).

From this plot, it is seen that even in the best of light, the silica gel subsystem is heavier than the cooler-condenser subsystem for vehicle power penalties below 300 lb per kw. If heat rejection load is taken into account, and moreso if the water balance is introduced into the picture, the silica gel subsystem is not at all competitive with the simple cooler-condenser subsystem on a weight basis.

Even at high vehicle power penalty, the slight weight advantage of the silica gel system (in ideal conditions) is not enough to offset the other advantages of the simpler cooler-condenser system, as discussed below.

#### Reliability

The cooler-condenser subsystem is orders of magnitude more reliable than the regenerable silica gel subsystem. Operation of the silica gel subsystem valves requires a complex mechanism. The number of valves, in itself, makes the system unreliable. In addition, all the valves seal against the vacuum to which the bed is desorbed; this presents a serious safety problem. In practice, two valves in series would be installed everywhere. Although single valves are shown in the subsystem diagram of Figure 35, the accessory weight estimate is based on the use of two.

#### Process Air Outlet Temperature

An undesirable feature of the regenerable silica gel subsystem is the temperature cycling of the process air at subsystem outlet. At the start of the adsorption period, the bed is hot, near 150°F, and the process air temperature will rise through the bed approaching the temperature of the bed at outlet. As the bed is cooled, the air temperature will decrease; the cyclic temperature of the outgoing air depends on the bed dynamic characteristics.

#### Integration Potential

Removal of the moisture from the cabin air by cooler-condenser offers the possibility of integration of the humidity control and cabin temperature control subsystems. This greatly reduces the installation number of components as well as control complexity. In actual practice, these two functions, humidity control and temperature control, are unified and effected in the same atmospheric control loop. In this report, the humidity control is assumed to be divorced from the temperature control to better assess the penalties involved in the process of controlling cabin humidity.

# LEGEND

- 1 NO HEAT REJECTION PENALTY  
NO HEATING PENALTY  
NO WATER CONSUMPTION PENALTY
- 2 NO HEATING PENALTY  
NO WATER CONSUMPTION PENALTY
- 3 NO HEATING PENALTY

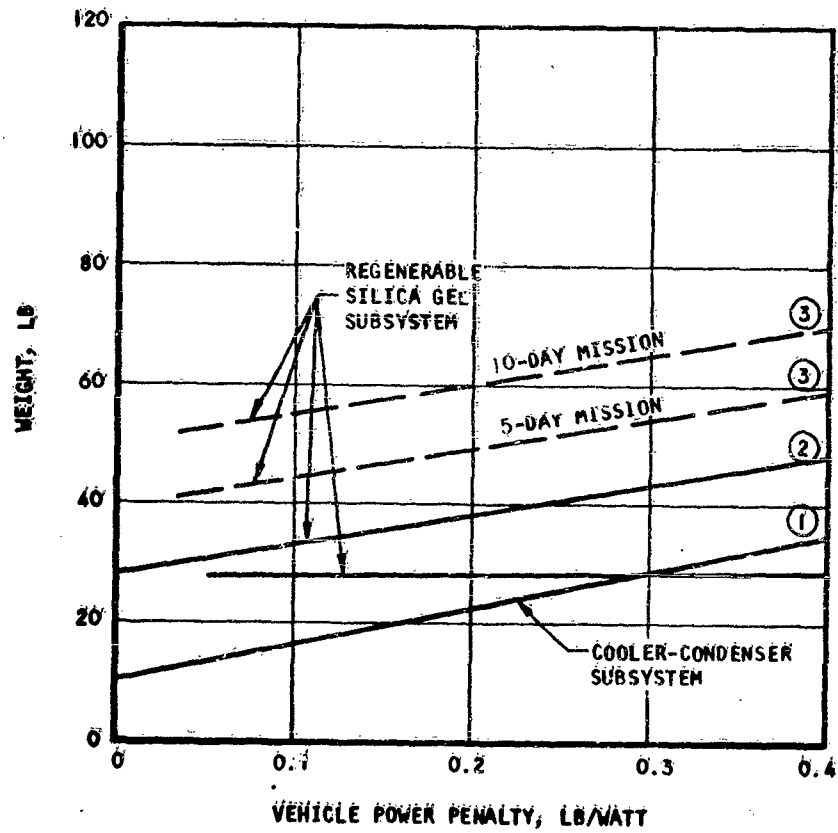


Figure 46. Humidity Control Subsystems Comparison

## SECTION VI

### CARBON DIOXIDE MANAGEMENT SUBSYSTEMS

#### INTRODUCTION

This section describes and characterizes carbon dioxide removal subsystems suitable for use in spacecraft atmospheric control systems. Only the most promising processes analyzed in Reference 1 are considered here: for limited mission durations - lithium hydroxide absorption, potassium and sodium superoxide absorption with generation of oxygen; for moderate to long mission durations - regenerable adsorbents, freeze-out heat exchanger processes, and continuous electrodialysis. Open-cycle carbon dioxide removal can be discarded because of excessive fluid requirements. On the other hand, closed-cycle carbon dioxide management systems using algae or plants can be discarded for reasons of weight and development status.

The systems are discussed in terms of vehicle and mission parameters. The weight penalties associated with power consumption will play an important role in selection of an optimum system. Other factors considered include heat dissipation penalties, state-of-the-art limitations, reliability, and integration problems.

Recovery of oxygen from the carbon dioxide is treated separately in the next section of this report.

#### SUMMARY AND CONCLUSIONS

For short mission durations, lithium hydroxide absorption appears the most attractive means of space vehicle atmosphere carbon dioxide control. Successfully used on the Mercury capsule, this method represents the state of the art. Oxygen-producing superoxide systems are at best heavier than competing lithium hydroxide systems. In addition, the tendency of superoxide beds to plug creates a control problem which does not exist in lithium hydroxide beds.

Regenerable adsorbents, such as "molecular sieves," can be used as the basis for regenerable carbon dioxide removal systems. The power requirements for these systems represent a serious limitation for mission durations on the order of two weeks and under. The main problem arises from the necessity of drying the process gas to a very low dew point with the presently available carbon dioxide adsorbents. Systems of this type require a large number of valves, some of which must seal tightly against a space vacuum. This poses a reliability problem.

Freeze-out heat exchangers can be used for carbon dioxide removal where a low-temperature heat sink is available. The most logical heat sink for these systems is the atmospheric make-up fluids stored as cryogenic liquids. At present, there is inadequate information concerning heat



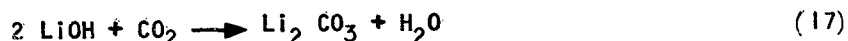
transfer to a subliming solid under conditions which exist in a freeze-out system to permit complete evaluation of freeze-out methods.

Diffusion and electrodialysis cells are potentially very attractive in that they are essentially static, continuous-flow devices. At present, however, they are in a fairly early research and development stage and have excessive power consumption and other operational limitations.

#### CARBON DIOXIDE REMOVAL BY LITHIUM HYDROXIDE ABSORPTION

##### General

Lithium hydroxide absorbs carbon dioxide according to the reaction:



Some water vapor is necessary for the reaction to take place. The amount of water vapor present in space vehicle cabin atmospheres (from 50 to 70 per cent relative humidity) is suitable to catalyze the reaction. Absorption of carbon dioxide by lithium hydroxide is exothermic, 1305 Btu per lb of carbon dioxide absorbed being released. Under normal operating conditions, some of this heat is expended in vaporizing the water of reaction. The amount of water vapor produced by the reaction is 0.41 lb of water per lb of carbon dioxide, and the lithium hydroxide consumption is ideally 1.059 lb per lb of carbon dioxide. Lithium hydroxide is commercially available at a purity of about 97 per cent and a bulk density of 25 to 30 lb per ft<sup>3</sup>.

The heat and mass transfer performance of a granular lithium hydroxide bed may be visualized by referring to Figure 47, which shows temperature and carbon dioxide concentration profiles at two different times in a typical canister. Most of the reaction takes place in an absorption zone which slowly moves from the inlet end to the outlet end of the canister. When the leading edge of the absorption zone reaches the outlet end of the granular bed, the so-called breakthrough point has been reached; after this point, carbon dioxide content of the gas leaving the canister rises fairly rapidly with time.

The theoretical capacity of lithium hydroxide for carbon dioxide absorption cannot be achieved in an atmosphere control system because of the bed dynamic characteristics. Typical closed-circuit test data are shown in Figures 48 and 49.

A closed-circuit process involves recirculation of the process gas and addition of carbon dioxide at a constant rate. The inlet and outlet carbon dioxide concentrations in the process air are plotted against test durations in Figure 48 for a typical bed design.

It is interesting to note that the relatively constant difference between the inlet and outlet concentrations, even after "breakthrough," indicates that all the carbon dioxide added to the air stream is removed.

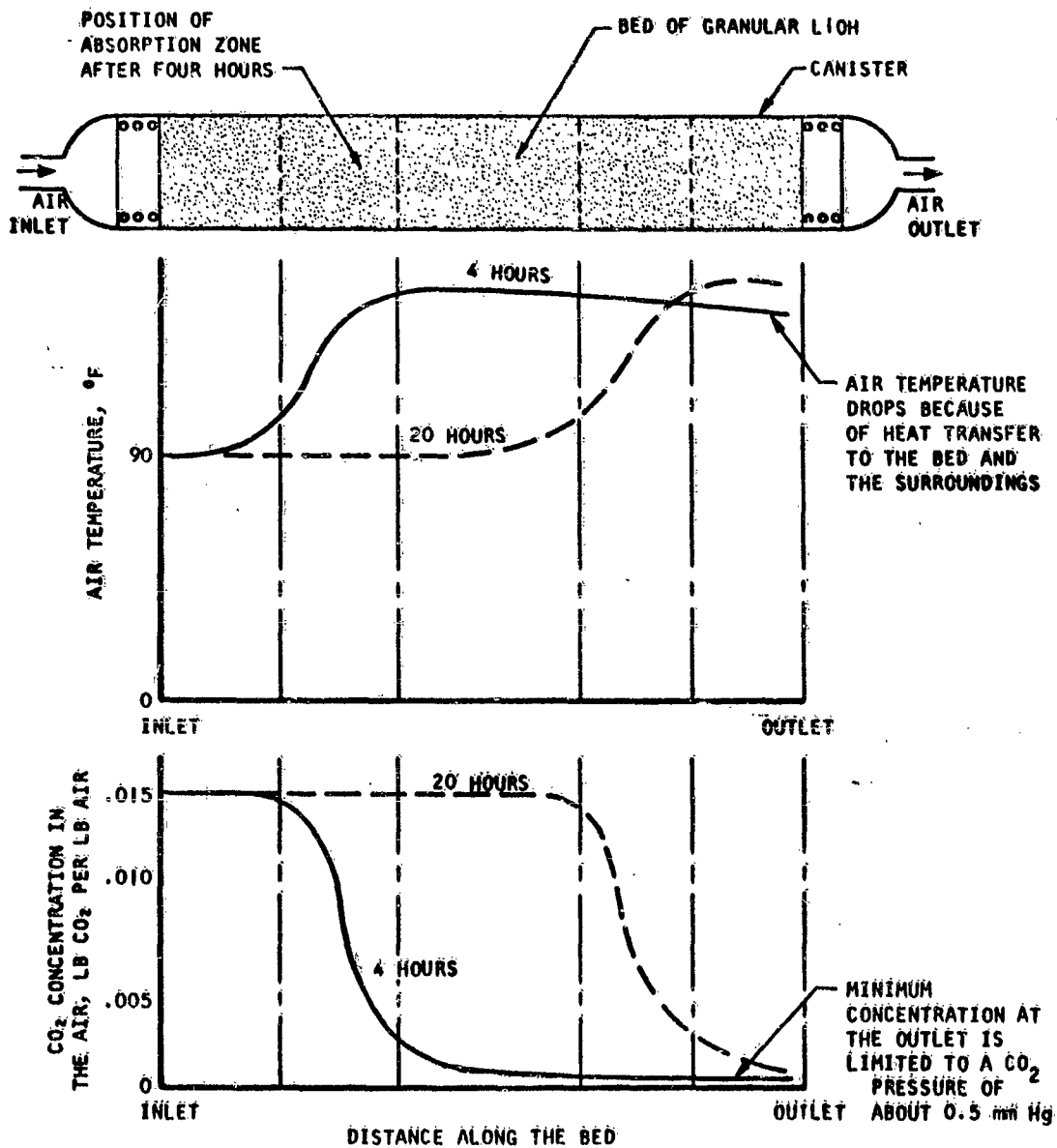


Figure 47. Temperature and Carbon Dioxide Concentration Profiles in a Typical Lithium Hydroxide Canister

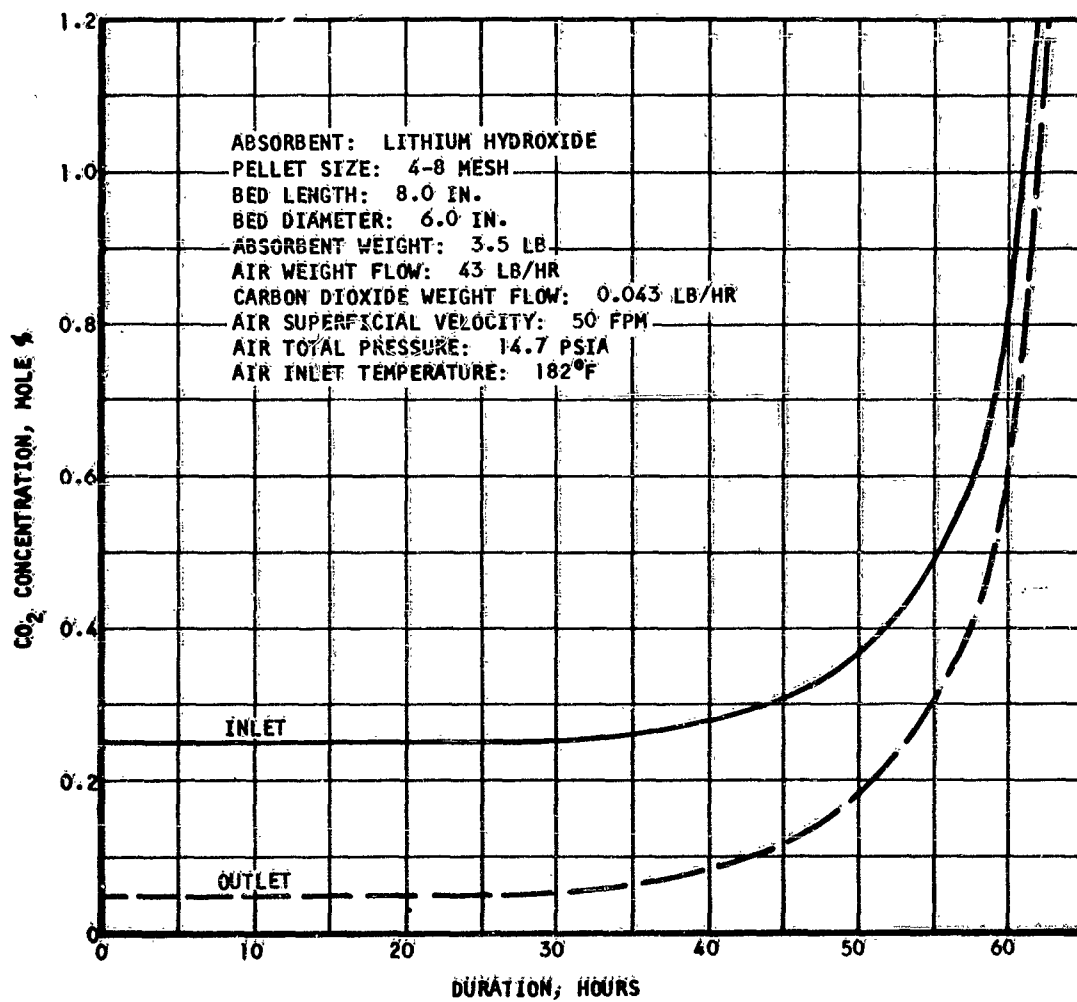


Figure 48. Typical Closed-Circuit Lithium Hydroxide Performance

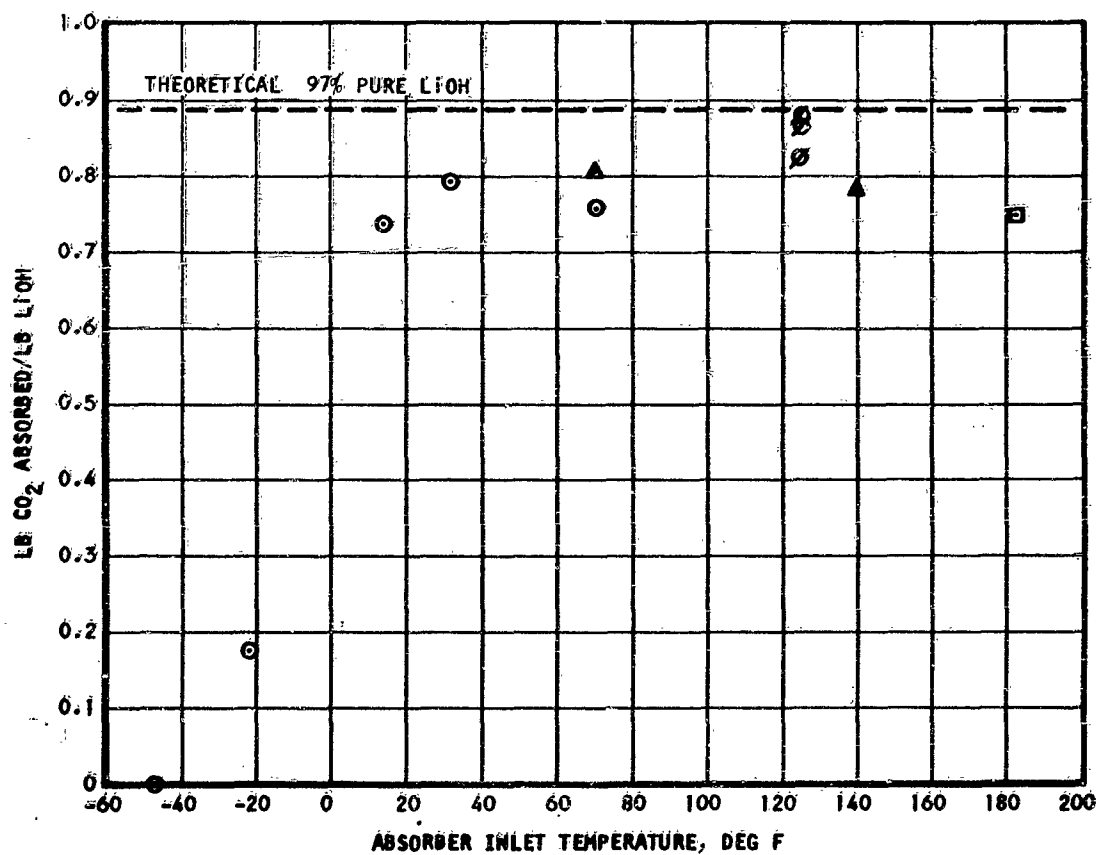


Figure 49. Lithium Hydroxide Absorption Capacity for Carbon Dioxide

The carbon dioxide concentration at bed outlet is about constant for a long period of time and increases rapidly before "breakthrough."

The exact shape of the curves presented in Figure 47 and the position of the "breakthrough" depend on the air superficial velocity, the canister dimensions, and the process air inlet temperature.

The carbon dioxide absorption capacity of several lithium hydroxide canisters of different configurations is shown as a function of inlet temperature in Figure 49. The two high values (0.88 and 0.87 lb carbon dioxide/lb lithium hydroxide) represent prototype canister tests using fresh lithium hydroxide. Production canisters of similar design provide capacities on the order of 0.825 lb of carbon dioxide/lb of lithium hydroxide. This last value corresponds to a bed utilization efficiency of 92.8 per cent.

In this report section, the characteristics of the lithium hydroxide carbon dioxide removal systems are based on the test data presented above. The bed utilization efficiency is taken as 92.8 per cent and the carbon dioxide partial pressure at bed outlet is assumed to be 0.5 mm of mercury. This last value is somewhat higher than shown in Figure 48.

The lithium hydroxide particle size is generally kept between 4 to 8 mesh size for high utilization efficiencies and low bed pressure drops. It appears that no channeling occurs with this particle size at gas velocities up to 1.0 ft per sec.

#### Subsystem Characteristics

##### 1. Flow Requirements

The process air flow requirement for carbon dioxide absorption by lithium hydroxide has been calculated for the following conditions and assumptions:

- a. The carbon dioxide partial pressure in the process air stream leaving the absorber bed is 0.5 mm Hg.
- b. The carbon dioxide production rate in the cabin is 2.25 lb/man day (Reference 3).
- c. The cabin air molecular weight is calculated assuming a cabin relative humidity of 60 per cent and an oxygen concentration given by Figure 4.

The results of these calculations are plotted in Figure 50 for various cabin atmospheric pressures.

##### 2. Temperature Rise

The process air temperature rise across the canister is shown in Figure 51 against the cabin air carbon dioxide concentration. The flows

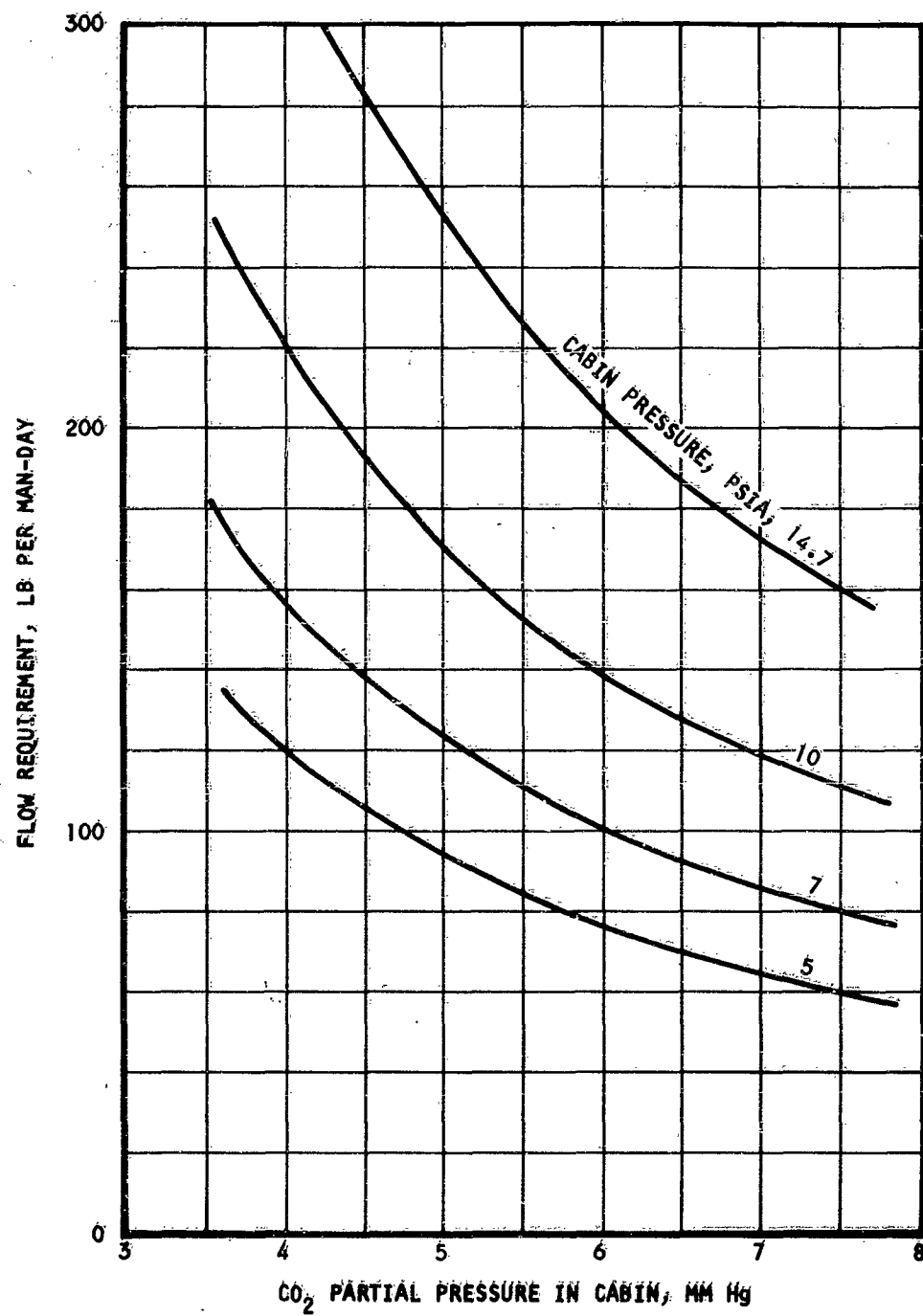


Figure 50. Lithium Hydroxide Subsystem Flow Requirement

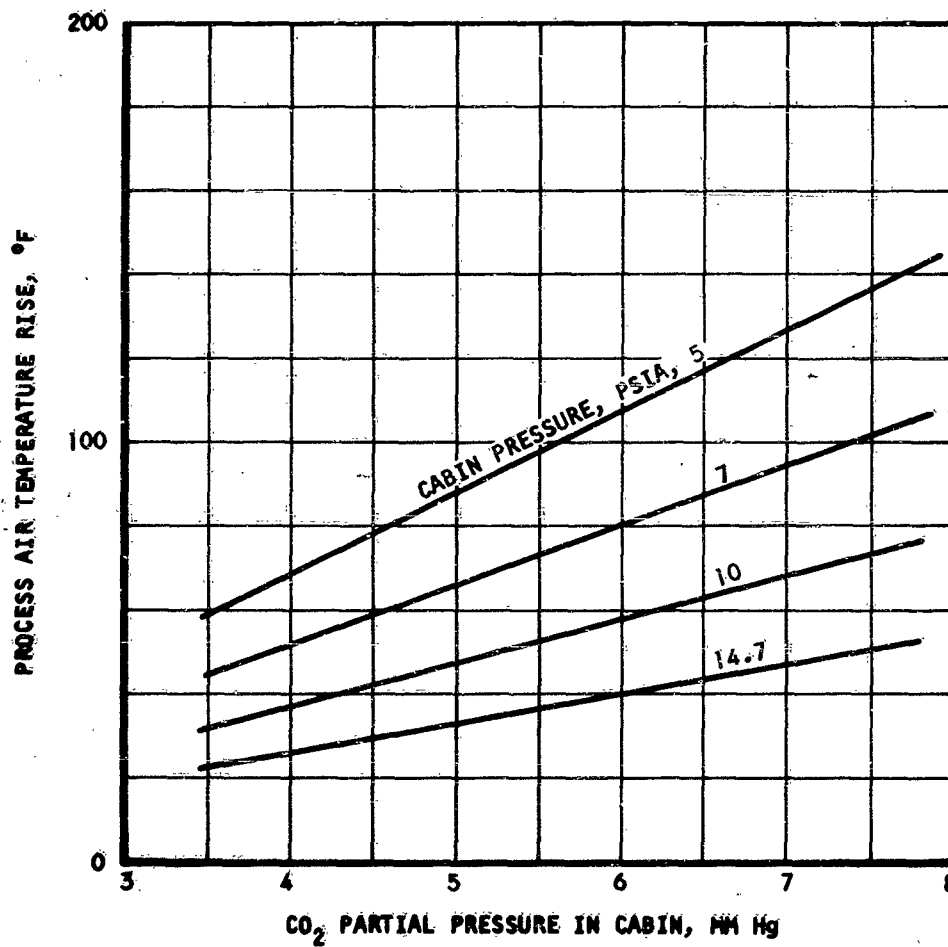


Figure 51. Lithium Hydroxide Subsystem Process Air Temperature Rise

calculated above were used in the computations. None of the heat of reaction is assumed transferred to the bed.

### 3. Subsystem Arrangement

The consumption of lithium hydroxide is a function of the number of crew members in the cabin and of the duration of the mission. Under normal average conditions, 2.728 lb per man-day are consumed; the corresponding volume consumption is 188 in.<sup>3</sup> per man-day. This leads to packaging problems as mission duration increases. In view of this, the use of rechargeable canisters is advisable for missions of long duration. It is reasonable to assume that an interval of one day between charges will not hamper crew operation unduly. Consideration of potential composition transients, particularly during emergency situations when suit circuit operation is required, leads to the recommendation of a system using two LiOH canisters in parallel for carbon dioxide removal. The two canisters are normally on stream, and operation on one canister involves a loss of system performance. Such a subsystem is illustrated in Figure 52.

### 4. Canister Weight Optimization

The weight of the canisters of the subsystem depicted in Figure 52 is optimum when the sum of the canister weight and the weight equivalent to the pressure loss in the LiOH bed is minimum. A canister design method based on this criterion is presented below.

Assume two cylindrical canisters as follows:

Material: Aluminum

Cylindrical wall thickness: 0.050 in. thick

Circular end plates: 0.200 in. thick

The weight of the two canisters based on this model can then be expressed by:

$$W_C = 2 \left[ 5.76 A_F + 2.552 \sqrt{A_F} L \right], \text{ lb} \quad (18)$$

Note that this weight includes the weight of the mounting brackets, flanges, filters, springs for loading the lithium hydroxide charge, etc.

The pressure drop through the lithium hydroxide bed is calculated by the method of Reference 1:

$$\Delta P = 4 f \frac{G^2}{2g\rho} \frac{L}{D_p}, \text{ lb/ft}^2 \quad (19)$$

where

$$f = \frac{850}{R_e} = \frac{850 \mu}{GD_p} \quad (20)$$



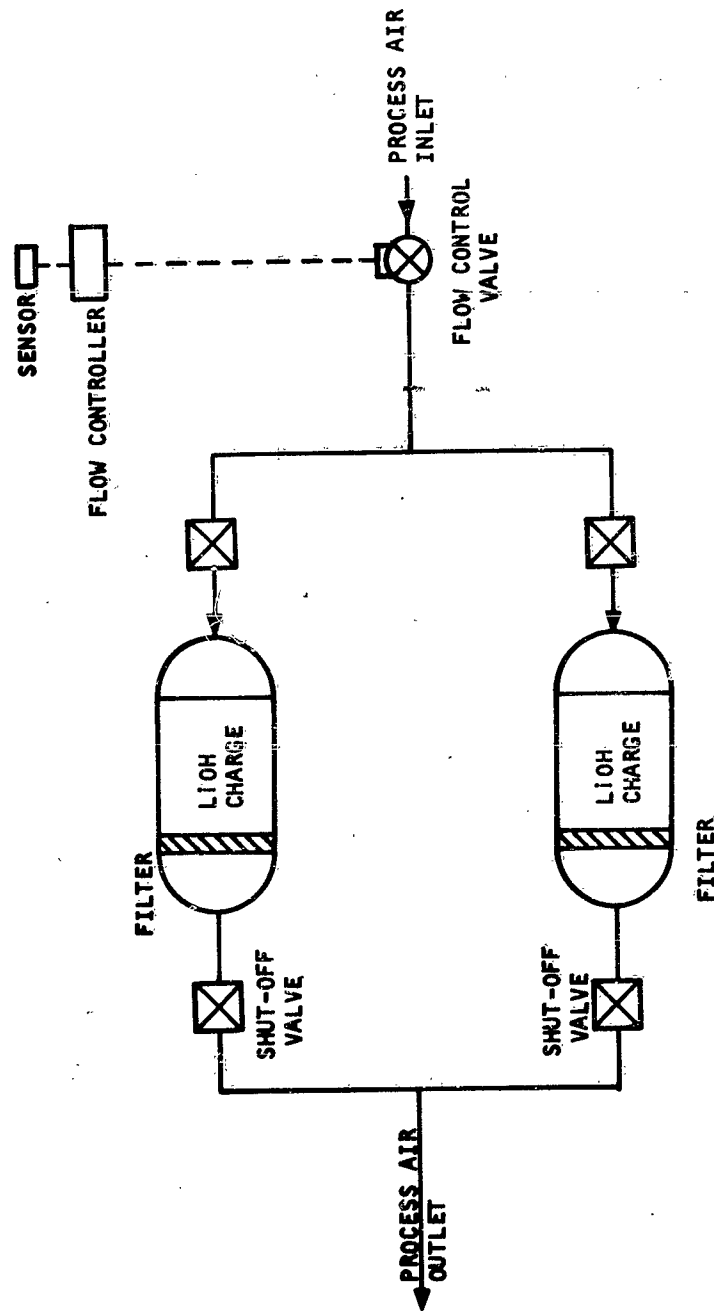


Figure 52. Lithium Hydroxide Subsystem Schematic Diagram

Therefore,

$$\Delta P = \frac{3400 \mu G L}{2g \rho D_p^2}, \text{ lb/ft}^2 \quad (21)$$

The lithium hydroxide volume consumption in one day is:

$$V = \frac{\bar{w}_c}{.825 \rho_{\text{LiOH}}} = \frac{2.728 N}{\rho_{\text{LiOH}}} = A_F L, \text{ ft}^3 \quad (22)$$

where  $\rho_{\text{LiOH}} = 25 \text{ lb per cu ft}$

Noting that  $G = w/2A_F$ , where  $w$  is in lb/sec, and introducing Equation 22 into Equation 21, the following expression is obtained:

$$\Delta P = \frac{242.2}{D_p^2} \left( \frac{\mu w}{\rho} \right) \frac{L^2}{N}, \text{ lb/ft}^2 \quad (23)$$

and the pumping power, assuming a fan-motor efficiency of 0.45, is given by:

$$(PL) = \frac{730}{D_p^2} \left( \frac{\mu w^2}{\rho^2} \right) \frac{1}{N} L^2, \text{ watts} \quad (24)$$

where  $D_p = 0.00909 \text{ ft}$  for a 6 to 8 LiOH particle mesh size.

Introduction of the expression for  $A_F$  from Equation 22 into Equation 18 yields

$$W_c = 1.256 \frac{N}{L} + 1.684 \sqrt{NL} \quad (25)$$

The optimum canister design is then found for a minimum of the function

$$(F) = 884 \times 10^4 \left( \frac{\mu w^2}{\rho^2} \right) \left( \frac{PP}{N} \right) L^2 + 1.256 \frac{N}{L} + 1.684 \sqrt{N} \sqrt{L}$$

where (PP) is the vehicle power penalty.

Differentiating (F) relative to  $L$ , the criterion for canister design is found:

$$1768 \times 10^4 \left( \frac{\mu w^2}{\rho^2} \right) \left( \frac{PP}{N} \right) L - \frac{1.256 N}{L^2} + \frac{0.842 \sqrt{N}}{\sqrt{L}} = 0 \quad (26)$$

The first term of Equation 26 is small compared to the other two, and its effect on the bed length is negligible. This means that the canister weight itself is much higher than the pressure loss weight penalty. For the purpose of system evaluation, Equation 26 reduces to

$$\frac{1.256 N}{L^2} = \frac{0.842 \sqrt{A_F}}{\sqrt{L}} \quad (27)$$

yielding the optimum canister length:

$$L = 1.305 N^{1/3}, \text{ ft} \quad (28)$$

The pressure drop, the power loss in the bed, and the weight of the bed are obtained by introducing the above value of L in equations 23, 24, and 25. Noting that  $w = N w$ , the following expressions are obtained:

$$\Delta P = 5 \times 10^6 \left( \frac{\mu \bar{w}}{\rho} \right) N^{2/3}, \text{ lb/ft}^2 \quad (29)$$

$$(PL) = 1.507 \times 10^7 \left( \frac{\mu \bar{w}^2}{\rho^2} \right) N^{5/3}, \text{ watts} \quad (30)$$

$$W = 2.885 N^{2/3}, \text{ lb} \quad (31)$$

In the above equations,  $\left( \frac{\mu \bar{w}}{\rho} \right)$  and  $\left( \frac{\mu \bar{w}^2}{\rho^2} \right)$  are functions of the cabin pressure and carbon dioxide concentration in the cabin. Equation 31 is plotted in Figure 53, and solutions of Equations 29 and 30 are given in Figures 54 and 55.

For missions of short duration, no problem arises from packaging all the required lithium hydroxide into a single canister. Redundancy is not necessary in this case, since the canister is in the circuit at all times. Results of an analysis of single canister weights are shown in Figure 56. Also shown for comparison is the canister weight of a double canister arrangement. On a weight basis, the use of single canisters is limited to mission durations of less than approximately two days.

##### 5. Subsystem Equivalent Weight

The total subsystem equivalent weight is made up of the terms below:

###### a. Lithium Hydroxide Consumption

This is readily calculated from the carbon dioxide production rate in the cabin and the lithium hydroxide bed utilization efficiency. An additional penalty is incurred for storing the charges aboard the vehicle; this is taken here as 3.0 per cent of the lithium hydroxide weight. The total weight of the stored hydroxide is then

$$W_{\text{LiOH}} = 2.81 N \tau \quad (32)$$

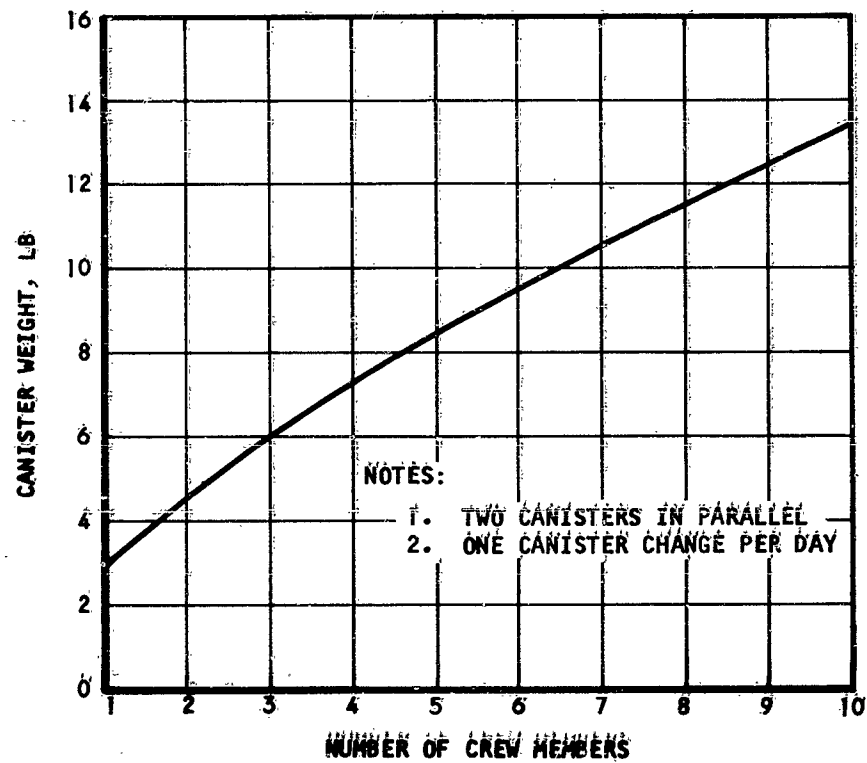


Figure 53. Lithium Hydroxide Canister Weight

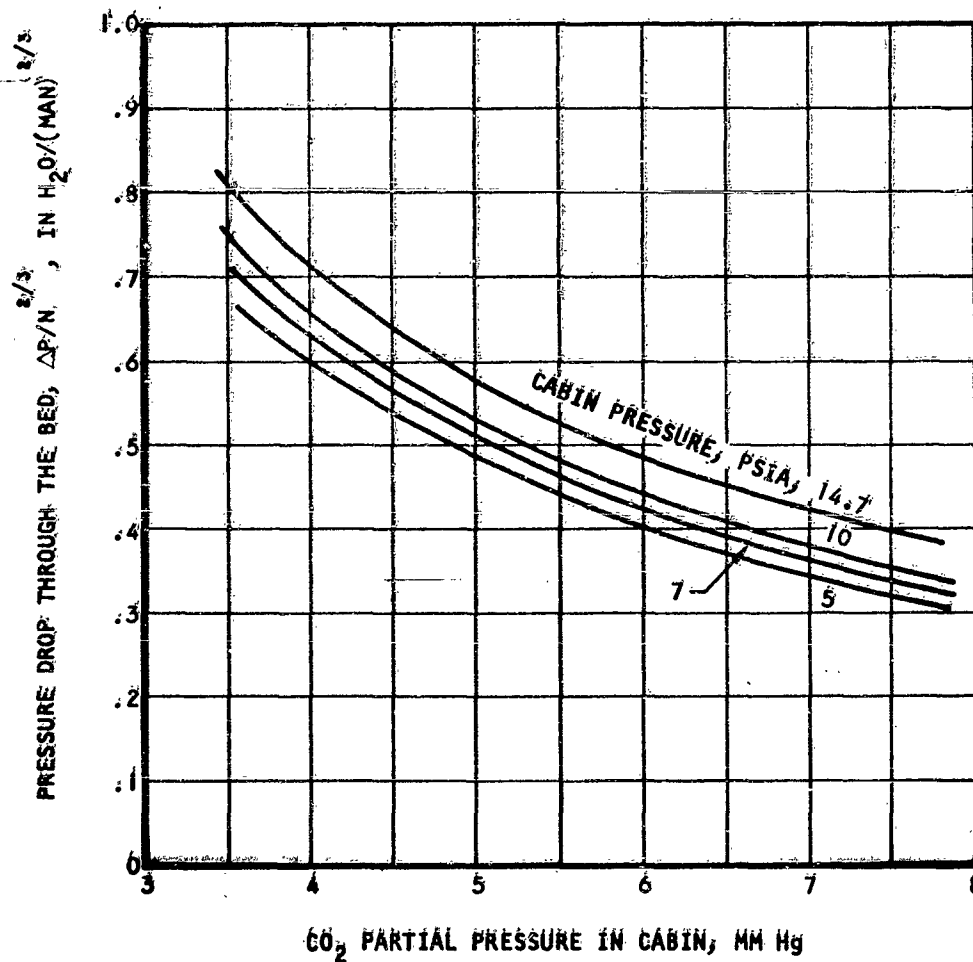


Figure 54: Lithium Hydroxide Bed Pressure Drop

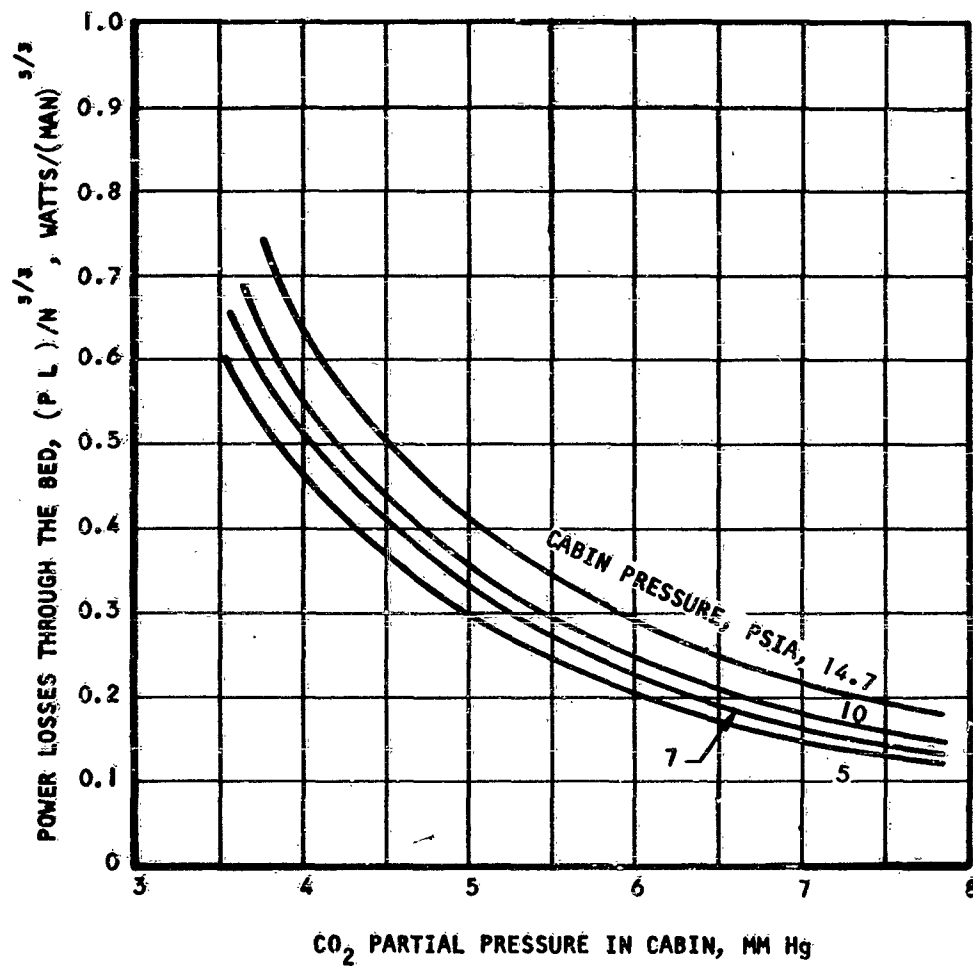


Figure 55. Lithium Hydroxide Bed Power Loss

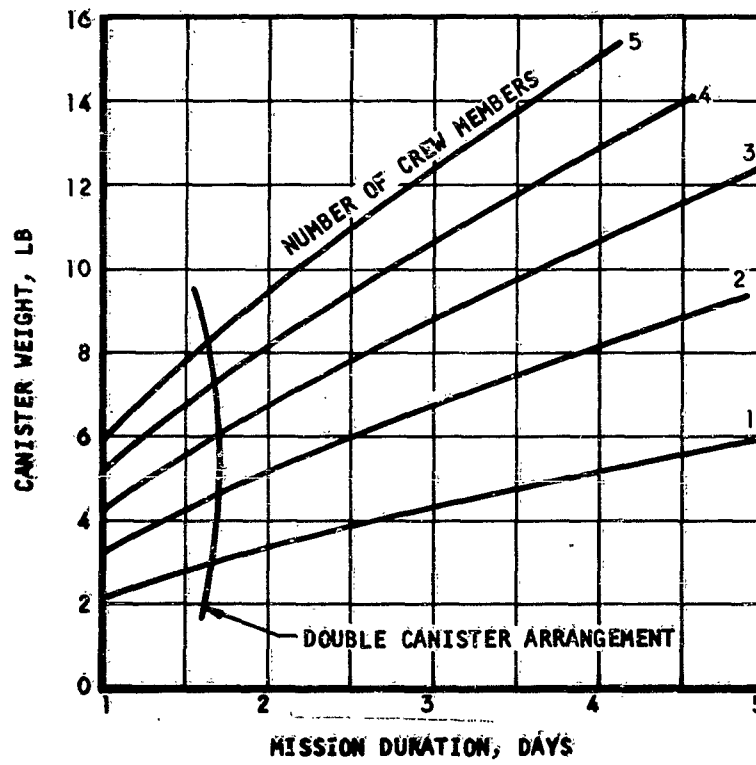


Figure 56. Single Canister Weight

b. Canister Weight

The canister weight has been found previously to be a function of the number of crew members and is expressed by the equation

$$W_C = 2.885 N^{2/3} \quad (33)$$

c. Accessory Weight

The weights of the accessories shown in Figure 52 are listed in Table 13 for a three-man system. The total accessory weight is a function of the number of crew members and can be estimated from the expression

$$W_A = 2.6 + 1.16 \sqrt{N} \quad (34)$$

d. Power Loss Penalty

The total subsystem pressure drop is made up of the losses in the bed itself (see Figure 55), and in the piping, manifolds, and valves of the system. The weight equivalent of the pressure drop can be calculated only when the vehicle power penalty in lb per watt is specified. It can be expressed as

$$W_P = (PL)_T (PP), \text{ lb} \quad (35)$$

e. Heat Rejection Penalty

The absorption process generates a total of 1305 Btu per lb of carbon dioxide absorbed. This is the heat load which must be disposed of by the thermal control system, since the water evolved in the reaction is ultimately condensed for humidity control purposes. The heat rejection load can, therefore, be written as

$$Q_R = 122.3 N, \text{ Btu/hr} \quad (36)$$

and the heat rejection weight penalty as

$$W_Q = (Q_R) (RP), \text{ lb} \quad (37)$$

where (RP) is the vehicle heat rejection penalty in lb per Btu/hr. This heat is rejected at a temperature level above 70°F. The exact temperature depends on the atmospheric and thermal control arrangement.

f. Material Balance

Water is produced in the carbon dioxide absorption process at the rate of 0.41 lb per lb of carbon dioxide absorbed. This water is relatively pure and can be used for drinking purposes after filtration through



TABLE 13

## LITHIUM HYDROXIDE SUBSYSTEM ACCESSORY WEIGHT

(3-MAN SYSTEM)

| Component            | Weight, lb |
|----------------------|------------|
| Flow control valve   | 0.6        |
| Sensor*              | 0.1        |
| Flow controller*     | 2.5        |
| Shutoff valves (4)   | 1.0        |
| Piping               | 0.2        |
| Total Weight: 4.4 lb |            |

\* Fixed weight accessory

activated charcoal beds. The system should be credited by the weight of the water evolved in the reaction. In addition, a further saving on the water management subsystem results from the use of a smaller container. Assuming the water storage weight penalty to be 8.5 per cent of the water stored, the total weight saving becomes

$$W_{H_2O} = 1.0 N\tau, \text{ lb} \quad (38)$$

The total subsystem equivalent weight is the summation of all terms given above and is written as:

$$W_E = 2.81 N\tau + 2.885 N^{2/3} + 2.6 + 1.16 \sqrt{N} + (PL) (PP) + (122.3 N) (RP) + 1.0 N\tau \quad (39)$$

where  $\tau$  is the mission duration in days.

The equivalent weight of a lithium hydroxide carbon dioxide removal subsystem was evaluated by the above equation for a typical case defined by the following parameters and data assumptions:

Cabin pressure: 10 psia

Cabin carbon dioxide partial pressure: 7.6 mm Hg

Vehicle heat rejection penalty: 10 per cent of the vehicle power penalty in lb per watt

Pressure losses through the system other than lithium hydroxide bed loss:  $0.8 \sqrt{N}$ , in  $H_2O$

Accessory weight:  $(2.6 + 1.16 \sqrt{N})$ , lb

The results of the calculations are given in Figures 57 and 58, where the subsystem equivalent weight is plotted versus the mission duration for the number of the crew members up to 5. Figure 57 applies when the subsystem is not credited for the water evolved in the process. Figure 58 shows the same plot applicable when the system is credited for the water of reaction. From these curves, it is apparent that for mission durations in excess of 10 days, the weight penalties due to pumping losses and heat rejection are only a small percentage of the total equivalent weight. The subsystem weight is mainly the hardware weight and the expendable lithium hydroxide weight. The plots presented can, therefore, with discretion, be used for estimating lithium hydroxide subsystem weight at operating conditions other than those defined above.

For mission durations shorter than two days, the weight of the lithium hydroxide subsystem is lower than shown by the difference in weight between the double and single-canister arrangement. The difference between the weight shown and the actual subsystem weight can easily be estimated from the data presented.

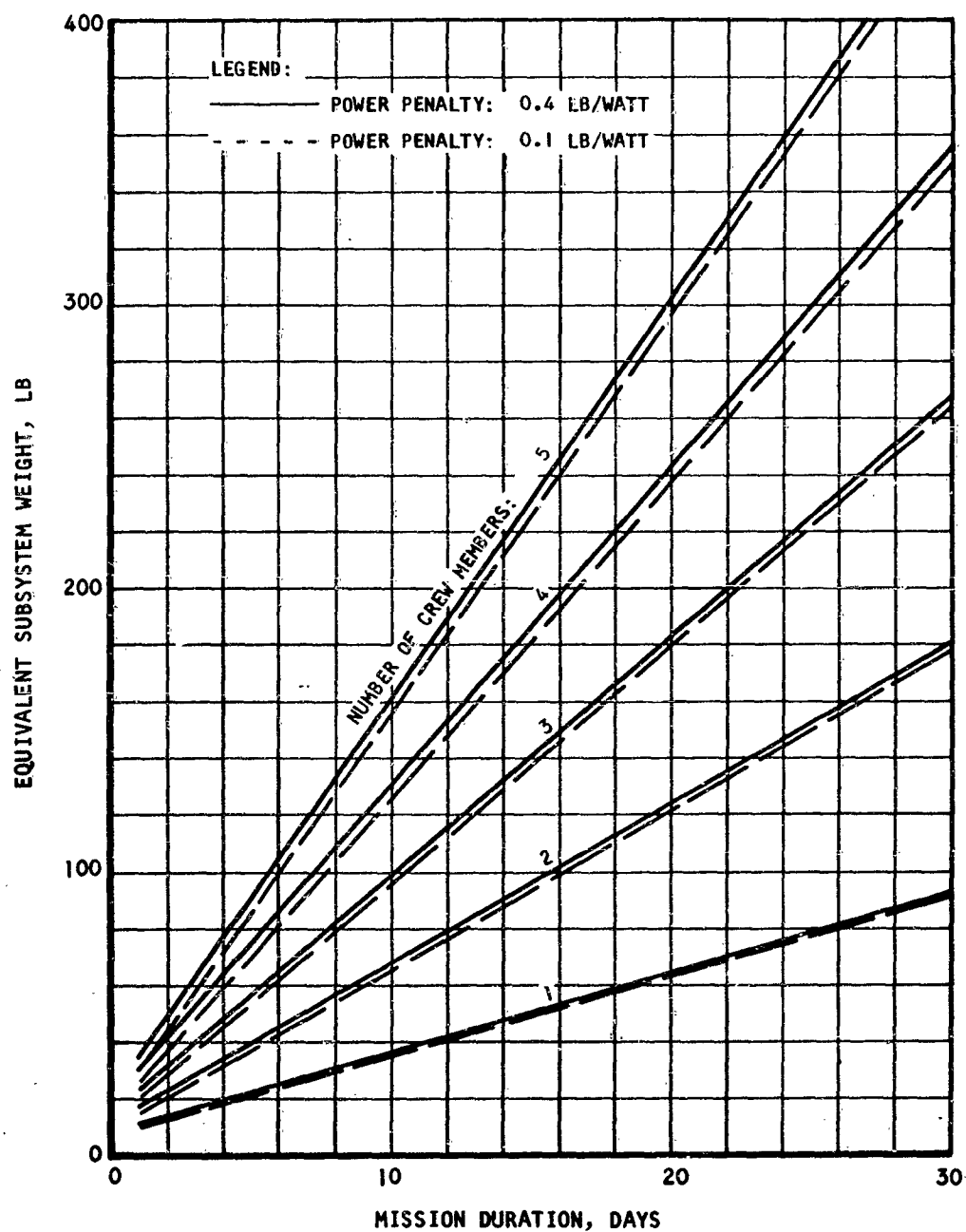


Figure 57. Lithium Hydroxide Subsystem Equivalent Weight  
(No Credit for Water Production)

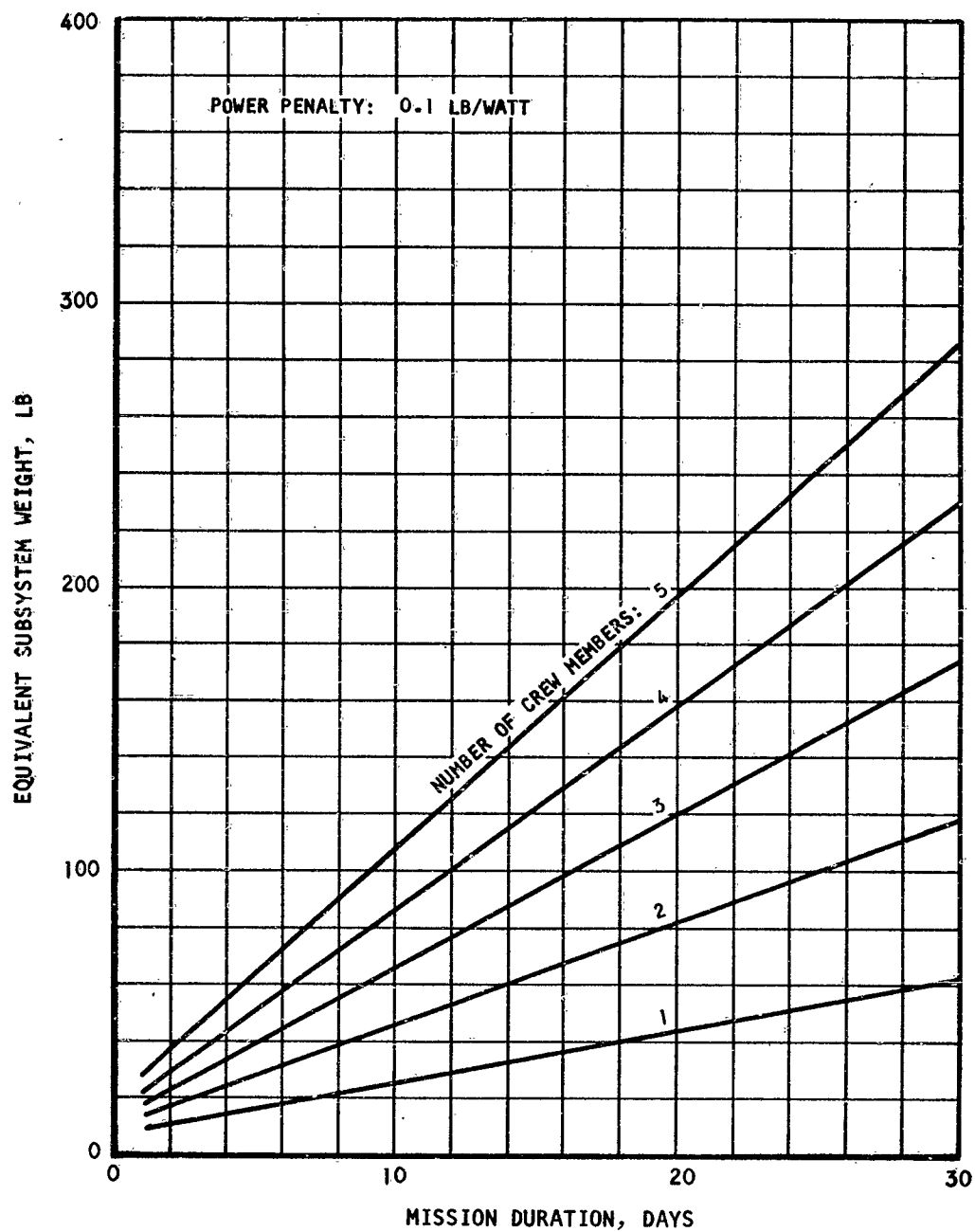


Figure 58. Lithium Hydroxide Subsystem Equivalent Weight  
(Credit for Water Production)

## Conclusions

The lithium hydroxide carbon dioxide removal subsystem whose characteristics have been presented in the preceding paragraphs is simple in construction and control. Its reliability has been proved by use in the Mercury capsule and numerous ground tests. Handling problems might arise from the necessity for charging the canister; however, if this operation is performed only once a day, it can hardly be considered to interfere with other crew activities. Reactant storage can in some cases present difficulties for missions of long duration.

As the absorber is expendable, the system weight is time-dependent. This limits its use to relatively short mission durations on the order of a few weeks. Because of its simplicity and reliability, the lithium hydroxide subsystem is attractive as an emergency system for long duration vehicles.

The water generated in the absorption process is not always a credit to the system. In vehicles where a water excess is produced from fuel cell power installation, for example, the water supply is already plentiful, and the water produced by carbon dioxide removal can hardly be treated as a subsystem credit.

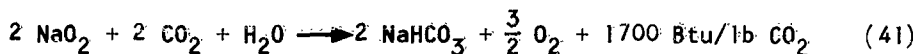
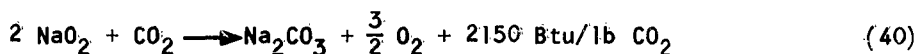
## **CARBON DIOXIDE REMOVAL BY ALKALI METAL SUPEROXIDE ABSORPTION**

### General

Alkali metal superoxides such as potassium superoxide and sodium superoxide act as both carbon dioxide absorbents and oxygen sources. This makes them very attractive for space vehicle usage, since it appears to dispense with the necessity of carrying oxygen for breathing purposes. However, as oxygen is required for leakage makeup, the oxygen produced in the carbon dioxide absorption reaction is not, in general, sufficient to fulfill all the space vehicle oxygen requirements. In some special cases when no leakage occurs, the process is of interest.

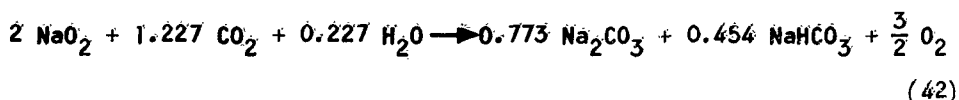
The use of such materials in atmospheric control is generally similar to that of lithium hydroxide in that they are packaged as granular beds through which impure gas is circulated. Superoxides are highly reactive, with strong oxidizing and alkaline properties; they appear to provide for odor control and sterilization of process air. Although this factor makes such materials promising for space vehicle use, this advantage is offset by handling problems incurred by their chemical reactivity.

In contrast to lithium hydroxide, the superoxides absorb both water and carbon dioxide; a variety of reactions is possible, depending upon operating conditions. Possible reaction products include carbonates, bicarbonates, and hydroxides, as well as hydrates of these compounds. The primary reactions of interest, yielding the carbonate and bicarbonate, are indicated below for sodium superoxide.



Analogous reactions exist for potassium superoxide; corresponding heats of reaction are 1875 Btu and 1625 Btu per lb of carbon dioxide absorbed.

In the carbonate formation reaction oxygen is produced at the rate of 1.09 lb/lb of carbon dioxide, while the bicarbonate reaction corresponds to the production of 0.545 lb of oxygen/lb of carbon dioxide. It appears possible to match these two reactions, by proper control of the process air humidity, to yield the amount of oxygen necessary for respiration while absorbing the carbon dioxide produced in the cabin. Assuming 2.25 lb of carbon dioxide is absorbed and 2.0 lb of oxygen is produced, such metabolic matching corresponds to an overall reaction of the form:



The heat released in this reaction is 2048 Btu/lb of oxygen; sodium superoxide expenditure is 2.29 lb per lb of oxygen. The analogous reaction for potassium superoxide would have a heat release of 1817 Btu/lb of oxygen and a potassium superoxide expenditure of 2.96 lb per lb of oxygen. The water absorbed in the reaction is 0.0758 lb per lb of carbon dioxide removed.

As it has not yet been shown possible to achieve reliability in control, some designers resort to the use of parallel beds of superoxide and lithium hydroxide, where all oxygen required is generated by the superoxide which handles part of the process air. The lithium hydroxide is then used for partial carbon dioxide removal. Such an arrangement is not considered here, since it can be shown that, under the ideal conditions described by the above reaction (Equation 42), a superoxide system is not competitive with the simple lithium hydroxide system described previously.

Test results summarized in Reference 1 have shown that, with careful bed design and appropriate control of the process air humidity level, utilization efficiencies on the order of 0.90 are attainable. Since the purity of available sodium superoxide and potassium superoxide is about 0.95, the consumption rates of these substances in carbon dioxide control systems are 5.36 and 6.93 lb per man-day respectively.

### Subsystem Characteristics

#### 1. Flow Requirements

The flow requirement is taken here to be the same as for the lithium hydroxide subsystem. Small variations in the carbon dioxide concentration

at outlet will not change the process gas flow rate appreciably. This flow is plotted in Figure 50 as a function of the carbon dioxide partial pressure in the cabin.

## 2. Process Air Temperature Rise

Based on the flows shown in Figure 50 and on the assumption that all the heat of reaction is dumped into the process air stream, the temperature rise of the air flowing through the superoxide bed has been calculated and is shown plotted in Figure 59 for a sodium superoxide and a potassium superoxide subsystem. The air temperature rise is much higher (double for sodium superoxide) than in the case of the lithium hydroxide subsystem.

## 3. Subsystem Arrangement

The use of a two-bed arrangement with daily replacement of one charge is considered, although this presents serious handling problems relative to lithium hydroxide. The subsystem arrangement is also more complicated because of the requirement for humidity control of the process air at canister inlet. A typical superoxide subsystem is illustrated in Figure 60.

Here, the water content of the process air is controlled by mixing of two air streams, one from the cabin and the other from the humidity control subsystem. The air entering the system is relatively cold under these conditions, and some preheating might be necessary at the start of the operation.

A preheater is not shown here, however. A catalyst mixed with the superoxide in the upstream portion of the bed will initiate the reaction, and the bed will be warmed up by the heat released in the reaction.

## 4. Canister Weight Optimization

The design problems for superoxide canisters are generally similar to those mentioned previously relative to lithium hydroxide; in addition, because of the highly oxidizing nature of the superoxides, stainless steel or plastic construction is indicated.

Canister design optimization follows the same lines as for lithium hydroxide. The model expressing the canister weight is assumed here to be the same as for lithium hydroxide. Using a 2 to 4 superoxide mesh size to reduce the tendency of the bed to plug up, the equations derived for lithium hydroxide become for sodium superoxide canisters:

$$L = 1.422 N^{1/3}, \text{ ft} \quad (43a)$$

$$W = 3.423 N^{2/3}, \text{ lb} \quad (44a)$$

$$\Delta P = 1.537 \times 10^6 \left( \frac{LW}{\rho} \right) N^{2/3}, \text{ lb/ft}^2 \quad (45a)$$

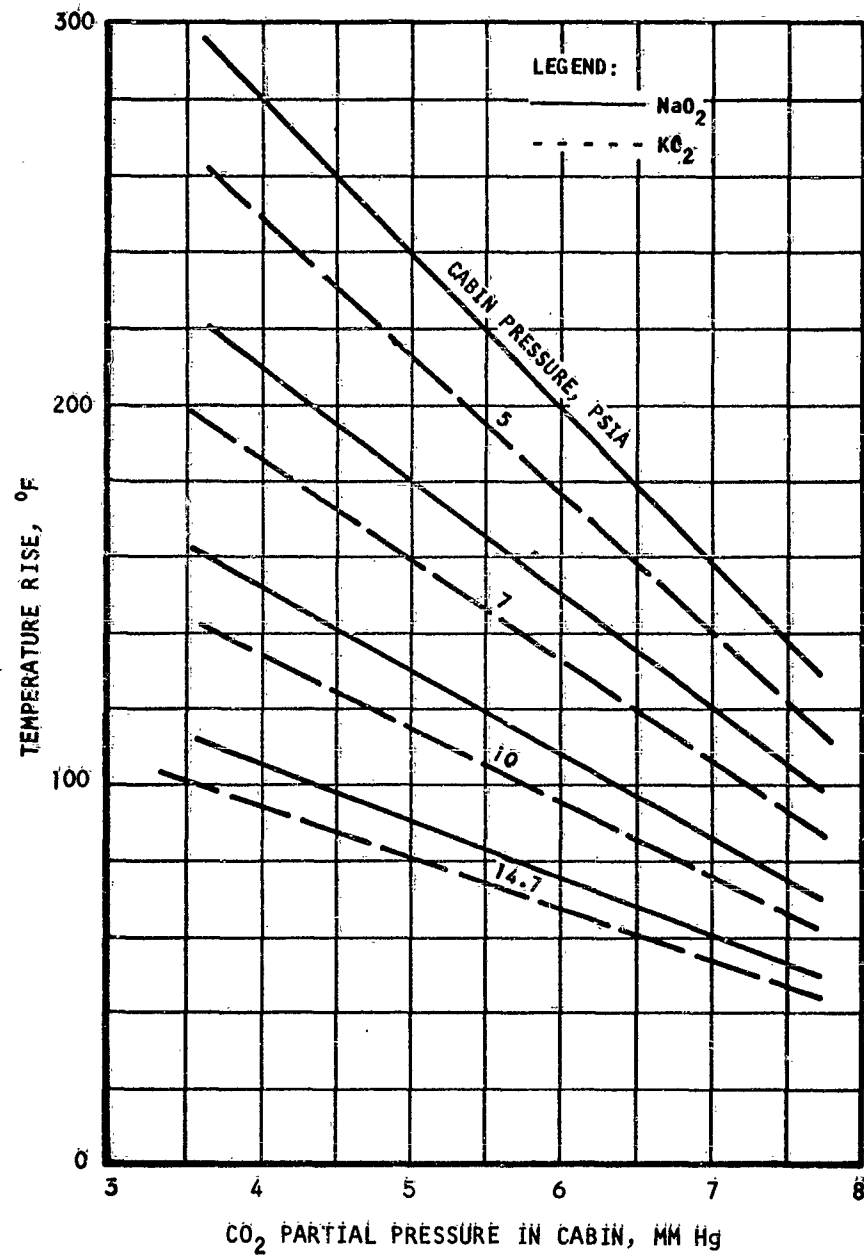


Figure 59. Process Air Temperature Rise Through Sodium Superoxide and Potassium Superoxide Canisters



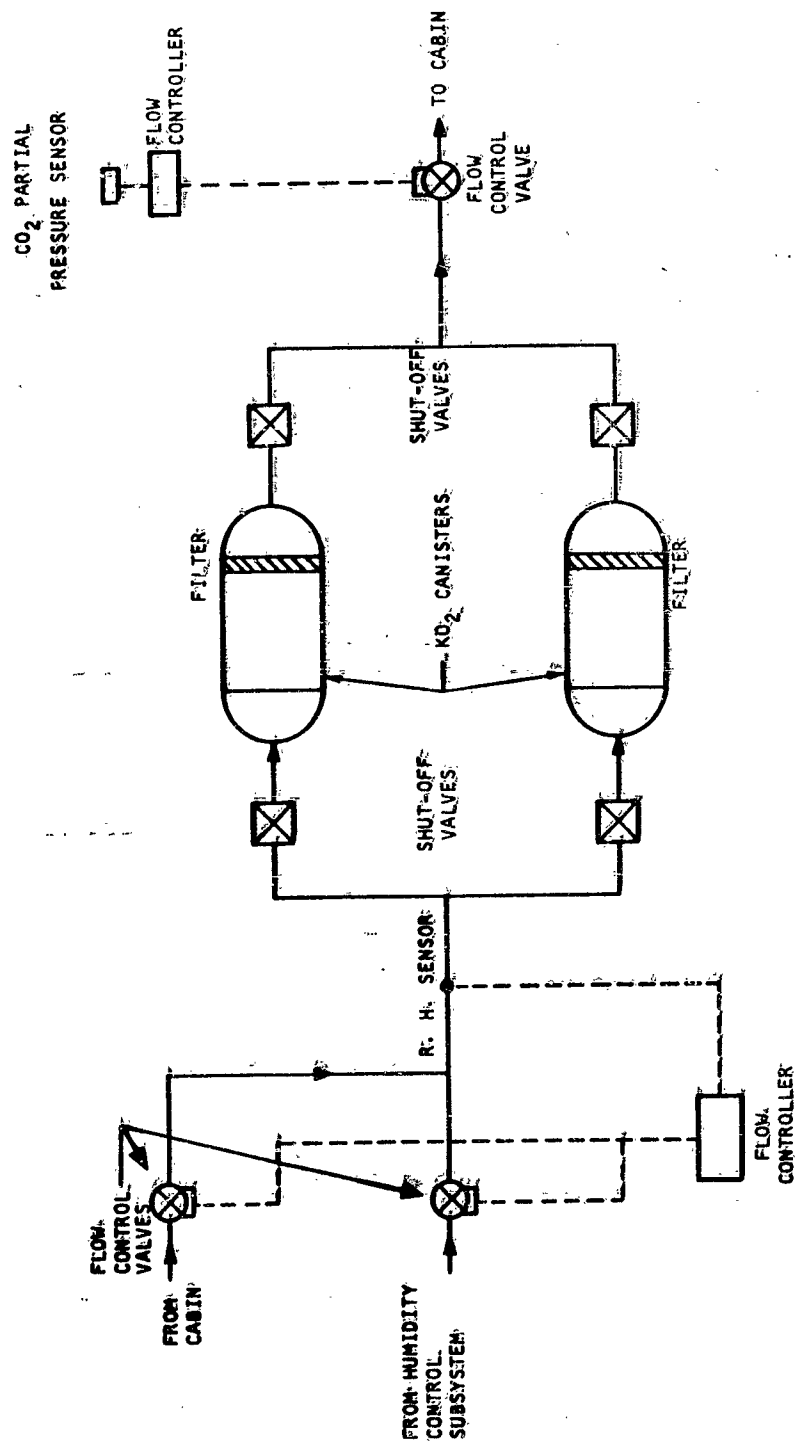


Figure 60. Alkali Metal Superoxide Subsystem Schematic Diagram

$$(\dot{P}L) = 4.62 \times 10^6 \left( \frac{\dot{U}W^2}{\rho^2} \right) N^{5/3}, \text{ watts} \quad (46a)$$

and for potassium superoxide canisters

$$L = 1.51 N^{1/3}, \text{ ft} \quad (43b)$$

$$W = 3.871 N^{2/3}, \text{ lb} \quad (44b)$$

$$\Delta P = 1.468 \times 10^6 \left( \frac{\dot{U}W^2}{\rho} \right) N^{2/3}, \text{ lb/ft}^2 \quad (45b)$$

$$(\dot{P}L) = 3.97 \times 10^6 \left( \frac{\dot{U}W^2}{\rho^2} \right) N^{5/3}, \text{ watts} \quad (46b)$$

Figure 61 shows the canister weight of sodium superoxide and potassium superoxide beds of optimum design.

Since the fixed weight and also the expendable superoxide weight of the potassium subsystem is considerable higher than that of the sodium superoxide subsystem, only the latter will be considered in the following discussions. The only advantage of the potassium superoxide is its slightly lower canister pressure drop and heat rejection load. These two parameters account for only a small percentage of the total subsystem equivalent weight, as will be seen later.

#### 5. Subsystem Equivalent Weight

The items to consider in computing the subsystem equivalent weight are discussed below.

- a. Sodium Superoxide Consumption - This has already been given, assuming a purity of 0.95 and a bed utilization efficiency of 0.90. Using a storage weight penalty of 3 per cent, the total weight of the sodium superoxide becomes

$$W_{\text{NaO}_2} = 5.52 N \quad (47)$$

- b. Canister Weight - The optimum canister design weight has been found previously to be

$$W = 3.423 N^{2/3}, \text{ lb} \quad (48)$$

- c. Accessory Weight - The weight of the accessories shown in the schematic diagram of Figure 60 is tabulated for a three-man system in Table 14. The variable part of this weight is taken to be a function of the number of crew members. The following expression is an estimate of the system hardware weight, other than the canister.

$$W_A = 5.2 + 1.79 \sqrt{N}, \text{ lb} \quad (49)$$

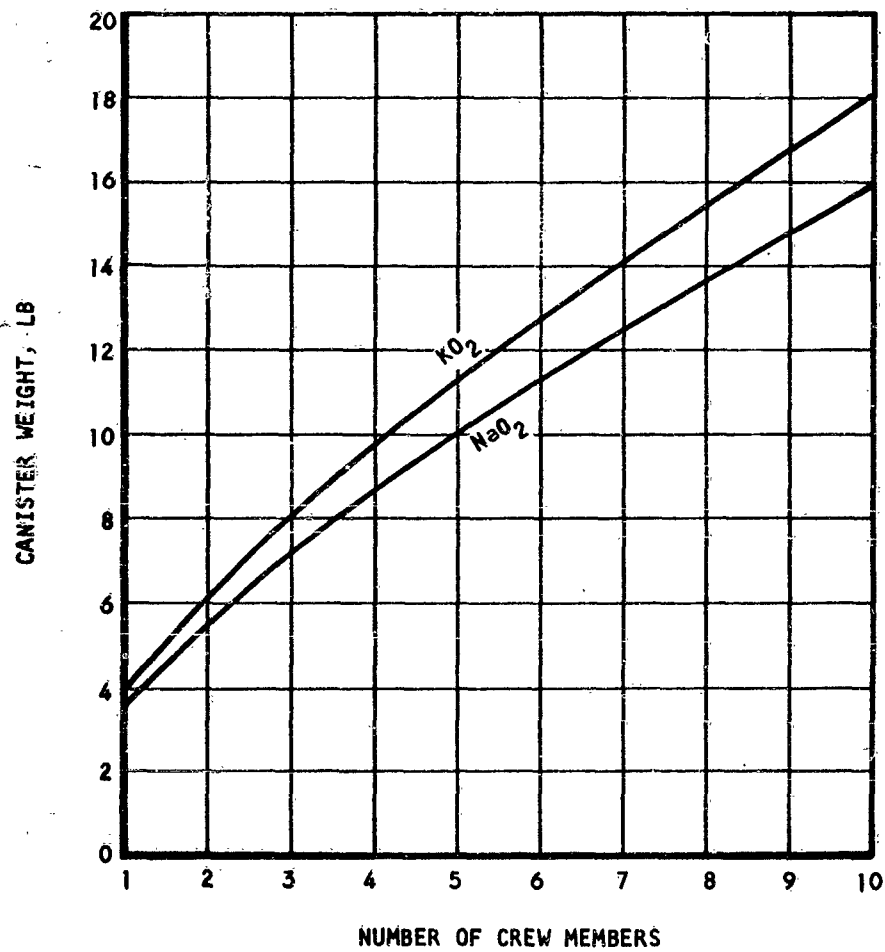


Figure 61. Alkali Metal Superoxide Canister Weight

TABLE 14  
SODIUM SUPEROXIDE SUBSYSTEM ACCESSORY WEIGHT  
(3-MAN SYSTEM)

| Component               | Weight, lb |
|-------------------------|------------|
| Flow control valves (3) | 1.8        |
| Flow controller (2)*    | 5.0        |
| Sensors (2)*            | 0.2        |
| Shutoff valves (4)      | 1.0        |
| Piping                  | <u>0.3</u> |
| Total Weight: 8.3 lb    |            |

\* Fixed weight accessory

- d. Power Loss Penalty - The total subsystem power loss is estimated from the canister pumping power loss and the subsystem valves, piping and manifold losses. The weight equivalent to the subsystem power loss is given by

$$W_P = PL_T (PP), \text{ lb} \quad (50)$$

- e. Heat Rejection Penalty - All the heat of reaction generated in the absorption of carbon dioxide is transferred either to the superoxide bed or to the process air. This heat is eventually rejected to the vehicle thermal management system. The carbon dioxide control subsystem must be penalized for this heat load. This penalty is calculated here from

$$W_Q = (Q_R) (RP), \text{ lb} \quad (51)$$

where  $Q_R = 170.6 \text{ N, Btu/hr} \quad (52)$

- f. Material Balance - Water is consumed in the reaction at a rate of 0.1706 lb per man-hr. In vehicles where a shortage of water exists, this constitutes a subsystem weight penalty which can be calculated by

$$W_{H_2O} = 0.185 \text{ NT}, \text{ lb} \quad (53)$$

assuming an 8.5 per cent storage weight penalty. On the other hand, oxygen is produced by the reaction at a rate of 2.0 lb per man-day, assuming the conditions for Equation 42 are satisfied. Considering a storage weight penalty of 1.14 lb per lb (Reference: Section IV of this report), the system is credited by

$$W_{O_2} = 2.28 N\tau, \text{ lb} \quad (54)$$

The total subsystem equivalent weight is the sum of the above terms and is expressed by

$$W_E = 3.262 N\tau + 3.423 N^{2/3} + 5.2 + 1.79\sqrt{N} + (PL)_T (PP) + 170 N (RP) \quad (55)$$

Equation 55 has been solved for a typical set of conditions defined by the following data assumptions:

Cabin pressure: 10 psia  
 Carbon dioxide partial pressure in the cabin: 7.6 mm Hg  
 Vehicle heat rejection penalty: 10 per cent of the vehicle power penalty in lb per watt  
 Pressure losses through the system other than  $\text{NaO}_2$  bed loss:  $0.8\sqrt{N}$ , in  $\text{H}_2\text{O}$   
 Accessory weight:  $(5.2 + 1.79\sqrt{N})$ , lb

Figure 62 is a plot of the sodium superoxide subsystem equivalent weight as a function of time. Number of crew members considered is from 1 to 5. In Figure 62, the system was assumed not penalized for the water consumed nor credited for the oxygen produced while removing the carbon dioxide. The plots were prepared for vehicle power penalties of 0.1 and 0.4 lb per watt. The same parameters are plotted in Figure 63 when the system is credited for oxygen and penalized for water; here the vehicle power penalty is 0.1 lb per watt.

### Conclusions

Although oxygen is produced by the superoxide while carbon dioxide is removed, the rate of oxygen production is not sufficient to supply the vehicle breathing and leakage gas. As an additional oxygen supply must be provided aboard the vehicle for cabin pressurization, the gas supply subsystem is in no way simplified by the use of superoxides for carbon dioxide removal.

Superoxide carbon dioxide removal systems have been tested and shown applicable to space vehicles; however, they have a tendency to form a hygroscopic hydroxide under certain conditions. This tends to plug the bed. The control problems associated with their use have not yet been solved completely. Usually, a lithium hydroxide bed is used in parallel with the superoxide bed to insure complete carbon dioxide removal. This, however, adds to the system control complexity and weight.

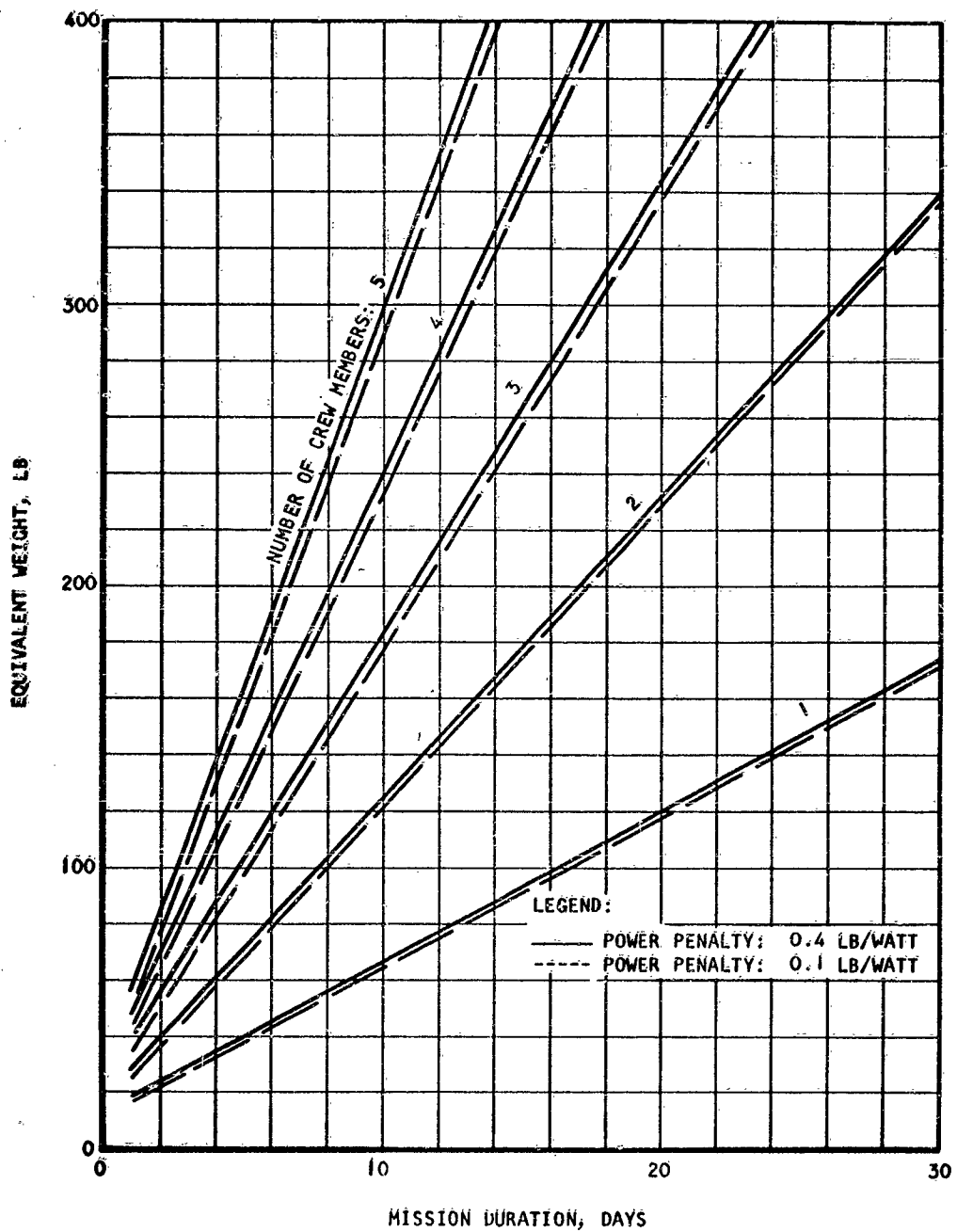


Figure 62. Sodium Superoxide Subsystem Equivalent Weight  
(No Credit for Oxygen Production)

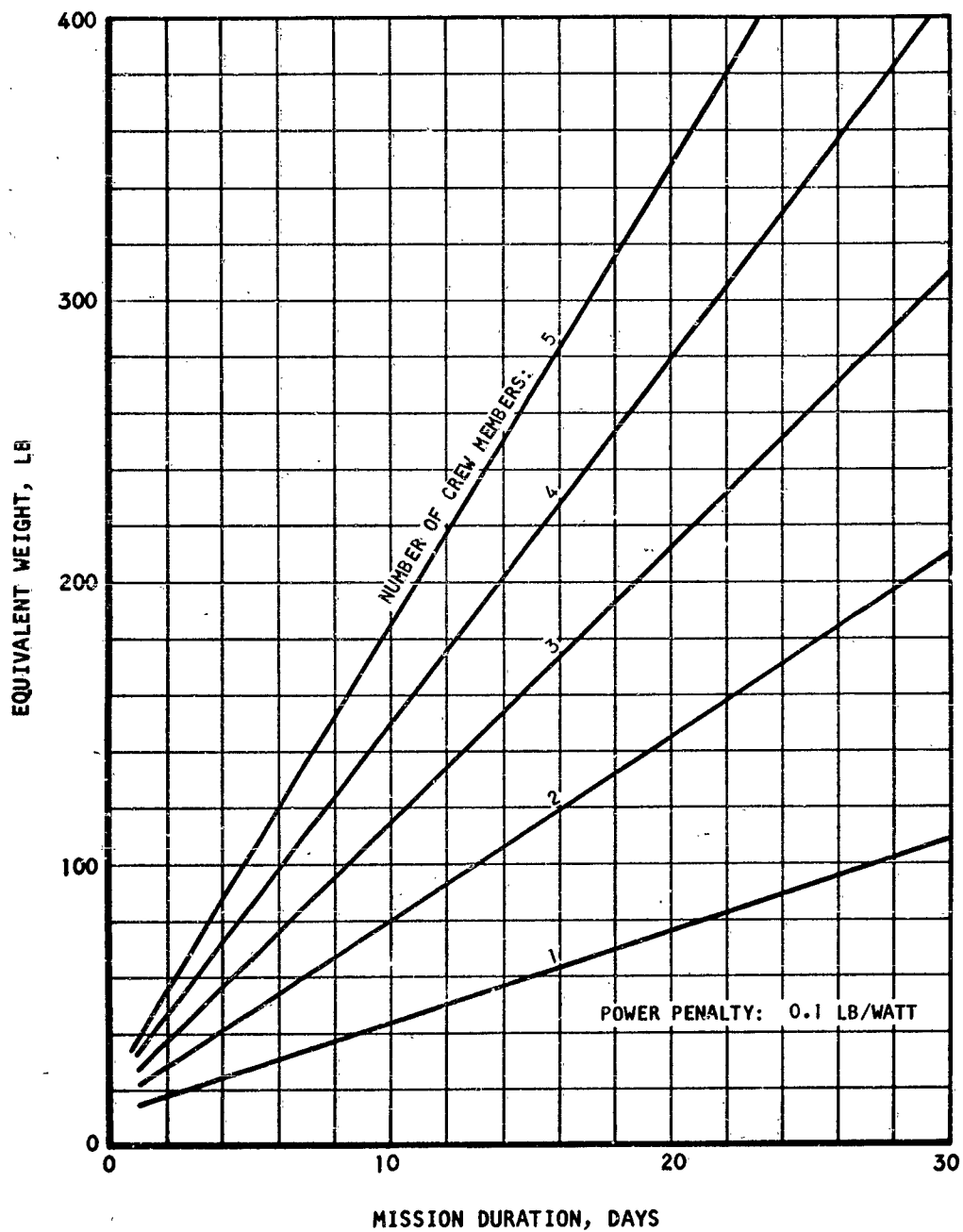


Figure 63. Sodium Superoxide Subsystem Equivalent Weight  
(Credited for Oxygen Production)

Handling of the sodium superoxide charges is more of a problem than in the case of the lithium hydroxide.

Like the lithium hydroxide, the sodium superoxide subsystem weight is time-dependent, and its application limited to relatively short mission durations. The system, however, is attractive for use in emergency situations because of its capacity for supplying oxygen. Superoxide subsystems might prove more reliable than lithium hydroxide for this application.

The water absorbed by the reaction might not be a penalty to the subsystem, where excess water is produced aboard the vehicle; this would occur if a fuel cell were used for power generation.

Lithium hydroxide and sodium superoxide subsystems are comparable on a mission duration basis. Figure 64 shows such a comparison for a 3-man system, a cabin pressure of 10 psia, and a cabin carbon dioxide partial pressure of 7.6 mm Hg. This plot shows that even in the case when the sodium superoxide subsystem is credited for the oxygen produced, it is still much heavier than the lithium hydroxide subsystem.

#### CARBON DIOXIDE REMOVAL BY MOLECULAR SIEVE

##### General

Carbon dioxide removal by the use of regenerable solid adsorbents is a means of obtaining low environmental control system weight in moderate-to-long duration applications. Materials considered suitable for this use include silica gel, activated alumina, and synthetic zeolites. The synthetic zeolites are most promising for space vehicle use and are the subject of consideration here. For ease of discussion, reference is made only to "Molecular Sieves" manufactured by Linde, although other manufacturers produce equally satisfactory materials. "Microtraps" by Davison Chemicals are another example.

Present regenerable carbon dioxide adsorbents also adsorb water; their affinity for water is considerably greater than for carbon dioxide. Thus, in adsorption, water will be picked up in preference to carbon dioxide, displacing carbon dioxide previously adsorbed if necessary. The capacity of the zeolites for water adsorption is shown in Figure 33.

Molecular sieves require temperatures on the order of 400 to 600°F for the desorption of water. This in itself prohibits their use for gas drying aboard space vehicles. Their greater affinity for water than for carbon dioxide also establishes a requirement for drying the process gas to a very low dew point if they are to be used for carbon dioxide removal. Silica gel is commonly used to dry the gas. Very low dew points are attainable by careful desiccant bed design, and silica gel can be regenerated by purging it with dry air at temperatures of approximately 250°F.

The carbon dioxide adsorbents can be regenerated by application of a vacuum with the bed at ordinary temperatures. A vacuum less than 50 microns is required for desorption at reasonable rates. In practice, it will not



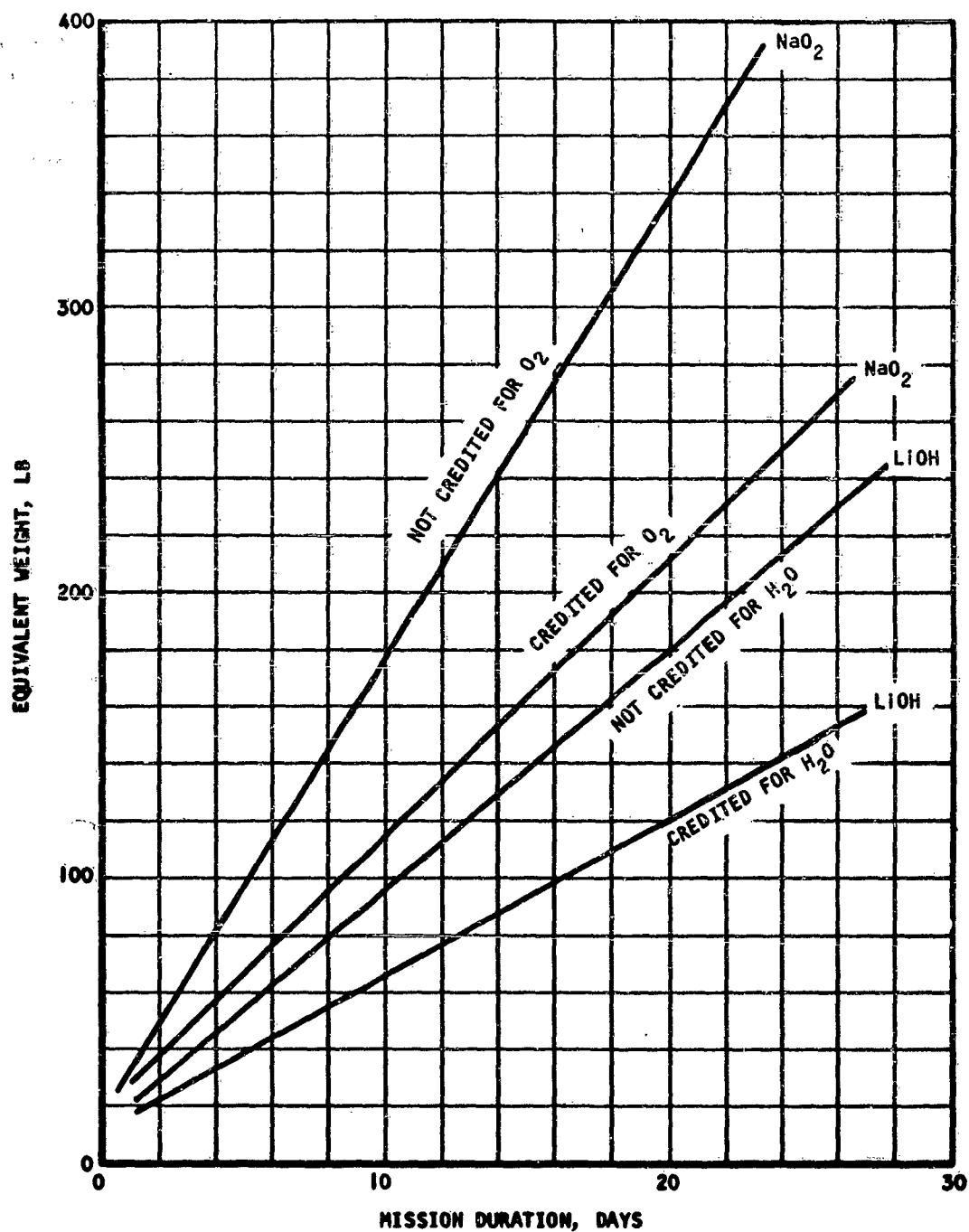


Figure 64. Carbon Dioxide Absorption Subsystem Comparison

usually be practical to completely desorb the bed, because of the time this process requires. As a consequence, there will be an initial carbon dioxide loading at the start of the adsorption cycle. This must be taken into account in bed design.

Figure 65 shows the comparative carbon dioxide adsorption capacity of molecular sieves at a temperature of 77°F. Other adsorbing materials also are shown. The temperature at which the adsorption process takes place has a marked effect on the molecular sieve loading capacity; this is shown in Figure 66, where the isothermal adsorption equilibrium capacity of molecular sieve Type 5A at various temperature levels is given.

Under dynamic adsorption conditions in an adsorber bed, the usable capacity is substantially less than the values given by the equilibrium curves. A large number of variables influence performance. These include superficial velocity, carbon dioxide partial pressure, temperature, bed length, particle size, and process gas composition.

#### Carbon Dioxide Removal System Description

Figure 67 shows a typical regenerable removal system configuration. To avoid poisoning the carbon dioxide adsorbent with water vapor, the process air is first dried to an extremely low dew point in a desiccant canister. The heat generated by dehydration of the air causes an increase in air temperature, and the air is cooled prior to entering an adsorber where the carbon dioxide is removed. The process air is reheated in the recuperative heat exchanger and is additionally heated by the compressor and an electric heater before entering the desiccant bed being regenerated. The carbon dioxide adsorbent is regenerated by application of a high vacuum.

The main internal design trade-off associated with the regeneration cycle of the desiccant beds involves the cycle time and purge gas temperature level. For example, using silica gel as the desiccant, the desorption time will be approximately 75 per cent of the adsorption time, using a purge gas temperature of 250°F. For a higher gas temperature, the desorption time will be shorter and, conversely, for a lower temperature, the desorption time will be longer. It is not necessary to completely desorb the desiccant bed with every cycle. As a means of reducing the power requirements, the desiccant bed can be partially desorbed for a number of cycles with periodic complete desorption at a higher temperature level. This will be reflected in a somewhat increased fixed weight. Many other trade-offs between power and fixed weight are to be found in the design of regenerable systems. The recuperative heat exchanger provides utilization of the heat stored in a freshly regenerated bed for regeneration of the bed being desorbed. Also, most of the heat of adsorption is recovered for the desorption of the saturated bed.

Figure 68 shows a modification of the previous system in which waste heat is used for desorption of the desiccant as a means of reducing the electrical power input to the system. The temperature level for the waste heat will be an important parameter in system design. If the cabin air is pre-cooled to a sufficiently low value, the heat exchanger will not be required.

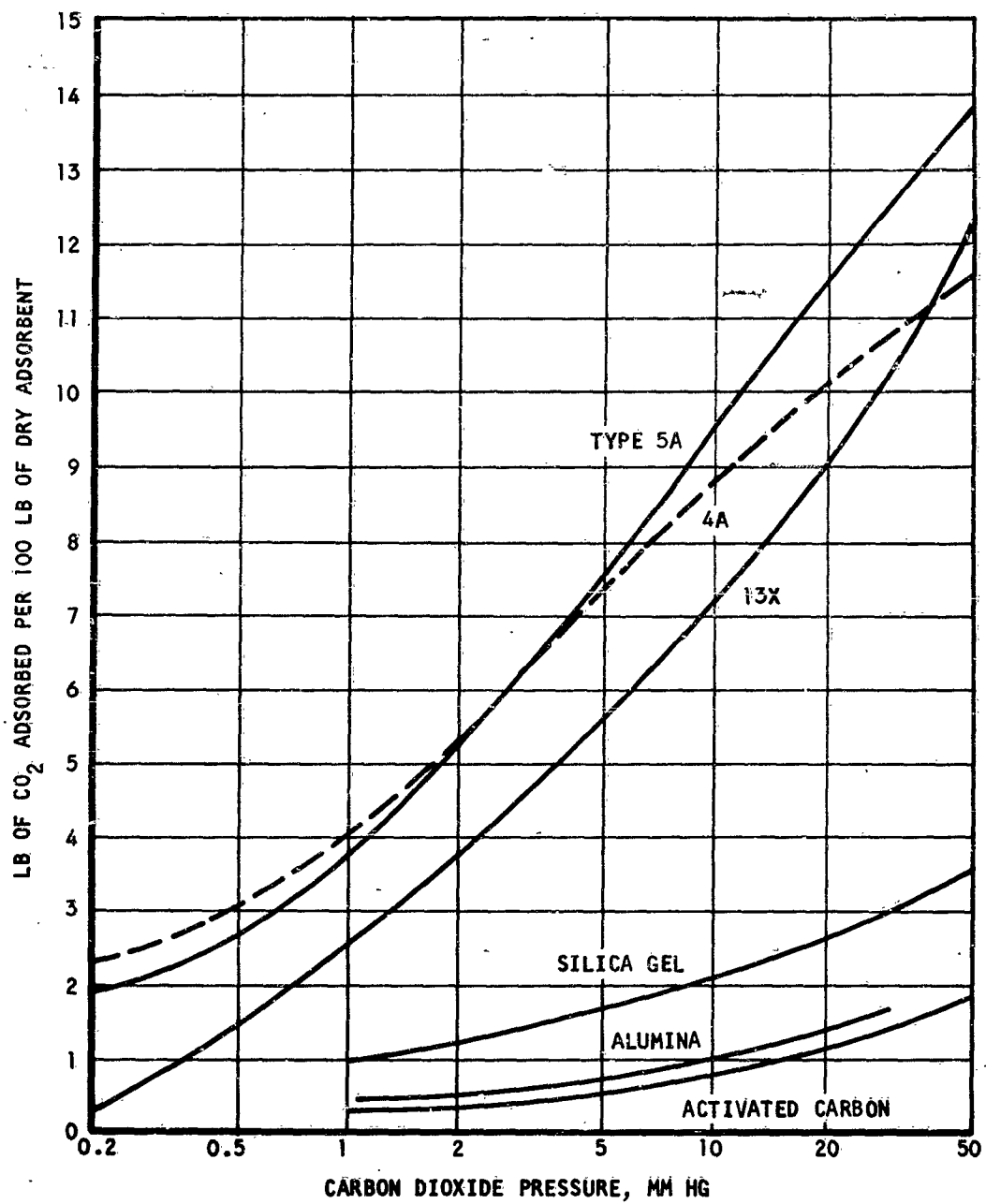


Figure 65. Comparison of Adsorption Capacity of Three Types of Molecular Sieves at 77°F

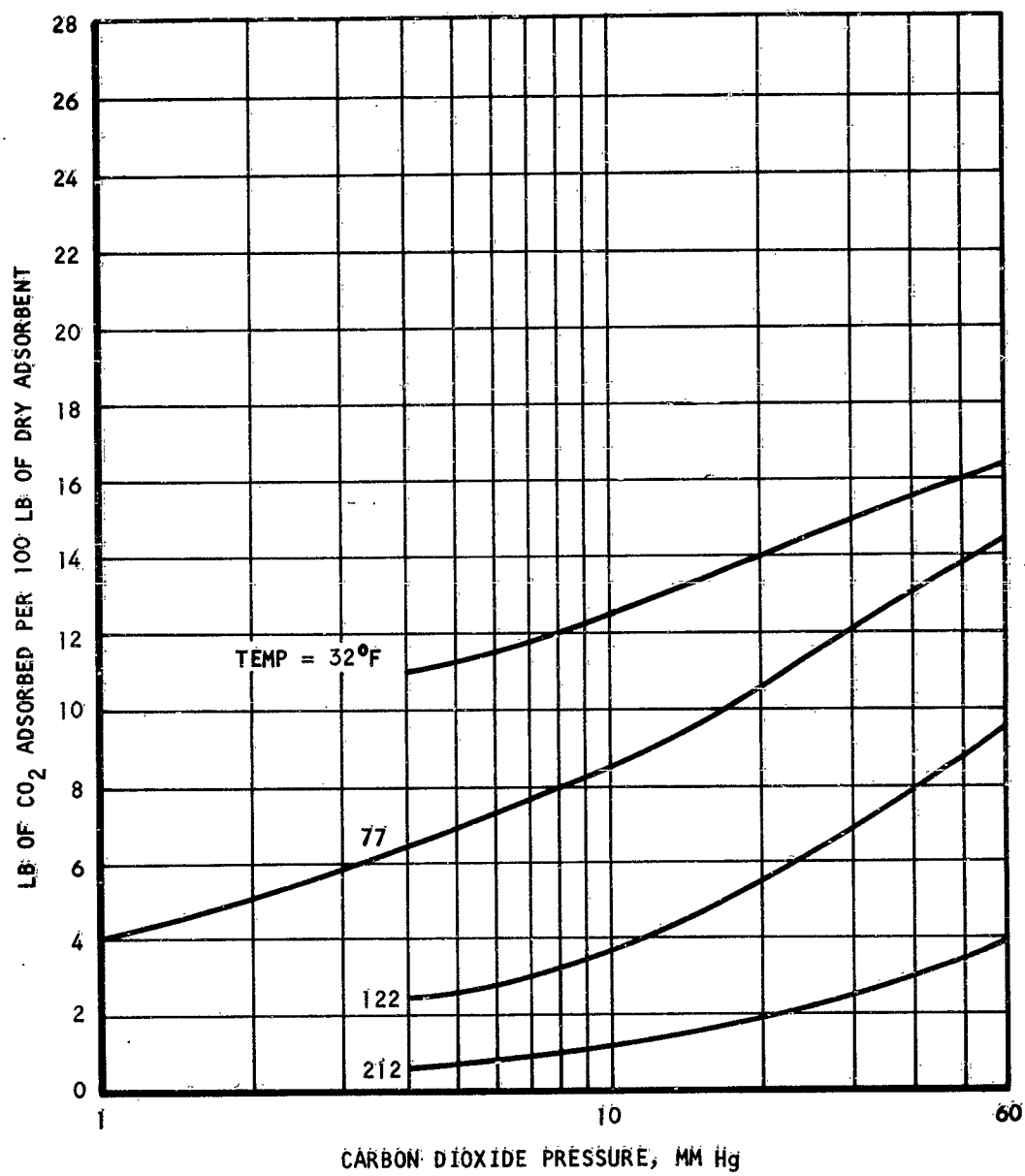


Figure 66. Adsorption Isotherms for Type 5A Molecular Sieve

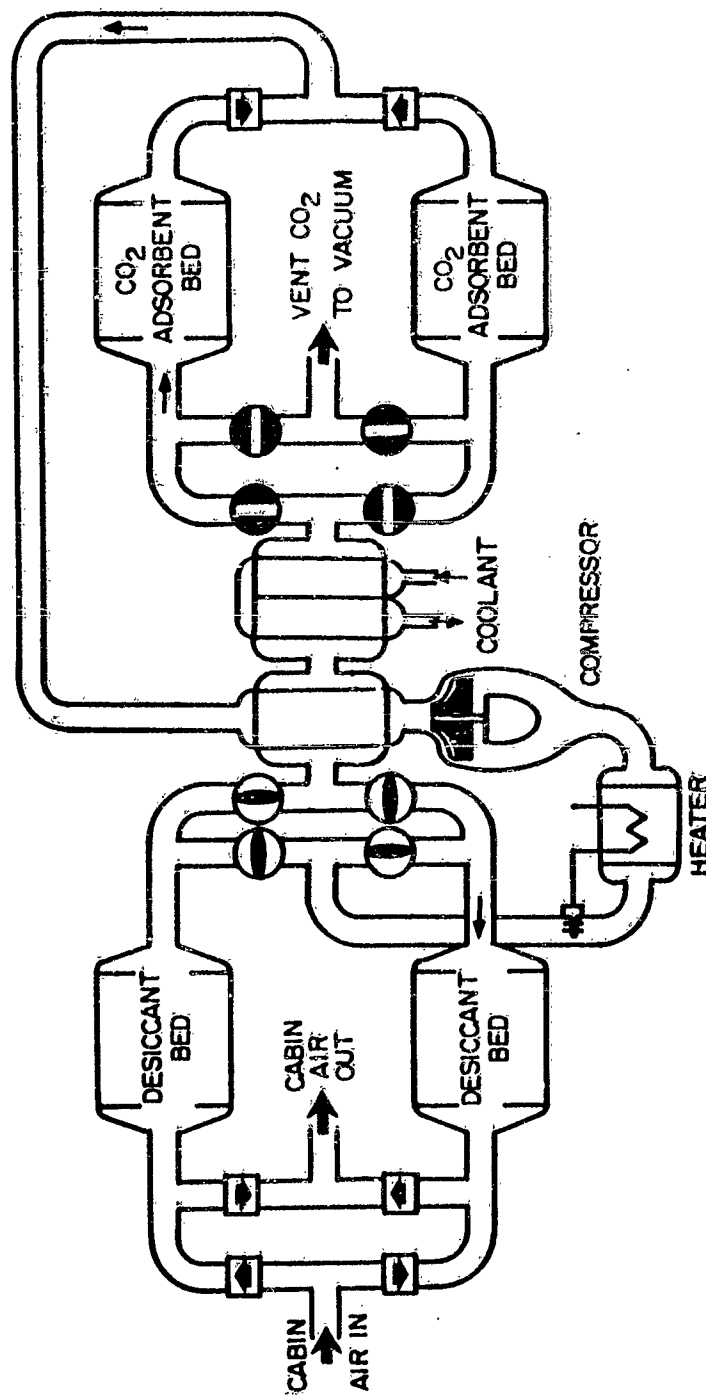


Figure 67. Typical Regenerable Adsorbent Carbon Dioxide Removal Subsystem (No Waste Heat Recovery)

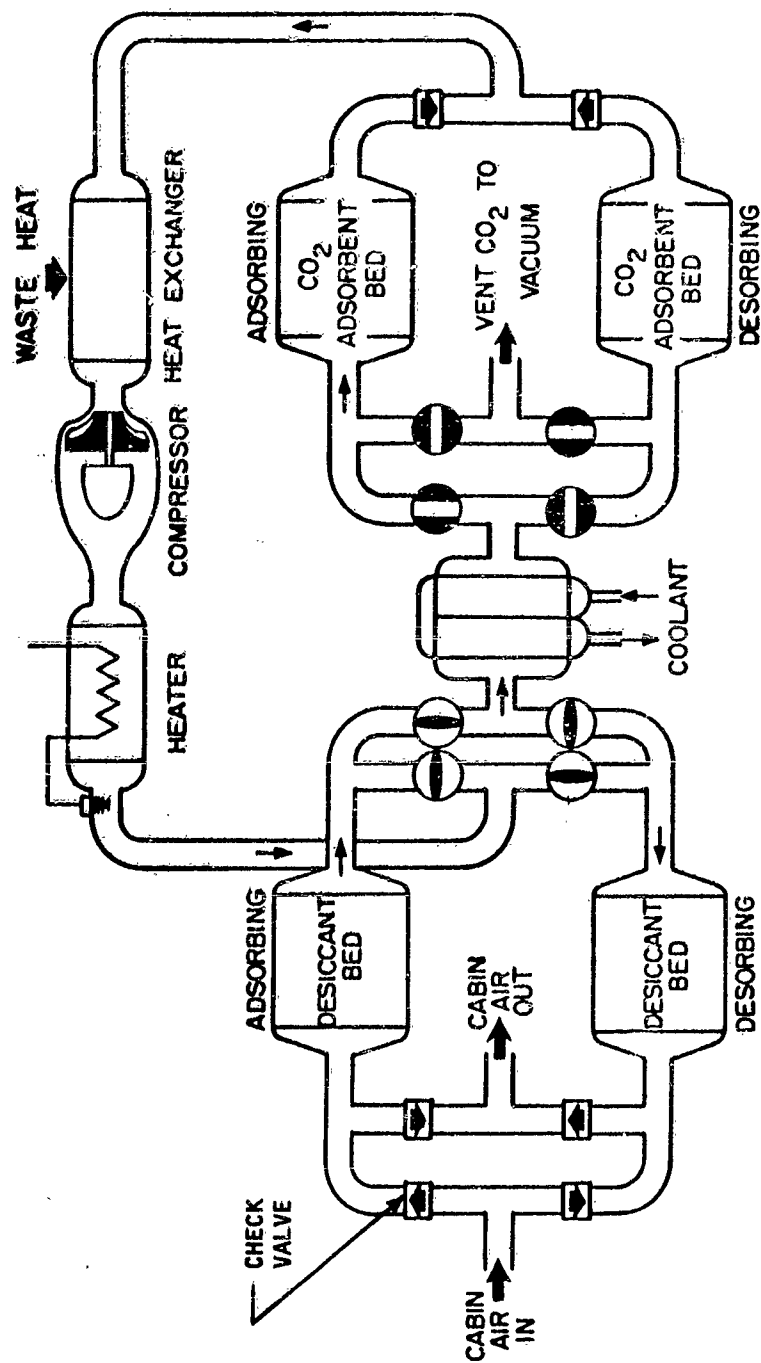


Figure 68. Typical Regenerable Adsorbent Carbon Dioxide Removal Subsystem (With Waste Heat Recovery)

## Subsystem Characteristics

### 1. Flow Requirement

The flow is determined on the assumption of complete removal of the carbon dioxide present in the process air at subsystem inlet. This flow, based on a carbon dioxide removal rate of 2.25 lb per man-day, is shown in Figure 69 as a function of the carbon dioxide partial pressure and the cabin total pressure.

The amount of water to be removed in the desiccant bed, assuming complete removal of the water, is plotted in Figure 70 for a dew point temperature at bed inlet of 45°F. The heat released in the adsorption process is shown in Figure 71. These two parameters, water adsorbed and heat load, are not functions of the cabin pressure but depend on the carbon dioxide partial pressure and on the process gas dew point.

### 2. Air Temperature Rise Through the Desiccant Bed

The heat and mass transfer processes taking place within the silica gel bed are very complex. At the beginning of the adsorption process, assuming the bed is cold, the face of the bed will be heated by the heat of adsorption. Some of this heat will be entrained downstream by the process air warming the rest of the bed. As the adsorption front moves downstream, the face of the bed, which is then saturated at some equilibrium temperature, will be cooled by the cold incoming air. Its capacity thus increases, and it adsorbs more moisture. At the end of the bed cycling period, the front portion of the bed will be relatively cold while the back portion will be warm. The same phenomenon will take place if the bed is warm at the beginning of the adsorption period. In this case, however, the bed is cooled somewhat by the process air to a temperature at which it can adsorb water at the partial pressure present in the process air.

Since at the end of the adsorption cycle most of the bed is at the inlet air temperature, only the downstream end being warm, the greatest part of the heat of adsorption is dumped into the air stream. In Figure 72 is plotted the process air temperature rise, assuming all the heat of adsorption is rejected to it at a constant rate.

Since the curve was plotted for a constant inlet dew point of 45°F, the temperature rise is the same for all values of the carbon dioxide partial pressure in the cabin, although the air flow through the subsystem varies with this pressure.

Only steady-state conditions are considered here. It should be noted that if the bed temperature is 250°F at the start of the adsorption period, the air temperature at bed outlet would approach the bed temperature. Since the adsorption efficiency of the warm bed is very poor, most of the water vapor present in the incoming air will not be adsorbed until the bed is sufficiently cooled; soon, poisoning of the molecular sieve beds will occur. Therefore, the heat stored during desorption of the silica gel bed should be removed after each cycle.

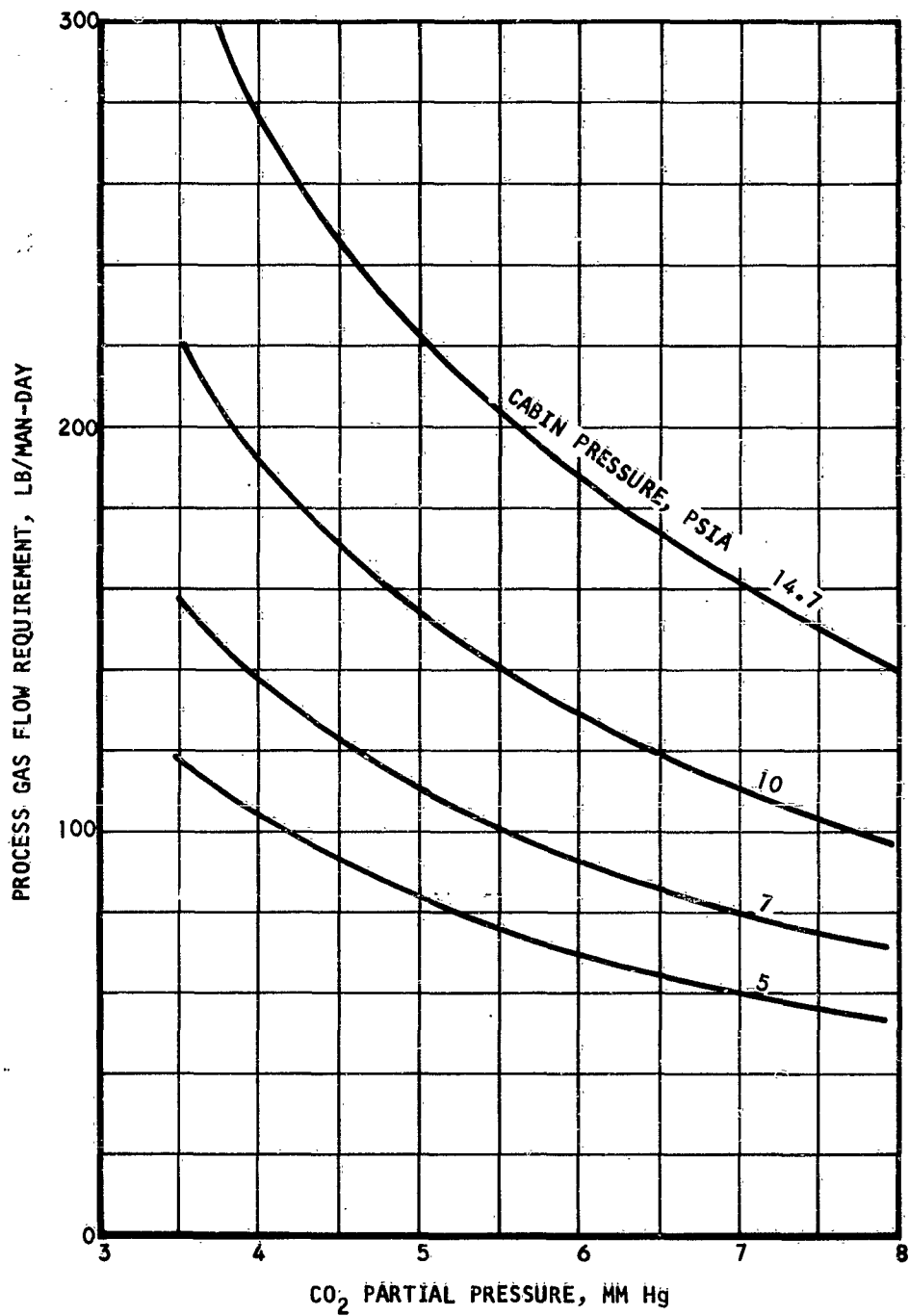


Figure 69. Flow Requirement Through the Molecular Sieve Subsystem



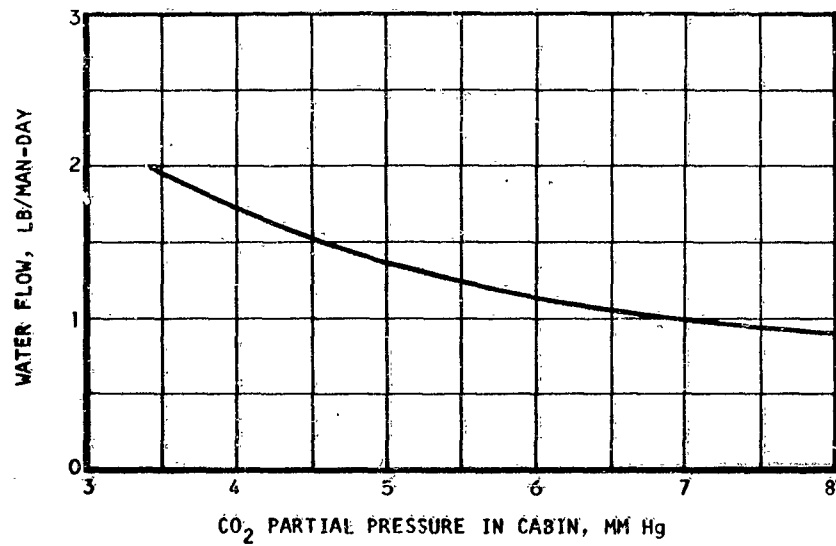


Figure 70. Water Vapor Flow to the Carbon Dioxide Management Subsystem

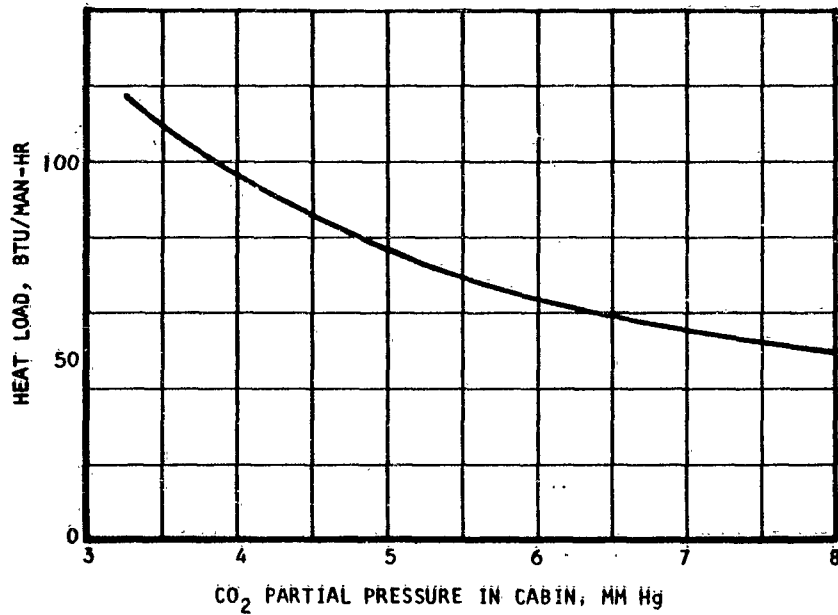


Figure 71. Heat Rejection Load from Water Adsorption

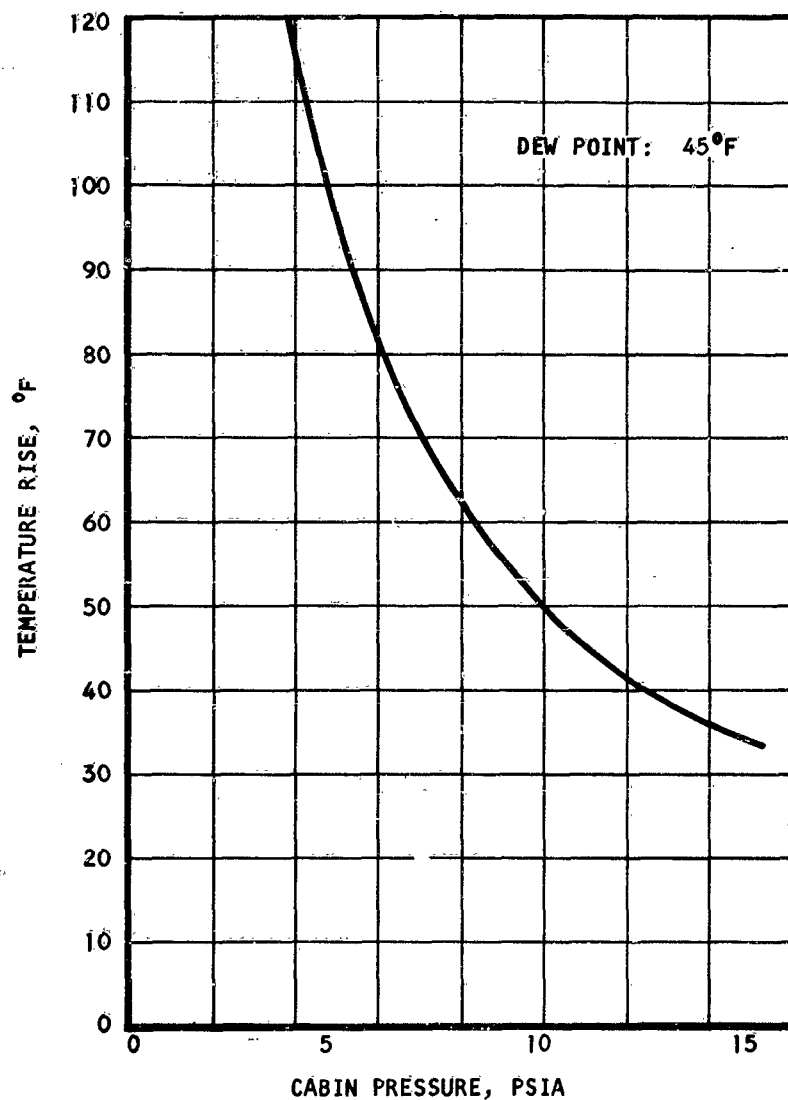


Figure 72. Process Air Temperature Rise Across Desiccant Bed

### 3. Silica Gel Canister Design

The silica gel bed utilization efficiency depends on the silica gel particle size, on the process air superficial velocity, and on the actual bed dimensions. However, for reasonable canister dimensions and air superficial velocities yielding acceptable pressure drops, the bed utilization efficiency based on the equilibrium capacity shown in Figure 33 is on the order of 30 per cent. This value was obtained from calculations performed assuming isothermal adsorption and outlet dew point temperatures on the order of  $-70^{\circ}\text{F}$ . The particle mesh size used in the calculations was 6 to 10.

Using this value of the bed utilization efficiency, an estimate of the silica gel bed canister weight was made for the purpose of system characterization. The following assumptions were used in the computations:

- a. The canister is assumed to be cylindrical. The wall of the cylinder is 0.050 in. thick and the circular ends 0.125 in. The canister material is aluminum. Using this model, the weight of the canister is expressed by

$$W_C = 3.6A_F + 2.553 \sqrt{A_F} L \quad (56)$$

- b. The pressure drop through the canister is taken as a function of the number of crew members and equal to

$$\Delta P = 0.7 + 0.3N, \text{ in } H_2O \quad (57)$$

- c. The canister length is calculated from the equation:

$$\Delta P = 4f \frac{G^2}{2g\rho} \frac{L}{D} \quad (58)$$

$$\text{where } f = \frac{850}{R_e} \quad (59)$$

- d. The temperature of the process air is taken as average between bed inlet and bed outlet. The air temperature rise of Figure 72 is used here.
- e. The adsorption-desorption cycle is taken as one hour.
- f. The calculations were performed for a silica gel particle mesh size of 8 to 10.

The results of these computations are given in Figures 73 and 74, where the silica gel charge weight and the canister weight are plotted as a function of the system pressure for three values of the carbon dioxide

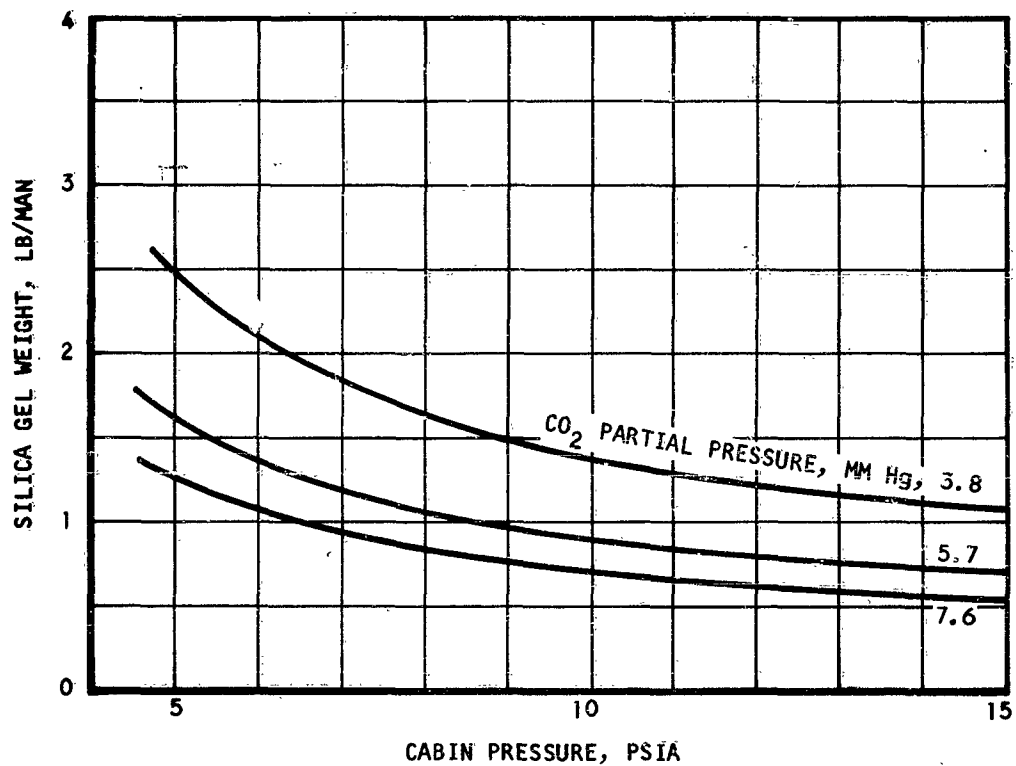


Figure 73. Silica Gel Charge Weight for Process Air Drying

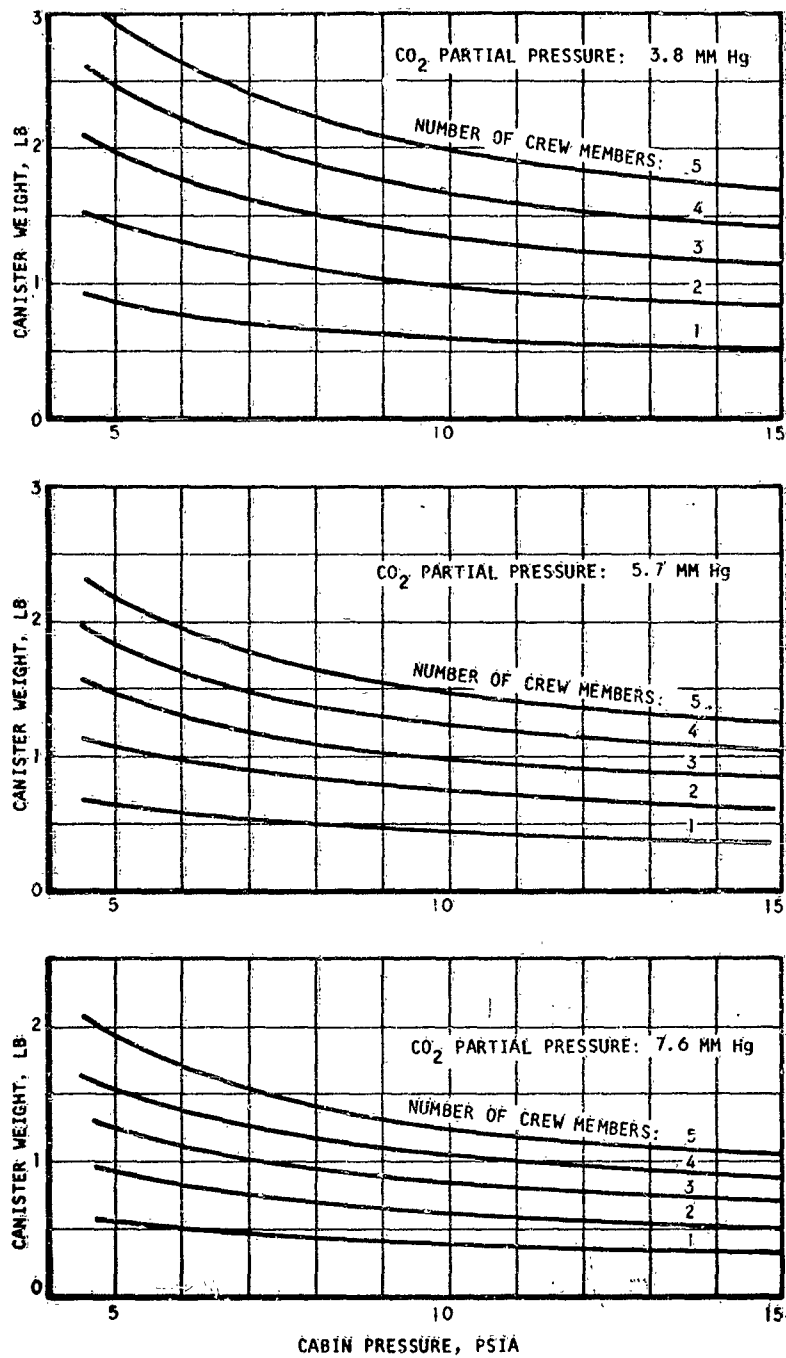


Figure 74. Desiccant Bed Canister Weight

partial pressure in the cabin: 7.6, 5.7, and 3.8 mm Hg. The canister weight is given for a number of crew members from 1 to 5. The weight of the canister varies between 30 and 50 per cent of the silica gel weight, depending on the amount of silica gel contained. The silica gel weight is plotted in Figure 73 as a function of the cabin pressure and the carbon dioxide partial pressure in the cabin.

Based on the above assumptions, the power loss incurred for pumping the process air through one bed during the adsorption cycle is plotted in Figure 75. Here the compressor-motor efficiency is taken as 30 per cent. During desorption, the friction power loss in the canister is about 1.8 to 2.0 times as large because of the higher process air temperature.

#### 4. Recuperator Optimization

The recuperative heat exchanger shown in the diagram of Figure 67 can in some operating conditions be used as a means of reducing the power necessary to heat the process air to the temperature required for bed desorption. While heat is transferred from the air leaving the adsorbing bed to the relatively cold air from the molecular sieve, the load on the cooler is also reduced; the recuperator, therefore, has a dual function. The power saved by the recuperator is especially large when the bed is not cooled after desorption. In this case, the heat stored in the bed at the end of the desorption cycle is used over again for desorption of the other bed.

A trade-off study between power saving, cooling load reduction, and heat exchanger weight was conducted to determine the optimum recuperator size and effectiveness. The weight of the exchanger and the pressure drop were estimated by the method derived in Reference 1. The heat transfer surface used in the study is defined as follows:

Construction: Plate fin, same fin on both sides

Fin type: Rectangular

Number of fins: 16 fins per in.

Fin dimensions: 0.153 in. high, 1/7 in. offset, 0.004 in. thick

Material: Aluminum

The system equivalent weight saving due to the use of the regenerator obviously depends on the vehicle power penalty (PP) and cooling load penalty (RP). For the purpose of system characterization, these parameters were taken as (PP) = 0.200 lb per watt of power and (RP) = 0.0200 lb per watt of cooling.

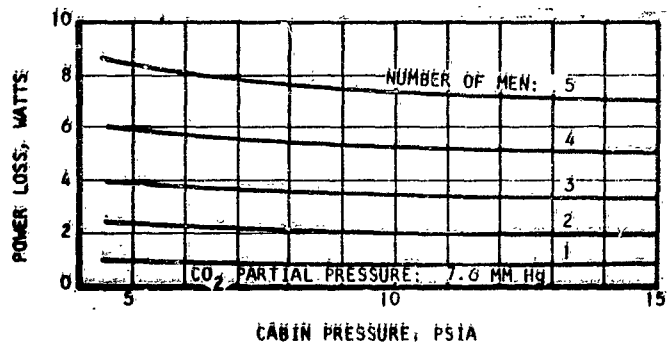
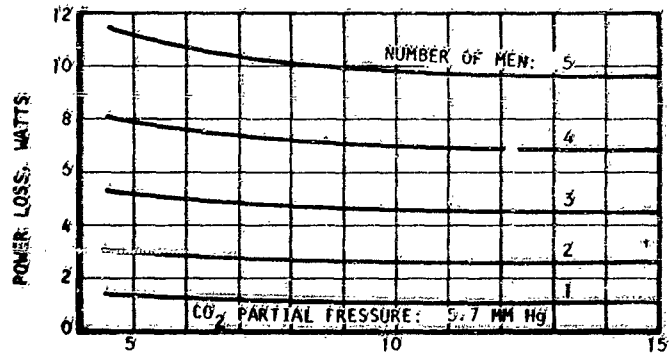
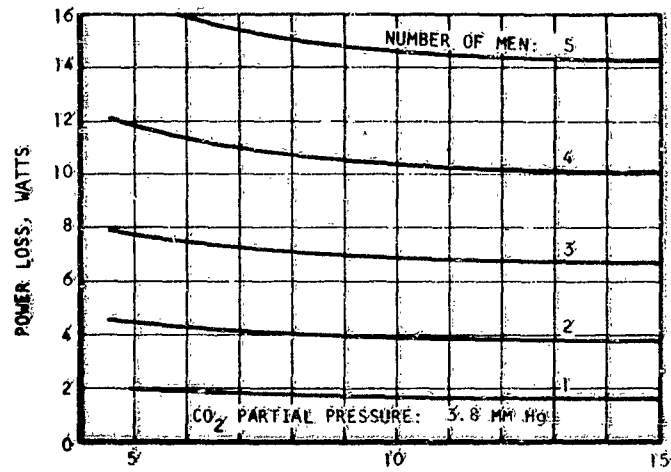


Figure 75: Power Loss Through Silica Gel Canister

The power reduction due to the recuperator is expressed for a one-man system by

$$PS = \epsilon \Delta T_{\max} \frac{w}{24} \times \frac{0.24}{3.413}, \text{ watts} \quad (60)$$

where  $\epsilon$  is the heat exchanger effectiveness

$\Delta T_{\max}$  is the temperature difference between the hot and cold streams at inlet.  $\Delta T_{\max}$  obtained from Figures 72 and 77, assuming the air temperature at silica gel bed inlet is 45°F, and at molecular sieve bed inlet, 50°F

$w$  is the air flow from Figure 69

The cooling load reduction,  $Q_R S$ , also is expressed by the same equation.

The equivalent system weight saving for any operating conditions can be written as

$$W_E = W_{HX} - PS (PP) - Q_R S (RP) \quad (61)$$

Calculations of heat exchanger weight and system penalties show that in the range of conditions considered here and for the penalties defined above, the optimum recuperator effectiveness is about 0.82. The system equivalent weight saving per man is shown plotted in Figure 76. Also shown in Figure 76 are the cooling load reduction and the heater power savings for optimum system weight. It should be emphasized that these calculations were performed for steady-state operation or average conditions, when the bed is cooled after desorption.

##### 5. Air Temperature Rise in the Molecular Sieve Bed

The air temperature rise in the molecular sieve bed was calculated in the same manner as for the silica gel bed. The carbon dioxide removal rate was taken as 2.25 lb per man-day, and it was assumed that the heat released in the adsorption process was entirely dumped into the air. The results of these calculations are shown in Figure 77.

##### 6. Molecular Sieve Canister Design

The characteristics of the molecular sieve canisters were determined in the same manner as for the desiccant canisters. Here the basic design assumptions are as follows:

Molecular sieve type: 5A

Bed utilization efficiency: 0.30



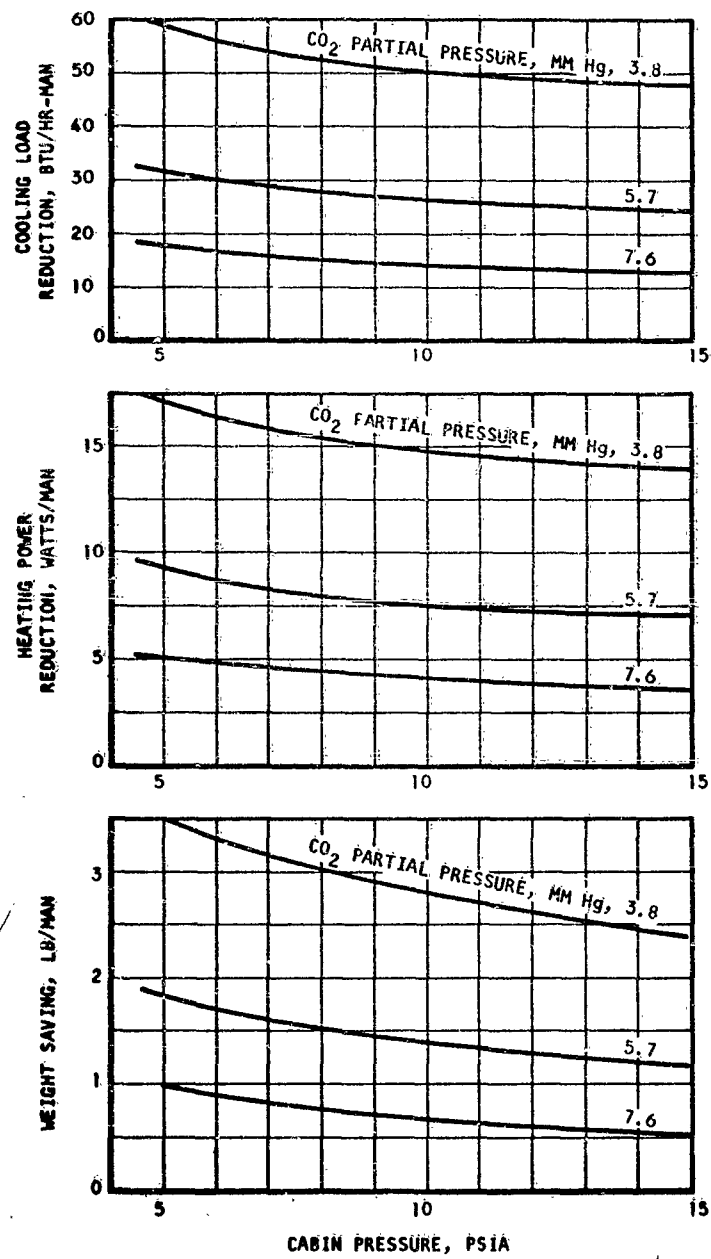


Figure 76. Effect of Recuperator on Subsystem

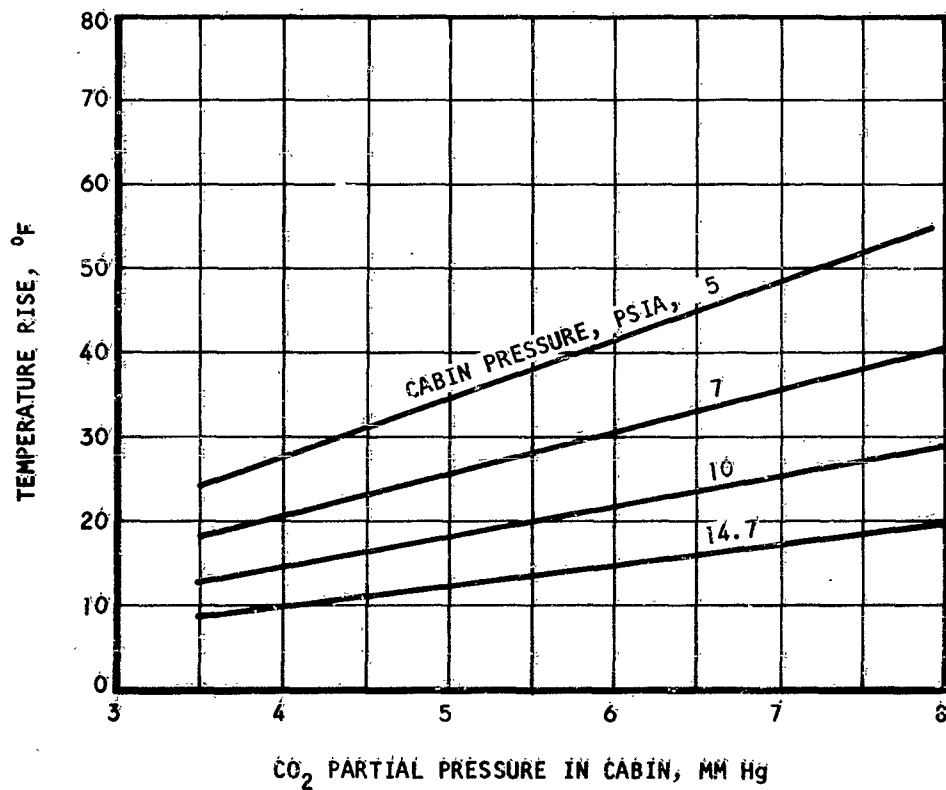


Figure 77: Process Air Temperature Rise Across the Molecular Sieve Bed

Particle mesh size: 8 to 10

Cycling time: 30 minutes

Canister weight:  $W_C = 3.6 A_F + 2.553 \sqrt{A_F} L$  (62)

(Reference: Equation 56)

Pressure drop through the bed:

$$\Delta P = 0.9 + 0.3 N, \text{ in. H}_2\text{O} \quad (63)$$

The significant results of the computations performed, based on the above assumptions, are shown in Figures 78, 79, and 80, in which the molecular sieve material weight, canister weight, and pumping power losses are plotted against the system pressure for three values of the carbon dioxide partial pressure in the process air: 7.6, 5.7, and 3.8 mm Hg. These parameters are only slightly dependent on the carbon dioxide concentration in the air stream.

#### 7. Subsystem Power Requirement

For space vehicle applications, it is important to minimize the power consumption of various systems because of the high weight penalties associated with power extraction. In the regenerable carbon dioxide removal system under consideration, electrical power is used to provide gas circulation and gas heating for desiccant bed desorption. The power input to the compressor will appear as a temperature rise in the gas flow. Thus, the compressor power input represents a direct contribution to desiccant bed desorption, in the arrangements shown in Figures 67 and 68. For the desiccant bed to undergo desorption in a period shorter than the adsorption cycle, the process gas must be heated to a temperature of 250°F before it enters the desiccant canister being desorbed. The power required for this process will determine the power input to the system. From the temperature effects previously calculated for the adsorbent beds, the total power input required to provide desiccant bed desorption can be calculated. This is shown in Figure 81 as a function of the cabin pressure for three different values of the carbon dioxide concentration in the cabin. Here it is assumed that the silica gel bed is cooled after desorption and that the temperatures at silica gel bed inlet and molecular sieve bed inlet are 45°F and 50°F, respectively. A large portion of this power is used to drive the compressor.

#### 8. Heat Rejection Load

Throughout the carbon dioxide removal system, heat is transferred from the adsorption beds to the air stream and inversely; heat also is exchanged in the recuperator, compressor, and heater element. A complete analysis of the heat transfer in the circuit is very complex; for the purpose of system evaluation, heat is assumed to appear in the system at three locations of interest only:

- a. In the cooler, upstream of the molecular sieve bed, where heat is rejected from the process air to the vehicle cooling loop. Here

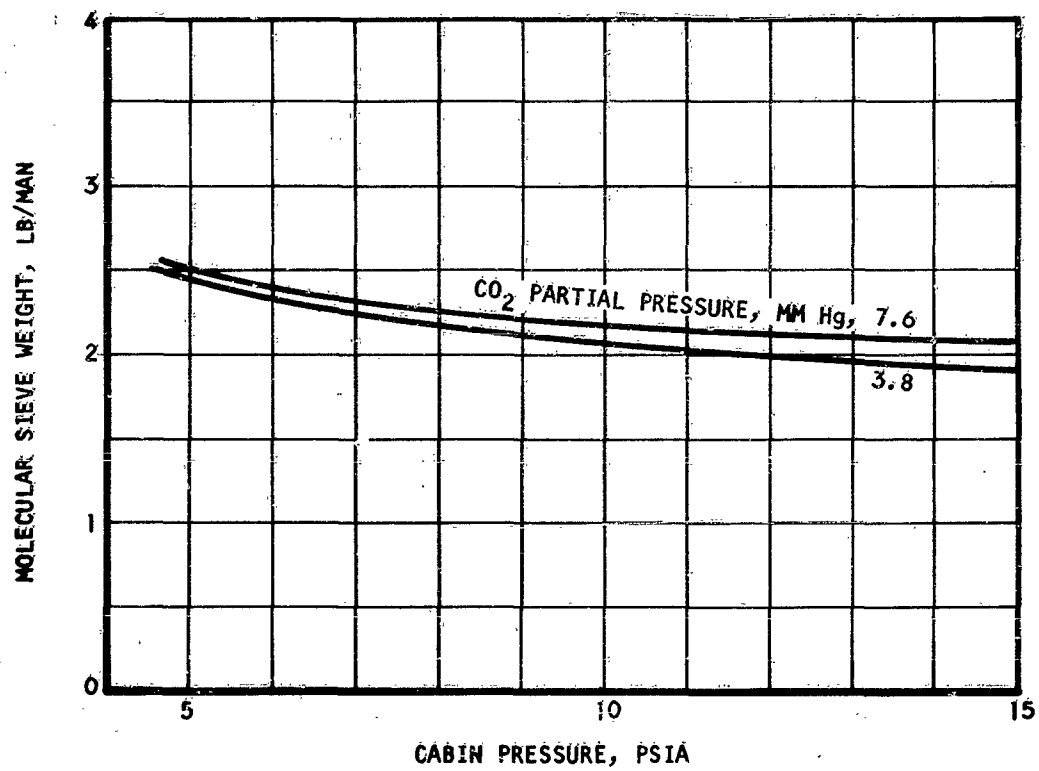


Figure 78. Molecular Sieve Weight for Carbon Dioxide Removal

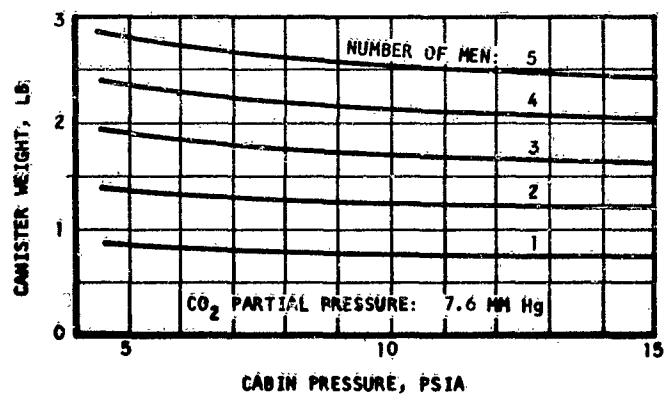
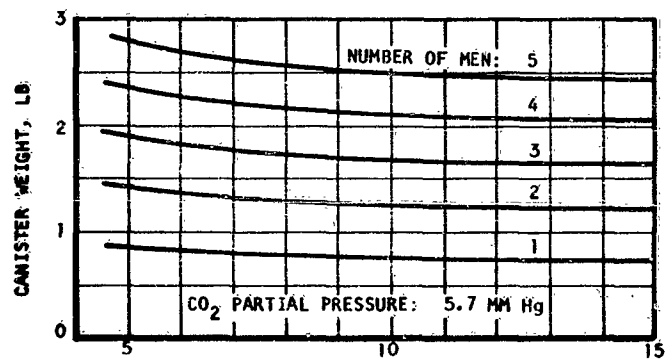
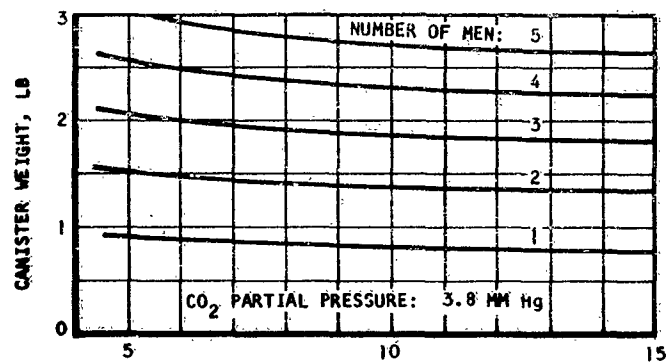


Figure 79. Molecular Sieve Bed Canister Weight

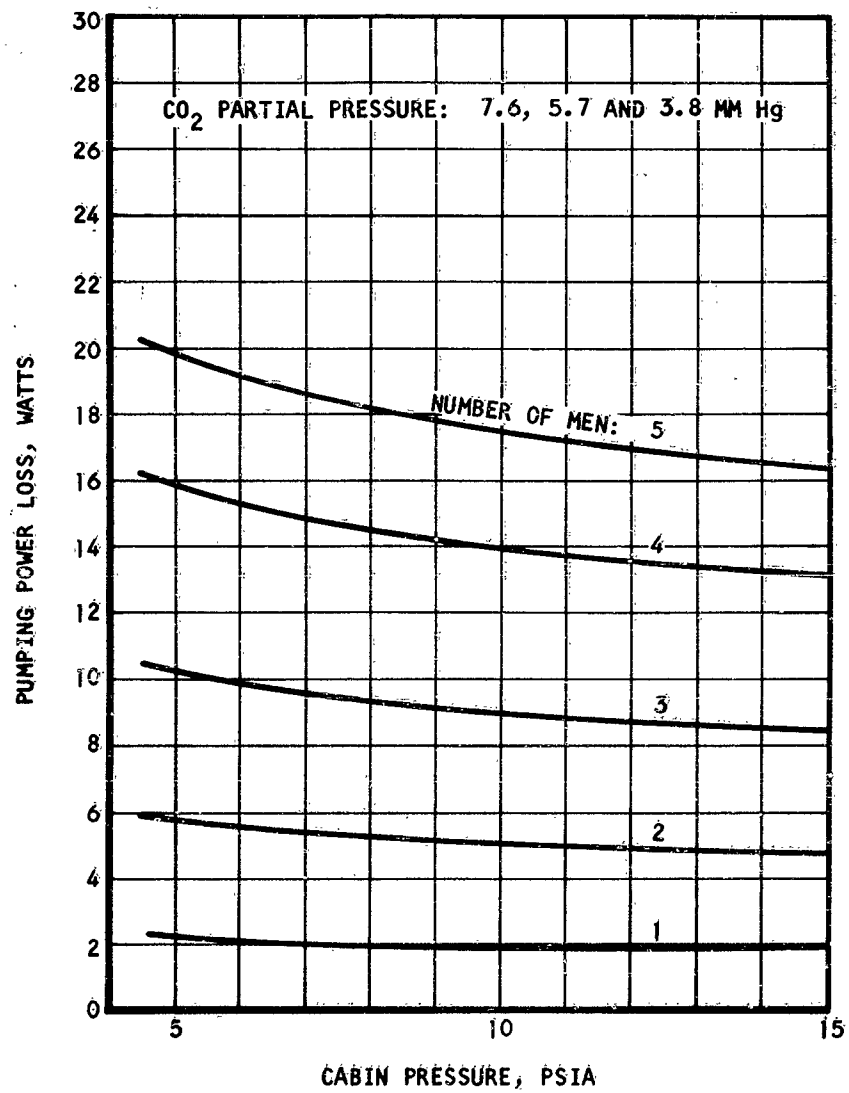


Figure 80. Molecular Sieve Bed Pumping Power Losses

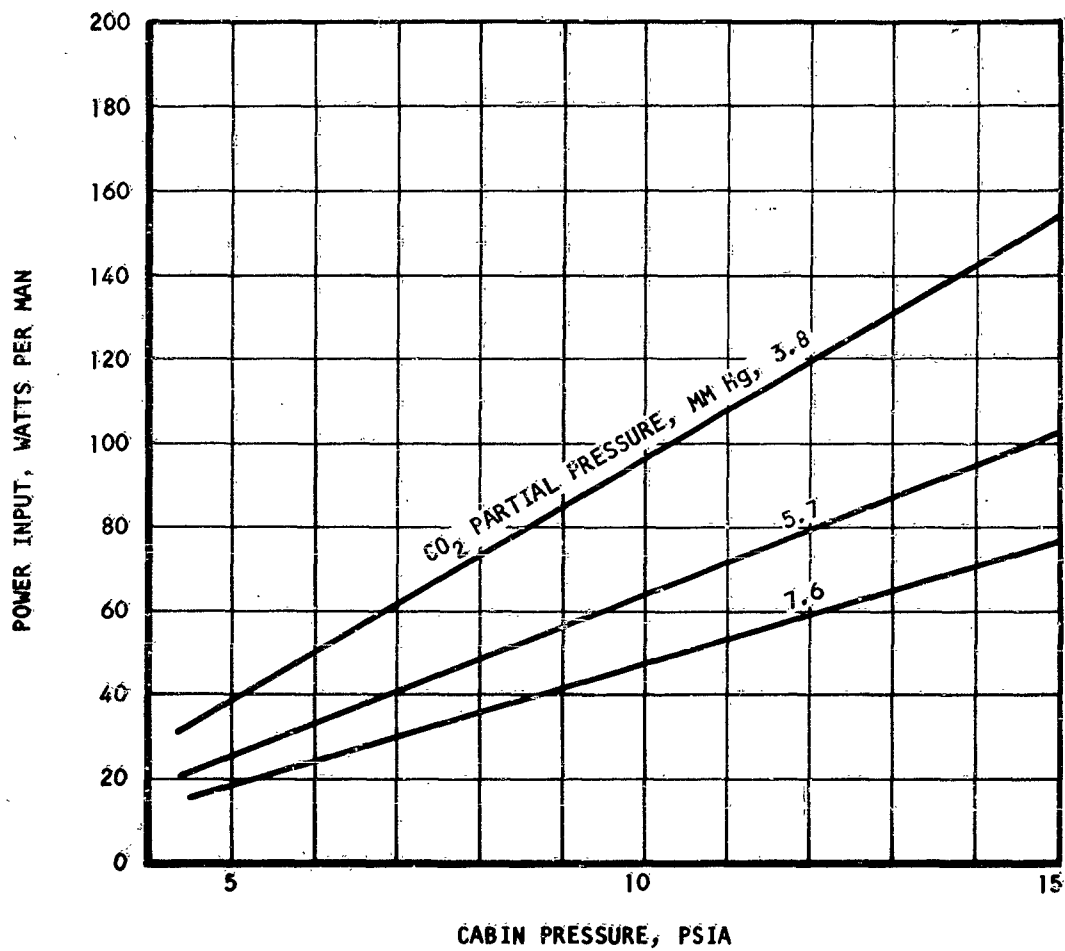


Figure 81. Molecular Sieve System Power Requirement

it is assumed that the air temperature at bed inlet is kept at a temperature of 50°F; the recuperator optimum effectiveness for a vehicle power penalty of 0.2 lb per watt was found to be 0.82. Under these conditions, the heat rejected to the vehicle cooling system is plotted in Figure 82.

- b. Heat is entrained by the process air exhausting from the system; this heat appears somewhere in the thermal balance of the vehicle and is considered here as a system penalty. The average value of this heat load is plotted in Figure 82.
- c. To prevent molecular sieve bed poisoning by entrained water, the silica gel beds are cooled before the adsorption cycle. The beds are not cooled during the adsorption process, since the heat of adsorption is partly recovered in the recuperator, thus reducing the system power requirement. This is achieved at the cost of a slight fixed weight penalty. The heat rejected to the vehicle cooling loop for bed cooling is calculated based on an initial bed temperature of 250°F and a final temperature of 70°F. It is plotted in Figure 82.

#### 9. Subsystem Equivalent Weight

The subsystem equivalent weight is made up of the subsystem hardware weight and the various penalties or credits associated with material balance, power requirements, heat rejection load, and heat sink potential of the subsystem. In the case of the molecular sieve subsystem, the total equivalent weight is expressed by

$$W_E = W_H + (PR)(PP) + (QR)(RP) \quad (64)$$

$W_H$  is the hardware weight including all the subsystem components. This weight can be estimated from the data presented in this section and from the weight of the accessories. The accessory weight of the subsystem depicted in Figure 17 is listed in Table 15 for a three-man subsystem. It is here, for the purpose of system evaluation, assumed to be a function of the number of crew members and is written as

$$W_A = 6.1 + 6.29 \sqrt{N} \quad (65)$$

The system hardware weight is plotted in Figure 83.

The total equivalent weight depends on the vehicle power penalty and heat rejection penalties. Figure 84 is a plot of the total system weight for power penalties of 0.1 and 0.4 lb/watt; the heat rejection penalty is here taken as one tenth of the power penalty. The plot has been prepared for a carbon dioxide partial pressure of 7.6 mm Hg. The equivalent weight for other values of the power penalty or other values of the carbon dioxide partial pressure is easily obtained from the data presented in this section.



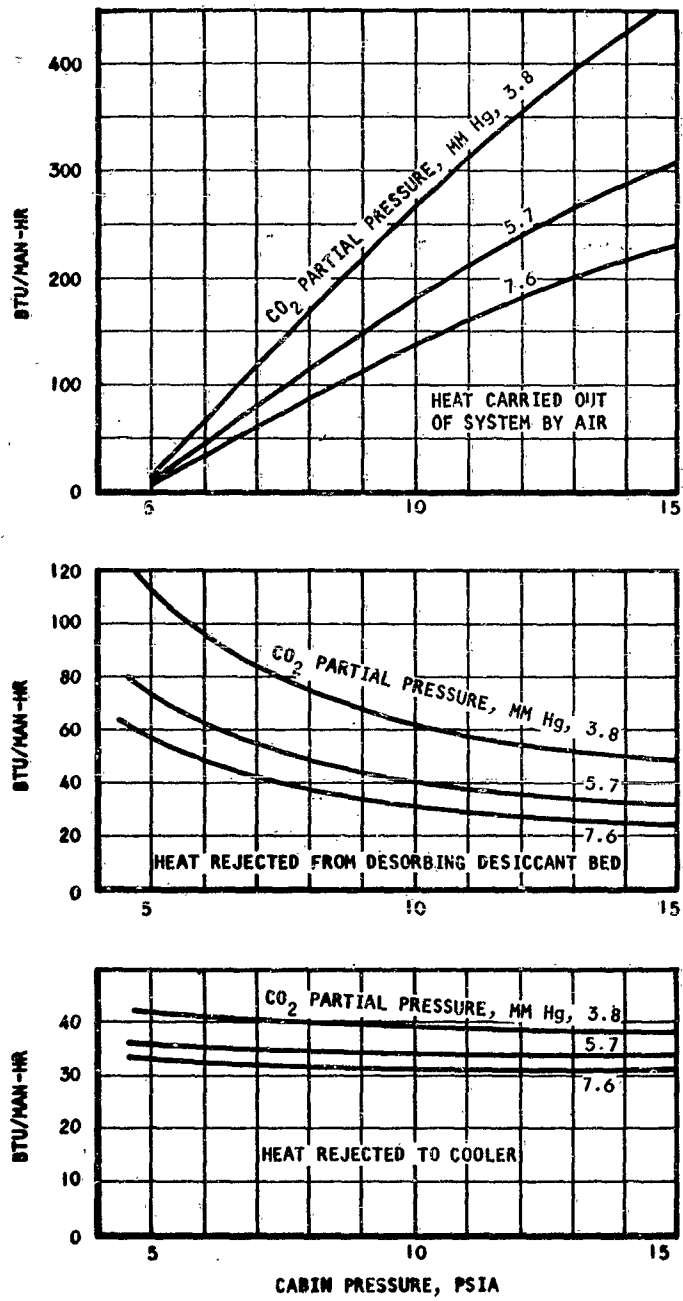


Figure 82. Molecular Sieve System Heat Rejection Loads

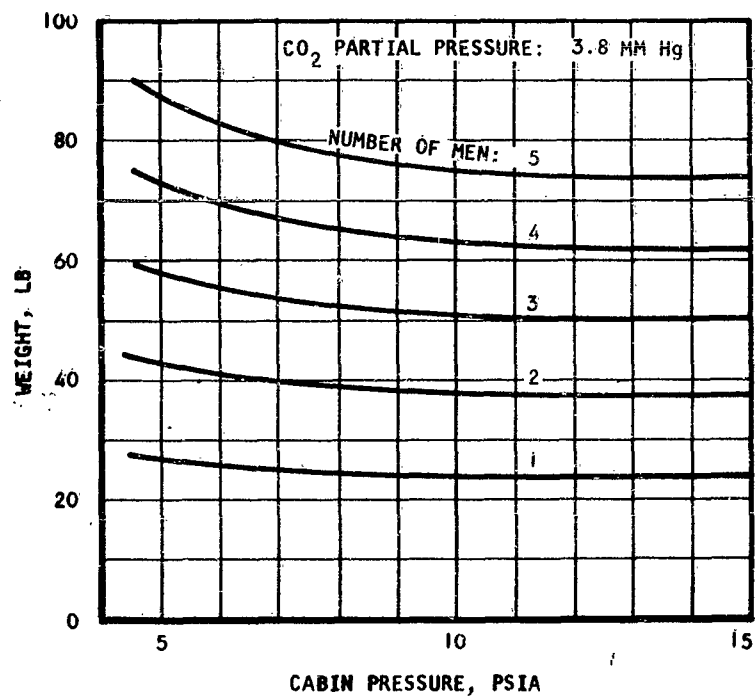
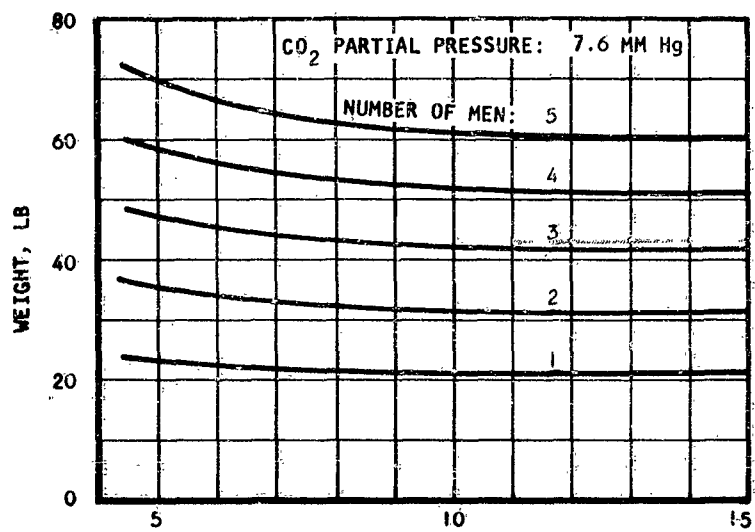


Figure 83. Molecular Sieve Subsystem Hardware Weight

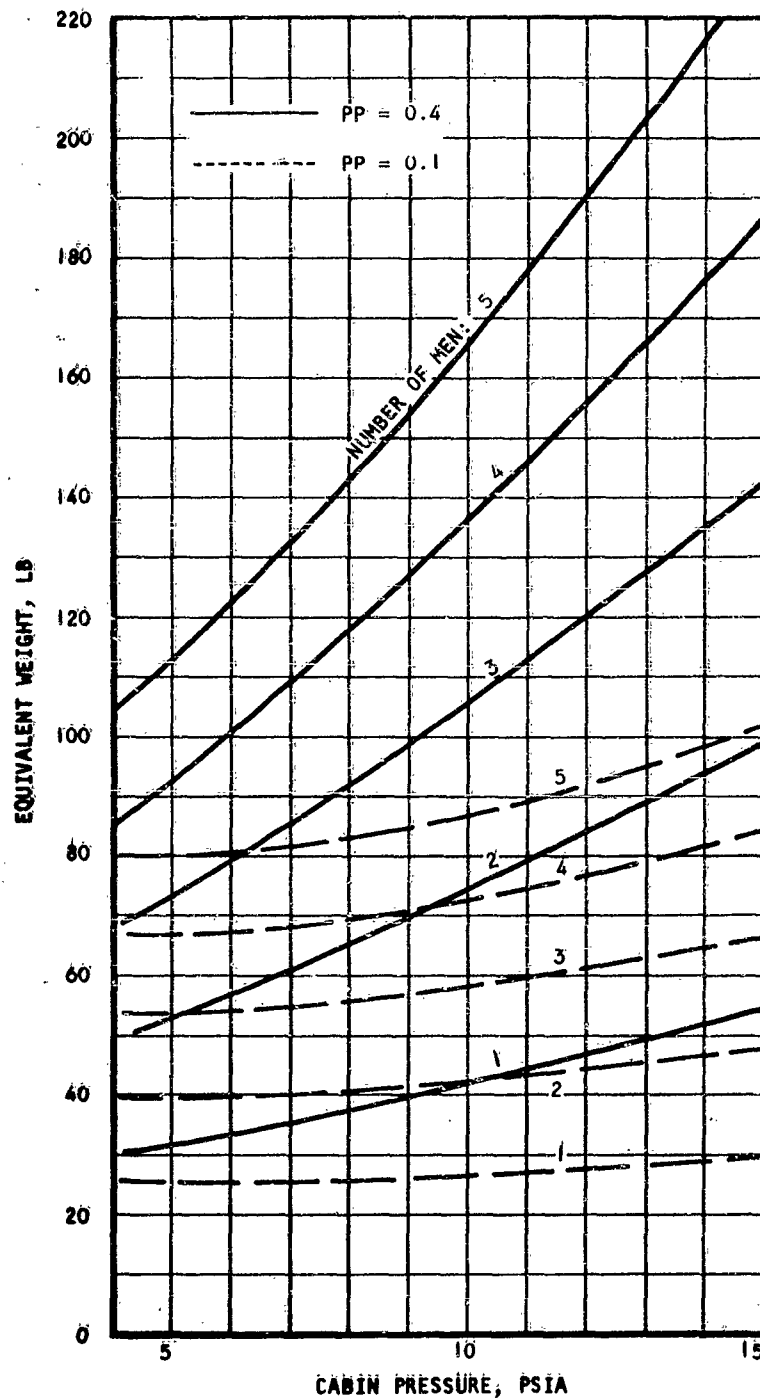


Figure 84. Molecular Sieve Subsystem Equivalent Weight

TABLE 15  
MOLECULAR SIEVE SUBSYSTEM ACCESSORY WEIGHT  
(3-MAN SYSTEM)

| Component                                | Weight, lb. |
|--|-------------|
| Desiccant loop check valves (4)          | 0.8         |
| Desiccant loop control valves (4)        | 1.0         |
| Molecular sieve loop check valves (4)*   | 1.2         |
| Molecular sieve loop control valves (8)* | 2.8         |
| Valve actuator and drive**               | 3.0         |
| Ducts                                    | 1.8         |
| Flow control valve                       | 0.5         |
| Sensor (not shown)**                     | 0.1         |
| Flow controller (not shown)**            | 2.5         |
| Heater control                           | 0.5         |
| Fan and motor drive*                     | 2.8         |
| Total Weight: 17.0                       |             |

\* Doubled for redundancy

\*\* Fixed weight component

## Conclusions

The analyses conducted in this section are based on steady-state operation of the molecular sieve system. Actual systems will be in a continual transient state: process air temperatures, heat rejection loads, and power requirement will vary all through the cycling period. A comprehensive analysis of the transients in a loop such as the one of Figure 67 is very complex and would require extensive use of computer techniques. Moreover, the characteristics of the adsorption and desorption beds under non-isothermal conditions are not well known at the present time, and considerable work in this area is required before a thorough system analysis can be performed. However, the results presented here are based on overall performance and provide relatively accurate values for system evaluation and comparison.

A carbon dioxide removal system using a molecular sieve is fairly complex. Cyclic operation of the 14 valves shown introduces a reliability problem which can be solved only by extensive testing of such a system. In practice, the valves isolating the system from the vacuum would be doubled to reduce the rate of leakage and the possibility of system failure.

Deterioration of the adsorption bed after a number of cycles may be remedied by bed replacement during the mission. Possibility of molecular sieve bed poisoning also indicates the desirability of carrying spare adsorption canisters aboard the vehicle. Provision also should be made for heating the beds to high temperature.

Carbon dioxide removal by molecular sieves is suitable for moderate to long mission durations. Although the system equivalent weight is not time-dependent, system reliability for long durations would necessitate some weight increase as discussed before. The system power requirement is high, and the total system equivalent weight is sensitive to the vehicle power source weight.

For a typical case, the duration of the mission in which a molecular sieve system instead of an expendable lithium hydroxide system would be used can be found from the equivalent weight plots of Figures 57, 58, and 84. The break-even point between the two systems depends primarily on the power consumption of the molecular sieve subsystem and on the vehicle power penalty. Vehicle parameters affecting these variables will greatly influence the field of application of these two carbon dioxide removal subsystems. Figure 85 is an estimate of the mission duration where the two subsystems have the same equivalent weight. The plot was prepared for two values of the vehicle power penalty, 0.1 and 0.4 lb per watt, and a three-man vehicle. The lithium hydroxide subsystem is credited for the water of reaction.

It should be emphasized that other considerations, such as state of the art and reliability, would favor the lithium hydroxide subsystem and shift upward the plots of Figure 85.

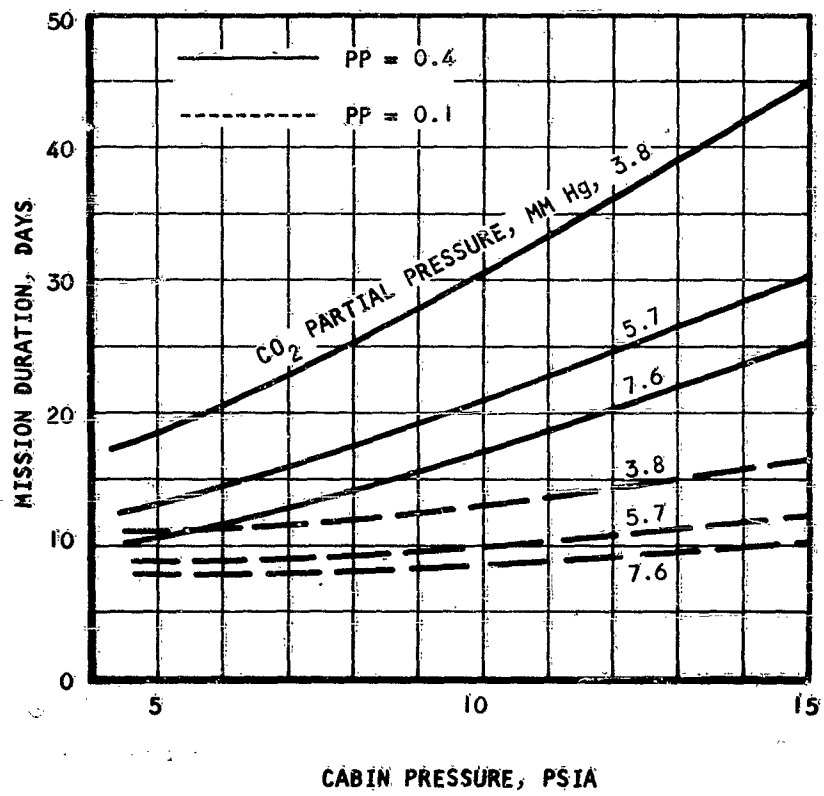


Figure 85. Lithium Hydroxide and Molecular Sieve Break-even Mission Duration

## CARBON DIOXIDE REMOVAL BY FREEZE-OUT PROCESS

### General

Carbon dioxide removal by freeze-out technique has been the subject of an extensive study conducted recently and reported in Reference 4. The study shows that, for space vehicle applications, the most attractive freeze-out system is one in which both the water entrained by the process gas and the carbon dioxide are removed by freezing; subsequently, the solids are sublimated to vacuum and the heat of sublimation recovered in a regenerative manner to cool the incoming gas. Such a system is shown in Figure 86.

While the process gas is cooled in a heat exchanger, water vapor is successively condensed and frozen; the ice formed adheres to the heat exchanger surface. This process takes place over a whole section of the heat exchanger, the freezing front moving downstream as ice deposits on the cold surface. Essentially, complete removal of the water necessitates cooling of the process gas to temperatures on the order of  $360^{\circ}\text{R}$ . Freezing of the carbon dioxide occurs at a much lower temperature, depending on the carbon dioxide partial pressure in the process gas. In the range of partial pressures encountered in space vehicle atmospheres, carbon dioxide will freeze at about  $270^{\circ}\text{R}$ . Removal is practically total at temperatures on the order of  $230^{\circ}\text{R}$ .

The heat sink required to pull the temperature of the process air to these low levels is, therefore, well defined. If the heat sink is provided by the oxygen and nitrogen stored in cryogenic form for breathing and cabin pressurization, supercritical techniques cannot be used for storing the gases. Figure 87 is a plot of the oxygen temperature in a supercritical vessel for constant pressure operation, and Figure 88, a pressure-enthalpy diagram for oxygen. From these plots it is seen that with low vessel contents, about 20 per cent, the oxygen temperature after expansion to system pressure is higher than the temperature required for carbon dioxide freeze-out. In addition, the enthalpy of the cold fluid increases with fluid usage until its useful heat sink potential completely disappears when its temperature reaches that required for carbon dioxide freezing.

Subcritical storage with positive expulsion appears to be the only storage technique capable of providing the constant heat sink corresponding to the constant heat load of the system. As discussed in Section IV of this report, this type of storage vessel is not as reliable nor as advanced in the state of the art as the supercritical storage vessels. Usage of subcritical storage with bladder pressurization is, therefore, in itself a drawback of the carbon dioxide removal system by freeze-out.

Freeze-out methods also are attractive when an external heat sink is available aboard the vehicle, such as hydrogen stored cryogenically. Here, an intermediate transfer fluid loop is used between the cold hydrogen sink and the process air to minimize the possibility of liquefying the process

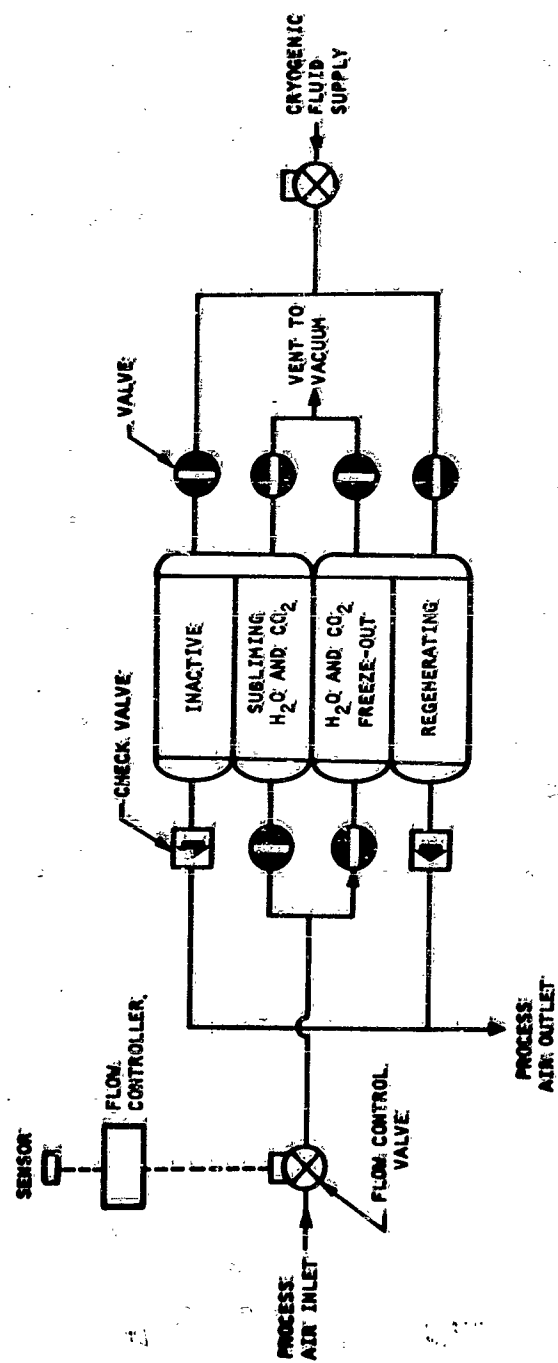


Figure 86. Simple Carbon Dioxide Freeze-out Subsystem Diagram



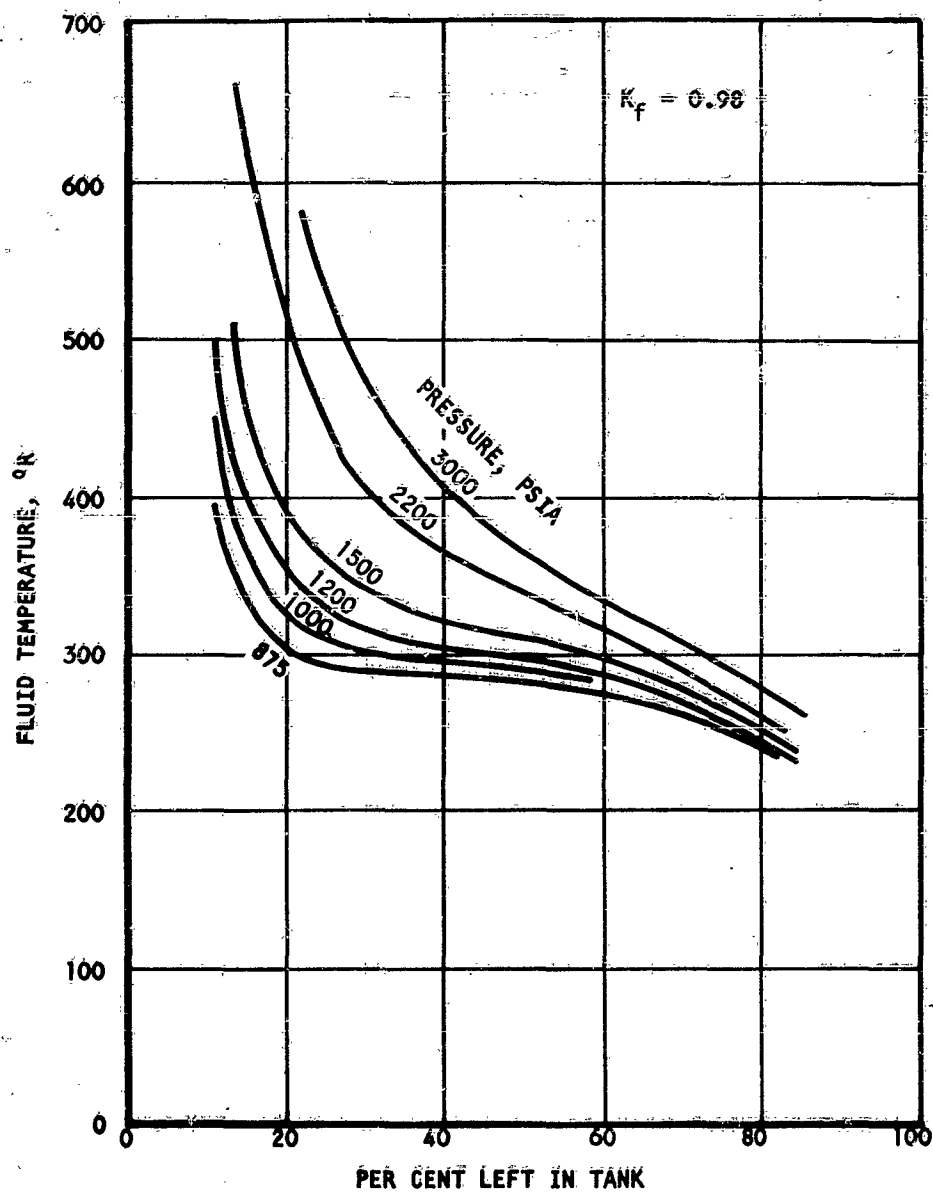
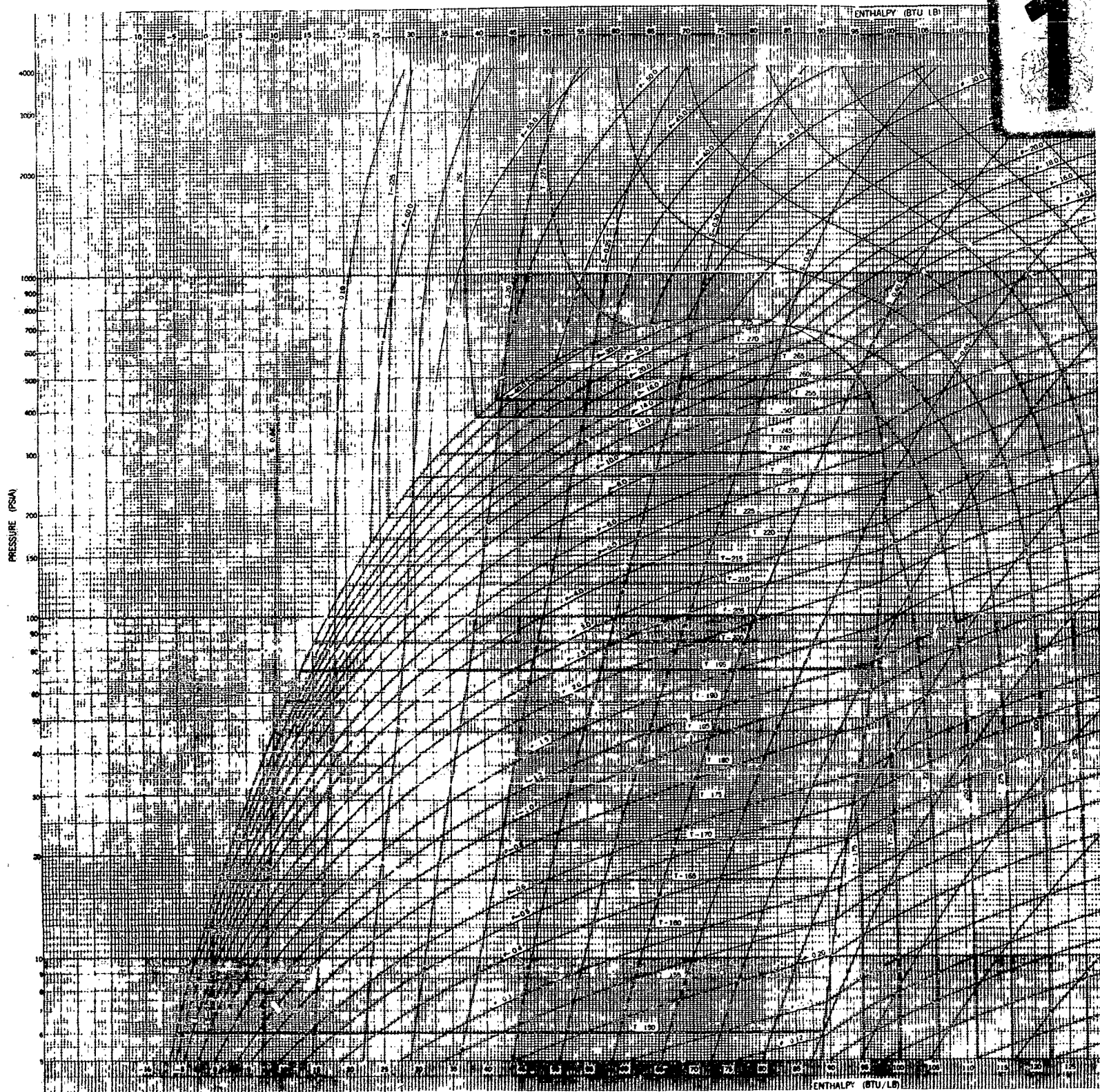


Figure 87. Fluid Temperature for Constant Pressure Delivery - Supercritical Oxygen Storage



2

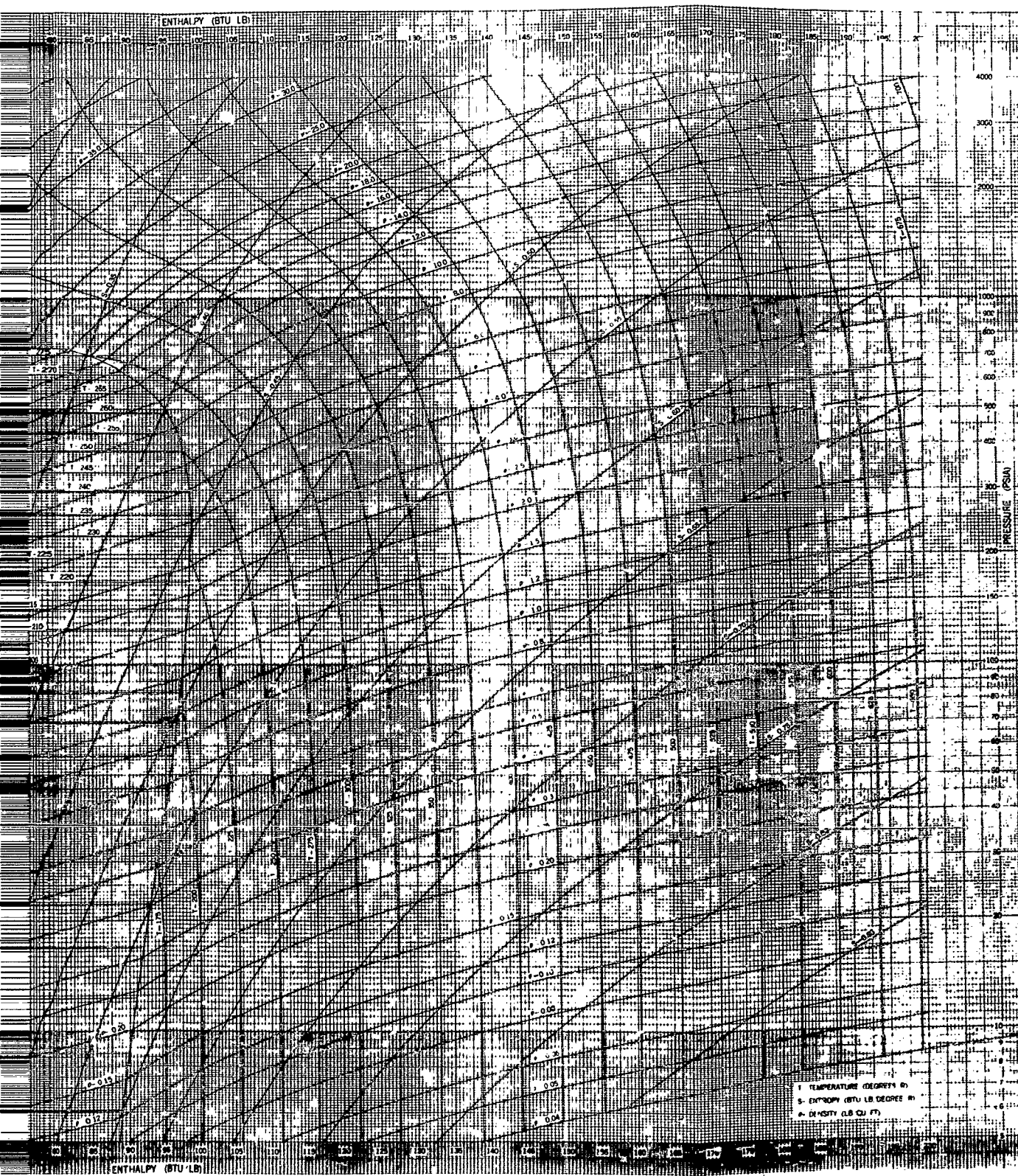


Figure 88  
Thermodynamic  
Properties  
Of Oxygen

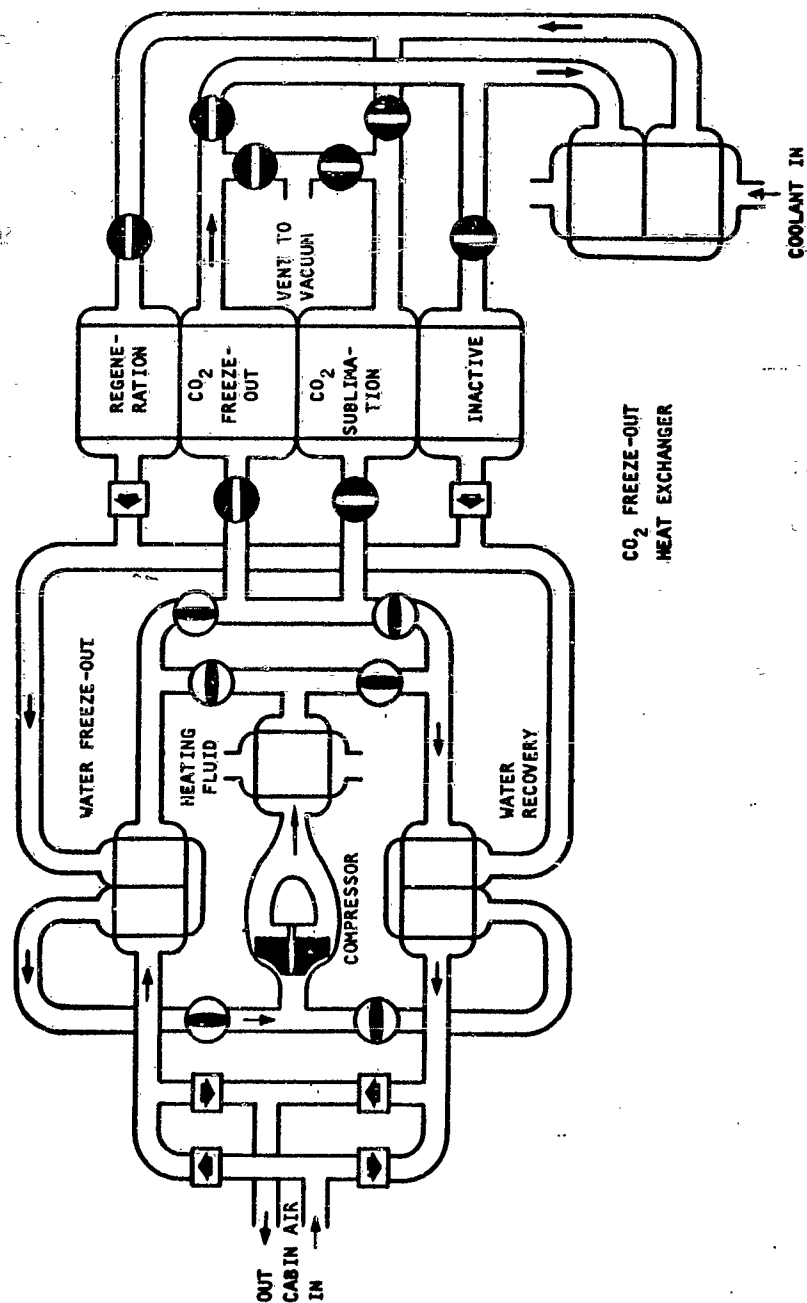


Figure 89. Carbon Dioxide Freeze-out with Water Recovery

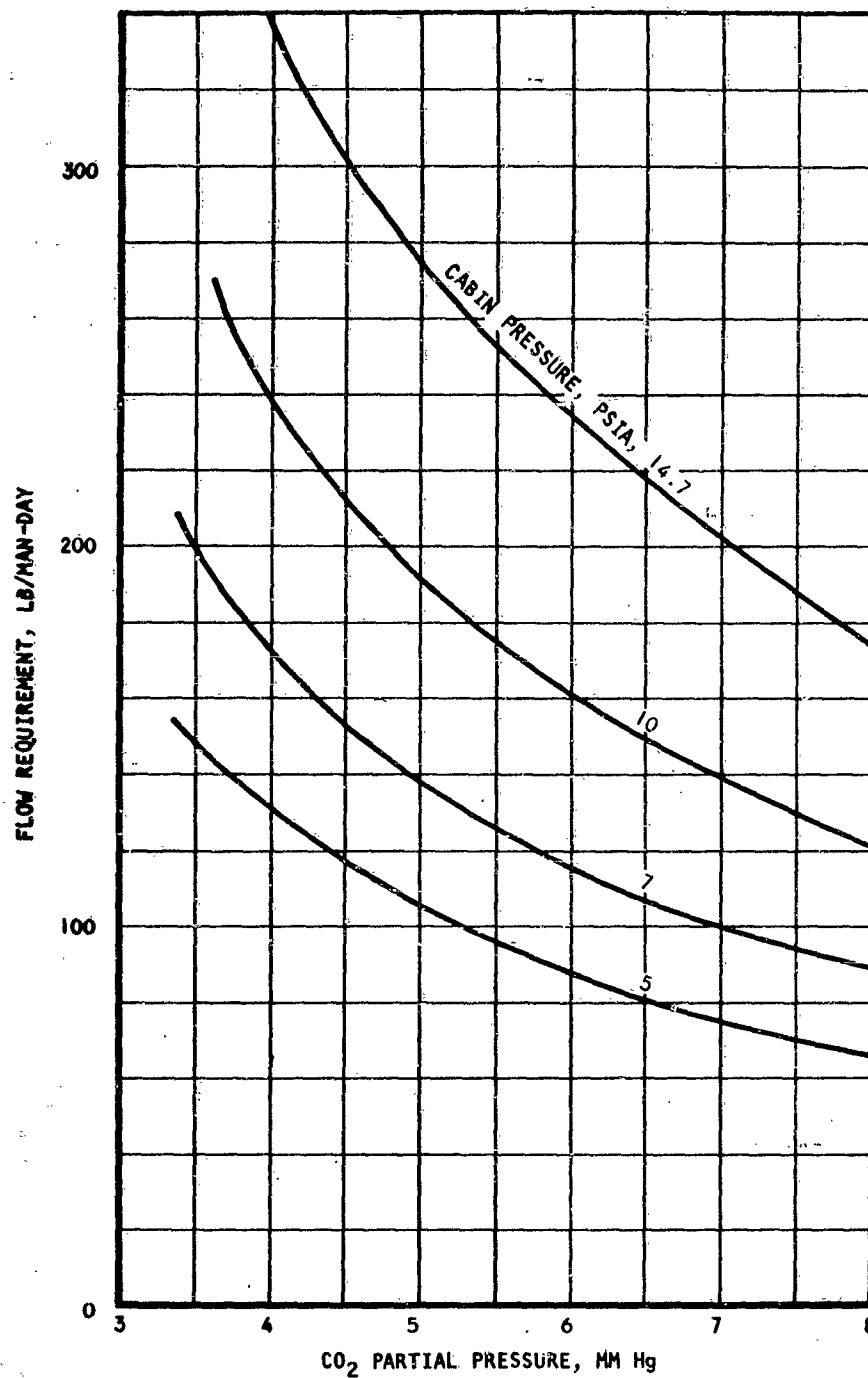


Figure 90. Carbon Dioxide Freeze-Out Subsystem Flow Requirement

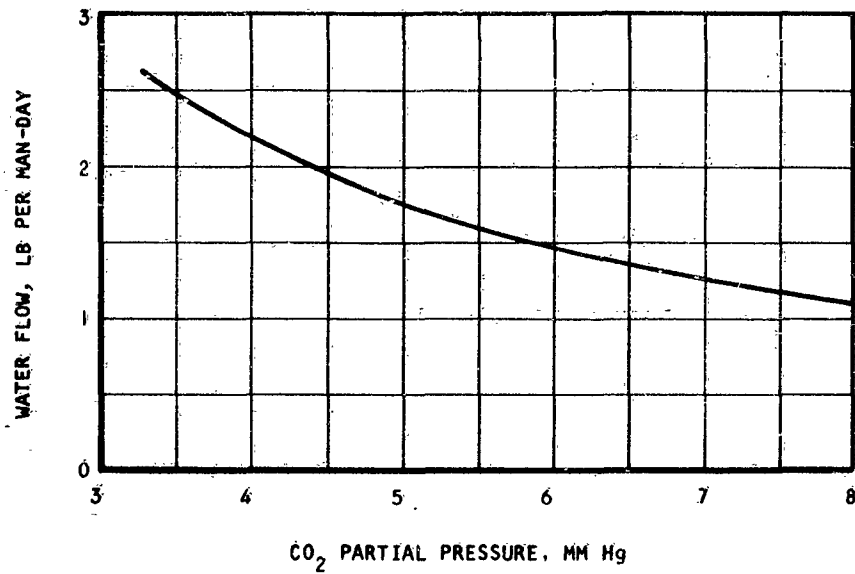


Figure 91. Water Vapor Flow To The Carbon Dioxide Freeze-out Subsystem.

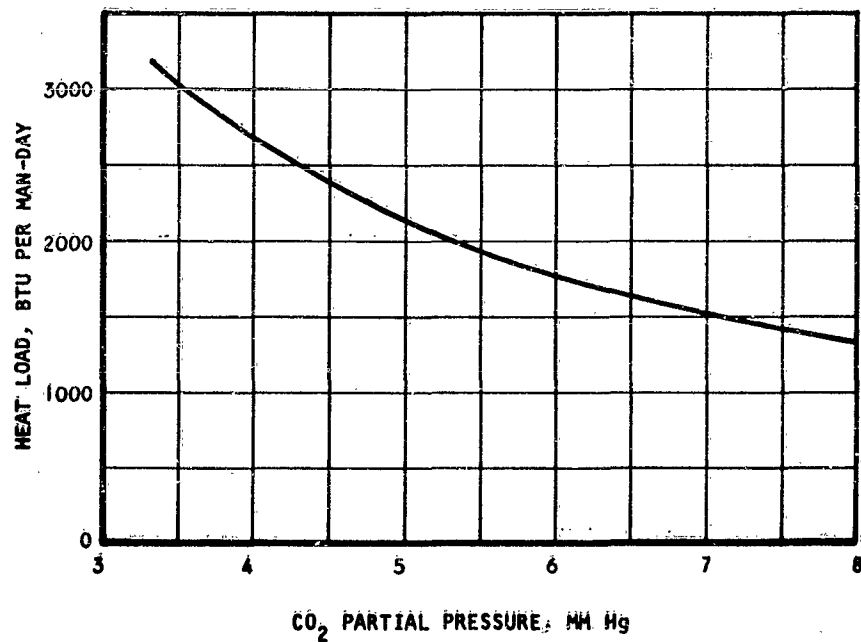


Figure 92. Heat Load for Water Freezing

## Simple Carbon Dioxide Freeze-Out Subsystem Characteristics

### 1. Subsystem Heat Sink

An analysis of the simple freeze-out system depicted in Figure 86 has been conducted. Oxygen and nitrogen are stored subcritically aboard the vehicle and delivered to the carbon dioxide subsystem as cryogenic liquids. Evaporation of these liquids by mixing with the process gas provides the heat sink required by the system. Since the process is of a regenerative nature, the capacity of the heat sink required is a function of the temperature difference between the inlet and outlet gas. Here it is assumed that the sublimating water and carbon dioxide are regenerated to the temperature of the outlet process gas. Based on these assumptions, the leakage flow rate from the cabin, insuring system operation, was determined as a function of the hot-end process gas temperature difference. This is plotted in Figures 93, 94, and 95 for three values of the carbon dioxide partial pressure in the cabin (7.6, 5.7 and 3.8 mm Hg). The zero leakage flow rate condition describes a system where metabolic oxygen only is used as a heat sink.

### 2. Heat Exchanger Optimization

The methods of Reference 1 were used to optimize the system heat exchanger weight. The optimum heat exchanger is defined here by

$$\frac{d(W_{HX})}{d(\Delta P)} + \frac{d}{d(\Delta P)} [(PL)(PP)] = 0 \quad (66)$$

where  $W_{HX}$  is the heat exchanger weight

$\Delta P$  is the pressure drop in the heat exchanger

$PL$  is the pumping power loss, watts

$PP$  is the vehicle pumping power penalty, lb per watt

The heat transfer surface used in the optimization procedure is defined as follows:

Aluminum plate fin exchanger

Single sandwich construction

16 rectangular fins per in., 0.153 in. high, 0.004 in. thick,  
1/7 in. offset

For this surface, the weight of the exchanger can be approximated by

$$W_{HX} = 0.01862 \bar{W} \frac{NTU^{1.166}}{(P\Delta P)^{0.166}} \quad (67)$$

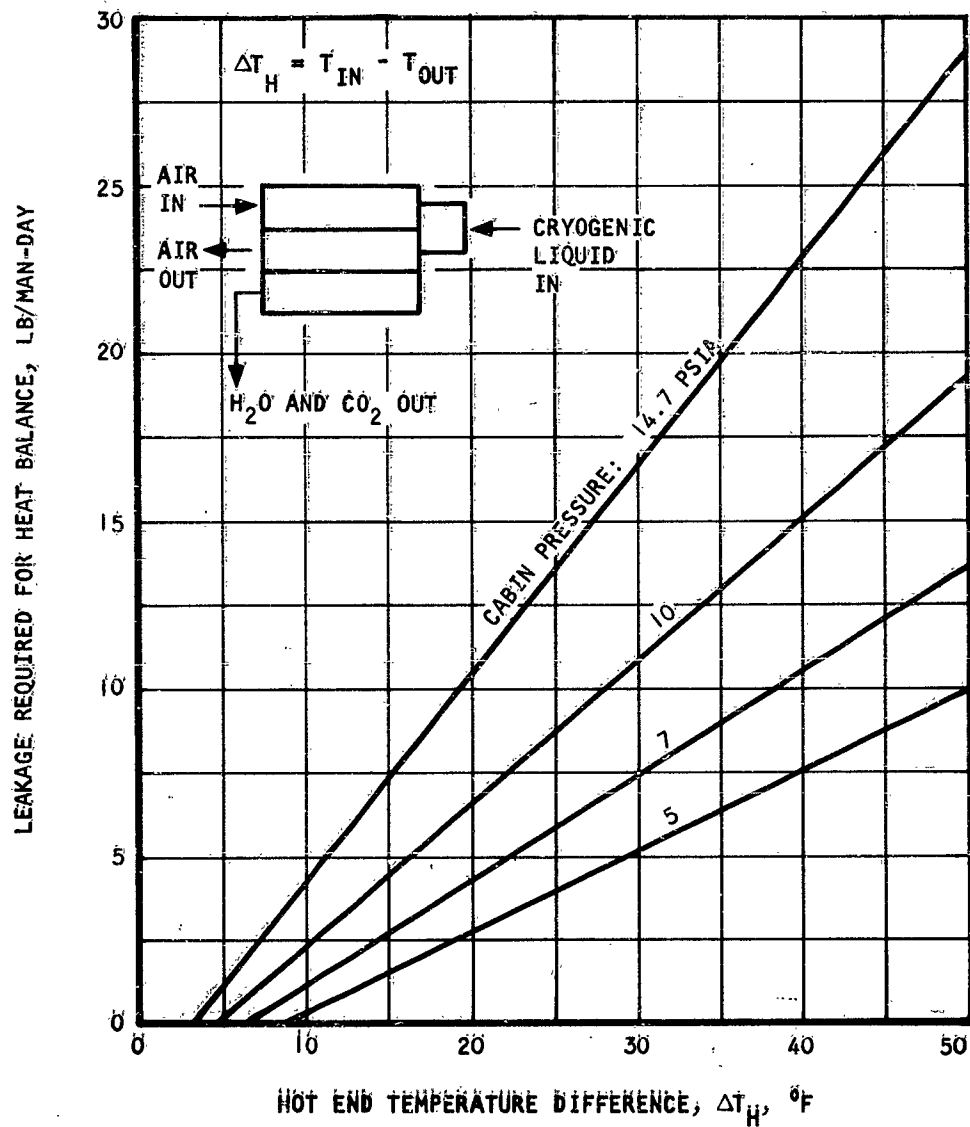


Figure 93. Simple Freeze-out Subsystem Metabolic and Cabin Leakage Flow Requirement  
( $P_{CO_2} = 3.8$  mm Hg)



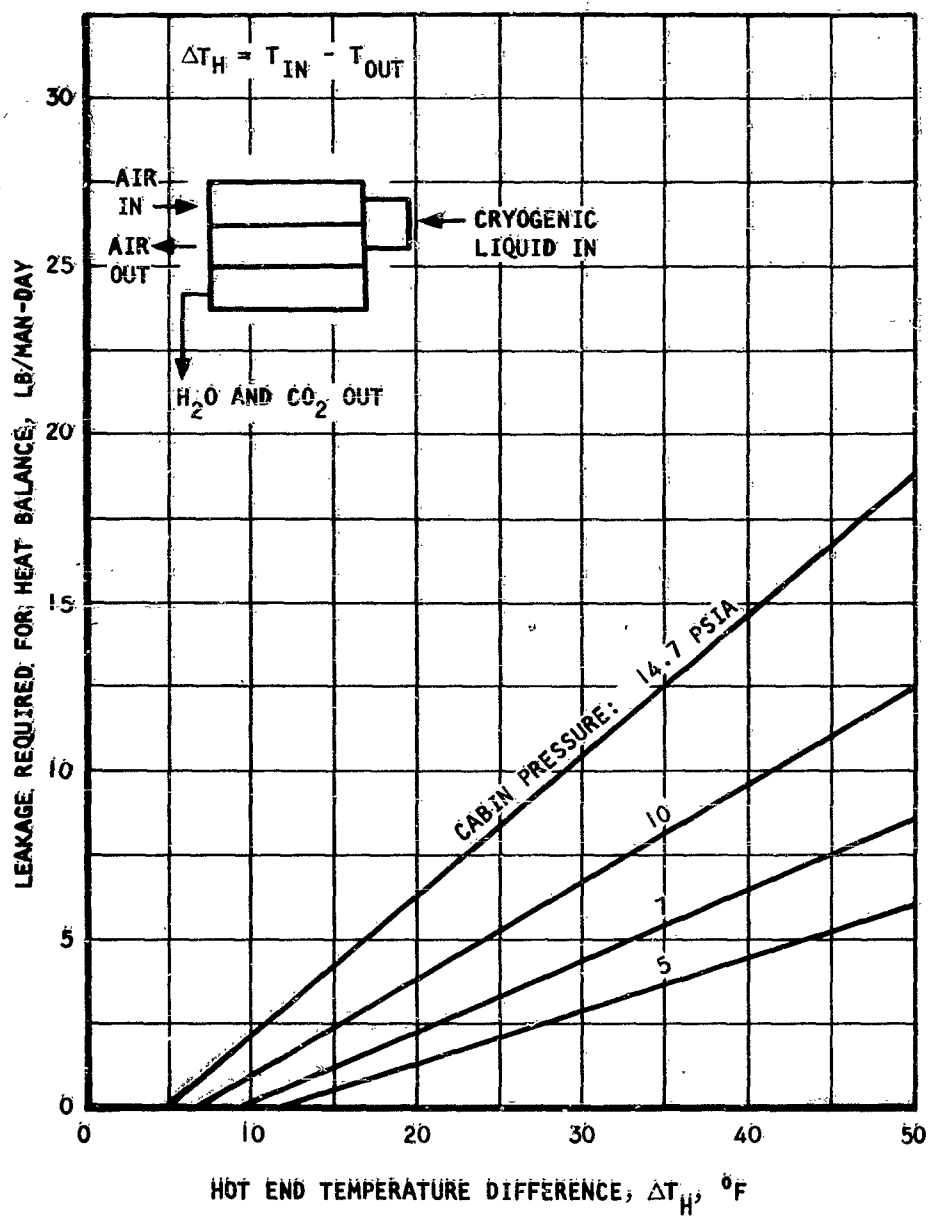


Figure 94. Simple Freeze-out Subsystem Metabolic and Cabin Leakage Flow Requirement  
( $p_{CO_2} = 5.7$  mm Hg)

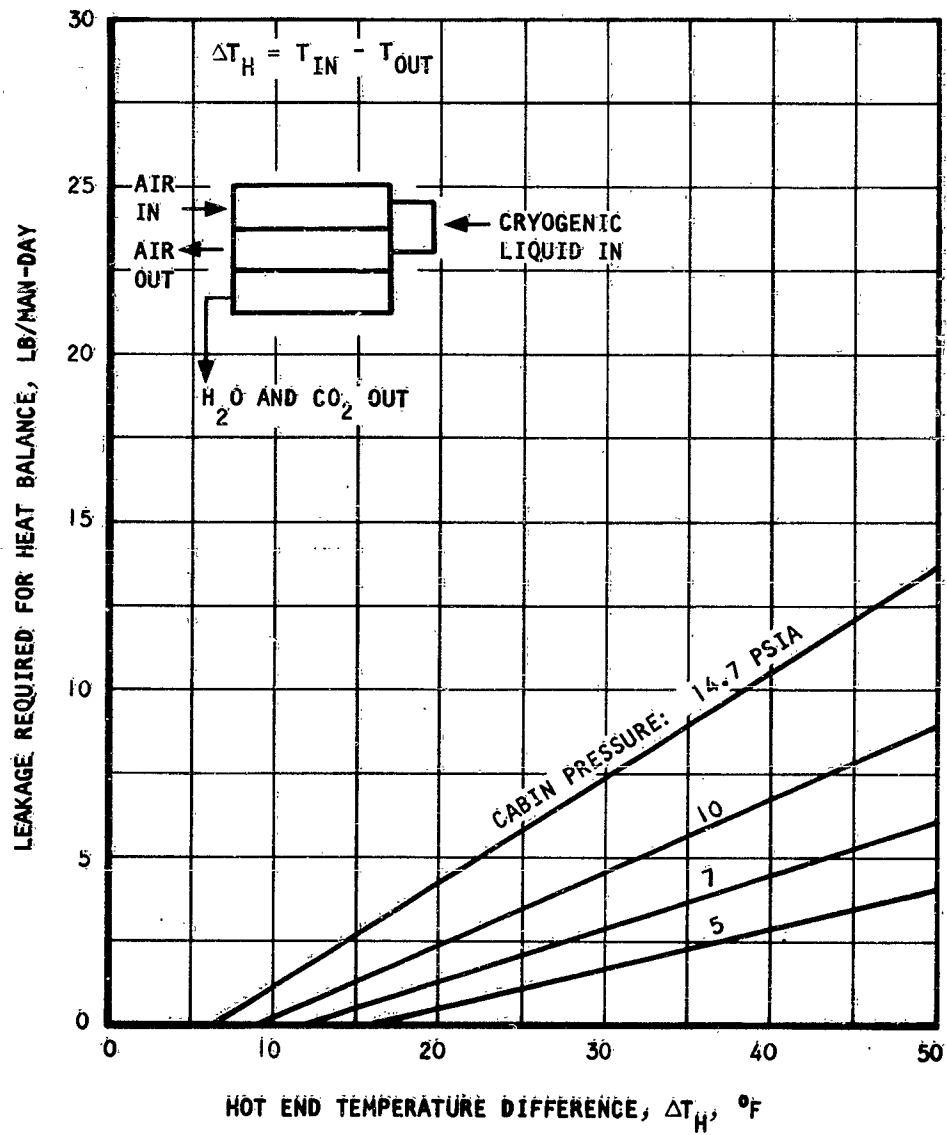


Figure 95. Simple Freeze-out Subsystem Metabolic and Cabin Leakage Flow Requirement  
( $p_{CO_2} = 7.6$  mm Hg)

where  $\bar{w}$  is the equivalent process air flow, lb/man-hr

$P$  is the system pressure, psia

$\Delta P$  is the pressure drop, in.  $H_2O$

NTU is determined assuming counterflow arrangement

Solution of Equation 66 yields optimum heat exchanger weight expressions of the form

$$W_{HX} = K_1 NTU, \text{ lb} \quad (68)$$

where  $K_1$  is a function of the system total pressure, carbon dioxide partial pressure, and vehicle power penalty. The pressure drop in the optimum heat exchanger system depends on the NTU and a constant,  $K_2$ , function of the system pressure:

$$\Delta P = K_2 NTU, \text{ in. } H_2O \quad (69)$$

$K_1$  and  $K_2$  are listed in Table 16 for various cabin conditions and a vehicle power penalty of 0.2 lb per watt.

The subsystem heat exchanger weights corresponding to the cryogenic oxygen and nitrogen flows of Figures 93, 94, and 95 have been calculated from these expressions and are given in Figures 96, 97, and 98 for various cabin conditions and cabin leakage rates.

### 3. Subsystem Equivalent Weight

In addition to the heat exchangers, several components are integral parts of the simple carbon dioxide freeze-out subsystem. Most of these components are shown in Figure 86; others not shown on the diagram are the valve-switching mechanism and the redundant valving used for safety reasons wherever a valve seals the system against vacuum. For a typical three-man subsystem, the weight of the system components, other than the heat exchangers, is given in Table 17. The variable portion of the accessory weight for the purpose of system analysis is taken as a function of the number of crew members. The weight of the accessories is expressed by

$$W_A = 5.1 + 3.75 \sqrt{N} \quad (70)$$

Other factors to be considered in computing the total subsystem equivalent weight are the water lost by sublimation to vacuum, the power losses due to friction, and the use of the cooling capacity of the gas supply for carbon dioxide removal.

TABLE 16

SIMPLE FREEZE-OUT SYSTEM OPTIMUM HEAT  
EXCHANGER CHARACTERISTICS  
(VEHICLE POWER PENALTY: 0.2 LB PER WATT)

VALUES OF  $K_1$ :

$$W_{HX} = K_1 \text{ NTU, lb}$$

| System Pressure, psia                  | 5      | 7      | 10     | 14.7   |
|--|--------|--------|--------|--------|
| Carbon dioxide partial pressure, mm Hg |        |        |        |        |
| 7.6                                    | 0.0975 | 0.1126 | 0.1256 | 0.1531 |
| 5.7                                    | 0.1258 | 0.1446 | 0.1643 | 0.2011 |
| 3.8                                    | 0.1823 | 0.2105 | 0.2407 | 0.2969 |

VALUES OF  $K_2$ :

$$\Delta P = K_2 \text{ NTU, in. H}_2\text{O}$$

| System Pressure, psia | 5    | 7     | 10    | 14.7  |
|-----------------------|------|-------|-------|-------|
| $K_2$                 | 0.11 | 0.144 | 0.182 | 0.238 |

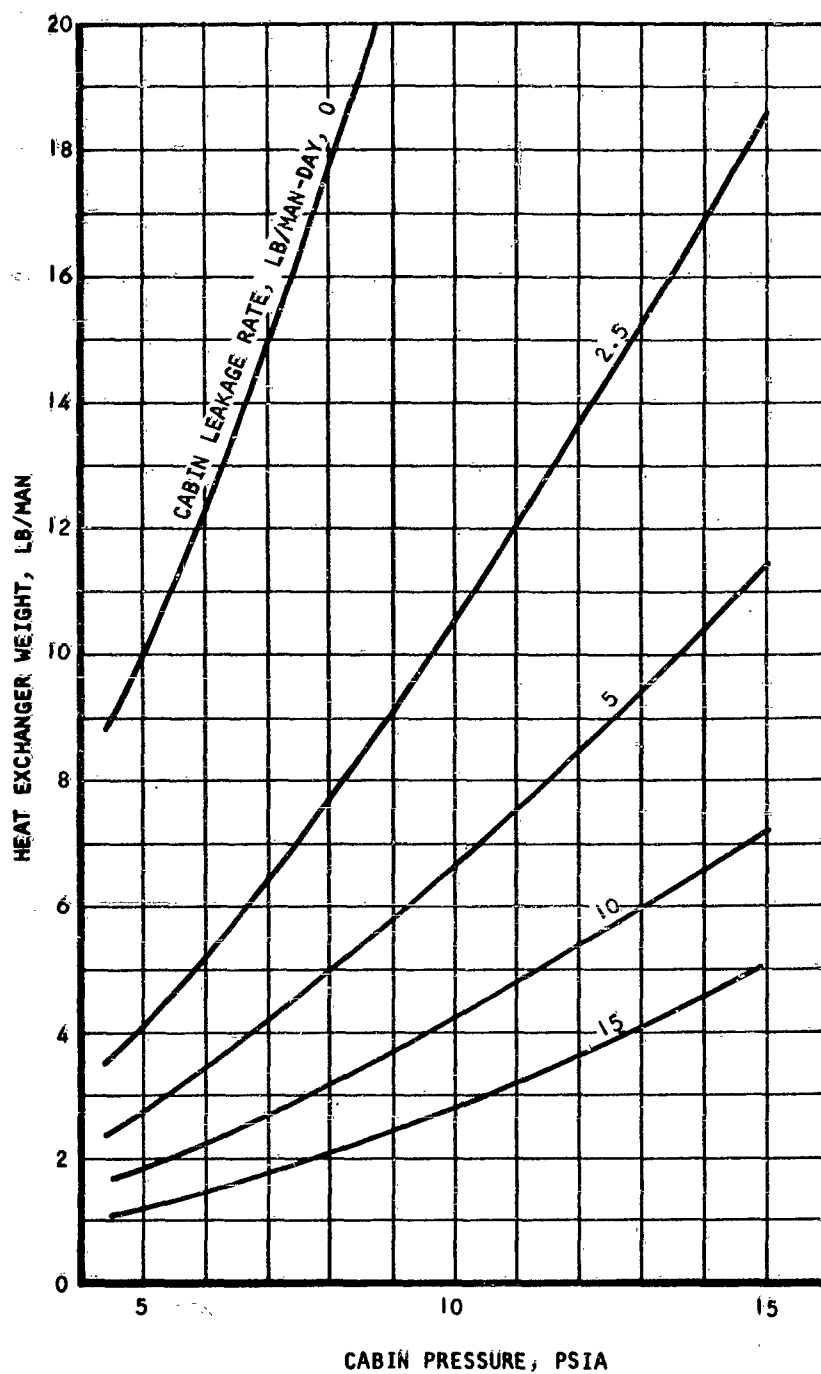


Figure 96. Simple Freeze-out Heat Exchanger Weight  
( $PCO_2 = 3.8$  mm Hg)

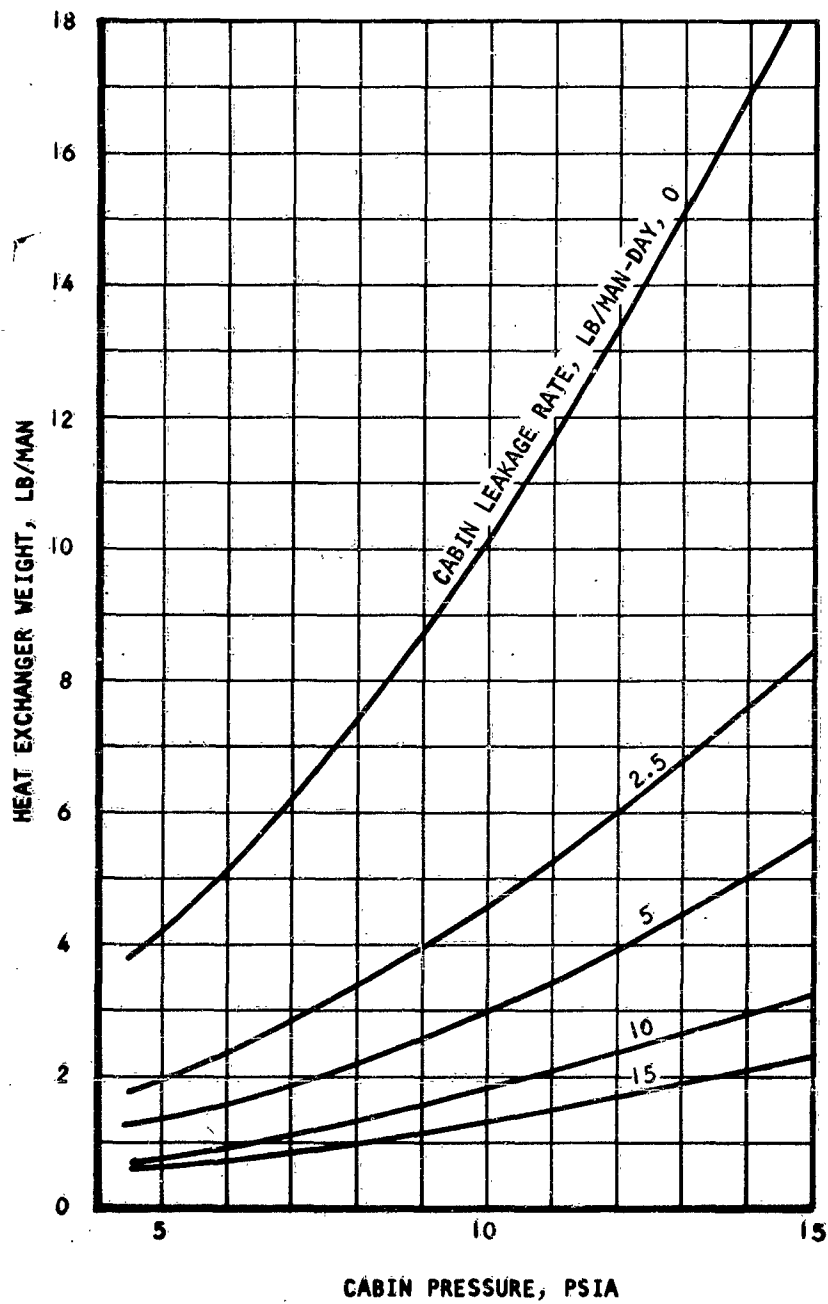


Figure 97. Simple Freeze-out Heat Exchanger Weight  
( $P_{CO_2} = 5.7$  mm Hg)

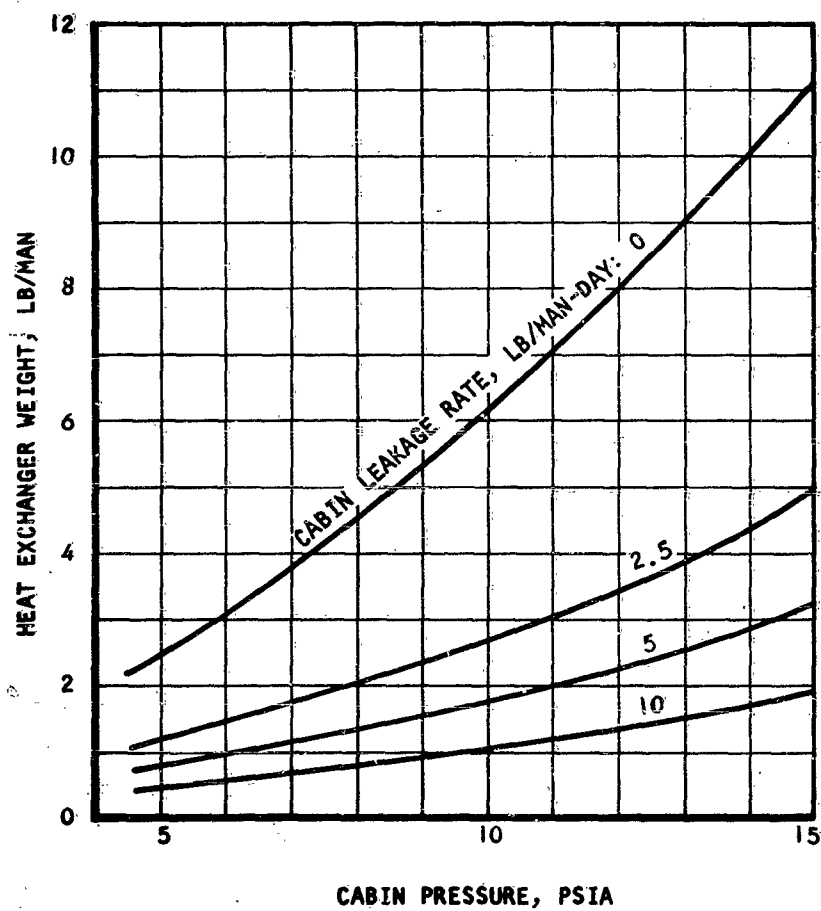


Figure 98. Simple Freeze-out Heat Exchanger Weight  
( $P_{CO_2} = 7.6$  mm Hg)

TABLE 17

SIMPLE CARBON DIOXIDE FREEZE-OUT SUBSYSTEM ACCESSORY WEIGHT  
(3-MAN SUBSYSTEM)

| Component                            | Weight, lb |
|--------------------------------------|------------|
| Heat exchanger control valves (12)** | 4.2        |
| Heat exchanger check valves (4)*     | 1.2        |
| Valve actuator and drive**           | 2.5        |
| Process air flow control valve       | 0.5        |
| Sensor**                             | 0.1        |
| Flow controller**                    | 2.5        |
| Cryogenic fluid check valve          | 0.2        |
| Piping                               | 0.4        |
| Total Weight:                        | 11.6 lb    |

\* Doubled for safety

\*\* Fixed weight component



The rate of water exhausted from the system is shown in Figure 91. The power losses due to friction can be calculated from the data of Table 16 for any cabin condition. The loss in cooling capacity of the gas supply subsystem is on the order of 90 Btu per lb of gas supplied to the cabin.

Since the leakage rate of a space vehicle is very difficult to predict with any kind of accuracy, and since it will most certainly differ greatly from one vehicle to the other of the same design, it is impractical to base the design of any vehicle system on this unknown parameter. On the other hand, the average oxygen metabolic use rate of the crew members can be estimated and the freeze-out system safely designed to operate on the crew metabolic oxygen consumption. Variations in this use rate can be adjusted by use of the inevitable leakage gas supply.

The total subsystem fixed weight is plotted in Figure 99 for two values of the carbon dioxide partial pressure. The plot was prepared for a vehicle power penalty of 0.2 lb per watt. The subsystem weight depends somewhat on the value of the power penalty, since the heat exchanger optimization procedure depends on this parameter. The heat exchanger weight at other vehicle power penalties can easily be calculated noting that it is proportional to the factor  $(pp)^{0.143}$ .

#### Discussions of Other Freeze-Out Subsystems

A number of carbon dioxide removal subsystems using freeze-out techniques are possible. Among them are the simple freeze-out subsystem discussed previously in which the heat sink is provided by an external cooling loop. This system is particularly attractive if cryogenic hydrogen is kept aboard the vehicle for purposes other than atmosphere control. Here, because of the danger of liquefying the process air, an intermediate heat transfer loop must be used. Helium is normally chosen as the heat transport fluid between the hydrogen and the process air stream. The size and weight of the freeze-out heat exchanger depends on the available heat sink as shown in Figure 100. However, numerous disadvantages offset this apparent advantage:

- a. Two additional heat exchangers are necessary for operation of the heat transfer loop.
- b. A pump is required to circulate the heat transport fluid.
- c. The additional valves and controls of the heat transfer loop decrease the reliability of the system.

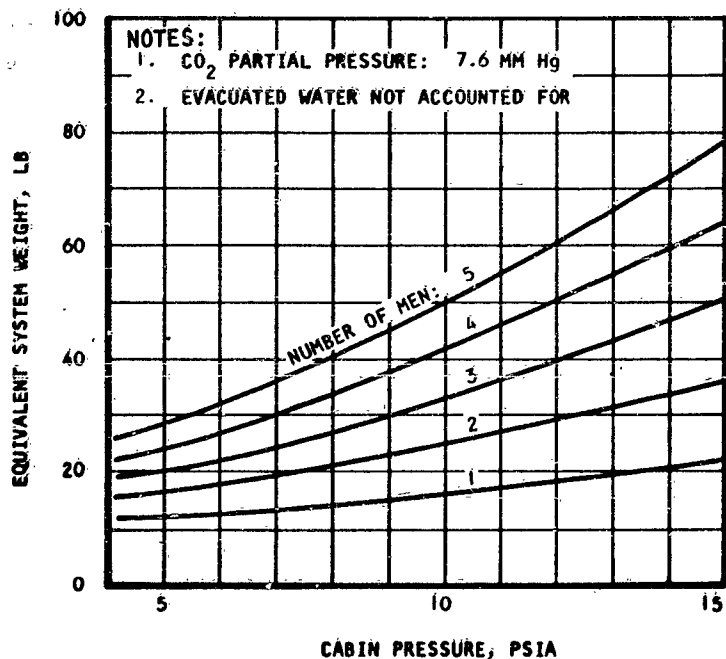
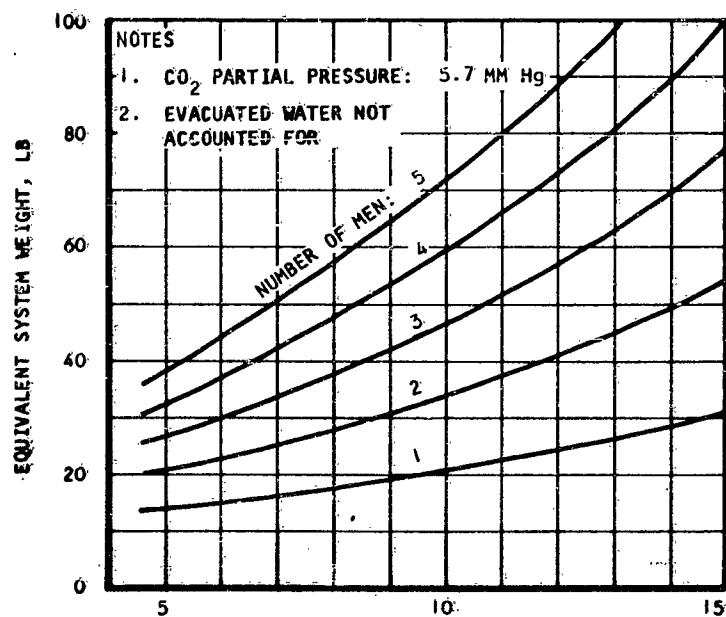


Figure 99. Simple Carbon Dioxide Freeze-out Subsystem Equivalent Weight

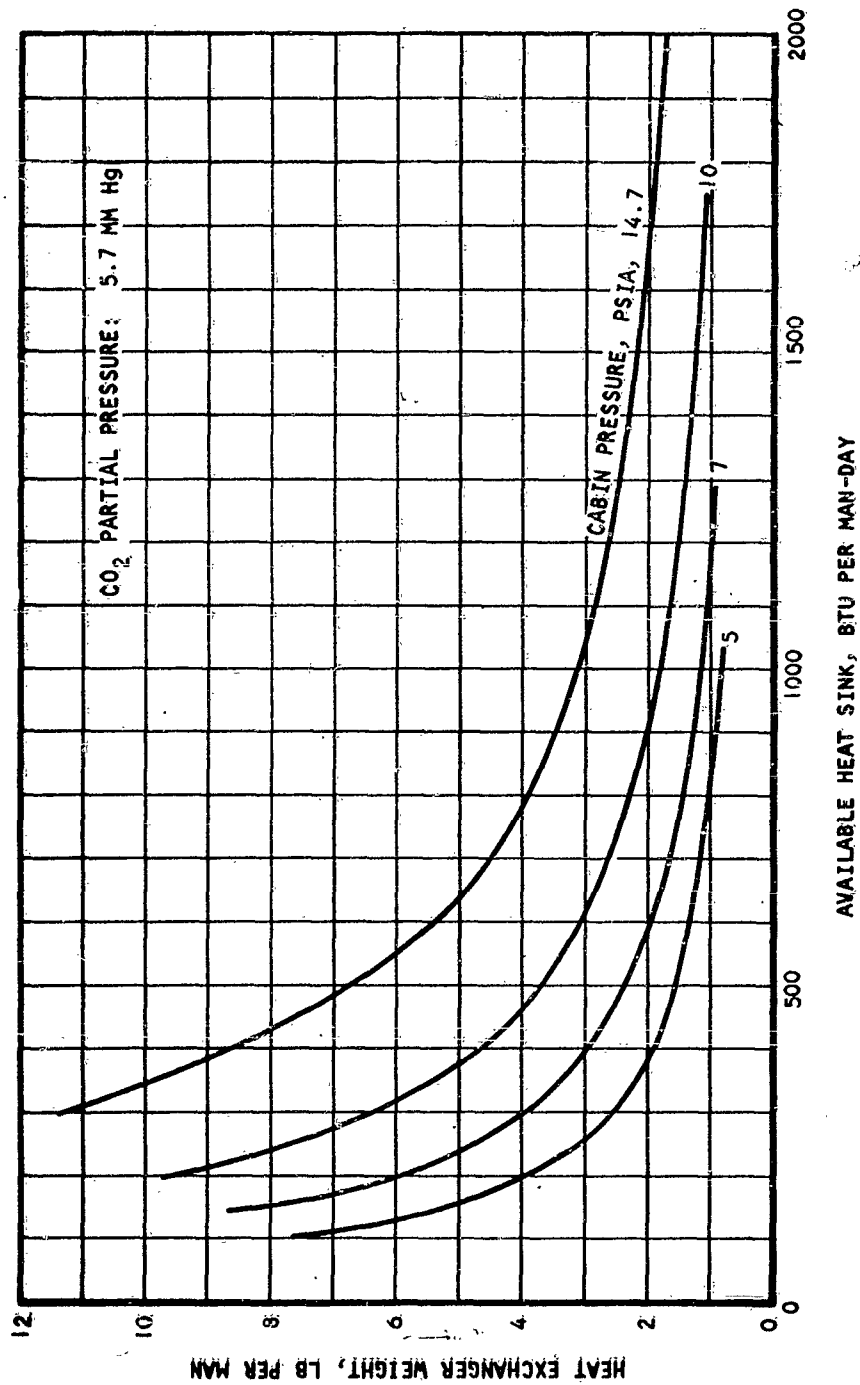


Figure 100. Freeze-out Heat Exchanger Weight - Subsystem with External Heat Sink

Freeze-out subsystems with water removal are essentially limited to short mission durations because of the cumulative weight of the water expelled overboard in the freeze-out process. Subsystems in which the water frozen out is recovered are feasible; one of them is shown in Figure 89. Because of the high heat load involved in freezing the water (Figure 92) and because this heat is not recovered regeneratively, the cryogenic metabolic oxygen supply does not provide a heat sink of the needed capacity for system operation. Even with a reasonable cabin leakage rate, on the order of 2 to 4 lb per man-day, the total cryogenic gas supply to the cabin is still not sufficient as a heat sink. Water recovery in freeze-out subsystems, therefore, necessitates the use of an external heat sink. In general, a heat sink of the size and temperature required here will be found only aboard vehicles where cryogenic hydrogen is stored for chemically fueled power generating units. This in itself limits the field of application of the freeze-out subsystem with water recovery to missions of short to moderate duration.

Thus, in a comparison of freeze-out subsystems with and without water recovery, the weight of recovered water must be balanced against the difference in hardware weight of the two systems. Other factors entering the comparison are system complexity and reliability. For a typical case, comparison on an equivalent weight basis is shown in Figure 101. The plot was prepared for a two-man system, a cabin pressure of 10 psia, and a carbon dioxide partial pressure in the cabin of 5.7 mm Hg. The carbon dioxide removal subsystems considered are the freeze-out subsystem with water recovery, the simple freeze-out subsystem with water overboard, the molecular sieve subsystem, and the lithium hydroxide subsystem credited for the water produced. The comparison is made on the basis of a power penalty of 0.2 lb per watt.

From this plot, it is evident that the slight advantage of the freeze-out system at mission durations over 10 days does not offset the reliability problems posed by the complexity of the system. In addition, molecular sieve system state-of-the-art is more advanced. The system has been shown workable, whereas considerable experimentation is needed to assess the removal efficiencies and general performance of freeze-out subsystems.

Moreover, for mission durations in excess of about three weeks, it is unlikely that cryogenic hydrogen would be stored aboard the vehicle in quantities sufficient to provide the heat sink required for water recovery in a freeze-out system.

### Conclusions

The simple freeze-out subsystem described in this section has several drawbacks which impose severe restrictions on its use aboard space vehicles:

- a. A large number of valves is necessary for continuous system operation. Eight of these valves seal the system against the ambient vacuum and pose a reliability problem which influences

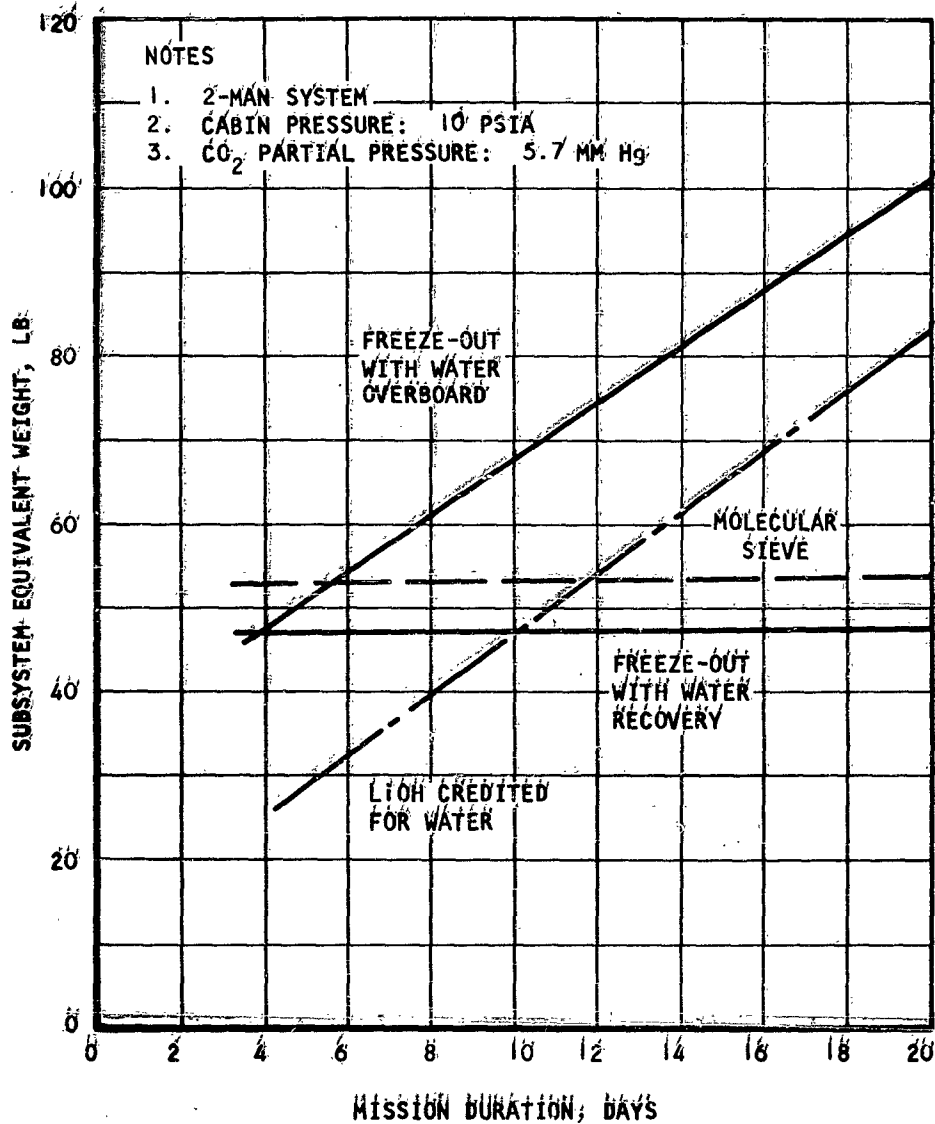


Figure 101. Carbon dioxide removal subsystem comparison

greatly the selection of the freeze-out subsystem in preference to simpler systems such as the lithium hydroxide subsystem.

- b. The vehicle gas supply must be stored and delivered as a cryogenic liquid. As the heat sink required for freeze-out uses the heat of evaporation of these cryogenic liquids, the delivery lines from the storage vessels must be well insulated and as short as possible. This introduces installation problems in addition to the cited disadvantages associated with the use of positive-expulsion type cryogenic vessels. It should be noted here that for short mission durations and liquid loads less than 100 lb, positive-expulsion vessels are somewhat heavier than their preferred supercritical counterpart; however, the freeze-out system is not here penalized for this added gas storage weight.
- c. Comparative development relative to other carbon dioxide removal subsystems represents a third disadvantage of the freeze-out subsystem. The carbon dioxide removal efficiency of various heat transfer surfaces is not well known; also, information is lacking in the field of heat transfer to and from a sublimating solid. In the analyses conducted here, it was assumed that the sublimation of water and carbon dioxide takes place at a rate consistent with the rate of solid build-up in the freezing passages of the heat exchanger. If the sublimating process were much slower than the freeze-out process, additional passages would be necessary within the heat exchanger at the cost of increased weight and additional valving.

Comparison on an equivalent weight basis was made, however, to assess the merits of the freeze-out subsystem as a means of atmospheric carbon dioxide control aboard space vehicles. The comparison initially considered short-duration missions on which water balance is unimportant. The simple freeze-out subsystem, not penalized for the water evacuated overboard, is compared with the lithium hydroxide subsystem using vehicle power penalty of 0.4 lb per watt. Figure 102 shows the freeze-out subsystem break-even mission time for various cabin conditions. On the basis of weight, it appears that the simple freeze-out subsystem can be considered competitive for mission durations on the order of 3 to 5 days and longer. Because of the disadvantages inherent in the freeze-out subsystem, however, this break-even time is in practice much higher than shown.

The simple freeze-out system next was compared on a medium-duration mission basis. Here, the power penalty used for the comparison was 0.2 lb per watt, and while the freeze-out subsystem was penalized for the water evacuated overboard, the lithium hydroxide subsystem was credited for the water generated in the reaction. The utilization field of the simple freeze-out subsystem is shown in Figures 103 and 104 for a carbon dioxide partial pressure of 7.6 mm Hg and cabin pressures of

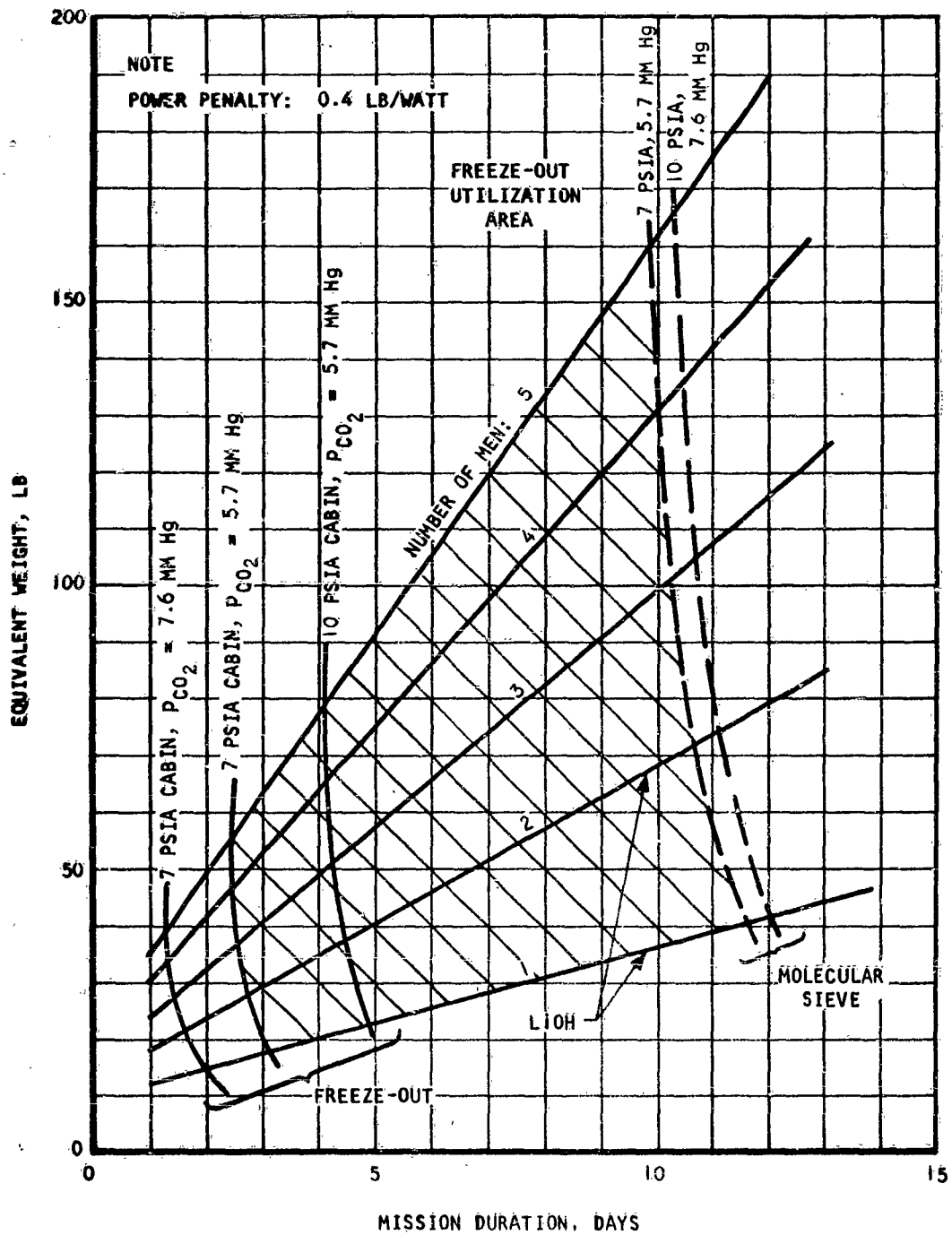


Figure 102. Freeze-out Subsystem Break-even Weight -  
Water Balance not Considered

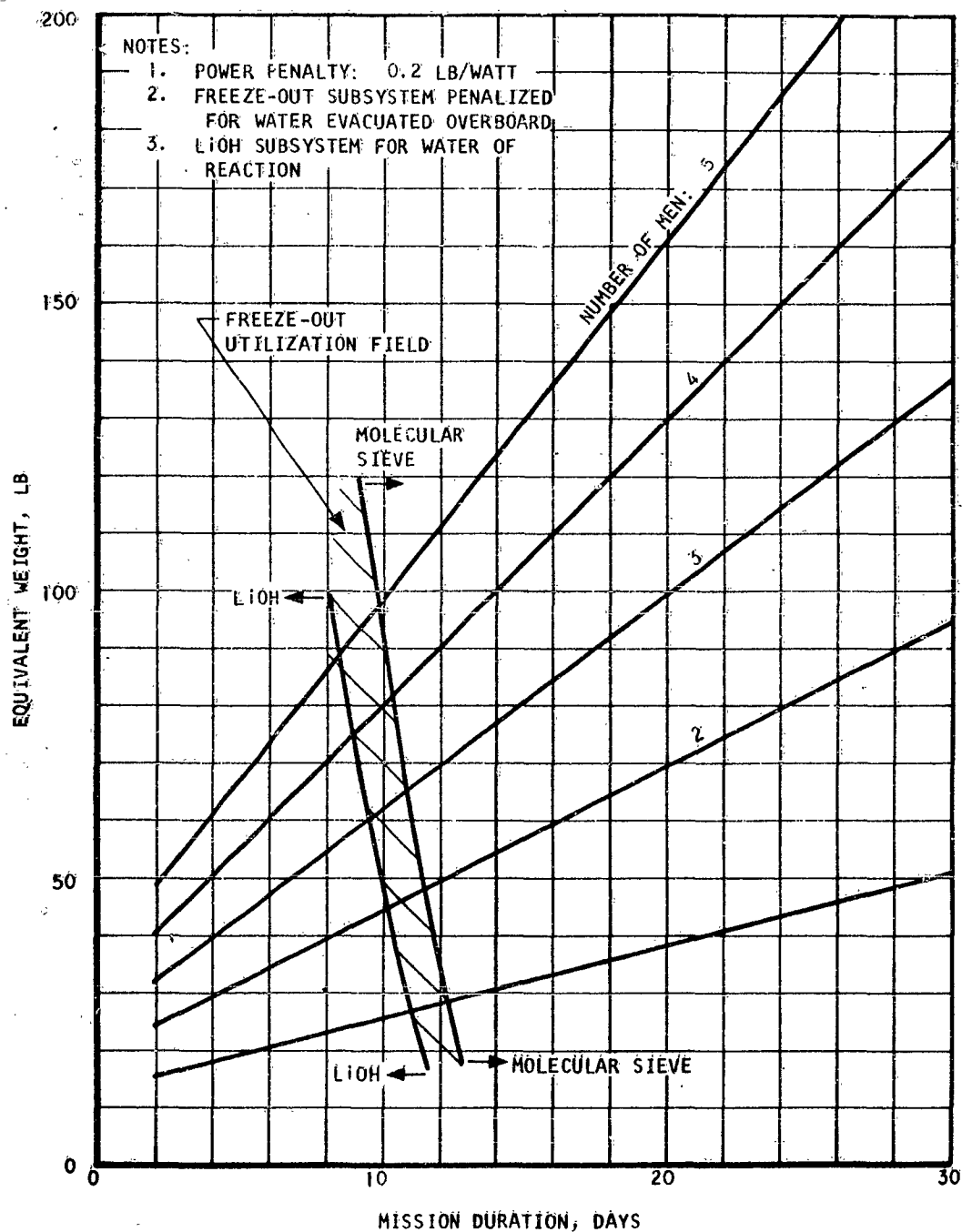


Figure 103. Freeze-out Subsystem Weight and Utilization Field  
( $P = 7.0$  psia,  $P_{CO_2} = 7.6$  mm Hg)



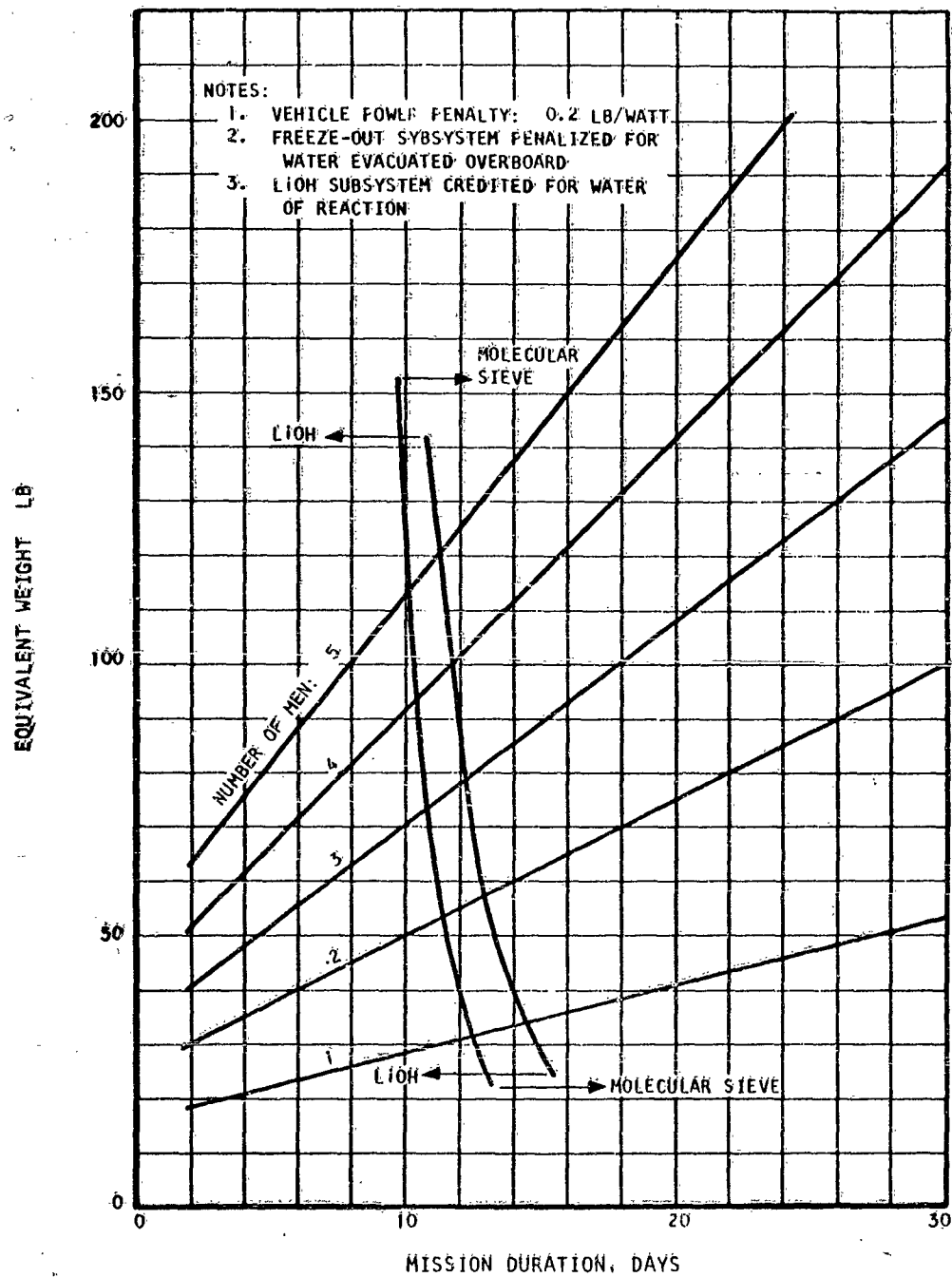


Figure 104: Freeze-out Subsystem Equivalent Weight and Utilization Field  
 ( $P = 10$  psia;  $P_{CO_2} = 7.6$  mm Hg)

7 and 10 psia. Under these conditions, the field of application of the freeze-out system is practically non-existent. Since the freeze-out system weight increases appreciably with a decreasing carbon dioxide partial pressure while the lithium hydroxide subsystem weight is fairly constant, the relative weight of the simple freeze-out system deteriorates at lower carbon dioxide partial pressures.

- d. Heat sink problems also are involved. Because of the size of the heat sink required, relative to the large amount of heat transferred in the exchanger, particular care in the design of the exchanger must be taken to reduce heat conduction from the warm to the cold end. Moreover, insulation of the heat exchanger to prevent heat leaks from ambient poses serious design problems, since any heat leaking into the heat exchanger corresponds to an increase in the cryogenic heat sink requirement of the subsystem.

#### **CARBON DIOXIDE REMOVAL BY ELECTRODIALYSIS PROCESS**

##### **General**

Electrodialysis has been proposed as a practical means of controlling the carbon dioxide concentration of space vehicle cabin atmosphere. This process appears very promising for long-duration missions in which system reliability becomes a primary factor in system selection. Also, since the process power requirements are high, its applicability is necessarily limited to vehicles on which the power source specific weight is relatively low, as for long-duration nuclear or solar power systems.

A schematic diagram of an electrodialysis cell illustrating the principle of operation is shown in Figure 105. The ion exchange membranes are separated by beds of ion exchange resins; as indicated, the carbonate ions, formed by reaction of carbon dioxide with the anionic exchange resin of the bed, migrate toward the anode through the anionic exchange membrane. On the other hand, hydrogen ions formed at the anode and migrating toward the cathode encounter the carbonate ions in an adjacent cell, where water and carbon dioxide gas is formed and discharged from the cell. In the resin system, hydroxyl ions generated at the cathode are constantly replacing those reacting with carbon dioxide in the passages where air flows. A large number of such cells are manifolded together. Small quantities of hydrogen and oxygen are discharged at the cathode and at the anode respectively.

Because the electrodialysis process is continuous compared to the batch type process previously considered for the removal of carbon dioxide, it offers the advantages of simplicity and reliability for long-duration missions. Another advantage lies in the ease with which the carbon dioxide removed can be recuperated for further processing.

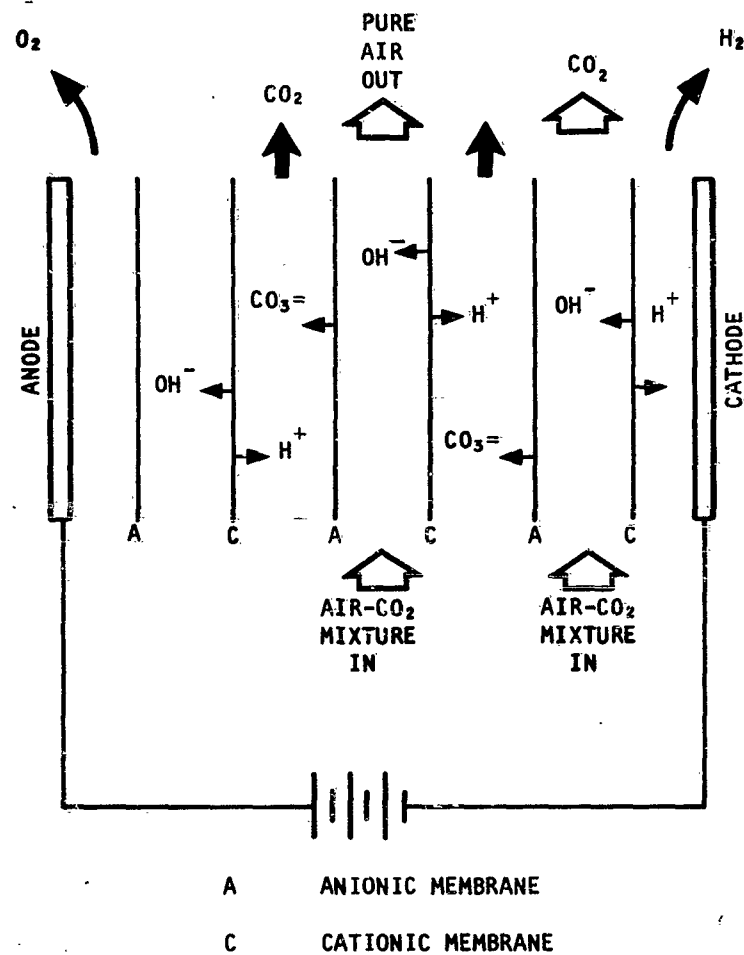


Figure 105. Ion Exchange Electrodialysis Unit for Continuous Carbon Dioxide Removal

### Performance Characteristics

At the present time carbon dioxide removal systems based on electro-dialysis techniques are in the early stages of development. Little is known about the performance characteristics of such systems; the weight, size, and power requirements of the existing experimental cells should be improved considerably in the near future. The effect of total pressure, operating temperature, and carbon dioxide partial pressure on cell design is not well defined. In this report, the following values, based on a literature search and information received from cell manufacturers, are used to evaluate this system:

Power requirement: 117.8 watt per lb of carbon dioxide removed per day

Cell weight: 18.2 lb per lb of carbon dioxide removed per day

Heat rejection: 302 Btu per hr per lb of carbon dioxide removed per day

Hydrogen produced: 0.000444 lb per lb of carbon dioxide removed per day

Oxygen produced: 0.003555 lb per lb of carbon dioxide removed per day

Net water consumption: 0.004 lb per lb of carbon dioxide removed per day

Pressure drop through the cell:  $\Delta P = 5$  in.  $H_2O$

A schematic diagram of a carbon dioxide removal subsystem using the electrodialysis technique is shown in Figure 106. An estimate of the weight of the accessories shown is listed in Table 18. The process air flow through the system necessary for the removal of carbon dioxide at the rate of 2.25 lb per man-day is the same as that calculated for the molecular sieve subsystem and is shown in Figure 69.

Part of the heat generated within the cell is dissipated to the surroundings; however, most of it is dumped into the gases flowing from the cell. These gases are saturated with water vapor at cell outlet. A considerable amount of water is, in this manner, dumped into the air processed in the cell. An analysis of the cell operating temperature was performed based on the cell characteristics listed above; 10 per cent of the heat generated in the cell was assumed lost to the ambient atmosphere. In these conditions, the cell operating temperature was found to vary between 120°F and 125°F, depending on the cell operating pressure. The amount of water carried by the air stream out of the cell is approximately 13.8 lb per man-day, whatever the cell operating pressure.

Based on the above considerations, the performance characteristics of the subsystem depicted in Figure 106 were estimated and are listed in Table 19 for a one-man vehicle. The carbon dioxide removal rate was taken as 2.25 lb per man-day, and the carbon dioxide was assumed completely removed from the process air as it flows through the electrodialysis cell. The relative humidity of the air at cell inlet was assumed to be 60 per cent.

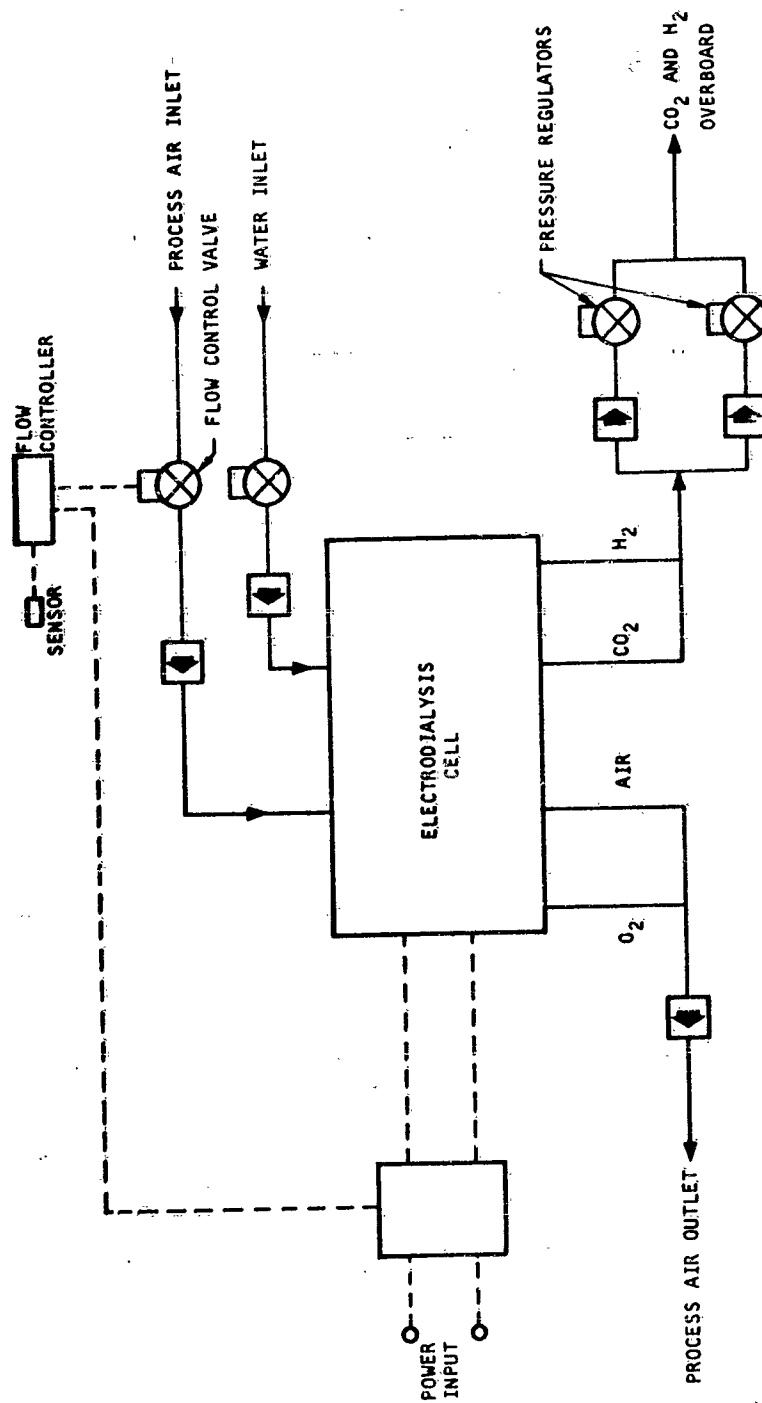


Figure 106. Carbon Dioxide Removal by Electrolysis Process - Subsystem Schematic Diagram

TABLE 18  
ELECTRODIALYSIS SUBSYSTEM ACCESSORY WEIGHT  
(3-MAN SUBSYSTEM)

| Component                 | Weight, lb |
|---------------------------|------------|
| Air flow control valve    | 0.3        |
| Water flow control valve* | 0.15       |
| Pressure regulators*      | 1.4        |
| Check valves              | 0.6        |
| Sensor*                   | 0.1        |
| Flow controller*          | 2.5        |
| Cell control*             | 2.2        |
| Total Weight              | 7.25 lb    |

\* Fixed weight accessories

TABLE 19  
ELECTRODIALYSIS SUBSYSTEM CHARACTERISTICS  
(10 PSIA SUBSYSTEM)

| Parameter                         | Value             |
|-----------------------------------|-------------------|
| Weight                            | 48.2 lb/man       |
| Power requirement                 | 265 watts/man     |
| Cell operating temperature        | 125°F             |
| Heat rejected to ambient          | 68 Btu/hr per man |
| Hydrogen production               | 0.001 lb/man-day  |
| Oxygen production                 | 0.008 lb/man-day  |
| Water entrained by carbon dioxide | 0.208 lb/man-day  |
| Water entrained by air            | 13.8 lb/man-day   |
| Net cell water consumption        | 12.66 lb/man-day  |

### Conclusions

Although accurate cell weight and performance characteristics are not available at the present time, the estimates listed in Table 19 are based on the information presently available and will be used in subsequent sections of this report for integrated system analysis and comparison. As mentioned previously, several design factors and their influence on cell design are unknown. Deterioration of the cell with usage also is an unknown design parameter.

Carbon dioxide removal subsystems using the electrodialysis process are, in their present state of development, much heavier than molecular sieve subsystems. Their power requirement also is much higher. However, because of their simplicity and possible improvement with development, they appear very attractive for long mission duration when the vehicle power penalty is small and the oxygen is recovered from the carbon dioxide, (Reference 6).

## SECTION VII

### RECOVERY OF OXYGEN FROM CARBON DIOXIDE BY HYDROGENATION TO WATER AND METHANE

#### GENERAL

For space vehicle missions of extended duration, it becomes essential to recover oxygen from metabolically produced carbon dioxide. The first step in this direction is based on the hydrogenation of carbon dioxide to methane and water. This reaction also is called Sabatier reaction and is described by the equation:



The reaction with suitable catalyst yields high conversion efficiencies at moderate temperatures. Tests conducted as part of Reference 5 have shown conversion efficiencies on the order of 95 per cent at temperatures of 600°F, with a catalyst consisting of nickel deposited on kieselguhr. These tests were conducted at atmospheric pressure; at reduced pressures, the conversion efficiency drops somewhat (85 per cent at 0.5 atmosphere, as reported in Reference 5).

In Sabatier reaction, which is exothermic, 1600 Btu are liberated per lb of carbon dioxide converted. This poses a problem of reactor design, since the reaction is temperature-dependent. If the temperature of the bed is excessive, the catalyst can be damaged, its life considerably reduced, and the conversion effected less efficiently. On the other hand, if the temperature is too low, little conversion will occur. A bed design used for experimentation with considerable success is shown schematically in Figure 107. The heater is used only to initiate the process; once started, the reaction is self-sustaining, with part of the heat of reaction carried away by the outgoing process gas.

The largest part of the heat released, however, is conducted from the bed through the fins and the insulation and dissipated to the ambient atmosphere. Since the rate of heat released is low, this poses no problem. Instead of being dumped to the atmosphere, this heat can be recovered for useful purposes in the atmospheric control system. This aspect of the reaction will be considered later. A catalytic reactor of the type shown in Figure 107 weighs about 3.0 lb for a three-man system. As will be shown, this weight is small compared to the weight of other components; a reactor weight of 1.0 lb per man will, therefore, be used in this section to evaluate the system.

The heat liberated by the reaction is available for use at other locations in the atmospheric control system. This heat is available at a relatively high temperature level (600°F to 800°F) and is of particular interest for the desorption of the silica gel beds of the molecular sieve system described in Section VI. Therefore, using the reactor as a heat source in some other part of the system offers a double advantage: first,



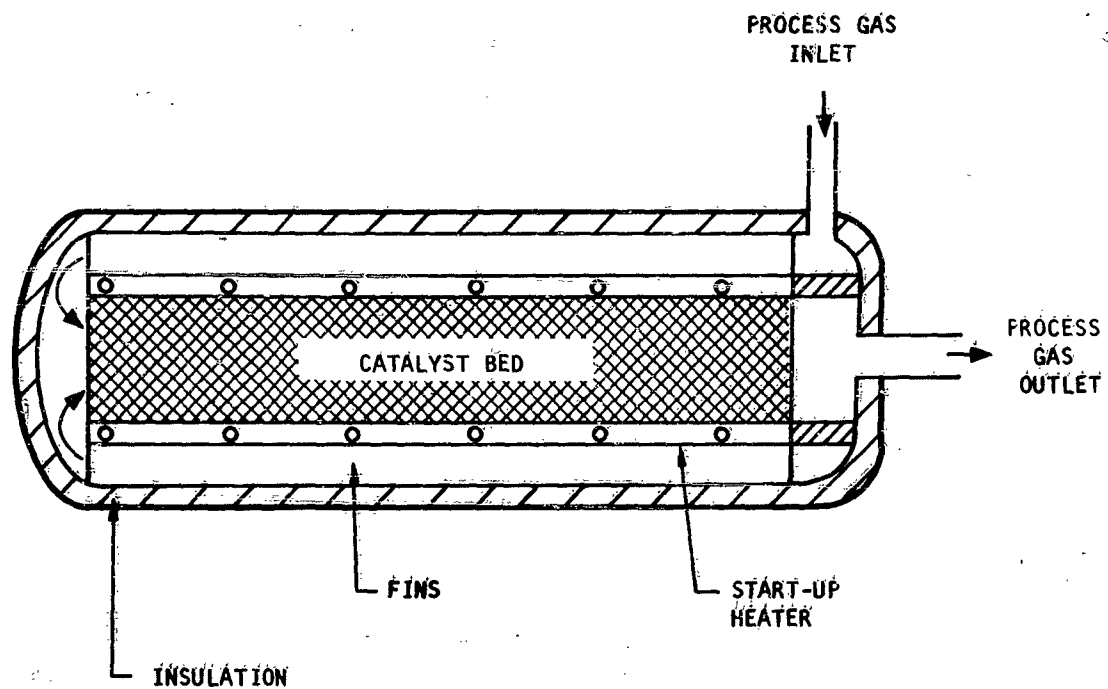


Figure 107. Catalyst Bed Design for Carbon Dioxide Methanation

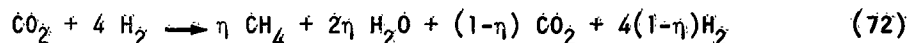
a reduction of the heat dumped into the vehicle cooling system; second, a saving in the system power requirement, since heat at the temperature level considered here is usually generated by electrical means. The heat flow rates in question here, however, are very small, and great care in packaging the whole atmospheric control system is necessary to prevent dissipation to the ambient atmosphere.

Under low loading conditions and good bed temperature control, the catalyst life is estimated to exceed 400 hours (Reference 5).

For the conversion of 2.25 lb per man-day of carbon dioxide, Equation 71 defines the following rates:

Hydrogen consumption: 0.409 lb/man-day  
 Methane production: 0.818 lb/man-day  
 Water evolved: 1.841 lb/man-day

At conversion effectiveness other than 1.0, Equation 71 is written



where  $\eta$  is the carbon dioxide conversion efficiency.

### System Description

In the Sabatier reaction, oxygen is recovered from carbon dioxide as water. This water is not, in itself, a very useful product on long-duration missions; however, by electrolysis the oxygen can be liberated from this water for further use in the cabin. Also, the hydrogen generated in the electrolysis process can be used as part of that required for the Sabatier reaction. Additional hydrogen is necessary for the methanation process, since only two moles of hydrogen are produced by electrolysis of the water of reaction, while four are required for the hydrogenation process (see Equation 71). For long duration missions, the storage of cryogenic hydrogen for the Sabatier reaction is impractical; the hydrogen balance is, therefore, achieved by supplying the electrolytic cell with additional water from the vehicle water management subsystem.

An oxygen recovery subsystem featuring water electrolysis in conjunction with the Sabatier reaction is depicted schematically in Figure 108. A discussion of the major components of the subsystem follows.

#### 1. Electrolytic Cell

The heat generated in the electrolytic cell by the inefficiency of the process is removed from the cell in two ways: first, part of this heat is dissipated from the cell itself to the surroundings; second, the remainder of this heat is used up in vaporizing water which is entrained by the outlet gases. Since these gases are saturated with water at the cell outlet, the operating temperature of the cell is fixed mainly by the cell operating pressure and by the heat leaking from the cell. The

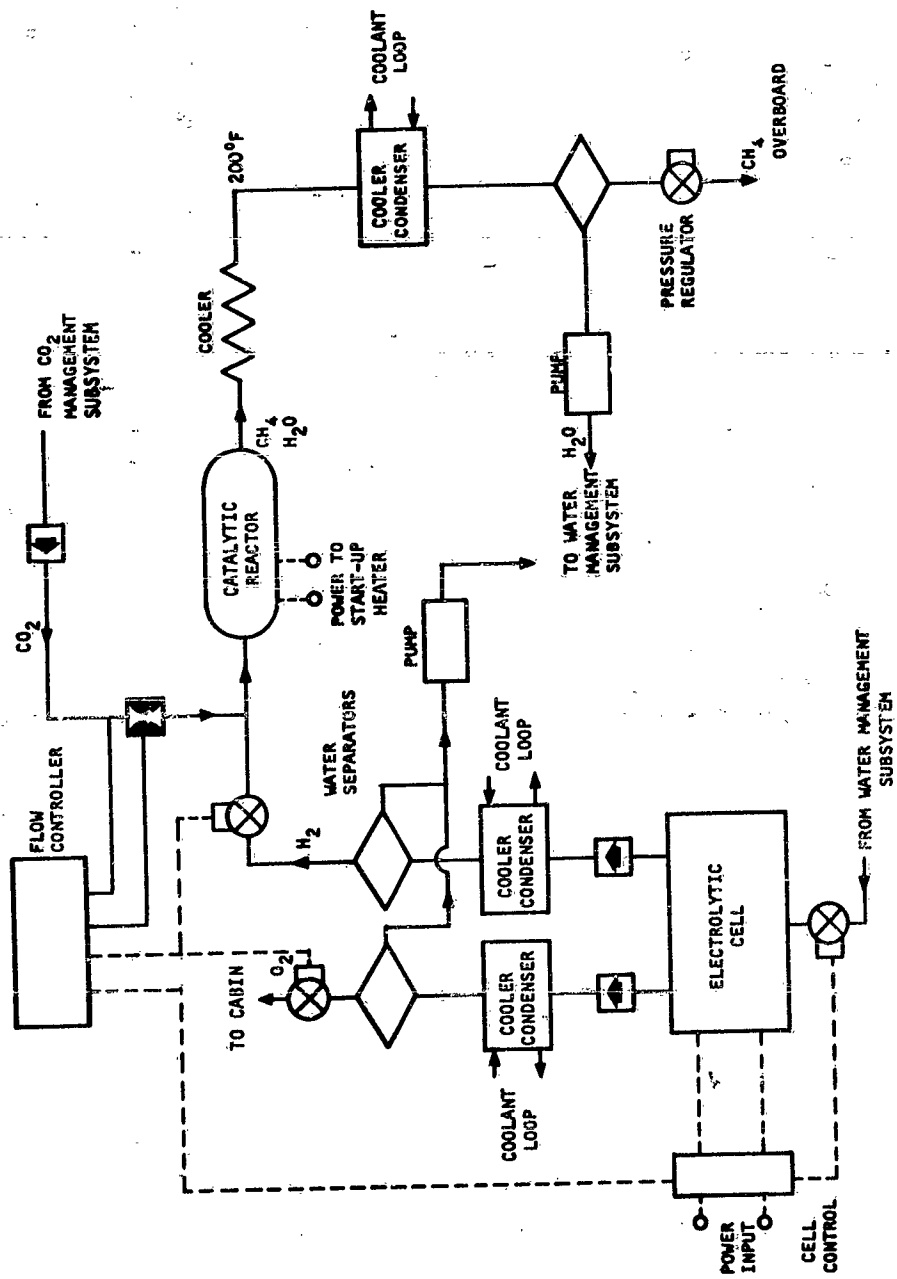


Figure 108. Carbon Dioxide Reduction Subsystem Schematic Diagram

electrolytic cell characteristics used here are the same as those reported in Section IV, namely,

Power input: 117 watts per lb of oxygen per day

Cell weight: 18.7 lb per lb of oxygen per day

Heat generated within the cell: 74.5 Btu hr per lb of oxygen per day

Using the above performance parameters, cell operating temperatures were estimated corresponding to pressures of 7, 10, and 14.7 psia. The heat dissipated to the surroundings was taken as 10 per cent of the heat generated in the cell. Temperatures of 144, 159, and 165°F respectively were estimated for the pressures listed. The amount of water entrained by the oxygen and hydrogen streams was calculated as practically independent of the cell pressure and equal to 0.473 lb per lb of oxygen and 7.58 lb per lb of hydrogen, or 1.546 lb per man-day entrained in the oxygen stream and 3.10 lb per man-day entrained in the hydrogen stream.

If the water carried by the oxygen stream is dumped into the cabin, the load on the cabin humidity control system will be nearly doubled. Since the oxygen stream is saturated with water at high temperature, it is advantageous to liquefy this water before it reaches the cabin. Removal of 1.5 lb of the 1.546 lb per man-day entrained can be achieved by cooling the oxygen stream to 50°F.

The water vapor carried by the hydrogen stream would greatly offset the Sabatier reaction equilibrium if piped to the catalytic reactor with the hydrogen. It is estimated that less than 15 per cent of the carbon dioxide could be converted under these conditions. It is, therefore, imperative to remove as much water as possible before the hydrogen enters the reactor, cooling the hydrogen stream to 50°F and making possible the separation as a liquid of 3.0 lb of water per man-day from this stream.

Removal of the heat dissipated in the electrolytic cell in situ would reduce the amount of water carried by the oxygen and hydrogen streams; however, the cell resistance would increase considerably with a corresponding drop in cell efficiency.

## 2. Catalytic Reactor

The heat of reaction, as mentioned before, is available as a heat source in some other part of the atmospheric control system; however, if this heat is to be used, the reactor itself and the lines carrying the hot fluid from the reactor must be carefully insulated. Here, since the carbon dioxide reduction subsystem is considered by itself, most of the heat of reaction is assumed dissipated to the ambient atmosphere. The methane and water vapor from the reactor are assumed to enter the cooler condenser at a temperature of about 175°F.

## Subsystem Characteristics

### 1. Material and Heat Balance

Figure 109 shows the material balance for the carbon dioxide reduction subsystem of Figure 108. Also shown are the power requirement and the heat loads generated within the subsystem. The values given are for a 7-psia subsystem. In general, the power requirement and heat loads are practically independent of the operating pressure. Table 20 lists the subsystem parameters of interest for operating pressures of 7, 10, and 14.7 psia.

### 2. Subsystem Weight

The weight of the electrolytic cell of the subsystem shown in Figure 108 contributes more than three quarters of the total subsystem weight. Since this weight is not known very accurately, a detailed estimate of the weight of other subsystem components is hardly justified. The total weight of the carbon dioxide reduction subsystem was estimated with this in mind: Table 21 is a list of the component weight showing a total subsystem hardware weight of 77.7 lb per man.

### 3. Equivalent Subsystem Weight

An estimate of the total subsystem equivalent weight can be calculated from the values of Tables 20 and 21. It can be expressed for a 10-psia subsystem by the equation

$$W_E = 77.7 N + 2.05 \times (WTP) N\tau + 383 N (PP) + 453 N (RP) \quad (73)$$

where  $N$  is the number of crew members

$\tau$  is the mission duration, days

(WTP) is the water tankage penalty, lb per lb of water stored

(PP) is the vehicle power penalty, lb per watt

(RP) is the vehicle heat rejection penalty, lb per Btu/hr

Obviously, since the recovery of oxygen is the function of the subsystem, it cannot be credited for the oxygen produced.

### 4. Subsystem Utilization

When the subsystem equivalent weight becomes smaller than the weight of the oxygen supply required with no oxygen recovery, the carbon dioxide reduction subsystem becomes necessary for minimum overall system weight. This occurs when the condition

$$W_E = 3.273 (OTP) N\tau \quad (74)$$

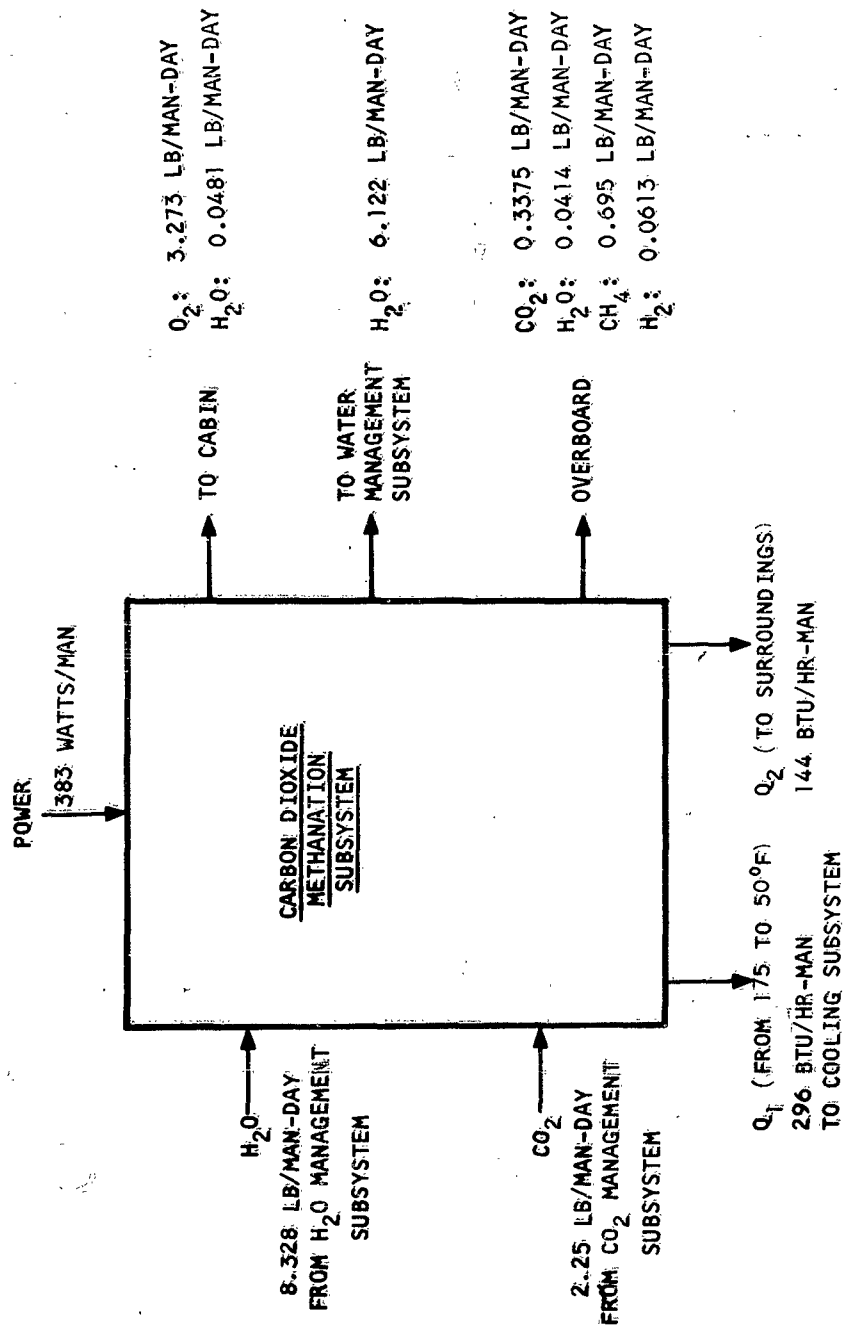


Figure 109. Carbon Dioxide Reduction Subsystem Material and Heat Balance

**TABLE 20**  
**CARBON DIOXIDE REDUCTION SUBSYSTEM CHARACTERISTICS**

| System Pressure, psia                             | 7      | 10     | 14.7   |
|---|--------|--------|--------|
| Power requirement, watts/man                      | 383    | 383    | 383    |
| Heat load to surroundings, Btu/hr-man             | 144    | 152    | 159    |
| Heat load to cooling system<br>(50°F): Btu/hr-man | 296    | 303    | 308    |
| Net water requirement: lb/man-day                 | 2.158  | 2.050  | 1.946  |
| Carbon dioxide overboard: lb/man-day              | 0.3375 | 0.225  | 0.1125 |
| Water overboard: lb/man-day                       | 0.0414 | 0.0249 | 0.0142 |
| Oxygen supply to cabin: lb/man-day                | 3.273  | 3.273  | 3.273  |

TABLE 21

## CARBON DIOXIDE REDUCTION SUBSYSTEM WEIGHT BREAKDOWN

| Component                                | Weight, lb/man |
|--|----------------|
| Electrolytic cell                        | 61.1           |
| O <sub>2</sub> stream cooler-condenser   | 0.65           |
| H <sub>2</sub> stream cooler-condenser   | 0.65           |
| O <sub>2</sub> stream water separator    | 0.5            |
| H <sub>2</sub> stream water separator    | 0.5            |
| Reaction products cooler-condenser       | 1.1            |
| Reaction products stream water separator | 0.5            |
| Water pump-reservoir                     | 1.5            |
| Pump actuator                            | 1.0            |
| Flow controller                          | 3.0            |
| Electrolytic cell control                | 1.2            |
| Water flow control valve                 | 0.2            |
| Catalytic reactor                        | 1.0            |
| CO <sub>2</sub> flow control valve       | 0.25           |
| Cooler                                   | 1.2            |
| Subsystem pressure regulator (2)         | 0.7            |
| Check valves (3)                         | 0.6            |
| Ducts and piping                         | 2.0            |
| <b>Total Weight</b>                      | <b>77.65</b>   |



is satisfied. Here, (OTP) is the oxygen tankage penalty. This equation was solved for the following conditions:

Oxygen tankage penalty: 1.16 lb per lb  $O_2$

Water tankage penalty: 1.05 lb per lb  $H_2O$

Heat rejection penalty: 0.04 lb/watt

The resulting mission duration plotted in Figure 110 against the vehicle power penalty gives the field of application of the subsystem on a weight basis alone. Other considerations, such as system simplicity and reliability, would shift upward the plot of Figure 103. The weight chargeable to carbon dioxide reduction would also be increased somewhat by integration with the atmospheric control subsystem.

### Conclusions

Recovery of part of the metabolic oxygen by reduction of the carbon dioxide offers the possibility of appreciable savings in weight for long-duration missions. The state of the art in the actual reduction process is fairly advanced; however, major problems associated with oxygen recovery subsystems remain.

The weight of the subsystem discussed in this section is largely dependent on the electrolytic cell weight and power requirement: any improvement in these two parameters would reduce considerably the duration of the mission when carbon dioxide methanation becomes applicable.

Another problem area is the recovery of the carbon dioxide from the carbon dioxide management subsystem. If carbon dioxide is to be recovered from the molecular sieve, two techniques can be used: the sieve can be desorbed by use of a pump; however, a better technique would be to desorb the sieve by flowing through it the hydrogen necessary for the reaction. This necessitates heating of the sieve bed and also drying of the hydrogen generated in the electrolytic cell. A control problem also arises to preserve the stoichiometric balance between the hydrogen and the carbon dioxide.

The carbon dioxide reduction system is particularly attractive for use in conjunction with carbon dioxide removal by the electrodialysis process. Here, carbon dioxide is continuously removed from the process air and fed to the methanation subsystem; thus, control problems are greatly simplified. However, as discussed previously, carbon dioxide removal by electrodialysis process is still in the early development stage and can only be accomplished presently at the cost of very high system weight and power requirement.

At the present time, carbon dioxide methanation subsystems are applicable to missions in excess of about 100 days' duration. It is felt that, in the near future, this value will be reduced considerably by the development of electrolytic cells and carbon dioxide removal processes.

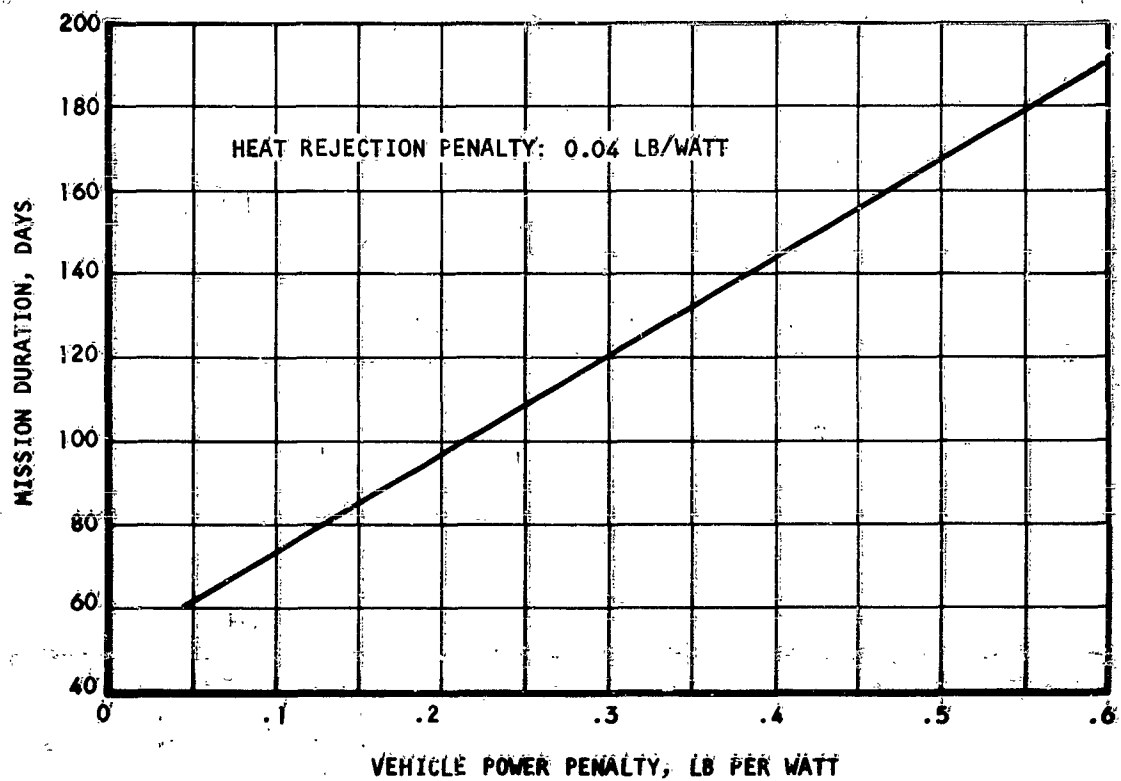


Figure 110. Mission Duration for Utilization of Carbon Dioxide Reduction Subsystem

## SECTION VIII

### TRACE CONTAMINANT MANAGEMENT

#### GENERAL

Trace contaminants may be expected to occur in space cabins as a result of the metabolic processes of the crew, vaporization of insulating and potting materials in electronic equipment, volatilization of lubricants and organic coatings, and leakage of stored materials and in-process materials from the equipment. Combustion processes or overheating caused by equipment malfunction could rapidly generate large quantities of toxic gases. Some of the possible contaminants are listed in Table 22. The occurrence and the exact amount of the contaminants are impossible to predict based on the present state of the art. These factors can be determined only by actual testing aboard vehicles; even then the accidental generation of contaminants remains an unknown parameter.

Various methods of controlling these contaminants have been considered. The methods suggested fall into several classifications, depending on the nature of the contaminant and on the removal process. These are listed below:

#### 1. Gaseous Contaminants

##### A. Contaminant Sorption by Solids

1. Activated carbon
2. Molecular sieves
3. Silica gel
4. Activated alumina

##### B. Chemical Conversion of Contaminants

1. Catalytic oxidation
2. Oxidation by superoxides
3. Oxidation by molybdenum and tungsten trioxide
4. Ozone oxidation
5. Photochemical conversion

##### C. Miscellaneous Methods

1. Electrodialysis
2. Freeze-out

TABLE 22

## POSSIBLE CONTAMINANTS OF SPACE CABIN ATMOSPHERE

| Contaminant                        | Allowable<br>Concentration, PPM |
|------------------------------------|---------------------------------|
| Hydrogen                           | $4 \times 10^4$                 |
| Carbon monoxide                    | 10                              |
| Methane                            | $5 \times 10^4$                 |
| Hydrogen sulfide                   | 20                              |
| Hydrogen cyanide                   | 10                              |
| Aldehydes                          | 0.5 to 200                      |
| Ketones                            | 50 to 200                       |
| Hydrocarbons                       | 500 to 1000                     |
| Hydrogens and halogenated organics | 0.1 to 100                      |
| Ozone                              | 0.1                             |
| Bacteria                           | ---                             |
| Aerosols                           | ---                             |

## **II. Ions, Aerosols, and Particulate Matter**

- A. Filtration**
- B. Electrostatic precipitation**
- C. Ultrasonic agglomeration**

Activated charcoal has a high adsorption capacity for many of the anticipated trace contaminants. It adsorbs effectively the vapors of most materials that are liquid at temperatures of 0°F or above. This classification includes most of the toxic or odor-causing materials likely to be present or generated in a space cabin. The major trace contaminants not effectively adsorbed by activated carbon are hydrogen, methane, and carbon monoxide.

Although synthetic zeolites are available which will adsorb hydrocarbons and other contaminants from the air, they have less capacity for these materials than activated carbon. They do not adsorb hydrogen, carbon monoxide, or methane effectively at room temperature. Furthermore, since a polar substance such as water displaces less polar materials from molecular sieves, the process air flowing through the molecular sieves must be thoroughly dry. Molecular sieves do not appear to offer as satisfactory performance as activated charcoal for the trace contaminant control system and, therefore, will not be discussed further.

Other solid adsorbents for gases, such as silica gel and activated alumina, are much less effective than activated charcoal for the adsorption of the trace contaminants expected to occur in space cabins.

Low molecular weight contaminants which cannot be effectively adsorbed, such as hydrogen, carbon monoxide, and methane, may be converted by catalytic oxidation into other materials which are adsorbable or are non-toxic. The best known catalyst for carbon monoxide and hydrogen oxidation is hopcalite, a mixture of copper and manganese oxides. Hopcalite is an effective catalyst for the oxidation of carbon monoxide and hydrogen at moderate temperatures, but methane is only approximately 30 per cent oxidized at 750°F. Recent work has demonstrated that other catalysts, notably cobalt oxide and palladium or alumina, are more effective than hopcalite for oxidizing methane. The hopcalite catalyst was chosen for consideration in this analysis because of the relatively greater amount of experience and information available for the newer materials. However, it is possible that improved performance could be achieved with the use of other catalysts; this, however, requires a comprehensive test program.

Other methods of oxidation have been considered, but the available information does not indicate effectiveness comparable to hopcalite. Superoxides appear of some value in oxidizing various odorous compounds. Molybdenum and tungsten trioxides have demonstrated good ability to oxidize hydrogen and carbon monoxide. Ozone is ineffective in non-toxic concentrations. Ultraviolet radiation does not seem practical for space vehicle application because of its power requirements and the associated production of undesirable compounds such as ozone.

Fiberglass filters appear the most satisfactory means of removing aerosols and particulate matter. These contaminants may also be destroyed during passage through the catalytic burner. Bacteria are also destroyed in a catalytic burner and, in addition, are adsorbed by activated charcoal.

#### System Description

The trace contaminant control system considered most practical on the basis of present experience consists of an activated charcoal canister and a hopcalite catalytic combustion bed with filters, valves, and piping. A sketch of the proposed system is presented in Figure 111. The activated charcoal, which adsorbs most of the organic, toxic, and odoriferous impurities in the air, is contained as a hollow cylinder within a canister. The airflow passes from the outside surface of the cylinder to the inside through the one-inch-thick carbon layer. Figure 112 is a diagram of the activated carbon canister.

A portion of the air coming from the activated carbon adsorption bed is piped through a heat exchanger and an electrical heater in succession before being circulated through a hopcalite bed. The temperature of the air entering the hopcalite bed is 750°F; the hot process air from the catalyst is cooled by the incoming air in a regenerator before being returned to the main atmosphere control circuit. In practice, the regenerator, heater, and hopcalite bed can be integrated as a unit within a single canister. Filters are located at the outlet of each unit to trap the particulate matter carried by the air stream.

The air circulated through the hopcalite bed is first partly decontaminated in the charcoal bed to reduce the load on the catalytic burner. A fiberglass filter is provided at the exit of the hopcalite bed to insure that no catalyst particles enter the process air. As the air processed in the burner is returned to the main air stream upstream of the fan, most of it flows through the main charcoal bed before being returned to the cabin.

#### System Analysis

Since little is known about the nature of contaminants and their production rates within space vehicle cabins, assumptions form the basis for system analysis. The following assumptions appear reasonable and should yield system weight, which is somewhat high; however, it is felt that, as the state of the art progresses in the field of trace contaminant management, lighter systems will be designed.

- a. The cabin atmosphere available to each crew member is 125 ft<sup>3</sup>.
- b. No cigarette smoking is allowed.
- c. The activated charcoal bed and hopcalite burner operates continuously.
- c. A volume of air equal to the cabin volume is processed through the charcoal bed every hour.

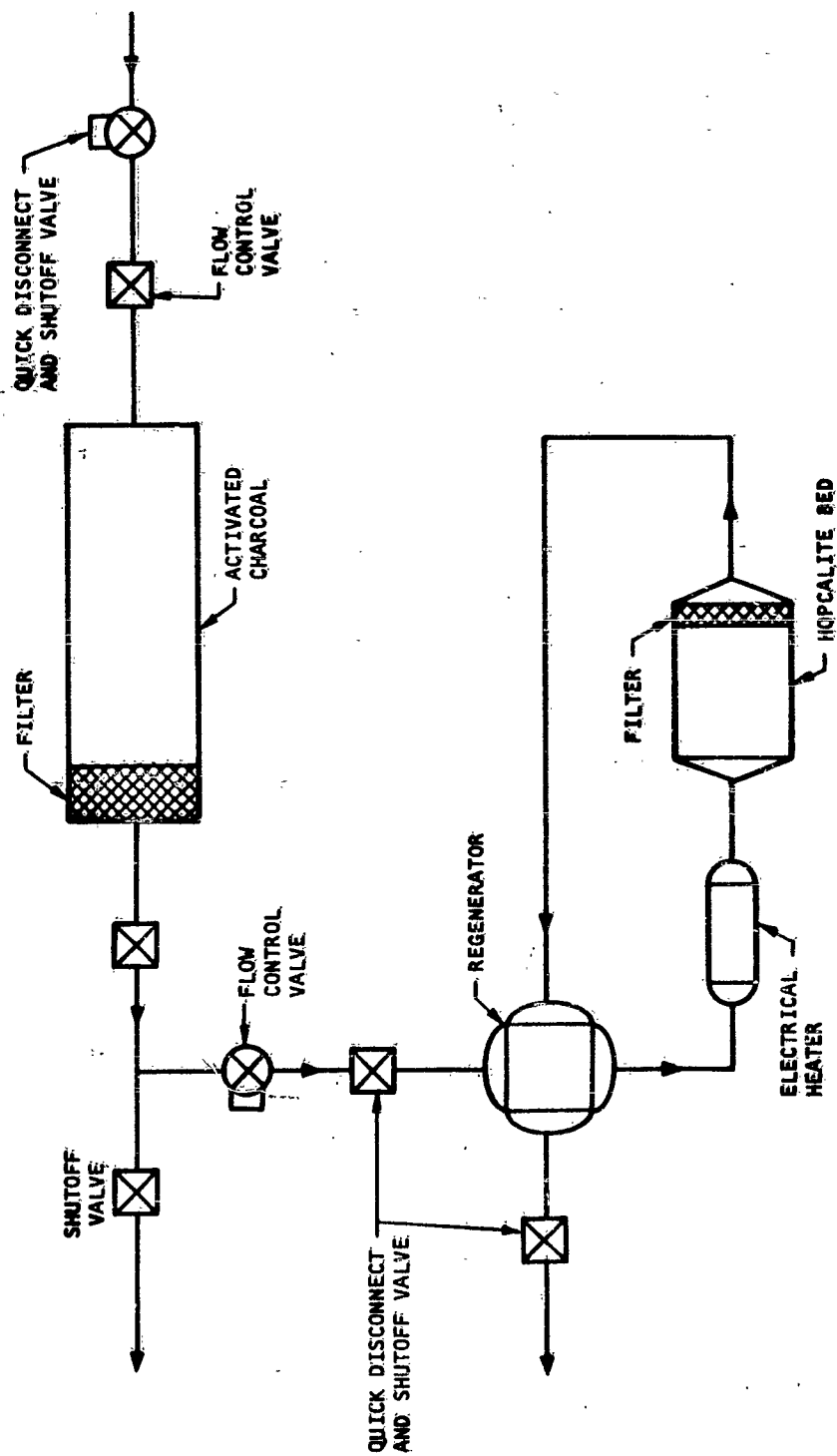


Figure 111. Trace Contaminant Removal Subsystem

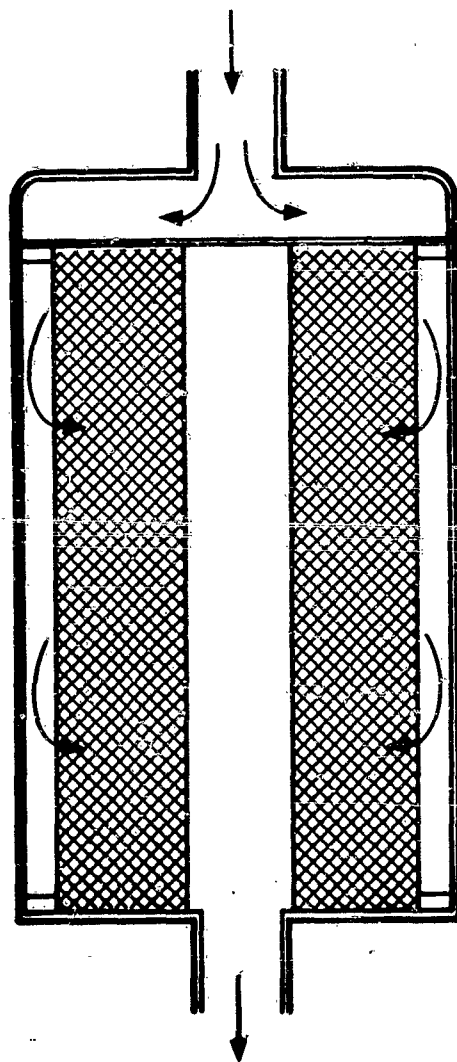


Figure 112. Activated Charcoal Canister.



- d. A volume of air equal to the cabin volume is processed through the charcoal bed every hour.
- e. The flow through the hopcalite bed under normal conditions is 5.21 ft<sup>3</sup> per hour, corresponding to one cabin volume per day.
- f. The activated charcoal bed life is taken as six months, and the weight of activated charcoal required in that period is 1.0 lb per man.
- g. The hopcalite catalyst life is assumed indefinite, and the weight of catalyst required for the emergency case is taken as 1.0 lb per man.

Considerable amounts of high-boiling-point acidic, odor-producing contaminants are removed from the process air stream in the humidity control and the carbon dioxide management subsystems. This somewhat alleviates the load on the activated charcoal bed under both normal and emergency conditions.

One important factor in the design of the contaminant removal subsystem is the trade-off between the regenerator weight and size and the power expended in heating the process air through the hopcalite bed to 750°F. Calculations performed on the weight of the regenerator show an optimum design at an effectiveness of about 90 per cent under normal conditions. Obviously, this value depends on the actual design of the unit and also on the vehicle power penalty. Here, a penalty of 0.2 lb per watt was used. The electrical power consumed by the unit under normal operating conditions is shown plotted in Figure 113.

The trace contaminant removal subsystem must be designed to handle a normal contaminant production rate within the cabin. In addition, emergency conditions in the case of a fire or electronic equipment breakdown must be considered. Two approaches to the solution of the emergency situation are: first, the contaminants can be disposed of by dumping the cabin atmosphere overboard; second, the system can be designed to process the air at an accelerated rate. The optimum solution will evidently be the result of a trade-off study between the additional system weight incurred in designing for emergency and the weight of the atmosphere dumped to vacuum. Because it is impossible to predict emergency conditions, both means of contaminant control will be made available to the cabin occupants. Figure 114, showing the weight of the gas contained in the cabin, is given for reference. The hopcalite unit is designed for very low pressure drop in normal operating conditions, and the air exhausted from the hopcalite unit is returned to the main atmosphere control loop upstream of the fan. Thus, in emergency conditions, the flow through the hopcalite unit can be increased considerably by using all the available pressure drop.

The electrical heater must also be designed with sufficient capacity to maintain the temperature of the catalyst bed at 750°F. The additional power used in this case cannot be charged against the system, since its occurrence cannot be predicted, and other non-essential electrical equipment could be shut off during the emergency period.

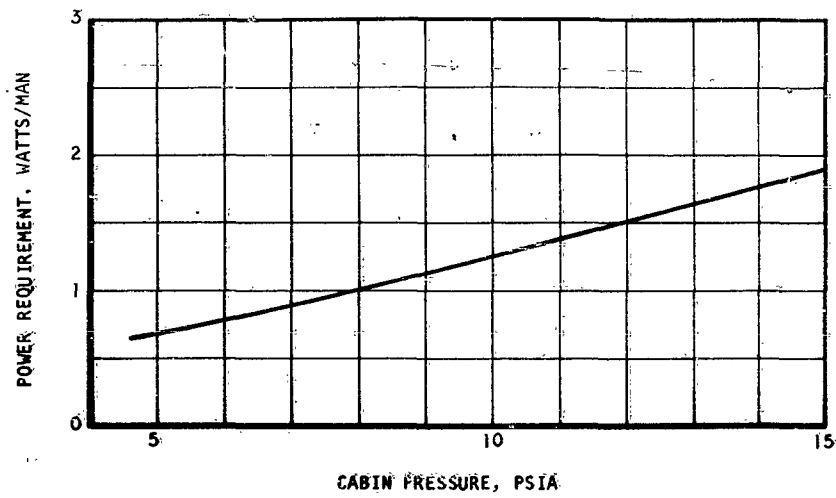


Figure 113. Heater Power Requirement

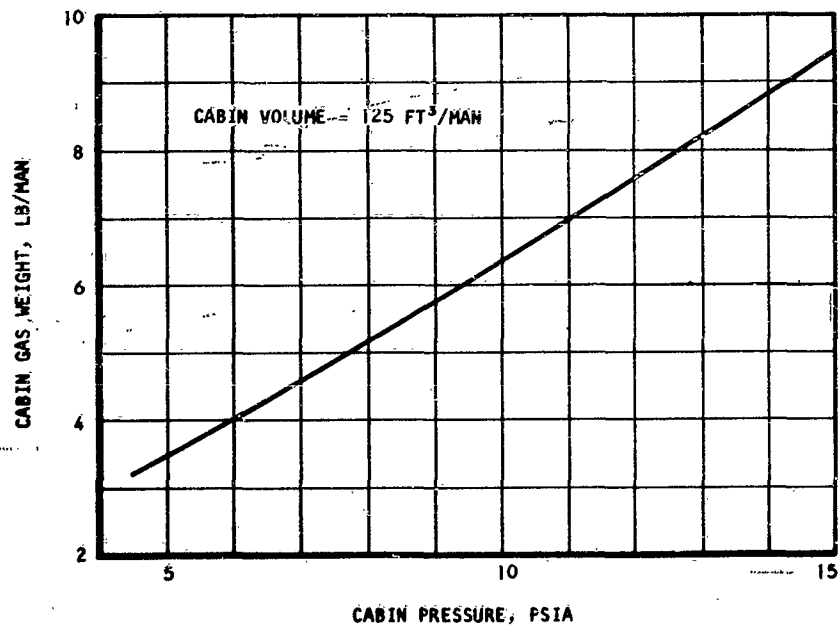


Figure 114. Cabin Atmospheric Gas Weight

An estimate of the subsystem weight is shown plotted in Figure 114 for a cabin pressure of 7 psia. The plot is given for a vehicle power penalty of 0.2 lb per watt of power consumed. The weight of the subsystem will vary slightly with the cabin pressure; however, in view of the assumptions used in the design, it is felt that the plot of Figure 115 is sufficiently accurate for any cabin pressure.

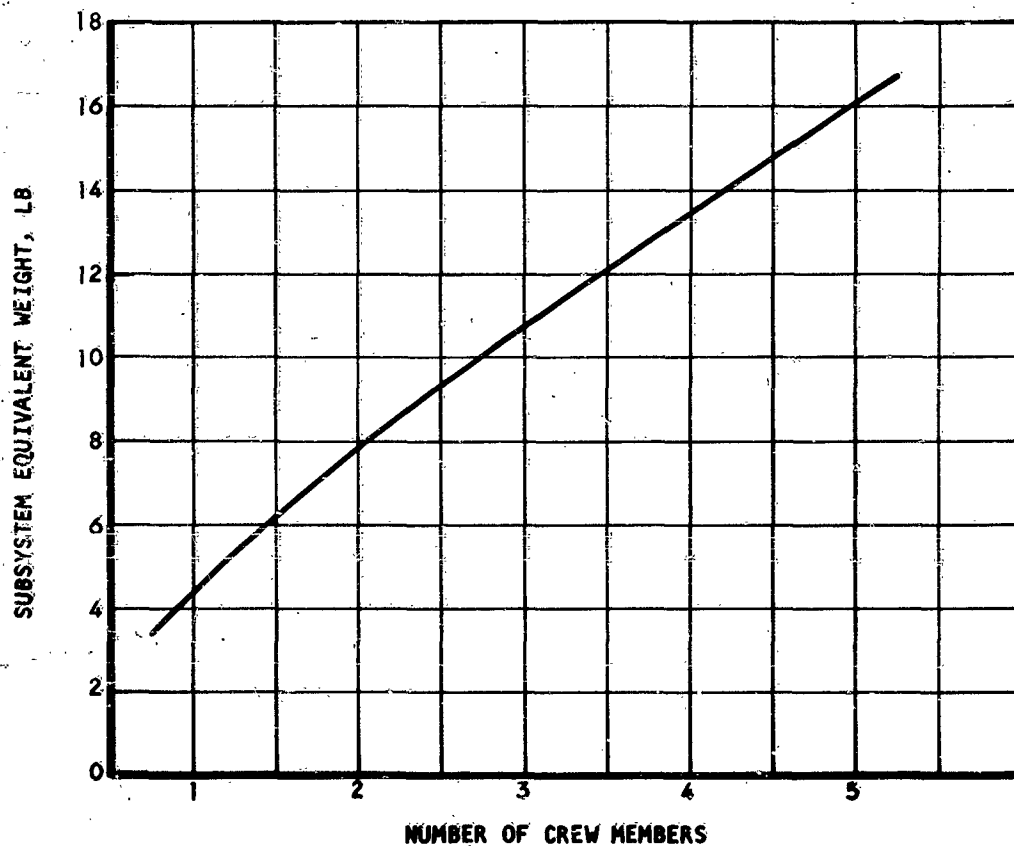


Figure 115. Trace Contaminant Subsystem Equivalent Weight

## SECTION IX

### LEAKAGE DETECTION AND REPAIR

The problem of leakage detection and repair in a space vehicle is largely a problem of leakage detection, and a question of access to the leakage area. The first requisite is, of course, to know that the leak has occurred. For large leaks a noticeable drop in pressure will take place and no special instrumentation is required to detect it. For intermediate size leaks, perhaps the most satisfactory warning indicator will be a drop in the nitrogen partial pressure. This is more satisfactory than a drop in the total pressure, since total pressure may vary somewhat for different levels of crew activity or for heating or cooling of the capsule. However, since it is not a part of any of the metabolic processes, the nitrogen tends to act somewhat as a trace gas. A satisfactory nitrogen partial pressure sensor should be a good indicator of leakage.

On a long-range basis, even minor leaks not accountable by other activity such as use of the airlock could be shown by a careful log of gas inflow. The fundamental problem then is whether or not the space vehicle walls are exposed or covered; that is, whether or not they are accessible to the astronauts. For accessible walls or portions of walls, a number of ideas may be considered. For example, the wall could contain a visual color indicator responding to any leakage. The cabin oxygen could react with a sublayer and cause a color change. The reactants causing a color change could be stored in adjacent films or capsules, as in some of the modern carbon papers, coming in contact only on puncture.

A wall puncture could cause an imbalance on an electrical capacity circuit, and, if this circuit were well subdivided for the small areas of the walls, this would immediately localize the leakage region. If it were feasible to go outside the vehicle to detect the leak, numerous oxygen-sensitive or possibly nitrogen-sensitive detectors could be used. They could be electrical, electrochemical, or chemical type, or they could operate on a physical property of oxygen such as paramagnetism. If it is possible for a man to go outside the vehicle, it should be quite easy to detect location of leaks, and this may well prove the most satisfactory method for detecting smaller leaks difficult to determine internally. If the capsule contains two solid walls which could be broken up into isolated sections, much like the watertight bulkheads on a ship, then it might be possible to isolate the leak by checking pressure of each of these sections. Possibly, too, a small amount of helium could be introduced in the cabin and then standard helium leak detectors utilized.

Once the leak has been found, a number of sealing techniques are possible. The holes could be hand-sealed by the astronaut; solder, varnish, various plastics, or bonded patches could be used. However, it would be desirable to have self-sealing walls, with hand-sealing used only as a backup, or for large holes. For example, the tubeless tire principle could be used, where a plastic coating would flow under a slight pressure and repair small leaks. The leaking air could react

chemically with an exposed material and thus seal small holes. Also, self-foaming plastic, contained in small cells under pressure, could fill the punctured area by foaming action if the cell is penetrated.

## SECTION X

### ATMOSPHERIC CONTROL SYSTEMS

#### GENERAL

Based on the results of the subsystem analyses performed in the preceding sections of this report, complete space vehicle atmosphere control systems are described integrating the following subsystems:

- Gas supply
- Carbon dioxide management
- Humidity control
- Trace contaminant removal

Although gas supply is, in general, the heaviest subsystem, the atmosphere control system arrangement is affected most by the carbon dioxide removal subsystem. Systems considered are, therefore, identified by these carbon dioxide management methods:

- Lithium hydroxide
- Freeze-out technique
- Molecular sieve
- Electrodialysis process
- Molecular sieve and oxygen recovery by carbon dioxide methanation
- Electrodialysis and oxygen recovery by carbon dioxide methanation

In this section, the above atmospheric control subsystems are described. Schematic diagrams showing the arrangement of the components and subsystems are given in Figures 116, 120, 128, 133, 134, and 136. The system weight, power requirement, heat load on the vehicle cooling system, and material balance are presented in parametric form. Sufficient data are given to make possible integration of the atmospheric control system with other vehicle systems, namely, power source, thermal control, and water management systems.

The gas supply subsystem is generally heavier than all the other atmospheric control subsystems. Its weight, if included in the computations of total system weight, tends to disguise the overall characteristics of any particular system. For this reason, the gas supply subsystem characteristics are excluded from the parametric data presented in this section. It should be noted here that the gas supply subsystem is the same for all the systems considered, except when oxygen is recovered from carbon dioxide by methanation and carbon dioxide removed by freeze-out.

By simple inspection of the schematic diagrams, it is evident that several features are common to all systems. To simplify the description of each one of the systems and to prevent unnecessary repetitions, these common components are reviewed below.

#### Gas Supply Subsystem

The preferred gas supply subsystem for space vehicle application uses supercritical storage of gases at cryogenic temperatures (See Section IV). This subsystem is incorporated in all the atmospheric control systems considered here, except when carbon dioxide is removed by freeze-out process. In this case, subcritical storage with positive expulsion is necessary to provide the heat sink required for freeze-out. The systems featuring oxygen recovery from carbon dioxide by methanation require hydrogen for this process; storage of hydrogen as a cryogenic fluid for long duration is impractical; in this case, hydrogen is produced by electrolysis of water. The oxygen generated in the process is used in the cabin. The pertinent characteristics of the gas supply subsystems are given in Section IV.

Quantity gages are installed in the cabin showing the amount of oxygen and nitrogen left in the storage vessels. This is done by density measurement in the case of supercritical storage vessels. Subcritical storage vessel quantity measurements are estimated from the pressurizing gas storage pressure.

Delivery of oxygen from the storage vessel is controlled by the oxygen partial pressure in the cabin, and the cabin total pressure is used to modulate the flow from the nitrogen storage tank.

#### Cabin Leakage Detection

The nitrogen rate of flow from the storage vessel is measured and translated into cabin leakage rate shown on an instrument inside the cabin.

#### Humidity Control Subsystem

In all the atmospheric control systems considered, cabin humidity control is effected by cooler-condenser process with subsequent separation of the water as a liquid. This technique is discussed in detail in Section V, where the subsystem characteristics are given parametrically. In some systems described later, several cooler-condenser-separators are used to control the moisture content of different gas streams.

Cabin relative humidity measurement is used to control the coolant flow to the cooler-condenser. This modulates the process air temperature at the outlet of the cooler and the rate of condensation of the water vapor.

The liquid separated from the process gas is returned to the vehicle water management system.

#### Trace Contaminant Removal Subsystem

Another feature common to all the systems considered is the removal of trace contaminants by circulating cabin air through an activated charcoal bed. Part of this flow is then directed to a hopcalite unit consisting of a regenerator, electric heater, and hopcalite catalyst bed where



low boiling point contaminants are oxidized. The flow from the hopcalite burner is returned to the system fan inlet for two reasons: first, the oxidization products from the hopcalite unit are themselves contaminants, and second, in case of emergency, the flow through the hopcalite unit can be increased considerably by manually opening the circuit flow control valve. All the pressure differential across the fan is then available to circulate cabin gas through the unit. A discussion of this subsystem and parametric data is given in Section VIII.

#### Redundancy for Safety and Reliability

In all the systems considered, two fans are installed in parallel to insure the flow through the atmospheric control system. Each fan can handle all the flow. For missions of long duration, three fans are used in the system.

Valves sealing the system against vacuum are also redundant for safety and reliability reasons.

The system studies were conducted for the following data assumptions defining cabin conditions and crew average metabolic processes:

- Cabin temperature: 70°F
- Cabin relative humidity: 60%
- Cabin pressure: 5 to 14.7 psia
- Carbon dioxide production rate: 2.25 lb/man-day
- Oxygen consumption: 2.0 lb/man-day
- Water evolved in respiration and perspiration: 2.2 lb/man-day
- Cabin oxygen partial pressure: (see Figure 4)
- Cabin carbon dioxide partial pressure: 3.8 to 7.6 mm Hg
- Leakage of carbon dioxide from the cabin: negligible
- Leakage of water from the cabin: negligible

These assumptions are common to all the systems analyzed; other assumptions applicable to particular systems are discussed with the system descriptions and analyses.

The weights plotted in this section are not a true criterion for system comparison. The other parameters relating the atmospheric control system to other vehicle systems must be considered to establish the relative merits of the various atmospheric control systems.

Thermal control of the cabin atmosphere and equipment is not considered in this report; however, it should be pointed out that part of the heat generated in the cabin is removed from the process air flow necessary for atmospheric composition control. First, the water vapor produced by the cabin occupants, through respiration and perspiration, is condensed in the atmospheric control system. Second, the process air is, in general, returned to the cabin at a temperature lower than the cabin air temperature. Third, the cryogenic gas supply provides a heat sink which must be considered in the overall vehicle thermal control.

## LITHIUM HYDROXIDE ATMOSPHERIC CONTROL SYSTEM

### General

This system, as seen from Figure 85, is applicable to mission durations up to 30 days, depending on the cabin pressure and the allowable carbon dioxide concentration in the cabin. The main advantage of this system, other than weight, is its great simplicity and reliability. Also, it is the most advanced in the state of the art.

### System Description

The system, shown schematically in Figure 116, uses supercritical storage of oxygen and nitrogen for metabolic and leakage make-up gas supply to the cabin. Humidity control is effected by cooler-condenser-separator technique. Trace contaminants are removed by activated charcoal adsorption and by catalytic oxidation in a hopcalite bed. Carbon dioxide is removed by adsorption in two lithium hydroxide beds. This subsystem arrangement is discussed in Section V of this report.

The flow through the system is clearly indicated on the system diagram. The carbon dioxide partial pressure in the cabin is used to control indirectly the flow through the lithium hydroxide canisters.

The humidity control is effected downstream of the lithium hydroxide beds to remove the water evolved in the carbon dioxide adsorption process without increasing the flow through the system.

### System Characteristics

#### 1. Weight

An estimate of the weight of the complete system, exclusive of the gas supply subsystem, is shown in Figure 117 plotted against mission duration for one- to five-man vehicles. Slight variations in weight, due to cabin pressure and carbon dioxide partial pressure in the cabin, are not shown.

#### 2. Power Requirement

Figure 118 is a plot of the system power requirement against the cabin pressure. Small deviations due to carbon dioxide partial pressure in the cabin and number of crew members are neglected. The plot shown here includes the power necessary for loop control.

#### 3. Heat Load

The heat rejected to the vehicle cooling system through the cooler-condenser is plotted in Figure 119. Here, it is assumed that all the power input to the system, including the power expended for loop control, is dumped into the process air stream and removed at the cooler-condenser. It should be noted that the air returning to the cabin from the cooler-condenser is saturated with water at 45°F, while the process air from the cabin enters the system at 70°F and 60 per cent relative humidity.

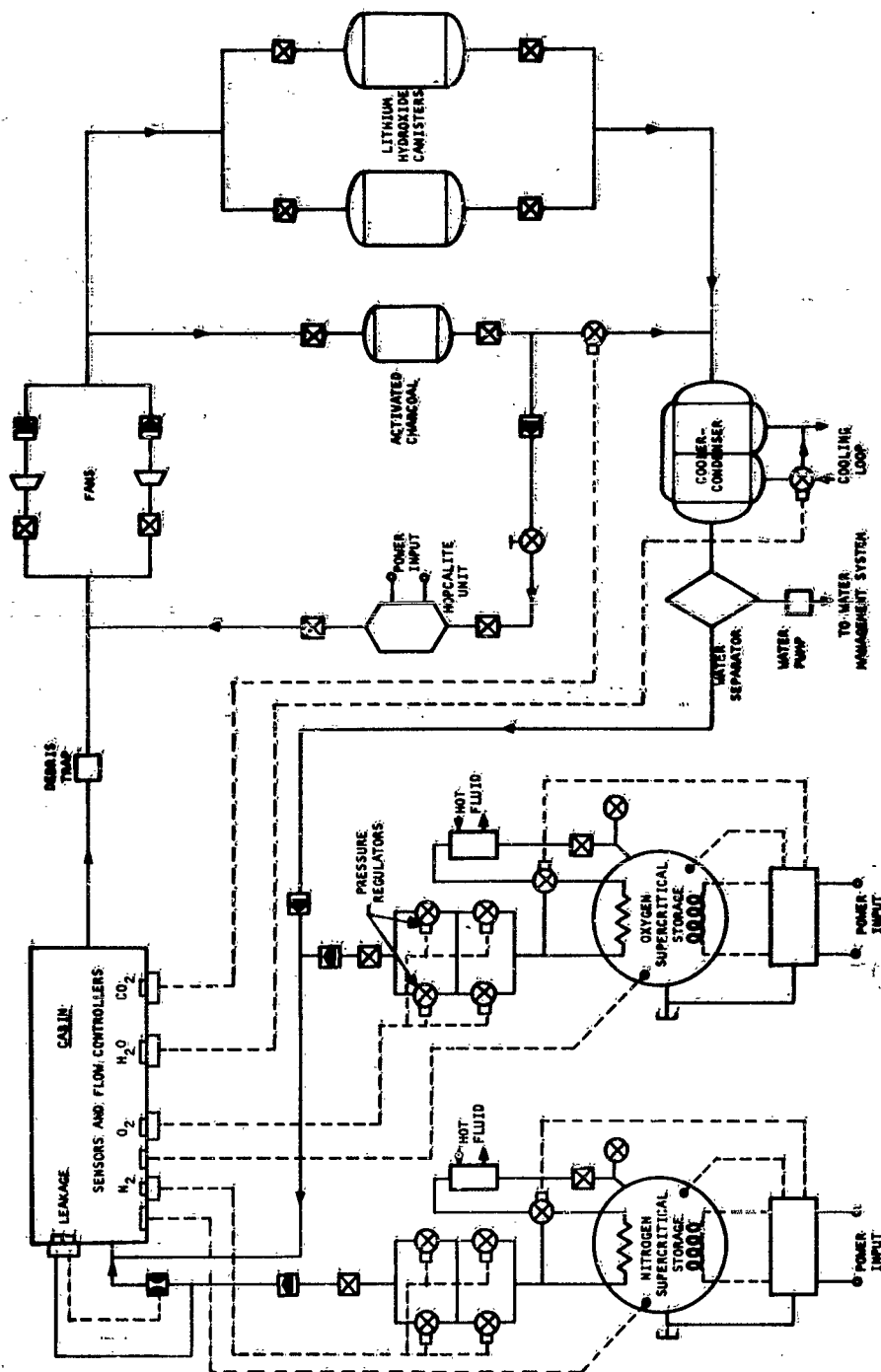


Figure 116. Lithium Hydroxide Atmospheric Control System

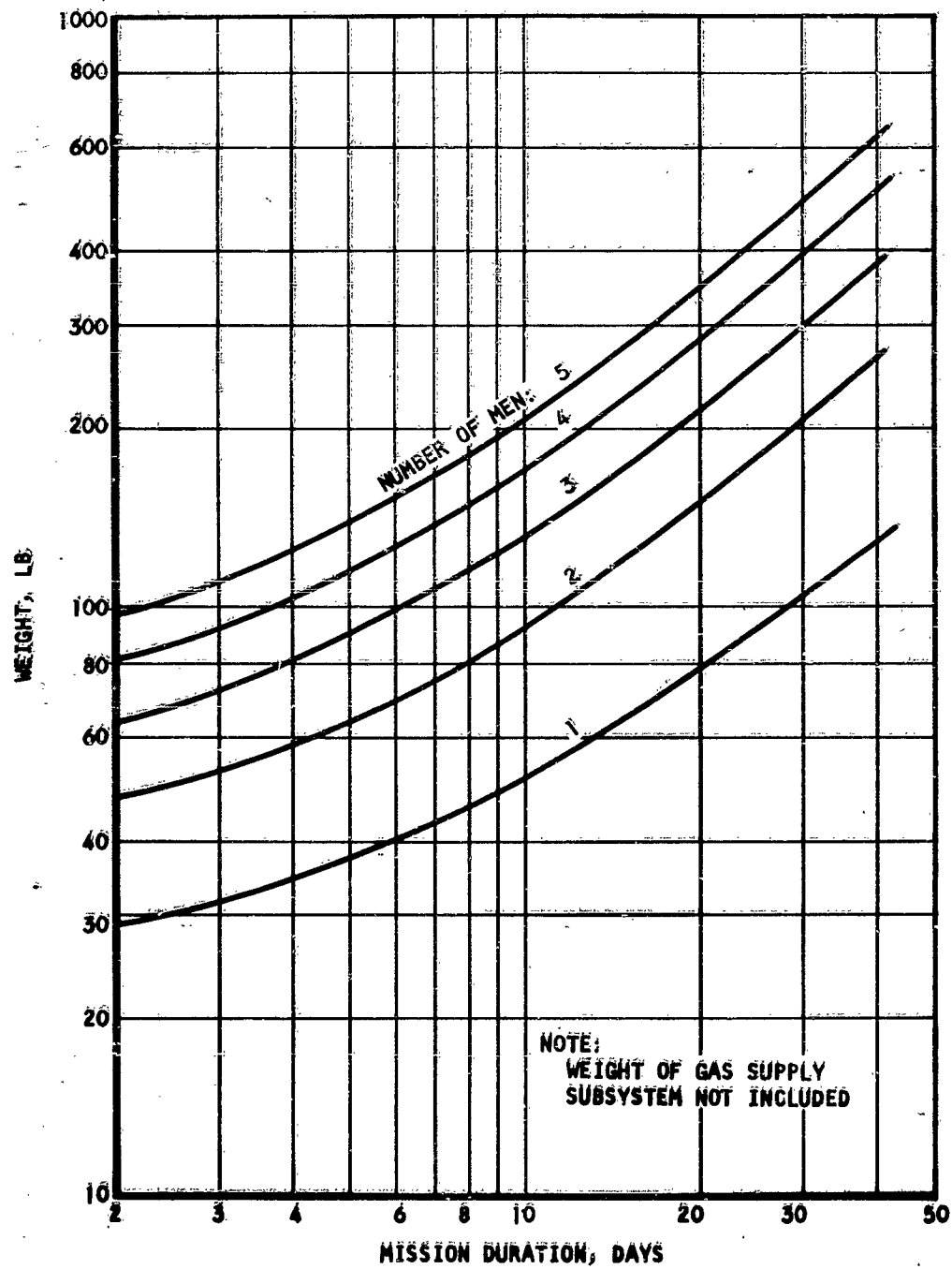


Figure 117. Lithium Hydroxide Atmospheric Control System Weight

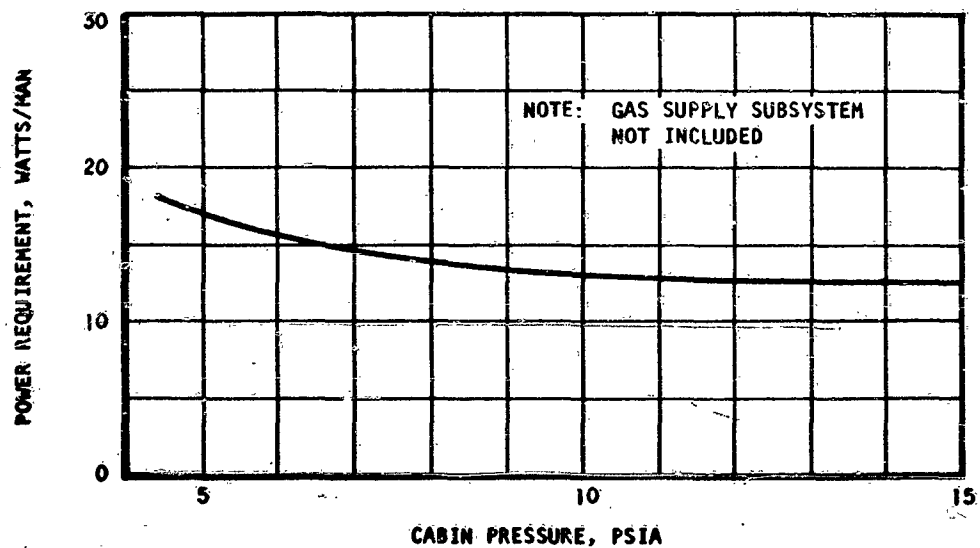


Figure 118. Lithium Hydroxide Atmospheric Control System Power Requirement

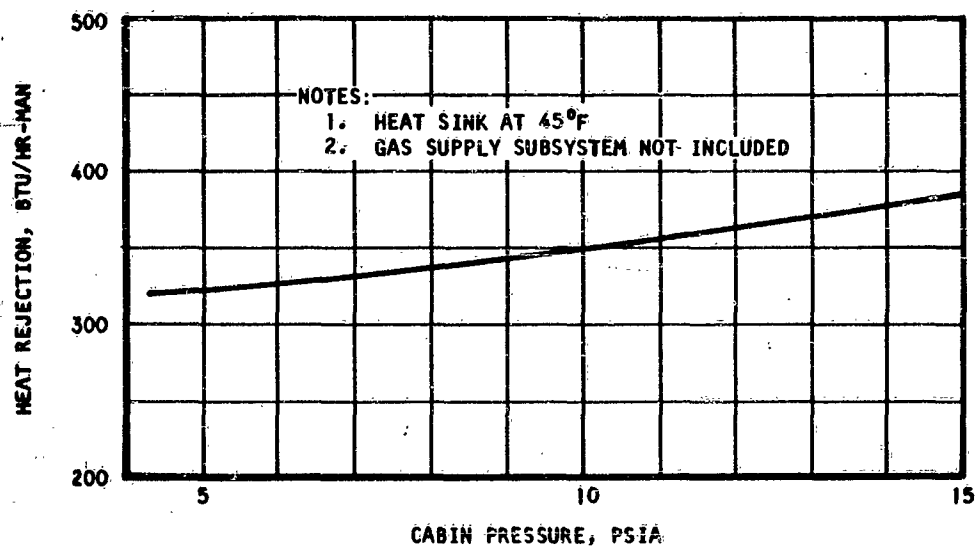


Figure 119. Lithium Hydroxide Atmospheric Control System Heat Rejection

#### 4. Material Balance

The atmospheric control system removes carbon dioxide from the cabin atmosphere at the rate of 2.25 lb per man-day and water vapor at the rate of 2.2 lb per man-day. Liquid water separated from the process air is returned to the water management system at the rate of 2.92 lb per man-day.

#### **FREEZE-OUT ATMOSPHERIC CONTROL SYSTEM**

##### General

Freeze-out processes, although relatively undeveloped, appear promising as a means of carbon dioxide removal. However, the water evacuated overboard limits the field of application of simple freeze-out systems to short-duration missions. System reliability is considerably less than for other short-duration systems using chemical processes.

##### System Description

The system uses a simple freeze-out heat exchanger where carbon dioxide and moisture are frozen and subsequently evacuated overboard in a regenerative manner. Figure 120 is a schematic diagram of the system showing the component arrangement and the process gas flow through the system.

Subcritical storage of atmospheric gases with positive expulsion is used here to provide the heat sink required for the freeze-out process.

The oxygen and nitrogen vessels are pressurized from two separate helium bottles. This greatly simplifies quantity measurements, and no weight penalty is incurred by the use of two bottles, other than the pressurizing subsystem accessory weight.

The liquid oxygen flow from the tank is regulated by the oxygen partial pressure in the cabin, and the liquid nitrogen flow is controlled by the cabin total pressure.

Moisture from the process gas is removed in a cooler-condenser-separator subsystem upstream of the freeze-out heat exchanger to reduce the heat load on this exchanger and also to reduce to a minimum the amount of water evacuated overboard. Trace contaminant removal is achieved by activated charcoal adsorption and catalytic oxidation in a hopcalite bed.

Operation of the carbon dioxide freeze-out heat exchanger is controlled as follows: the flow of cabin air is modulated by the carbon dioxide partial pressure in the cabin. The valve switching mechanism is activated when the pressure drop of the process air flowing through the exchanger exceeds a preset value. This occurs when the heat exchanger passages where freezing occurs become blocked by deposited solids. The flow of cryogenic liquids, oxygen, and nitrogen to the freeze-out heat exchanger is controlled by the temperature of the process gas at the heat exchanger outlet. The excess cryogenic liquid delivered from the storage vessels is dumped into the process air returning to the cabin.

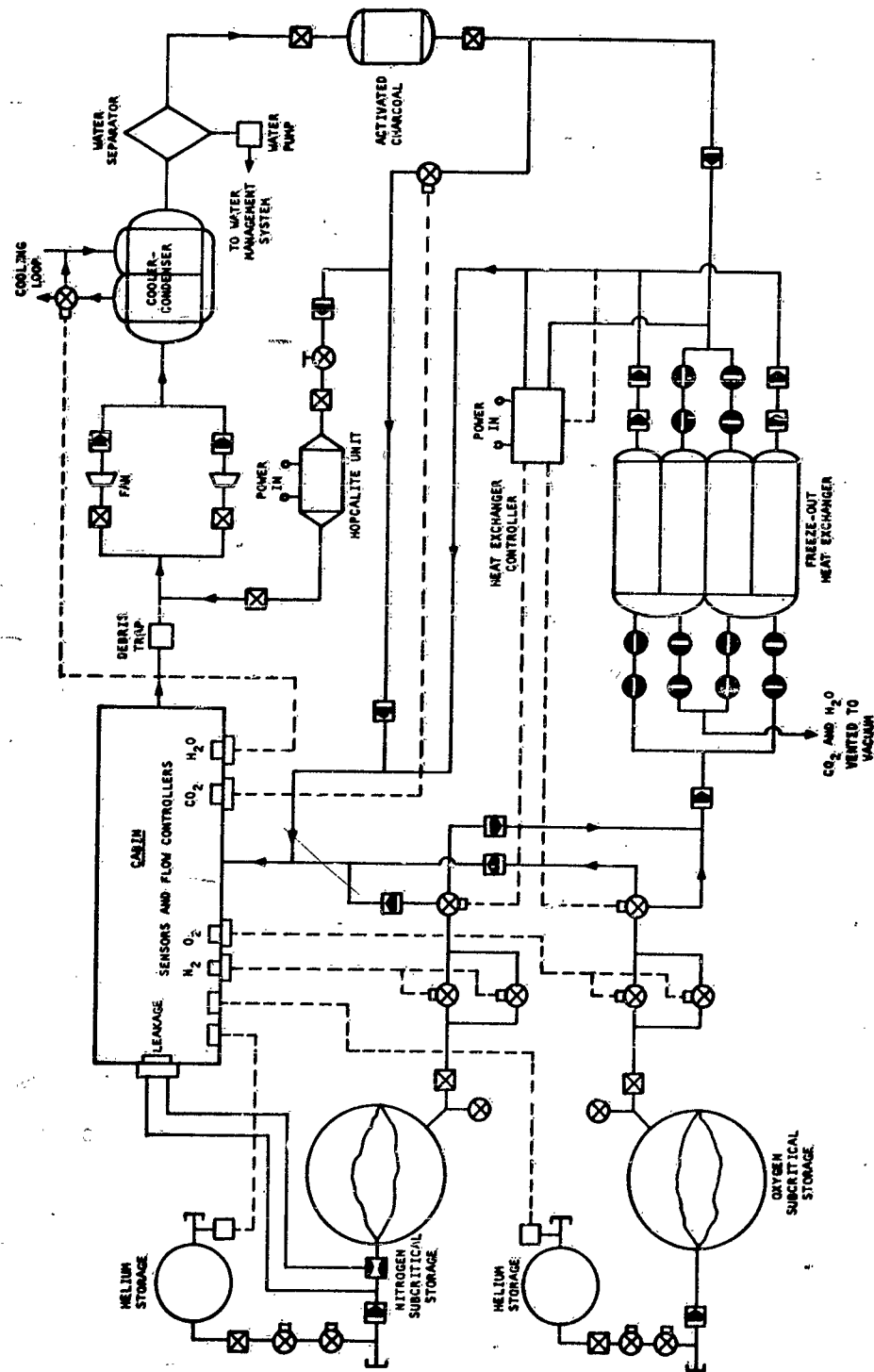


Figure 120. Freeze-out Atmospheric Control System

## System Characteristics

### 1. Weight

The weight of the system is plotted against the carbon dioxide partial pressure in the cabin in Figures 121 and 122 for two values of the cabin pressure: 7 and 10 psia. This weight estimate was based on a cabin leakage rate of 2.5 lb per man-day. This value seems reasonably conservative for short-duration mission vehicles where the simple freeze-out system applies.

### 2. Power Requirement

Figure 123 gives a plot of the system power requirement on a one-man basis. Power is plotted as a function of the cabin total pressure for a range of carbon dioxide partial pressures. The small variations due to the number of crew members are neglected.

### 3. Heat Load

The heat rejected to the vehicle cooling system at the cooler-condenser is plotted in Figure 124. The process air at cooler-condenser outlet is taken as 45°F. The cryogenic heat sink required for the freezing process is provided by the flow of 4.5 lb per man of liquid oxygen and nitrogen from the subcritical vessels; this corresponds to a heat sink of approximately 26.1 Btu per man-hr at a temperature on the order of 225°R. More accurate values are given in Section VI where freeze-out subsystems are discussed.

### 4. Material Balance

Carbon dioxide is removed from the process air and evacuated overboard at the average rate of 2.25 lb per man-day. Part of the water vapor produced in the cabin at the rate of 2.2 lb per man-day is frozen in the carbon dioxide removal process and evacuated overboard with the carbon dioxide. The rate of water lost in this manner is plotted in Figure 125 as a function of the carbon dioxide partial pressure in the cabin. This water is not recovered by the water management subsystem; however, the flow through the humidity control subsystem is considerably reduced, since complete water removal is effected in the freeze-out heat exchanger. Calculations were performed to determine the amount of water carried by the process air required for carbon dioxide removal. This is plotted in Figure 126 as a function of the cabin relative humidity for a cabin temperature of 70°F. This plot shows that at low carbon dioxide partial pressure, water is removed from the air stream at such a rate that the cabin relative humidity cannot be kept at 60 per cent. The amount of water removed in the cooler-condenser and returned to the vehicle water management system is plotted in Figure 127 for the cabin relative humidity shown in Figure 126 (60 per cent maximum).



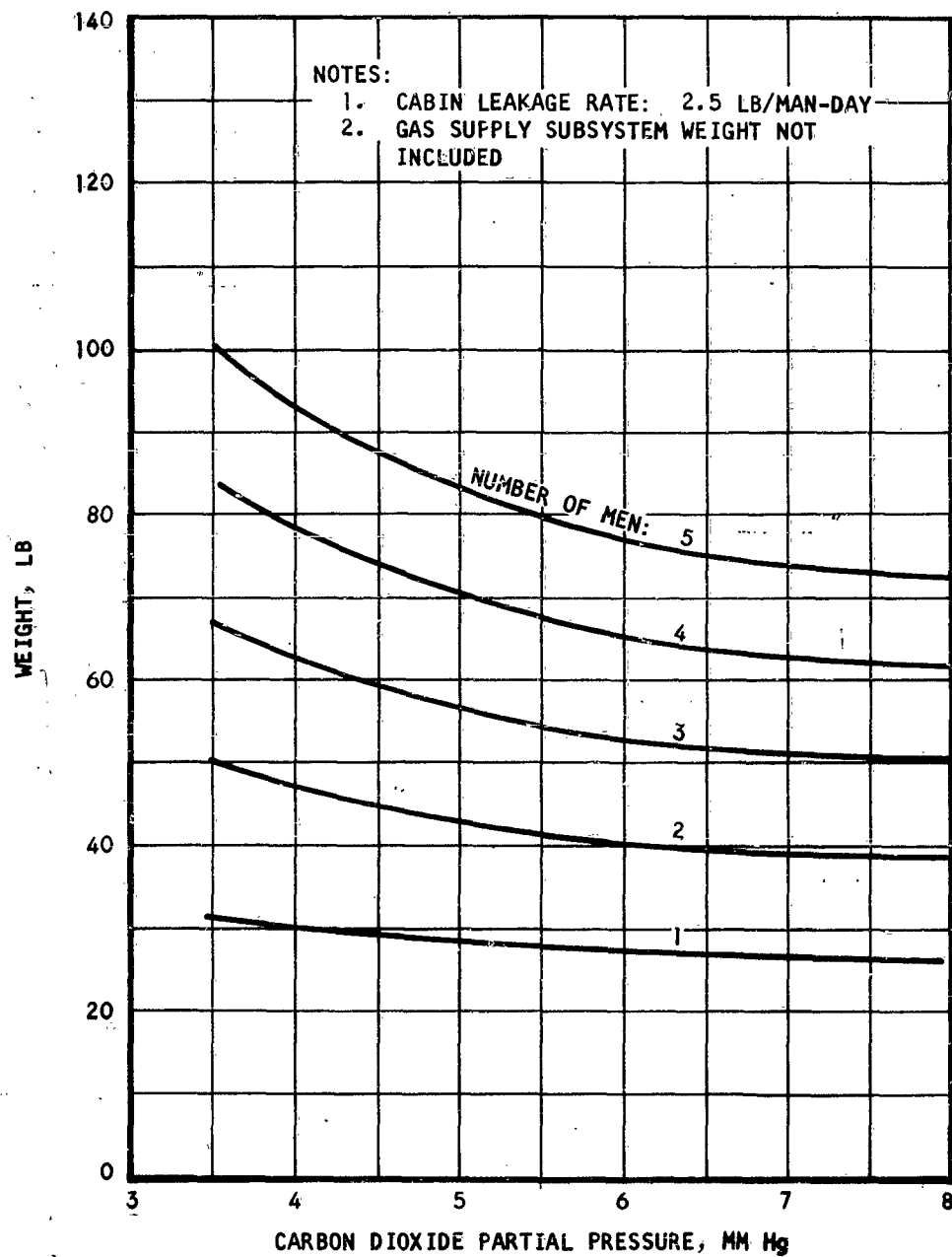


Figure 121. Freeze-out Atmospheric Control System Weight  
(Cabin Pressure: 7 psia)

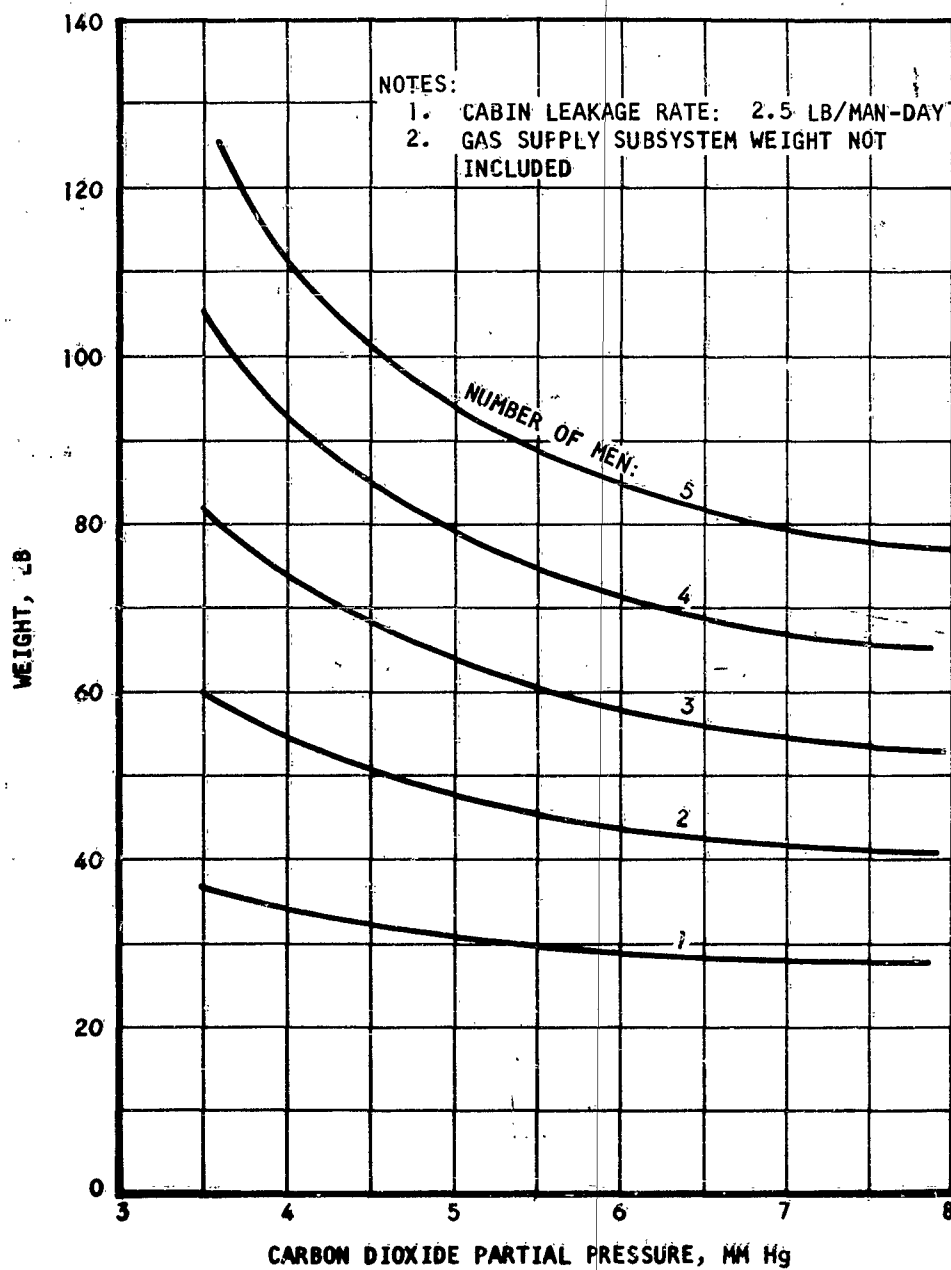


Figure 122. Freeze-out Atmospheric Control System Weight  
(Cabin Pressure: 10 psia)

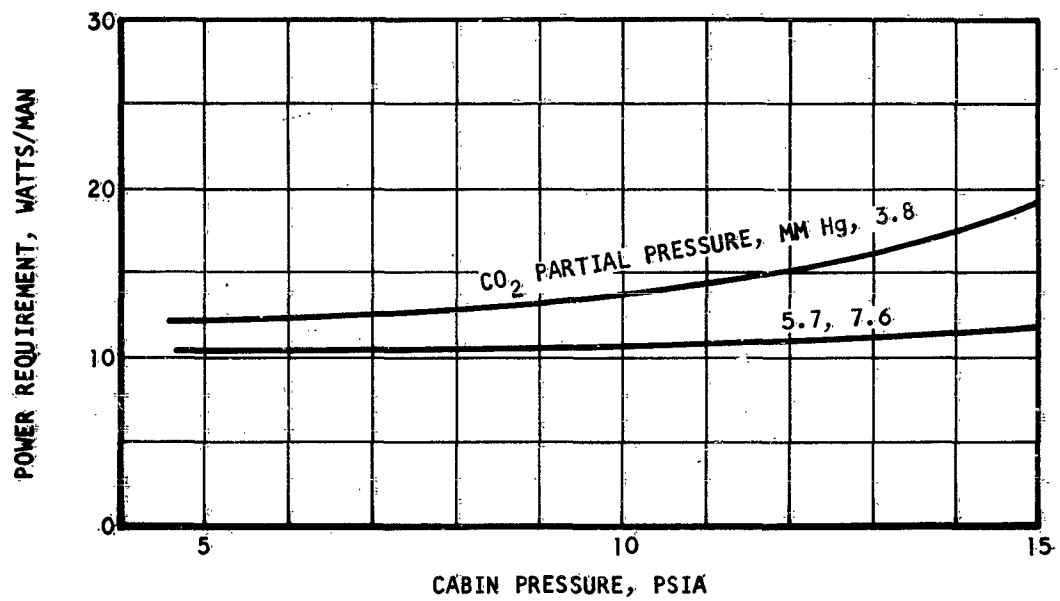


Figure 123. Freeze-out Atmospheric Control System Power Requirement

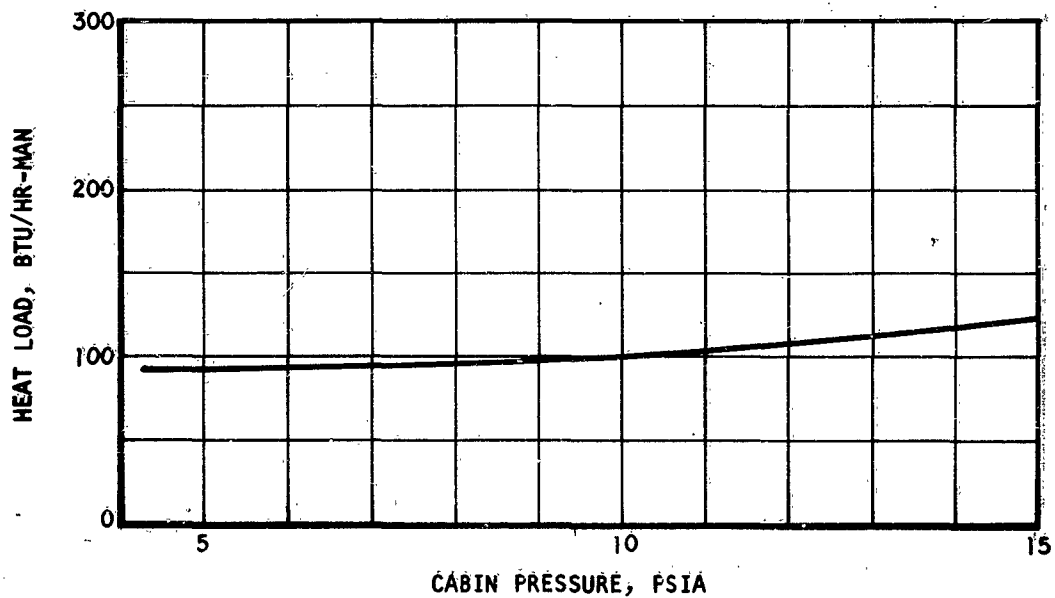


Figure 124. Freeze-out Atmospheric Control System Heat Load

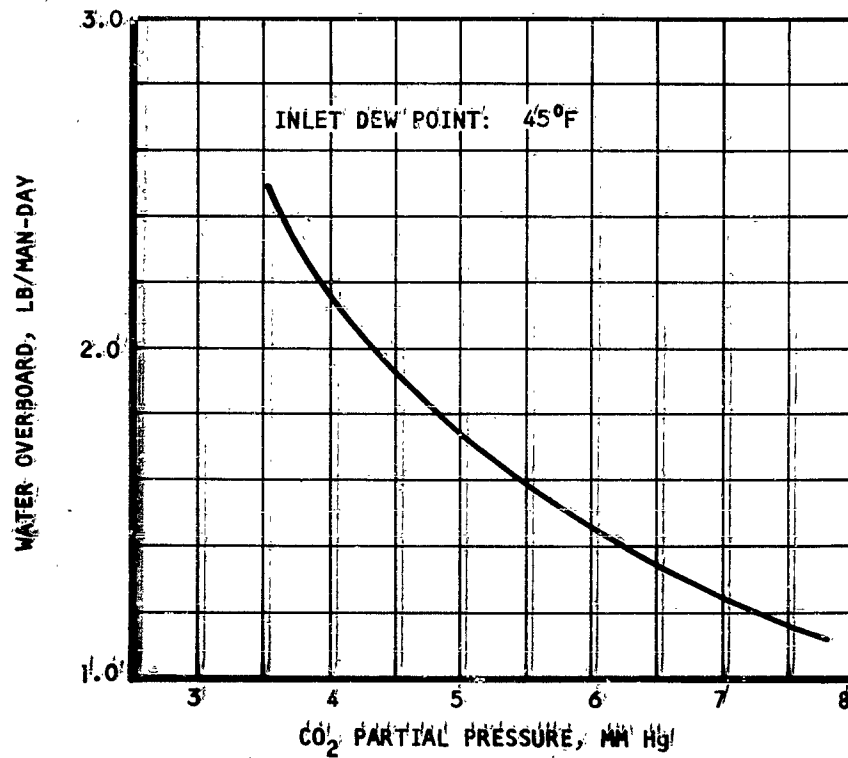


Figure 125. Rate of Water Evacuated Overboard in a Simple Freeze-out Atmospheric Control System

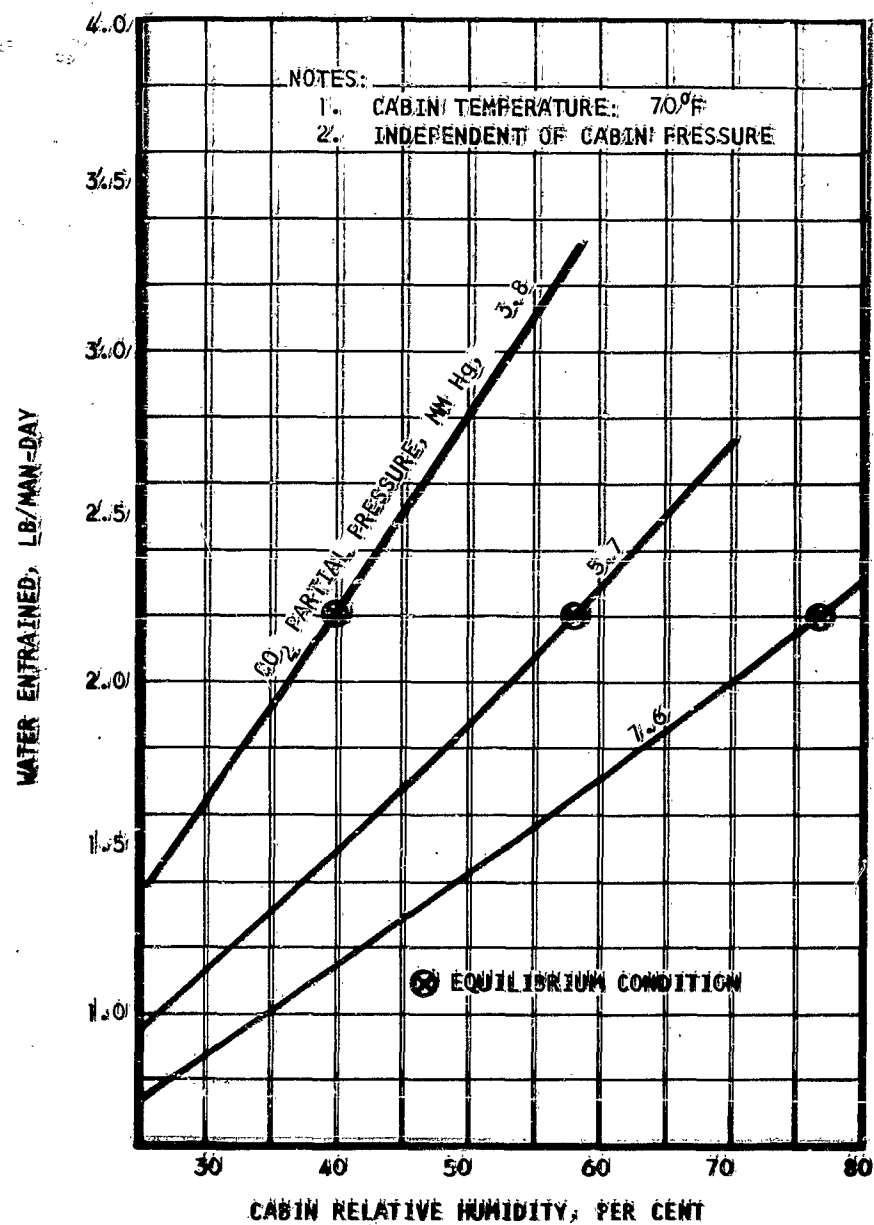


Figure 126: Water Entrained to the Carbon Dioxide Removal Subsystem in a Freeze-out Atmospheric Control System

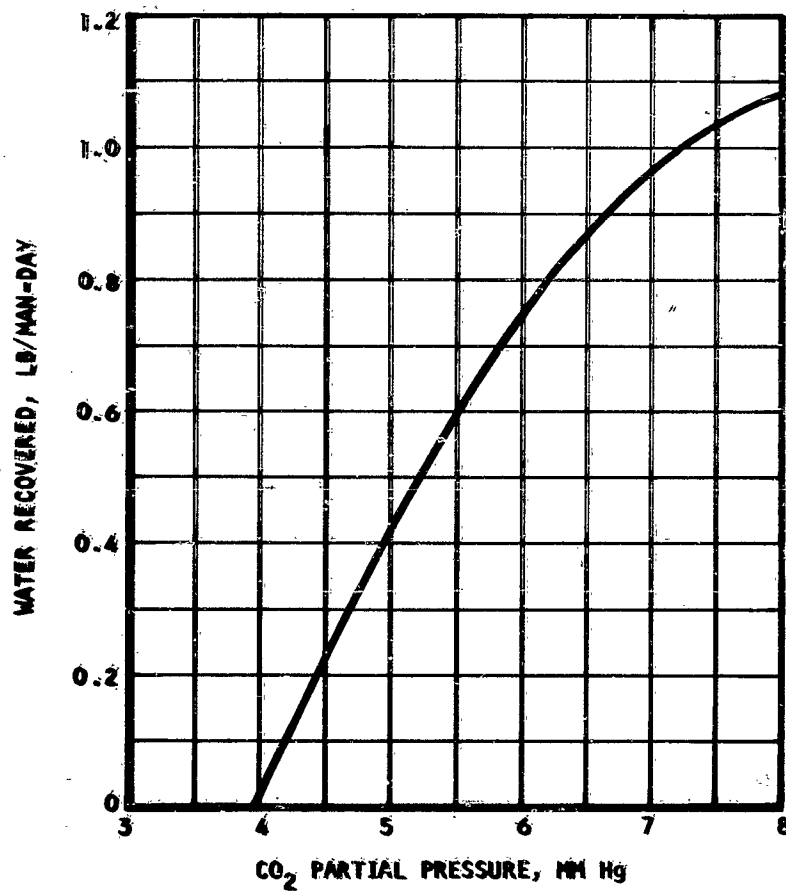


Figure 127. Water Recovered in Simple Freeze-out Atmospheric Control System

## **MOLECULAR SIEVE ATMOSPHERIC CONTROL SYSTEM**

### **General**

For missions of moderate to long duration, molecular sieve atmospheric control systems presently appear the most attractive means of controlling space vehicle atmospheric compositions. The system, however, is complex and incorporates a large number of valves, which makes it unreliable, especially for long-duration missions. This stems from the cyclic nature of the adsorption-desorption processes of the desiccant and molecular sieve beds.

### **System Description**

The system is shown schematically in Figure 128. Both oxygen and nitrogen are stored supercritically; cabin humidity is controlled by the cooler-condenser-separator process; trace contaminant removal is effected in activated charcoal and hopcalite catalyst beds.

The carbon dioxide removal subsystem is basically that described in Section VI of this report. A cooler is shown on the switching silica gel beds. Its purpose is to cool the beds between the desorption and adsorption cycles to prevent poisoning of the molecular sieve by water entrained through the desiccant at the beginning of each cycle.

The valve-actuating mechanism of the silica gel bed arrangement is activated when the water partial pressure at the desiccant bed outlet reaches a fixed preset value. Similarly, cycling of the molecular sieve beds is controlled by the carbon dioxide partial pressure at the molecular sieve outlet.

For safety, three fans are used in the main system and in the carbon dioxide removal subsystem. All the valves controlling the flow through the molecular sieve beds seal the system against vacuum and are redundant. A complete analysis of the carbon dioxide management subsystem is given in Section VI of this report.

### **System Characteristics**

#### **i. Weight**

The weight of the system shown in Figure 128 is a function of all the cabin parameters and of the number of men aboard the vehicle. An estimate of the system weight is plotted in Figure 129 as a function of the number of crew members. The plot was prepared for a carbon dioxide partial pressure in the cabin of 5.7 mm Hg and a cabin pressure of 7 psia. The system weight is slightly dependent on the carbon dioxide partial pressure. The analyses of Section VI shows a carbon dioxide removal subsystem hardware weight variation of approximately 10 per cent when the carbon dioxide partial pressure varies from 3.8 to 7.6 mm Hg. This corresponds to a system weight variation of about 5 per cent.

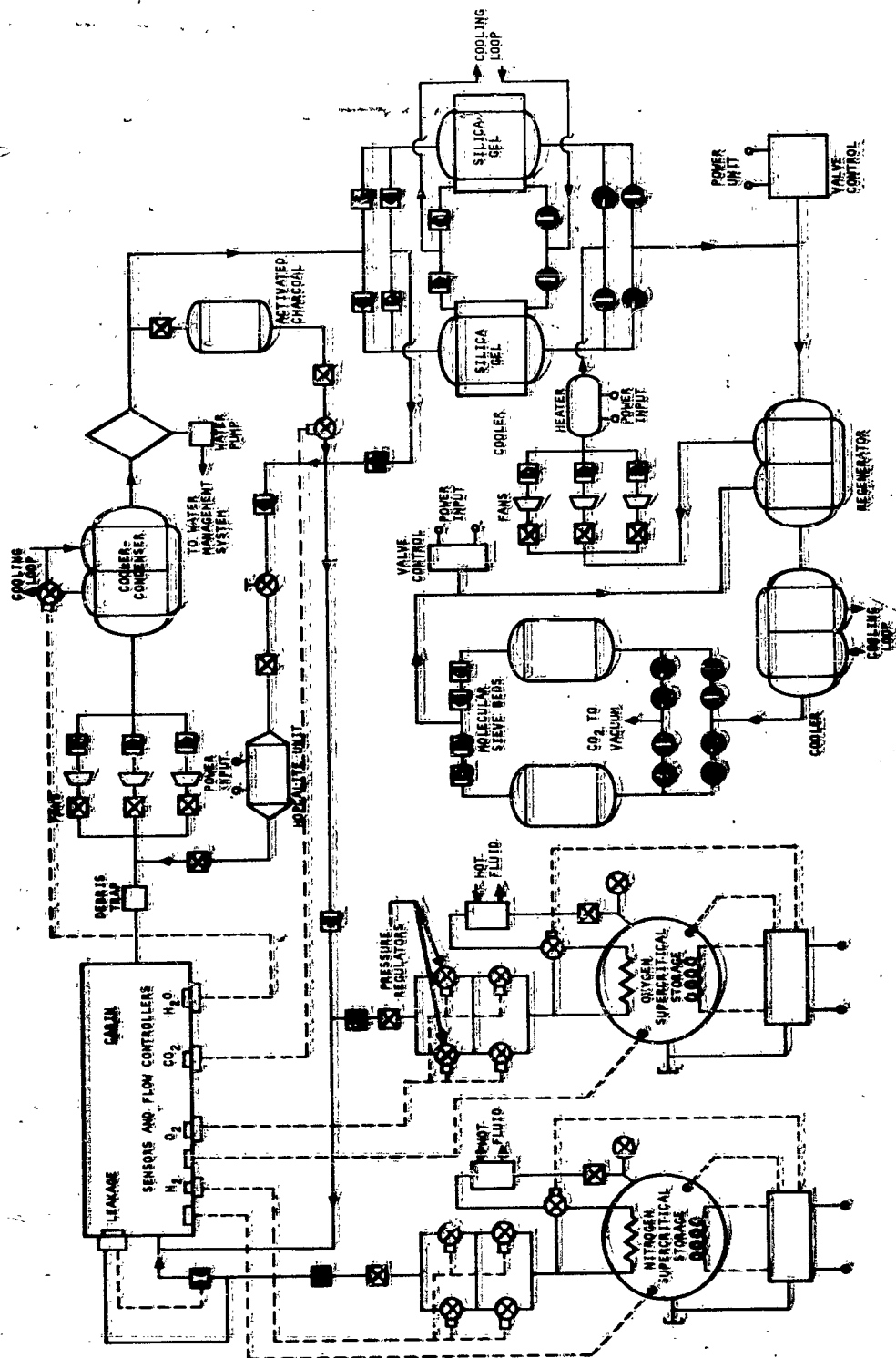


Figure 129. Molecular Sieve Atmospheric Control System



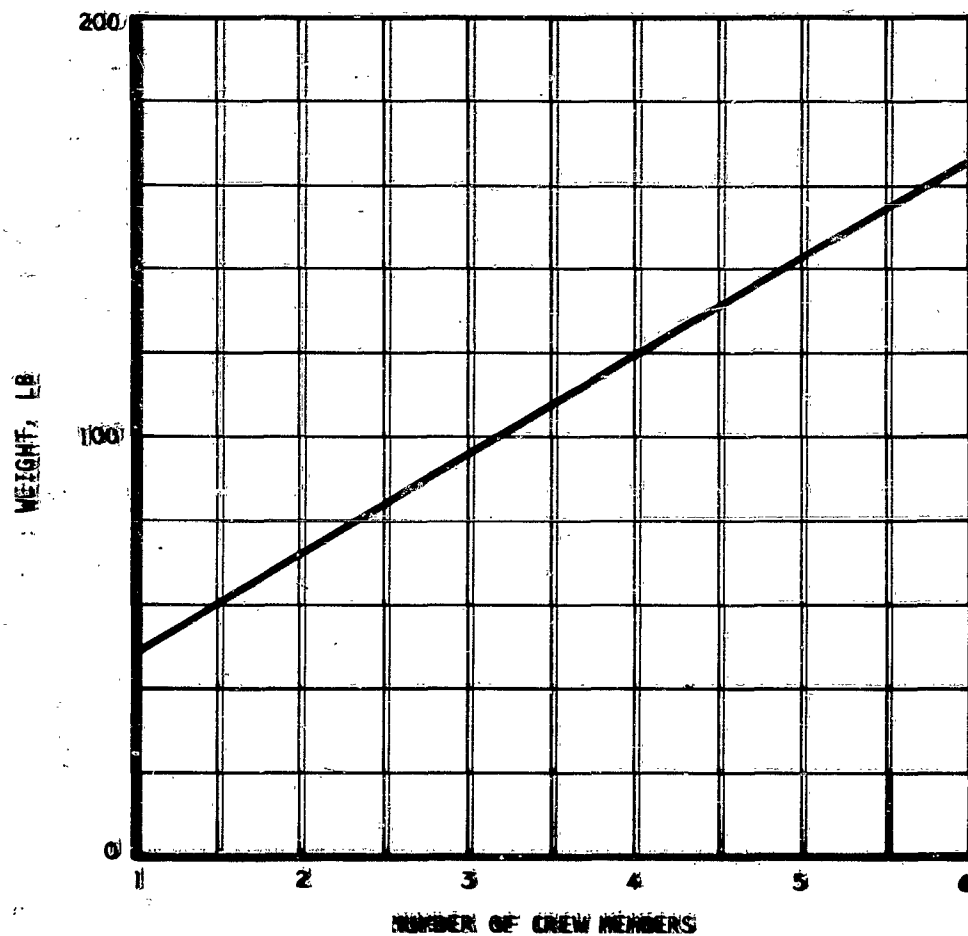


Figure 129. Molecular Sieve System Weight

## **2. Power Requirement**

The system total power requirement is shown in Figure 130 plotted versus the cabin pressure for various carbon dioxide partial pressures in the cabin. The plot was prepared for a one-man system. Small variations for the number of crew members were ignored.

## **3. Heat Load**

Heat is dumped from the atmospheric cooling system into the vehicle cooling system at three locations: first, through the cooler-condenser, where the process air is assumed cooled to 45°F; second, through the cooler upstream of the molecular sieve bed, where the air temperature is dropped to 50°F; third, in the silica gel bed cooling process between the desorption and the adsorption cycles. The total amount of heat rejected to the vehicle cooling system at these three locations is plotted in Figure 131 as a function of the carbon dioxide partial pressure in the cabin.

Heat also is carried to the cabin from the hot air discharged from the carbon dioxide management subsystem. This amount of heat, calculated as the difference between the subsystem heat content at outlet and inlet, is shown plotted in Figure 132.

These plots are based on average values and do not take into account the transient nature of the cycle; maximum heat loads in an actual system are higher than shown here.

## **4. Material Balance**

Carbon dioxide is removed from the cabin atmosphere and evacuated overboard at the rate of 2.25 lb per man-day. Water vapor generated in the cabin is condensed, separated from the process air as a liquid, and returned to the vehicle water management system at the rate of 2.2 lb per man-day.

# **ELECTRODIALYSIS CELL ATMOSPHERIC CONTROL SYSTEM**

## **System Description**

Carbon dioxide removal by electrodialysis has been discussed in Section VI of this report. An atmospheric control system using this technique is shown schematically in Figure 133. The system uses supercritical storage of atmospheric gases, humidity control by cooler-condenser-separator process, and trace contaminant management by activated carbon and hopcalite catalyst. The system is essentially for long-duration missions because of its high power requirement and high specific weight; therefore, three fans are installed in parallel to insure process air flow through the system.

Humidity control is effected downstream of the electrodialysis cell, because the air processed in the cell is saturated with water vapor at cell outlet. This moisture is removed in the same cooler-condenser-separator as the humidity from the cabin.

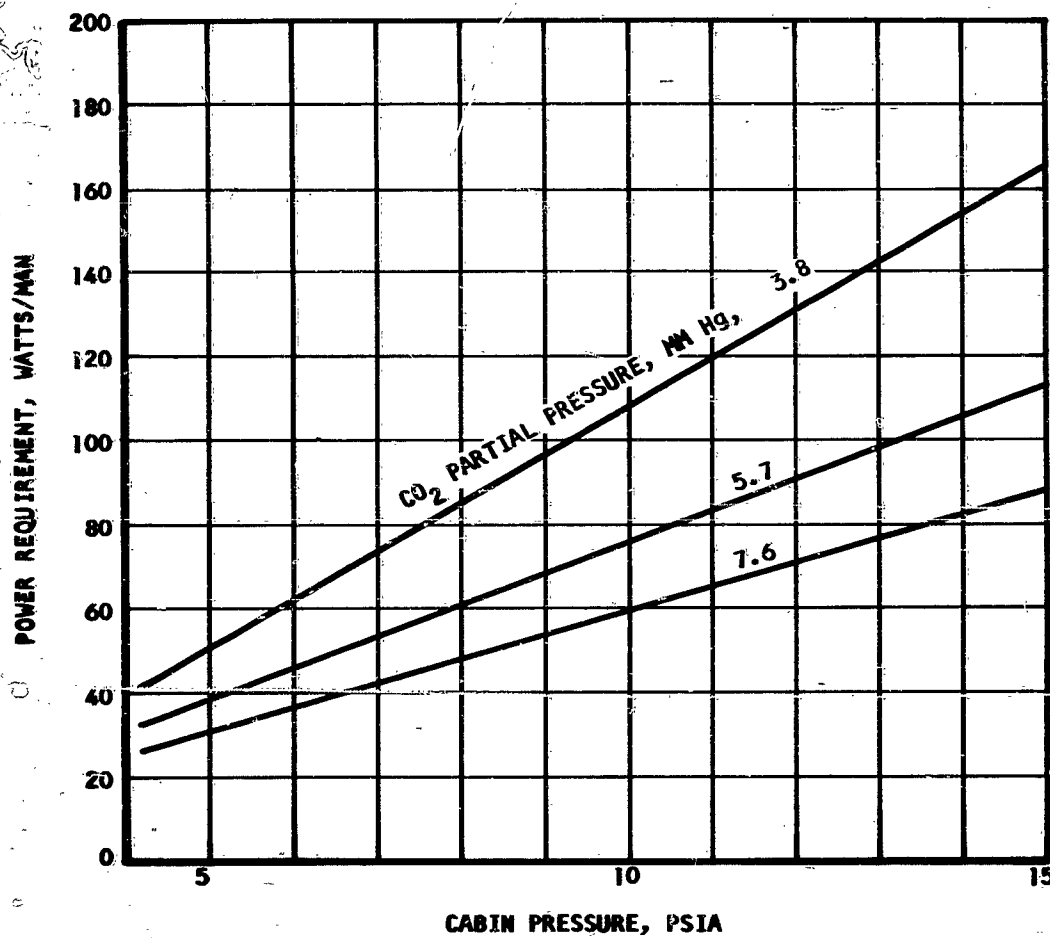


Figure 130. Molecular Sieve System Power Requirement

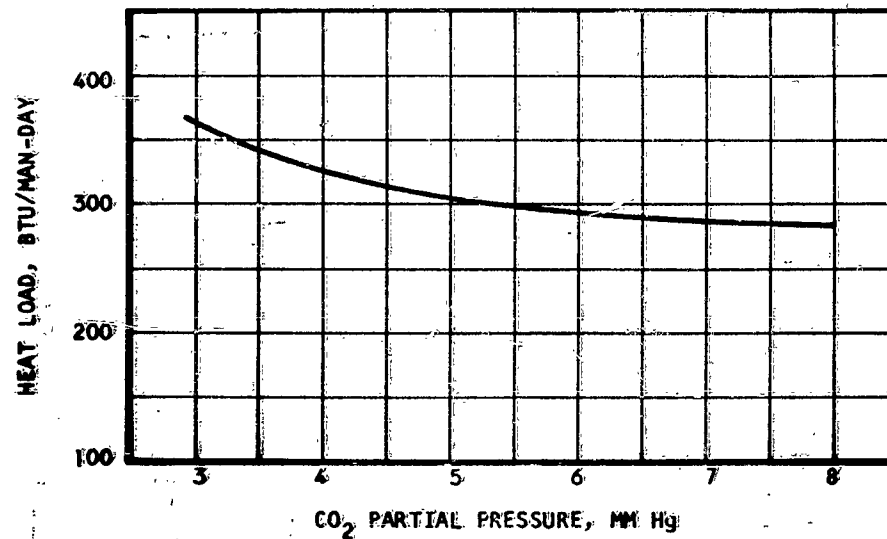


Figure 131. Heat Rejected to Vehicle Cooling System - Molecular Sieve Atmospheric Control System

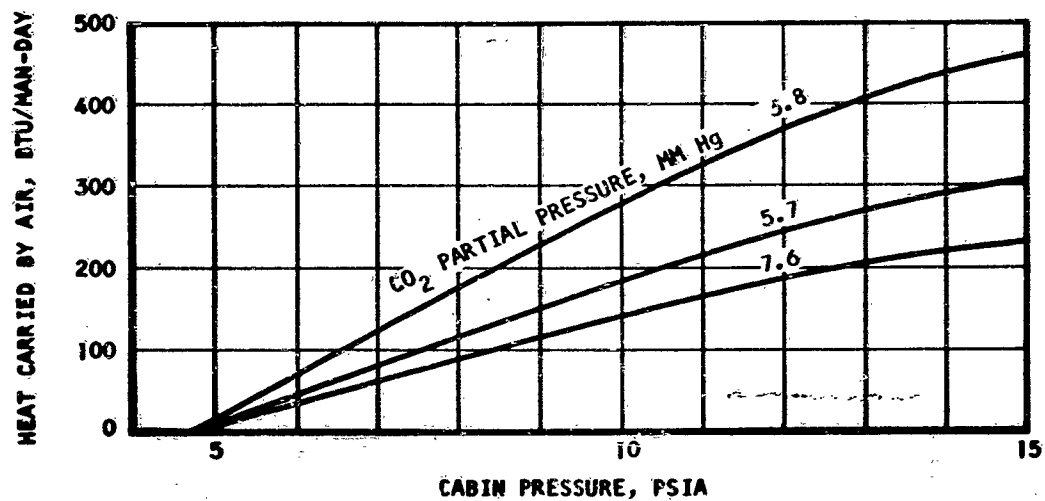


Figure 132. Heat Carried by the Process Air - Molecular Sieve Atmospheric Control System

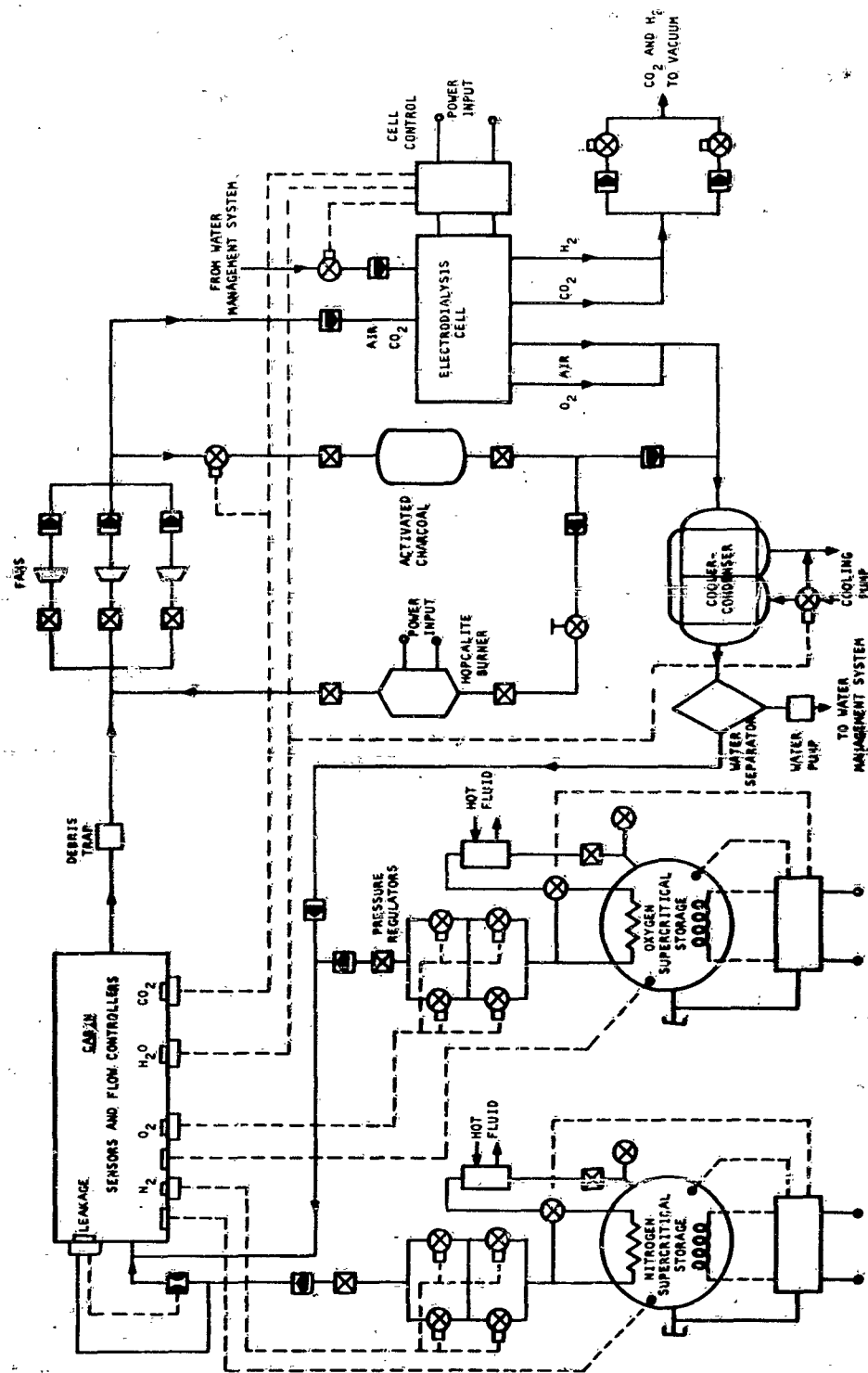


Figure 133. Atmospheric Control System with Electrolysis Cell

The process air flow to the cell is indirectly controlled by the carbon dioxide partial pressure in the cabin. The water flow to the cell is modulated by the amount of air processed in the cell, its relative humidity, and the cell operating temperature.

#### System Characteristics

By far, the heaviest subsystem (excluding gas storage) of the atmospheric control system depicted in Figure 133 is the electro dialysis carbon dioxide removal subsystem. It comprises about 75 per cent of the total system weight. Similarly, the other characteristics of the electro dialysis cell far outweigh those of the other subsystems. Since the electro dialysis cell parameters cannot be estimated accurately, only rough estimates of the overall system characteristics can be made. The atmospheric control system parameters of interest are listed on a one-man basis in Table 23. The carbon dioxide removal subsystem parameters used here are given in Section VI.

#### ATMOSPHERIC CONTROL BY MOLECULAR SIEVE WITH CARBON DIOXIDE METHANATION

##### System Description

For long-duration missions (in excess of 100 days), recovery of oxygen from the carbon dioxide produced by respiration becomes a necessity. A complete atmospheric control system, in which the carbon dioxide is removed by molecular sieve adsorption, recovered, and reduced to methane with hydrogen, is shown schematically in Figure 134. This system is basically the same as the molecular sieve system described previously with three additional features. First, the carbon dioxide is recovered from the molecular sieve instead of being evacuated overboard. Second, the hydrogen necessary for methanation of the carbon dioxide is produced by water electrolysis; the electrolytic cell is also used as an oxygen supply for the cabin. Third, the system incorporates a catalytic reactor where the methanation process takes place. The methanation subsystem incorporating an electrolytic cell is described and discussed in Section VII. Here, only the integration aspect of the subsystems is discussed.

System operation is as follows: hydrogen produced by water electrolysis is first circulated and cooled in a cooler-condenser-separator unit. Most of the moisture carried by the stream is condensed, separated, and returned to the vehicle water management system. The hydrogen stream is further dried by flowing it through a silica gel bed. It is then used to desorb the "off-stream" molecular sieve bed. The mixture of carbon dioxide and hydrogen exhausting from the bed is introduced in the catalytic reactor where methanation takes place. Part of the heat of reaction leaks through the reactor wall into the molecular sieve bed to make possible the desorption process. The hot gases exhausted from the reactor are cooled by the incoming hydrogen and piped to a cooler-condenser-separator unit where the water of reaction is recovered and returned to the water management subsystem.

TABLE 23

ELECTRODIALYSIS CELL ATMOSPHERIC CONTROL SYSTEM CHARACTERISTICS  
(10 PSIA SYSTEM)

| Parameter  | Value                             |
|--|-----------------------------------|
| Weight   | 62 lb/man                         |
| Power requirement  | 310 watts/man                     |
| Heat load on the vehicle cooling system                                  | 900 Btu/hr-man                    |
| Heat rejected to ambient   | 68 Btu/hr-man                     |
| Temperature of process air at system outlet                              | 45°F (sat. with H <sub>2</sub> O) |
| Water returned to vehicle water management system                        | 14.2 lb/man-day                   |
| Hydrogen overboard   | 0.001 lb/man-day                  |
| Carbon dioxide overboard   | 2.25 lb/man-day                   |
| Water overboard  | 0.208 lb/man-day                  |
| Oxygen production  | 0.008 lb/man-day                  |
| Water required for system operation from vehicle water management system | 12.20 lb/man-day                  |

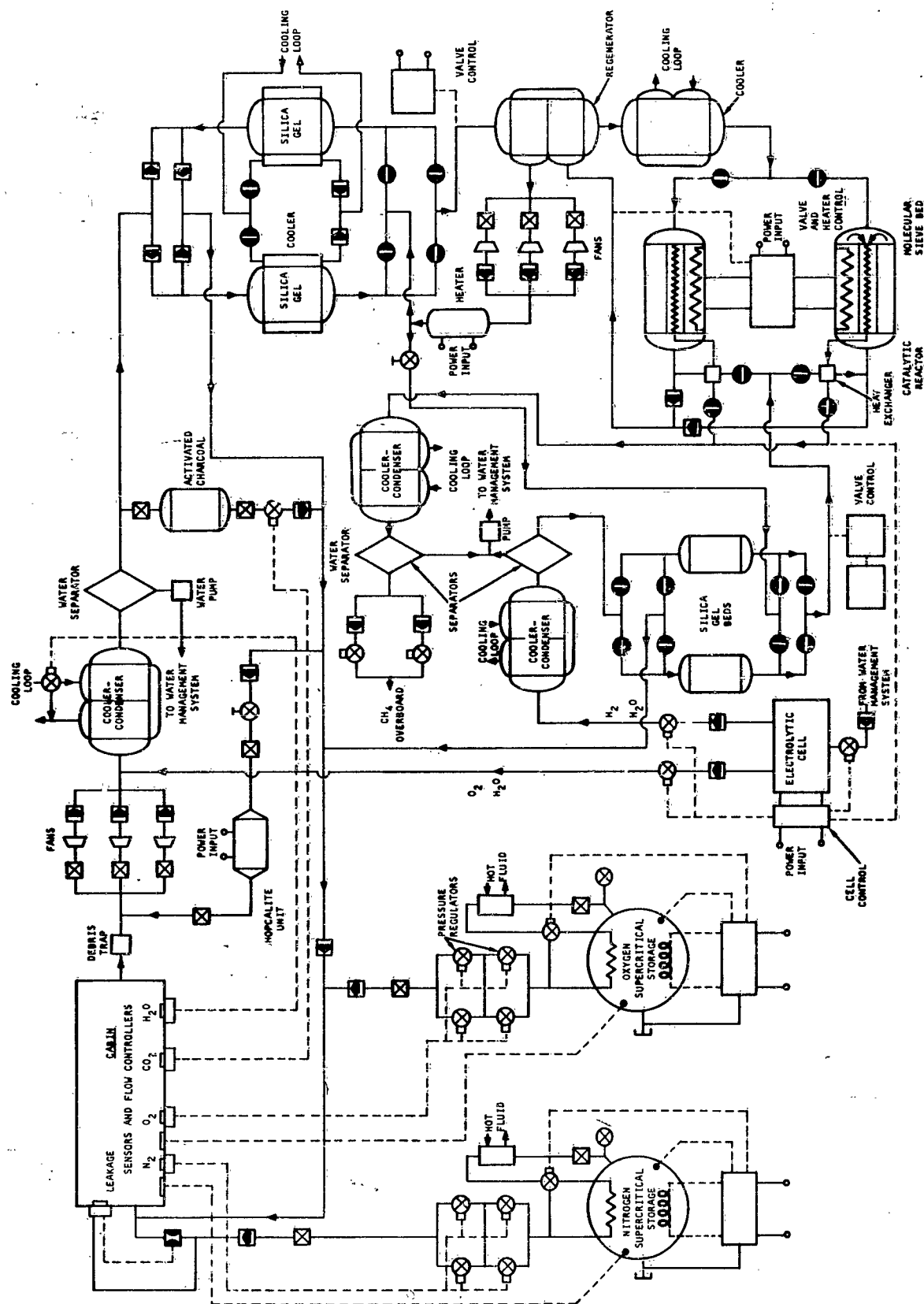


Figure 134. Atmospheric Control System By Molecular Sieve With Carbon Dioxide Methanation



The catalytic reactor is built into the molecular sieve bed. In this manner, the temperature of the catalyst bed can be maintained at a reasonably low level by allowing most of the heat of reaction to leak out. Fins are used to carry the heat of reaction to the sieve and to increase the contact area between the heat source and the molecular sieve pellets.

Heating elements are provided within the molecular sieve bed to insure desorption at the start of operation and to maintain stoichiometric composition of the mixture entering the methanation reactor. To initiate the methanation process, a start-up heater also is provided within the catalytic reactor.

The valves controlling the hydrogen flow path into the molecular sieve beds are actuated by the same mechanism operating the process air flow valves. Carbon dioxide partial pressure at sieve outlet signals valve switching. The hydrogen drying silica gel bed valves are switched when the moisture content of the hydrogen stream reaches a preset value. The silica gel bed is desorbed by hot air from the main atmospheric control system.

The flow of hydrogen to the methanation circuit is regulated by the amount of hydrogen and carbon dioxide present in the gases exhausted from the catalytic reactor. If this stream is hydrogen-rich, the hydrogen flow is reduced and the pressure inside the electrolytic cell builds up. The power and water inputs to the cell also are reduced when the cell operating pressure reaches a maximum value. If the gases at reactor outlet are carbon dioxide-rich, the hydrogen flow is increased with a corresponding increase in power and water inputs to the electrolytic cell.

### System Characteristics

#### 1. Weight

The weight of the electrolytic cell of the system shown in Figure 134 comprises more than half of the total system weight. Thus, the effect of parameters such as cabin pressure and carbon dioxide partial pressure can be ignored, since the electrolytic cell weight cannot be predicted accurately. An estimate of the system weight was made using a cell weight of 18.7 lb per lb of oxygen per day produced; the corresponding system weight, exclusive of the gas supply subsystem, is then estimated at 110 lb per man.

#### 2. Power Requirement

The system total power requirement was computed from the subsystem parametric data given in preceding sections. Figure 135 is a plot of the power required for system operation. Again, the power input to the electrolytic cell far outweighs that of the rest of the system. In this plot, the power necessary for molecular sieve desorption was neglected.

#### 3. Heat Rejection Load

The amount of heat rejected to the vehicle cooling system from the atmospheric control system is estimated to be about 750 Btu/hr per man.

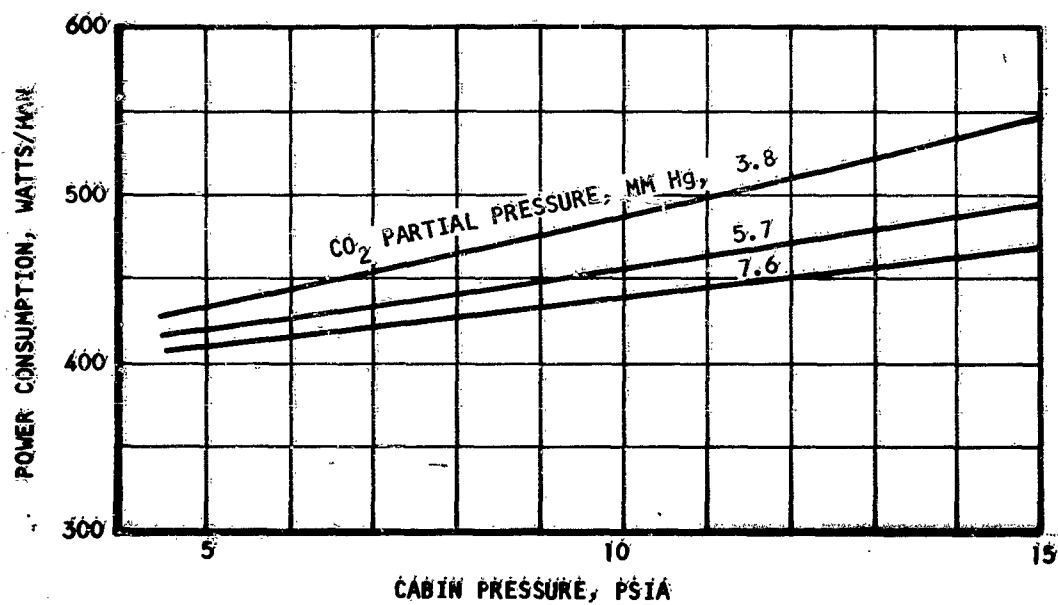


Figure 135. Molecular Sieve System with Methanation - Power Requirements

Heat also is dumped from the system to the surroundings at the rate of about 50 Btu/hr per man. The heat generated within the carbon dioxide removal subsystem and carried to the cabin by the process air is shown plotted in Figure 82.

#### 4. Material Balance

In Table 24 are listed data pertinent to the system material balance. A large amount of water is circulated to and from the water management system. This water is pumped into the electrolytic cell where part of it is converted into hydrogen and oxygen; a larger portion of it, however, is entrained by the gases produced in the cell and subsequently condensed and separated from these streams to be returned to the vehicle water management subsystem.

### ATMOSPHERIC CONTROL SYSTEM BY ELECTRODIALYSIS PROCESS WITH OXYGEN RECOVERY

#### System Description

This system offers the advantage of great simplicity over the molecular sieve system with oxygen recovery discussed previously. This stems from the fact that carbon dioxide removal by electrodialysis is a continuous process compared to the cyclic type of operation of the molecular sieve system. Figure 136 is a system schematic diagram. The basic system has been described before; the only addition here is the methanation subsystem. This subsystem has also been described previously in Section VII. Integration of the carbon dioxide removal and carbon dioxide reduction subsystem presents no problems, as seen from the system diagram. As shown, the electrolytic cell is controlled by the carbon dioxide flow from the electrodialysis cell. Most of the heat generated in the methanation process is dissipated to the surroundings, and contributes to the load on the vehicle thermal management system.

#### System Characteristics

The weight, power consumption, and effectiveness of the two major components of this system are not well-known at present, and only a rough estimate of the system characteristics can be made. Table 25 lists the pertinent system parameters and material balance data.

TABLE 24

ATMOSPHERIC CONTROL BY MOLECULAR SIEVE  
WITH CARBON DIOXIDE METHANATION

## SYSTEM MATERIAL BALANCE

| Parameter                                     | Flow Rate,<br>lb/man-day |
|---|--------------------------|
| Oxygen production                             | 3.273                    |
| H <sub>2</sub> O from water management system | 8.275                    |
| H <sub>2</sub> O to water management system   | 8.42                     |
| H <sub>2</sub> O overboard                    | 0.025                    |
| CO <sub>2</sub> overboard                     | 0.225                    |
| H <sub>2</sub> overboard                      | 0.041                    |
| CH <sub>4</sub> overboard                     | 0.736                    |

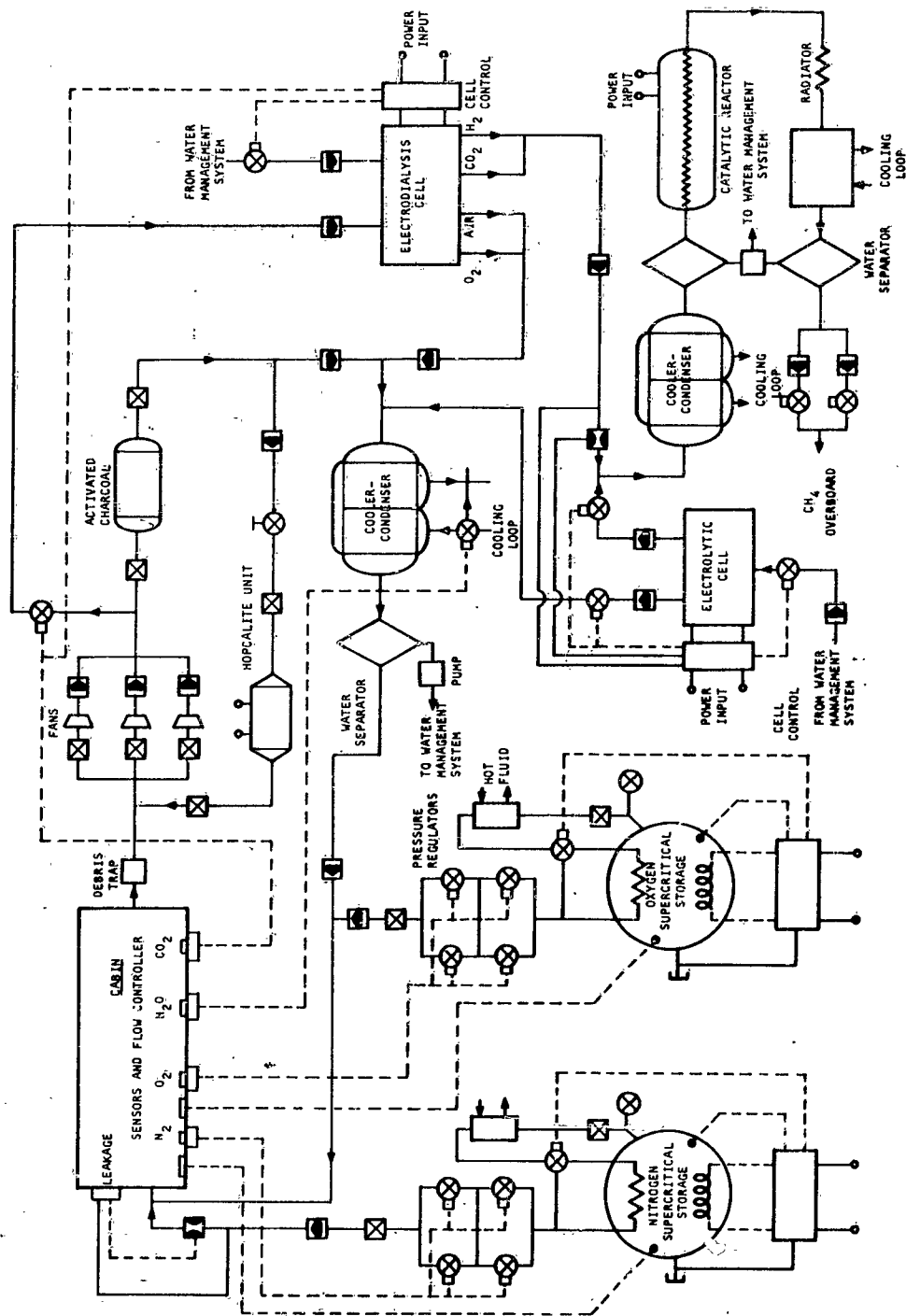


Figure 136. Atmospheric Control System by Electrodialysis  
With Carbon Dioxide Reduction

TABLE 25

ATMOSPHERIC CONTROL SYSTEM BY ELECTRODIALYSIS  
WITH OXYGEN RECOVERY

## SYSTEM CHARACTERISTICS

| Parameter  | Value             |
|--|-------------------|
| Weight   | 135 lb/man        |
| Power requirement                                  | 710 watts/man     |
| Heat rejection to vehicle cooling system (45-50°F) | 1200 Btu/hr-man   |
| Heat rejection to ambient                          | 220 Btu/hr-man    |
| Oxygen production                                  | 3.281 lb/man-day  |
| Water consumption (from water management system)   | 20.28 lb/man-day  |
| Water to water management system                   | 20.42 lb/man-day  |
| Carbon dioxide overboard                           | 0.225 lb/man-day  |
| Methane overboard                                  | 0.736 lb/man-day  |
| Water overboard                                    | 0.0300 lb/man-day |
| Hydrogen overboard                                 | 0.0409 lb/man-day |

## SECTION XI

### CONCLUSIONS

In this report, analyses of the various subsystems, which are integral parts of complete atmospheric control systems, were performed. Parametric data were given, and subsystems that perform particular functions were compared on an equivalent weight basis. The parameters introduced in the concept of equivalent weight were the subsystem hardware weight, power consumption, heat rejection load, and material balance. Subsystem reliability also was discussed. Trade-off studies were presented delineating the field of application of particular subsystems.

The studies performed on gas supply subsystems have shown that, at the present state of the art, supercritical storage of atmospheric constituents is preferable to other storage methods. Subcritical storage with single-phase delivery poses operating problems which are presently being studied experimentally. None of the chemical methods of atmospheric gases generation appears competitive with cryogenic storage techniques. However, water electrolysis will be applicable as a source of hydrogen for long-duration missions when oxygen is recovered from carbon dioxide. Intensive experimental work is required to develop an efficient, lightweight, electrolytic cell for zero-gravity operation. Experimental work also is necessary for the development of a reliable subcritical cryogenic storage vessel with liquid delivery. This type of storage vessel is very attractive for use in conjunction with carbon dioxide freeze-out systems. It provides the heat sink necessary for the freezing process which appears to have a definite field of application in vehicles where water is plentiful.

Cabin humidity control by the cooler-condenser process, with subsequent liquid water separation, seems to be the only suitable method of water removal at present. The subsystem based on this process is very simple and offers a double advantage: first, it can be used for complete thermal control of the cabin atmosphere; second, the moisture removal from the cabin air is recovered as liquid water.

An excess production of liquid water aboard a space vehicle is desirable, since it can be used in an evaporator as a low-temperature heat sink. Sink temperatures on the order of 40°F are not easily attained with liquid loop cooling systems; however, evaporation of excess water can, for a very low weight penalty, produce these sinks with a considerable overall cooling system weight reduction.

While the selection of subsystems, such as gas supply and humidity control, are virtually independent of time, the choice of a carbon dioxide management subsystem is essentially based on the vehicle mission duration. The design of the atmospheric control system is, in this manner, critically dependent on the carbon dioxide management subsystem. A number of such systems were analyzed in this study. Parametric data have been presented and trade-off studies were performed. The results of trade-off studies are given in Sections IV through IX of this report.

For short-duration missions, lithium hydroxide appears the only attractive chemical means of carbon dioxide control. Depending on the design cabin conditions, carbon dioxide removal by freeze-out technique is definitely applicable to missions shorter than two weeks. Freeze-out systems, however, are inherently less reliable than lithium hydroxide systems. Experimental testing of freeze-out heat exchangers is recommended to determine the characteristics of the freezing process.

For moderate to long-duration missions, carbon dioxide removal by molecular sieve adsorption is indicated. Problem areas here are the high system power requirement, the system reliability arising from the large number of valves, and the desorption characteristics of the desiccant and molecular sieve beds. Considerable analytical and development work is required to fully understand the complex mass and heat transfer problems involved in these systems, and to establish realistic design criteria.

For long-duration missions, carbon dioxide removal by the electro-dialysis process appears attractive because of the simplicity resulting from the continuous nature of this process. Considerable development, however, is indicated to reduce the electrodialysis cell weight and power requirement.

The problems associated with oxygen recovery from carbon dioxide arise from the integration of the carbon dioxide reduction subsystem with the rest of the atmospheric control system. Hydrogen required for the process is produced by water electrolysis, which has been discussed previously. A control problem is associated with the desorption of molecular sieve beds at a rate consistent with stoichiometric composition of the gases entering the catalyst bed. Heat recovery from the methanation process also presents a problem.

In the present state of the art, trace contaminant removal subsystem design is based on assumptions relative to the contaminant production rates within the space vehicle cabin. Efforts should be expended on the determination of the nature and the generation rates of these contaminants. Once the problem statement is established, a better design can be effected with present methods of control.



#### REFERENCES

1. Coe, C.S., Rousseau, J., and Shaffer, A., Analytical Methods for Space Vehicle Atmospheric Control Processes, ASD TR-61-162, Part 2, 1962.
2. Shaffer, A., and Woodworth, L.R., Comparison of Cryogenic Storage Methods for Space Vehicle Environmental Control Systems, Report No. AAC-3843-R, AiResearch Manufacturing Company, August 1960.
3. Environmental Control Systems Selection for Manned Space Vehicles, ASD TR 61-240, Part 1, Volume 1, October 1961.
4. Wright, C.C., Contaminant Freeze-Out Study for Closed Respiratory Systems, Life Support Systems Laboratory Report No. MRL-TDR-62-7.
5. Rydelek, R.F., Investigation of Integrated Carbon Dioxide Hydrogenation Systems, ASD TDR 62-581.
6. Water Electrolysis and Carbon Dioxide Separation, AF33(657)-7938.

Aeronautical Systems Division, Dir/Aero-  
mechanics, Flight Accessories Lab., Wright-  
Patterson AFB, Ohio.  
Rpt Nr ASD-TDR-62-527, Part I. ATMOSPHERIC  
CONTROL SYSTEMS FOR SPACE VEHICLES. Mar 63.  
247 p. incl 136 illus., 25 tables, and 6  
references.

#### Unclassified Report

Studies are presented of subsystems perform-  
ing one single atmosphere control function  
and of complete atmospheric control systems.  
The subsystems considered are the following:  
gas supply, humidity control, carbon dioxide  
management, trace contaminant removal, and  
oxygen recovery from carbon dioxide. Para-

metric data are presented whereby the sub-  
systems and systems are characterized in  
terms of vehicle and mission parameters;  
interfaces between the atmospheric control  
system and other vehicle systems also are  
taken into account. Comparison of the sub-  
systems considered are performed on an  
equivalent weight basis where the equivalent  
weight includes hardware weight as well as  
penalties for material balance, power con-  
sumption, and heat rejection load. Areas of  
utilization of the various subsystems are  
defined in terms of mission duration, crew  
complement, and cabin atmosphere parameters.

1. Atmospheric Con-  
trol System
2. Environmental  
Control System
3. Space Ships
4. Astronautics

- I. AFSC Project 6146  
Task 614609  
Contract No. AF  
33(616)-8323
- III. AirResearch Mfg.  
Company, Los  
Angeles, Calif.
- IV. J. Rousseau
- V. Secondary Rpt No.  
SS-716-R
- VI. Not avail fr OTS
- VII. In ASTIA collection

Aeronautical Systems Division, Dir/Aero-  
mechanics, Flight Accessories Lab., Wright-  
Patterson AFB, Ohio.  
Rpt Nr ASD-TDR-62-527, Part I. ATMOSPHERIC  
CONTROL SYSTEMS FOR SPACE VEHICLES. Mar 63.  
247 p. incl 136 illus., 25 tables, and 6  
references.

#### Unclassified Report

Studies are presented of subsystems perform-  
ing one single atmosphere control function  
and of complete atmospheric control systems.  
The subsystems considered are the following:  
gas supply, humidity control, carbon dioxide  
management, trace contaminant removal, and  
oxygen recovery from carbon dioxide. Para-

metric data are presented whereby the sub-  
systems and systems are characterized in  
terms of vehicle and mission parameters;  
interfaces between the atmospheric control  
system and other vehicle systems also are  
taken into account. Comparison of the sub-  
systems considered are performed on an  
equivalent weight basis where the equivalent  
weight includes hardware weight as well as  
penalties for material balance, power con-  
sumption, and heat rejection load. Areas of  
utilization of the various subsystems are  
defined in terms of mission duration, crew  
complement, and cabin atmosphere parameters.

1. Atmospheric Con-  
trol System
  2. Environmental  
Control System
  3. Space Ships
  4. Astronautics
- I. AFSC Project 6146  
Task 614609  
Contract No. AF  
33(616)-8323
  - III. AirResearch Mfg.  
Company, Los  
Angeles, Calif.
  - IV. J. Rousseau
  - V. Secondary Rpt No.  
SS-716-R
  - VI. Not avail fr OTS
  - VII. In ASTIA collection